Comparative functional study of the development of the photoreceptive organs in *Danio rerio* and *Scophthalmus maximus*, two phylogenetically distant Teleost fish species

Inauguraldissertation

zur

Erlangung der Würde eines Doktors der Philosophie

vorgelegt der

Philosophisch-Naturwissenschaftlichen Fakultät der Universität Basel

von

Robin Vuilleumier

aus

La Sagne

Ausgeführt unter Leitung von:

Prof. Dr. Walter J. Gehring

Abteilung Zellbiologie

Biozentrum der Universität Basel

CH-4056 Basel

Prof. Dr. Gilles Boeuf/

Dr. Jack Falcon

Physiologie environementale

Laboratoire Arago (Paris VI)

66650 Banyuls/Mer (France)

2006

Genehmigt von der Philosophisch-Naturwissenschaftlichen Fakultät auf Antrag

Prof. Dr. W. J. Gehring	**Prof. Dr. Gilles Boeuf**	**Prof. Dr. S. Arber**
Referent	Koreferent	Vorsitz
.....	.....	.....

Dr. Jack Falcon

Gast

.....

Basel, den 21 November 2006

.....

Prof. Dr. H-P. Hauri

Dekan

Philosophisch-Naturwissenschaftlichen Fakultät

Universität Basel

Abstract

In ectothermic vertebrates, the retina and the pineal gland are the two main photoreceptive organs. Whereas the first one is involved in visual information, the second one acts as a detector of day length and synchronizer of the different functions in the organism through rhythmic secretion of melatonin. Both organs display common and specific features, which suggest the existence of differences in the molecular mechanisms leading to their formation. However, until today, scant progress has been made in understanding the fundamental questions of how their respective functions are established during embryonic development, and whether the genetic actors, critical for their correct morphogenesis, are shared or organ specific.

In an attempt to tackle these questions, we first examined the expression pattern of several photoreceptive organs and cell division markers in the zebrafish (*Danio rerio*) and the turbot (*Scophthalmus maximus*), two phylogenetically distant Teleost fish species. We found that the pineal gland differentiates before the retina in both species, suggesting that the former mediates photic responses during embryonic development. Although this feature is conserved between the zebrafish and turbot, differences in the expression pattern of marker genes were found between both species, suggesting that the molecular mechanisms controlling the early pineal functions have been modified during Teleost evolution. Finally, we investigated the role of two alternative *Pax6.2* splice variants in the formation of the central nervous system including the pineal gland and the eyes in zebrafish through a knock down strategy. We show that both isoforms display specific and similar functions suggesting that the general gene networks triggering the patterning of these organs have been highly conserved during vertebrates' evolution.

Acknowledgments

I am very grateful to Prof. Walter J. Gehring, Prof. Gilles Boeuf and Dr. Jack Falcon for giving me the opportunity to perform my PhD in their respective laboratory. I am profoundly indebted to them for the enthusiasm they put in my projects and the trust they gave me during these four years. To perform a PhD between these two laboratories was a great honour for me, thanks a lot Walter, Jack and Gilles!!!

Special thanks to my supervisor commitee: Prof. Silvia Arber, Prof. Gilles Boeuf, Dr. Jack Falcon and Prof. Walter J. Gehring.

I would like to thank warmly Annaïck Carles, Jack Falcon, Frédéric Prince, Makiko Seimiya and Hiroshi Suga for critical reading of this manuscript and comments.

I am very grateful to the following people of the Banyuls Fish Team for their invaluable help and friendship during my PhD: namely Laurence Besseau, Michael Fuentes, Elodie Peyric, Esther Isorna, Aurélien Pipparelli, Sandrine Sauzet and Béatrice Rivière. Laurence was a very nice and encouraging person for me. I will miss the fruitful discussions we had, especially the ones of the saturday morning in the lab! Thanks a lot! I would like to thank Michael for his valuable help to have taking care of the zebrafish and turbot. This is not an easy task, but without him, this work could never have been done. Also, a special thank for his enthusiasm in the missions in Noirmoutiers, it was very fun! I am indebted to Elodie and Esther, they helped me a lot during all my stay in Banyuls and I will never forget the "impossible night missions" we had in the lab !!! Also, thanks a lot for their encouragments and for fruitful discussions which gave me new ideas and hope on my projects. I would like to acknowledge warmly Aurélien for the expert and valuable help he gave me to finish a part of this experimental work. Without him, I would not have been done so easily. Finally, I would like to say thank you to Sandrine and Béatrice for their valuable help in the lab and for their graciousness. You were very nice person to work with.

To perform a PhD between two laboratories does not only allow to learn a lot on a scientific point of view but also to meet a lot of very nice people. Because I began my studies in Banyuls, first I would like to thank for their friendship and their help the following people that I met there, namely: Antoine Aze, Alain Camasses, Antoine Carlier, Carolina Concha, Gilles Doignon, Guillaume Drillet, Yasmine Even-Le Gac, Anne-Marie Geneviève, Karine Gérard, Mickael Le Gac, Céline Labrune, Laure Lapasset Isabelle Quiroga, Caroline Rocher, Olivier Zemb, Nicholas Offner, Olivier Maire, Christian Schwarz, Elodie Magnanou, Carmen Palacios de la Cruz, Hector and Stéphanie Escriva, Arturo Rodriguez Blanco, Sabine Matanalla Surget, Mickael Moulager, Raphaël Lami, Benoît Farinas, Jean-Claude Lozano, Valérie Vergé, Philippe Schatt, Prof. Gérard Peaucellier, Florence Corellou, Sigurd von Boletsky, Patricia Fuentes, Bérangère Pradet-Ballades, Isabelle Valdeperez, Adriana and Marcio, Joel, Marc, Damien, Anthonin, Lisa, Suzanna, Rozenn, Matthieu, Bachir, Marine, Hélène, Fred, Delphine, Julie, Matan, Antonio, Carmen and Christian and all the other I might have forgotten.

Almost half of the time of my PhD was done in the Biozentrum of Basel, where the environment is ideal for a scientific emulation. I would like to acknowledge sincerely the following people for having participated in it and for good atmosphere in the lab, namely: Paul Baumgartner, Urs Kloter, Makiko Seimiya, Christopher Brink,

Jorge Blanco, Frédéric Prince, Georges Gentsch, Raphaël Fünfschilling, Daria Grazussi, Christina Gonzales, Daniel Felix, Nicole Grieder, Sacha Glardon, Polychronis Dimitrakis, Ilias Charlafti, Lydia Michaut, Yoshi and all the persons of the second floor.

I am very grateful to Véronique Charpignon, Lukas Keller and Hiroshi Suga for their friendship, their help and for having kindly lodged me several times during these four years. I will miss a lot all the excellent moments we had, especially the one in Banyuls and St-Luc. I hope never loose contact with them and that in the future we will have still very nice time together!!!

Also I would like to thank warmly Heinz-Georg Belting, Elin Ellertsdottir and Markus Affolter for having kindly provided zebrafish embryos to me when I needed at this end of PhD.

Many thanks to the kitchen team, namely Karin Mauro, Gina Evora and Bernadette Bruno. They facilitate my work so much!!!

Special thanks to the secretaries of Banyuls and Basel who organized all the administration staff to make our life easier and for their graciousness, namely Elisabeth Goetchy and Greta Backhaus.

I am indebted to Prof. Jochen Wittbrodt and the members of his laboratory for their kind hospitality and nice atmosphere they provided during my stay in Heidelberg. Especially, I would like to thank Felix, Caroline, Martina, Maru, Mirana, Hiroki and Thorsten for their valuable help and friendship.

I would like to thank the collaborators we had in France Turbot in Noirmoutier, especially Michel Guennoc and Sophie Jeu, for their warm reception, their valuable help and enthusiasm for sampling the turbot embryos and larvae.

Je voudrais aussi remercier profondément mes parents pour m'avoir tant encouragé et conseillé tout au long de ces années. Sans vous, je n'y suis serais jamais arrivé, merci infiniment!!!

I am very grateful to Annaïck for her encouragments, invaluable help and love during these years. Also, I would like to say thank you to her for having always respected my professional choices in spite of the distance which separated us.

Finally, a special thank to the little fish I worked on. Whitout them, this work could never have been done.

Table of contents

List of figures, tables and appendix

Figures

Tables

Appendix

Abbreviations

Aanat1/2: arylalkylamine N-acetyltransferase 1/2 genes
AP: antero-posterior
Ash1a: achaete/scute homologue 1a
bHLH: basic helix loop helix motif
Bmp2/4: bone morphogenetic protein 2/4 genes
BrdU: bromo-deoxyuridine
cDNA: complementary deoxyribonucleic acid
Chx10: Ceh 10 homeobox containing gene
CLZ: circumferential larval zone of the retina
CMZ: ciliary marginal zone of the retina
CNS: central nervous system
Crx: cone rod homeobox gene
Cry: cryptochrome gene
D3: type 3 deiodinase gene
DD: constant dark
Dig: digoxygenin
Dlx: distal-less homeobox homolog gene
Dpf: days post-fertilization
Dpp: decapentaplegic gene
DV: dorso-ventral
Ef1a: elongation factor 1 alpha
eGFP: enhanced green fluorescent protein
Emx: empty spiracles homeobox genes
ExR: exo-rhodopsin gene
ey: eyeless gene
Ey: eyeless mutant
eya: eye absent gene
Fgf: fibroblast growth factor gene
Flh: floating head gene
FoxE3: forkhead homeobox E3 gene
RGC: retinal ganglion cells
HD: homeodomain
Hh: hedgehog gene
Hiomt: hydroxyindole-O-metyltransferase gene
Hpf: hours post-fertilization
INL: inner nuclear layer of the retina
Irbp: interphotoreceptor retinoid-binding protein gene
L: lens
LL : constant light
LD : light/dark
Mab21l1: mab21 like 1 gene
Mbl: master blind gene
Mitf: Microphtalmia-associated bHLH transcription factor gene.
Myr: million years
NeuroD: neurogenic differenciation gene
Ngn1: neurogenin 1 gene
Notch: notch gene
NR: neural retina

O: octapeptide
OC: optic cup
ON: overnight
ONL: outer nuclear layer of the retina
Onecut: one cut domain, family member 1 gene
Optix: optic homeobox gene
Otx5: orthodenticle homeobox 5 gene
OV: optic vesicle
Pax: paired box genes
PAX6(5a): paired box 6 protein containing the exon 5a
PAX6.2(2a): paired box 6.2 protein containing the exon 2a
PCR: polymerase chain reaction
PD: paired domain
PDE: cyclic guanosine monophosphate phophodiesterase
Per: period gene
PFA: paraformaldehyde
PL: photoreceptors layer of the retina
Prox1: prospero-related homeobox 1 gene
PSB: pallium/subpallium boundary
Rh: rhodopsin photopigment
RPC: retinal progenitor cells
RPE: retinal pigmented epithelium
RT: room temperature
Rx: retinal homeobox gene
RxR: retinoic acid receptor gene
SE: surface ectoderm
sey: small eye gene
Sey: small eye mutant
Shh: sonic hedgehog gene
Six3: Sine oculis homeobox homolog 3 gene
Sm: Scophthalmus maximus
so: sine oculis gene
T3: tri-iodothyronine
T4: thyroxine
Tbx5: T-box 5 gene
TGF: transforming growth factor
THs: thyroid hormones
TR: thyroid homone receptor genes
toy: twin of eyeless gene
Vax: ventral anterior homeobox genes
Wnt: wingless type gene
Zf: zebrafish

Chapter 1

1. General introduction

Historically, the study of the development of the central nervous system (CNS) including the eye has begun as early as during the XVI century with the italian scientist **Leonardo da Vinci** (1452-1519). In the years 1510-1512, he was the first one to leave us precise descriptions of the human female organs and foetus (Figure 1). It was necessary to wait three centuries more until several scientists made important advances in the field of eye development. One of them, the belgien Professor **Daniel Van Duyse** (1852-1924) was the first one to publish reports concerning malformations of the optic nerve, the absence of the iris, the macular coloboma, the cyclopia, etc. During the same period, the english Professor and surgeon **Ida Mann** (1893-1983) helped to develop the field of ophtalmology and wrote several books including the development of the human eye (1928, 1949, 1950 and 1964) and developmental abnormalities of the eye (1957).

Figure 1. Pictures of the human female organs and human embryos designed by Leonardo Da Vinci. From http://www.wga.hu/frames-e.html?/bio/l/leon ardo/biograph.html.

However, the real bases of eye development were established by the german biologist **Hans Spemann** (1869-1941). In 1902, he made several experiments using the frog eye as a

model and found the phenomenon of induction and specialization occuring during eye development. Thus, he discovered that the formation of this organ is under the dependance of the brain and if it is cauterized, the eyes do not appear. In addition, transplantation experiments showed that the formation of the lens in vertebrates requires the contact between the optic vesicle and the adjacent surface ectoderm. Currently, the eye is certainly one of the most studied organ due to its nervous origin, its very complex cell structure and, maybe also because it is at the border between our environment and our mind.

In ectothermic vertebrates, the eye is not the only photosensitive organ. The pineal gland, an outgrowth of the forebrain, is also able to receive light signals that are transformed in nervous impulses and hormonal signals. However, the formation of this organ during development has been much less studied.

The molecular understanding of the complex processes of eye and brain development were in part resolved with the apparition of new powerfull technologies in the field of molecular biology during the last three decades. The identification of several highly conserved factors acting upstream of the genetic cascade governing eye and brain patterning in both vertebrates and invertebrates has resolved the origin of several previously described mutant phenotypes. Because of their dramatic effects caused by mutations and their highly conserved mode of action, it has been proposed that the different eye types and also different brain types found in eumetazoa may have a monophyletic origin (Gehring and Ikeo, 1999; Sharman and Brand, 1998; Gehring, 2002; Lichtneckert and Reichert, 2005).

This PhD study focuses on developmental aspects of the CNS and photoreceptive organs in ectothermic vertebrates. The first part of this work introduces the anatomical and functional description of the retina and the pineal gland, the two main photoreceptive organs present in ectothermic vertebrates. Then, the formation and remodeling during embryonic and metamorphic development will be described. More particular, focus will be put on an essential factor of the development of these organs, namely *Pax6*, and its interactions with other crucial genetic factors. In the second part, the results obtained during my PhD thesis work concerning the ontology of the photoreceptive, circadian and endocrine functions of both the retina and pineal gland in the zebrafish and turbot, two Teleost species, will be presented. Finally, the results concerning the functions of two different alternative *Pax6* splice variants in the formation of the photoreceptive organs and forebrain during zebrafish embryonic development will be described.

2. The two main photoreceptive organs in vertebrates

2.1 The vertebrate eye

The vertebrate eye or "camera-type" eye is composed of one single unit complex optical organ allowing the animal to gain knowledge of its environment by the sense of vision. One additional function is the biosynthesis of hormones such as melatonin (see section 2.2.4 : the two major sites of melatonin biosynthesis, the pineal gland and the retina).

2.1.1 Anatomy of the vertebrate eye

2.1.1.1 General information on the vertebrate eye

The vertebrate eye is composed of three main tissues (Figure 2) :

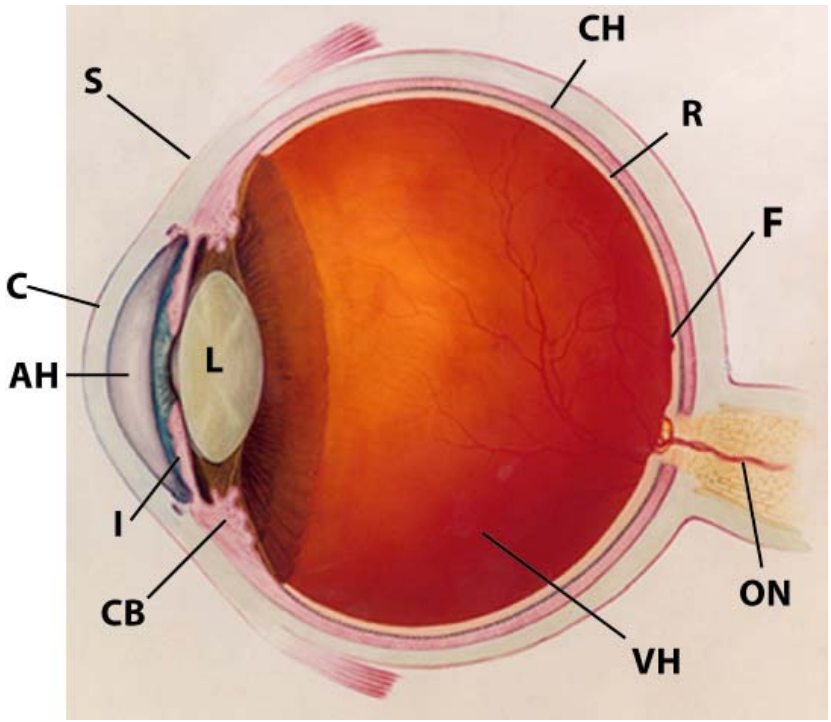

Figure 2. Schematic representation of a transverse section of a human optic lobe. AH, aqueous humor; C, cornea; CB, ciliary body; CH, choroid; F, fovea; I, iris; L, lens; ON, optic nerve; R, retina; S, sclera; VH, vitreous humor. Adapted from http://www.nei.nih.gov/photo/eyean/.

- The external fibrous tunic is composed of the sclera and the cornea. The sclera is a rigid tissue giving the form to the eye and preventing excessive light to enter the eye. The cornea is a transparent, avascular, rigid laminated tissue covering the anterior part of the eye. Its convex surface acts as a lens which bends, deviates or refracts the rays of light from their course of direction so that they can form an image on the retina.

- The uveal tunic is composed of three elements, the iris, the ciliary body and the choroid. The iris is a pigmented structure giving its colour to the eye. It surrounds a black, round opening, called the pupil through which light enters after passing through the cornea. The iris contains two muscles which act by opening or closing the pupil depending on the amount of light reaching the ocular globe. The ciliary body is a ring muscle located just behind the iris that is able to modify the form of the lens. The choroid is the third continuous and posterior portion of the uveal tract. It consists of blood vessels providing the important nourrishment and oxygen to the retina.

- The nervous tunic is composed of the retina, which transforms the light information into nervous impulses. A detailed description of the retina is presented below.

In addition, the eye contains three mediums acting each as a converging lens. The aqueous humour is formed in the cilliary body and passes along the back surface of the iris and around the lens to the pupil. One of its most important functions is to maintain the intraocular pressure within certain levels. The second is the lens which is a transparent, colourless body suspended in the front of the eyeball. Its function is to bring the rays of light to a focus on the retina. Finally, the vitreous humour is a transparent gel located behind the lens, iris and ciliary body. It extends to the retina and optic nerve. The vitreous humour gives support to the retina in maintaining its attachment to the choroid.

2.1.1.2 The main structure of the retina

As mentionned above, the main function of the retina is to translate the light signals from the environment in nervous impulses which travel through the optic nerve to the brain. It is noteworthy that it is the only element of the eye having a neural origin (see development of the eye in section 3.1). Thus, the retina belongs to the central nervous system (CNS) and contains eight cell types organized in four main layers (Figure 3).

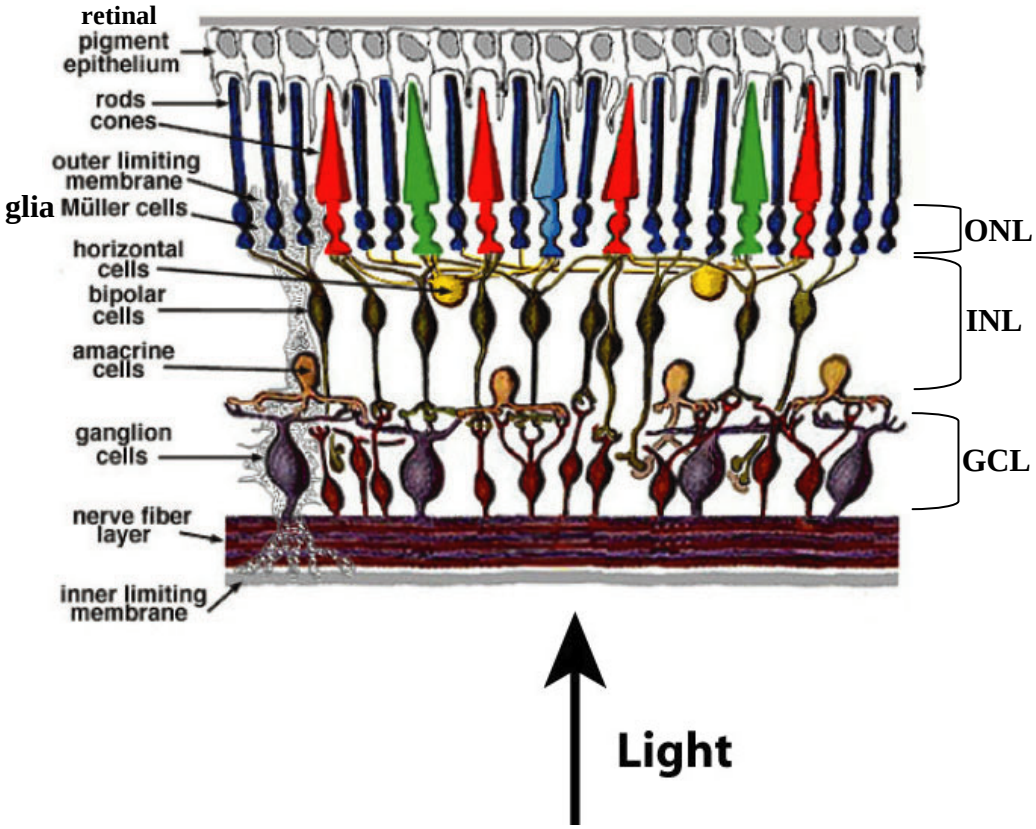

Figure 3. Schematic presentation showing the complex cellular structure of the retina. GCL, ganglion cell layer; INL, inner nuclear layer, ONL, outer nuclear layer. From webvision.med.utah.edu.

The layers from the outermost surface to the innermost surface of the retina is the retinal pigment epithelium (RPE) followed by the photoreceptor layer containing the inner and outer segments of the photoreceptors, the outer nuclear layer (ONL) containing the cell bodies of the photoreceptors, the outer plexiform layer (OPL) including the axons of the photoreceptors, horizontal and bipolar cell dendrites, the inner nuclear layer (INL) containing the nuclei of the horizontal, bipolar and amacrine cells, the inner plexiform layer (IPL) including the axons of bipolar and amacrine cells and dendrites of the retinal ganglion cells. The ganglion cell layer (GCL) contains the nuclei of retinal ganglion cells. Finally, the axons of the retinal ganglion cells form the optic nerve connecting the retina to the brain. The retinal glial cells (also called Müller cells) compose the retina but extends from the RPE to the retinal ganglion cells.

2.1.1.3 *The outer plexiform layer of the retina and the mechanism of phototransduction*

The light from the environment crosses all the innermost cell layers before reaching the outer segments of the photoreceptor layer where the light sensitive molecules such as molecules of the opsin family reside. When light reaches the photoreceptors, the latter transforms the light energy into nervous impulses, through a complex process named phototransduction (Figure 4).

In vertebrates, two major photoreceptors types are present in the retina, the cones and the rods, which are distinguished by their form. The cones are involved in the perception of color vision and are able to perceive finer details and more rapid changes in images through their fast response times to stimuli (Michaelides et al., 2006). There are different kind of cones which carry different opsins sensitive to different wavelengths. Moreover, these wavelengths are species specific. The second type of photoreceptors, the rods, contain the rhodopsin pigment, and are involved in the scotopic (night) vision through their high sensitivity to light. The human retina has about 100 million of rod cells concentrated at the outer edges of the retina and only 6 million of cone cells concentrated at the fovea and sparsed gradually in the remainder retina.

The mechanisms of phototransduction have been more intensely studied in the retinal rod cells as compared to the cone cells (Figure 4).

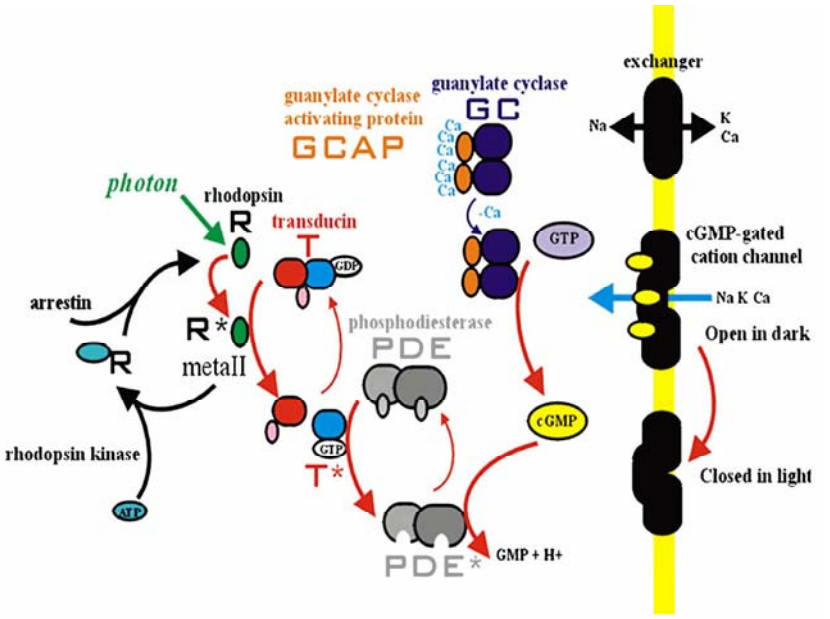

Figure 4. Schematic representation of the retinal phototransduction cascade typical for ciliary photoreceptors. R*, activated rhodopsin. From Michaelides et al., 2006.

The photopigment rhodopsin (Rh) is concentrated in the apical part of the cell, in the plasma membrane, which is folded into a stack of discs forming the outer segment. Rhodopsin is a seven transmembranes protein covalently linked to the 11-cis-retinal by a Lysin at position 296 of the protein (Lys296). The chromophore activation by a photon leads to the isomerisation to the all-trans-retinal accompanied by changes in the protein moiety. Photo-excited rhodopsin (R*) activates transducin (T), a guanine nucleotide binding protein (G protein), which in its turn activates a membrane bound cyclic guanosine monophosphate (cGMP) phosphodiesterase (PDE). In the dark, the intracellular concentration of cGMP is high. This second messenger binds to ion channels in the plasma membrane of the photoreceptor cell keeping them open allowing the influx of ions into the outer segment. Due to this circulating dark-current along the rod photoreceptor, the membrane potential of the photoreceptor cell is slightly depolarized. This depolarization allows the release of the neurotransmitter glutamate at the synaptic junctions with the second order neurones. Upon illumination, the cGMP hydrolysis by the PDE leads to the closure of the Na^+ and Ca^{2+} cationic channels inducing an hyperpolarization of the cell and the inhibition of neurotransmitter release at the synaptic junctions. The change in neurotransmitter release is registered by bipolar cells, which relay this information onto retinal ganglion cells. The retinal ganglion cells then convey the information to the brain.

2.1.1.4 The retinal pigment epithelium

The retinal pigment epithelium (RPE) is a highly specialized monolayered epithelium containing melanosomes, the cells producing and storing the melanin pigment. The RPE, located between the choroid and the photoreceptors of the neural retina, is involved in several functions: it participates in the outer blood-retinal barrier, it maintains the adhesion and the water/ions flow between the neural retina and the choroid, it absorbs stray light preventing the degradation of the visual image, it protects against free radicals, it controls retinoid metabolism and phagocytoses the outer segment of the photoreceptors ensuring their renewal (reviewed by Martinez-Morales et al., 2004; Bok, 1993; Boulton and Dayhaw-Barker, 2001). Furthermore, it has been shown that the RPE is able to transdifferentiate and regenerate a new neural retina in many vertebrate species (Del Rio-Tsonis and Tsonis, 2003).

2.1.1.5 The inner nuclear and retinal ganglion cell layers

The inner nuclear layer contains three cell types including the amacrine, horizontal and bipolar cells. They are principally involved in the treatment of the neural impulses generated by the photoreceptors following their activation by light. The horizontal cells are contacted by the photoreceptor synapses; they are principally involved in the development of the contrasts. The bipolar cells transmit the information received from the afferences of the photoreceptors and horizontal cells to the ganglion cells in the form of graduated potentials. Then, the axons of the retinal ganglion cells transmit the nervous impulses as action potentials to the optic area of the brain. The functions of the amacrine cells are not well underderstood yet.

2.1.1.6 The ciliary marginal zone (CMZ) and circumferential larval zone (CLZ)

In fish and amphibians, the retina grows throughout all the life by adding rings of new neuronal cells at the periphery from stem cells located in a proliferative region, namely the ciliary marginal zone (CMZ) (Figure 5).

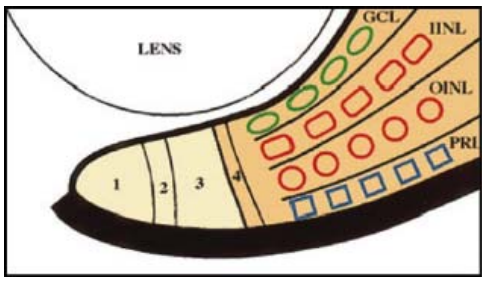

Figure 5. Schematic representation of the ciliary marginal zone (CMZ) of the retina. This zone is divided in four regions specified by their cellular type: 1, retinal stem cells; 2,3 proliferative retinoblasts; 4, post-mitotic cells. GCL, retinal ganglion cell layer; IINL, inner part of the inner nuclear layer; OINL, outer part of the outer nuclear layer; PRL, photoreceptor layer. From Perron et al., 1998.

The CMZ which has the capacity to generate all retinal cell types except rods, is spatially ordered with respect to cellular development and differentiation. The less determined stem cells are located in the peripherical part of the retina. The proliferative retinoblasts are in the middle and the cells that have stoped dividing are located at the central edge (Figure 5). Recently, it has been shown that the CMZ also exists in birds and marsupial but not in mice

(Kubota et al., 2002). In Teleost, in contrast to the other retinal cell types generated by the ciliary marginal zone (CMZ), the rod photoreceptors are generated from rod precursors located in the outer nuclear layer and in a zone previously described in goldfish (*Carassius auratus*), namely the circumferential larval zone (CLZ) (Otteson et al., 2001; Johns, 1982; Raymond and Rivlin, 1987). This region which is adjacent to the CMZ of the retina has not been described so far in retina of other vertebrates species.

2.2 The pineal gland

2.2.1 Anatomy and main functions of the pineal gland

The anatomy of the pineal gland (also called epiphysis) has changed dramatically during the course of evolution (Figure 6). In ectothermic vertebrates, the pineal gland is located just below the skull and is connected to the diencephalon by a stalk. The epiphysis of Teleost and frogs is a vesicle, filled with cerebrospinal fluid, and its lumen is usually opened to the third ventricle. In lizards and birds, the pineal gland is folliculated whereas it is glandular in mammals. In ectothermic vertebrates, the pineal gland is composed of three main cell types: photoreceptors, neurones and glial cells. The organization of the epiphysis displays similarities with the vertebrate retina but with a lesser degree of complexity. For instance, the pineal gland contains only cone-like photoreceptor cells directly connected to the pineal ganglion cells. The rod, amacrine, bipolar and horizontal cells present in the retina are absent. The axons of the pineal ganglion cells converge dorsally to the pineal stalk and form the pineal nerve, which enters the brain. In Sauropsids, the photoreceptors are rudimentary : they have no outer segments and do not contact neurons anymore. In the pineal organs of snakes and mammals, the regression of the photoreceptor characteristics are even more pronounced than in birds: the mammalian pinealocyte displays only a cell body and one or several pedicles but no inner and outer segments (For review see Falcon, 1999).

The mechanisms of phototransduction occuring in the pineal photoreceptor seem quite similar to that of the retinal photoreceptors (Figure 7); the pineal photoreceptor is depolarized in the dark and hyperpolarizes upon light exposure. Hyperpolarisation of the photoreceptor results in the inhibition of release of an excitatory neurotransmitter at the synaptic junction with the second order neuron.

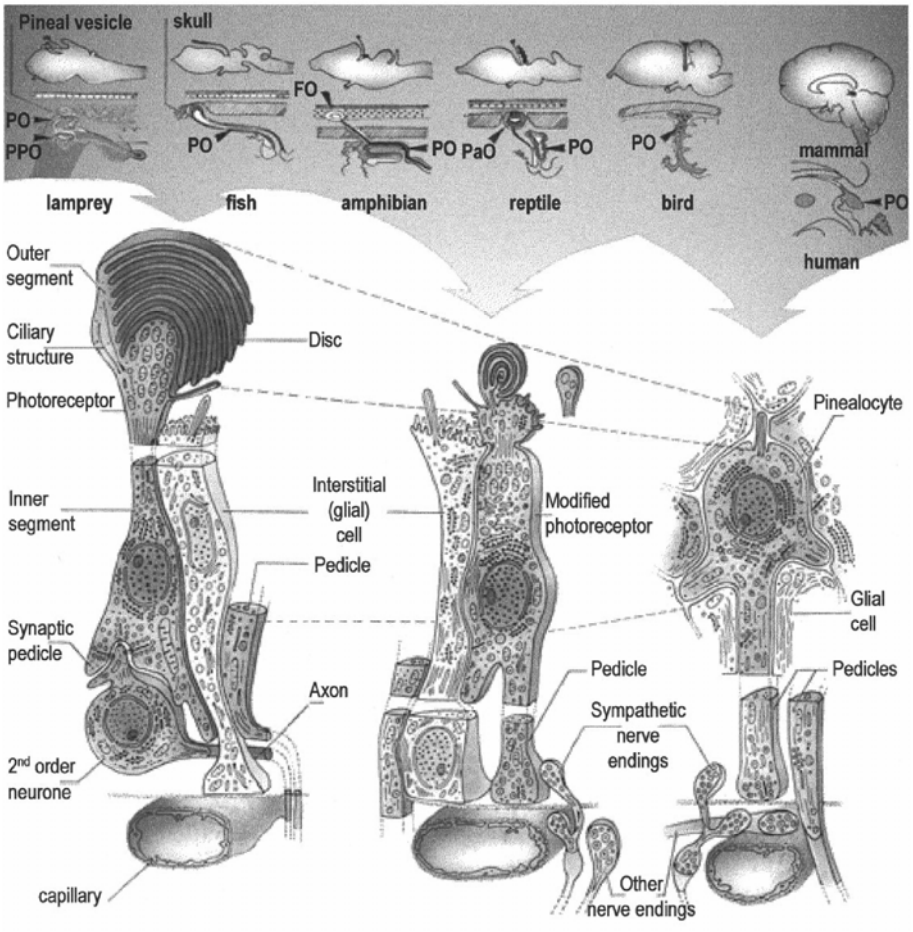

Figure 6. Evolution of the different pineal glands and pinealocytes found among vertebrates. FO, frontal organ; PaO, parietal organ; PO, pineal organ; PPO, parapineal organ. From Colin et al., 1989.

Compared to the retinal photoreceptors, the pineal photoreceptor responds to light with a greater latency and recovery time (Figure 7) (For review see Falcon, 1999). This indicates that the pineal gland is not able to discriminate rapid light changes as the retina does and thus, may act only as a mediator of gradual light intensity changes. Hence, in ectothermic vertebrates, the pineal gland functions as a dosimeter of ambient illumination and detector of day length. As a consequence, the pineal allows time measurement, generally related to the synchronization of internal circadian clocks. This function allows the living organisms to predict and to anticipate the environmental changes in order to optimize their physiological, biochemical and behavioural functions.

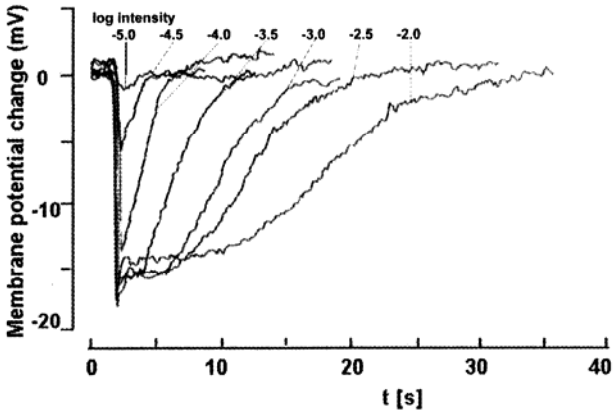

Figure 7. Electrophysiological response of the pineal photoreceptor cell exposed to different light pulse times. From Falcon, 1999, data from Dr. Hilmart Meissl (Max Plank Institut; Frankfurt (G)).

In vertebrates, this function is primarily driven by a circadian system containing three main components: (i) an input or photoreceptor with photoreceptive molecules which synchronizes (ii) a circadian clock formed by several activator and repressor transcription factors and (iii) an output which synchronizes the different functions in the organism.
The retina, the pineal gland and the suprachiasmatic nuclei are key components of this system. The anatomic organization of this system has changed dramatically during the course of evolution. In mammals, the photoreceptors of the retina detect light allowing to synchronize the circadian clock located in the suprachiasmatic nuclei of the hypothalamus. Then, the rhythmic signals from the CNS synchronize a number of other rhythms. Among them is the rhythmic production of melatonin by the pineal gland. In ectothermic vertebrates, the pineal photoreceptor contains all three elements of this system. Hence, pinealectomy in fish and lizards leads generally to a loose of circadian rhythmicity. In addition, pineal organs of non-mammals are able to maintain a rhythmic activity *in vitro* under light/dark or under constant photoperiodic conditions including constant light (LL) or constant dark (DD) (For review see Falcon, 1999).

2.2.2 The nature of the molecular circadian oscillator

The circadian clock (from the latin *circa diem*: about a day) or circadian oscillator is composed of several transcription factors acting in a negative feedback loop. In vertebrates, five genes have been identified as the core component of the clock machinery. The *Periods*

(*Per*), *Cryptochromes* (*Cry*) and *Rev-erba* genes encode the negative components whereas the Clock and Bmal genes encode the positive ones. The functional mechanism of the clock can be divided in three successives steps. In a first step, as presented in Figure 8, the CLOCK/BMAL heterodimer binds the E-box enhancer located in the Per(s), Cry(s) and Rev-erbα genes and activates their transcription. Then, the PER and CRY proteins bind together to form a heteropolymeric complex and, when it reaches a critical concentration in the cell, interacts with the CLOCK/BMAL heterodimer titrating these transcription factors. In parallel, the REV-ERBα transcription factor inhibits the expression of both the Clock and Bmal genes. Finally, as a consequence of this inhibition, the mRNAs and proteins levels of the Per(s), Cry(s) and Rev-erbα genes decrease in the cell and once their levels are insufficient for repression, a novel cycle can start with the transcription of the Clock and Bmal genes (for review see Gachon et al., 2004; Albrecht and Eichele, 2003).

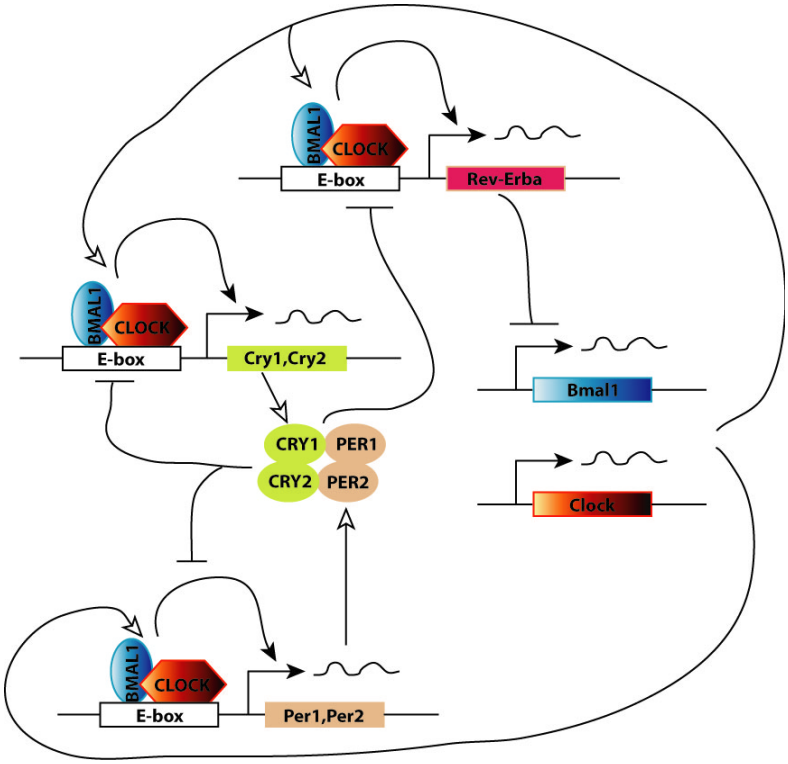

Figure 8. Simplified model of the molecular clock found in vertebrates. Adapted from Gachon et al., 2004.

2.2.3 The melatonin: a major output of the circadian clock

In 1917, McCord and Allen observed that when bovine pineal extracts were fed to amphibians, their skins lightened in color. The extracts were subsequently shown to produce

this effect by causing the melanin granules in the melanophores to agregate around the cell nucleus (Lerner and Case, 1959). Using lightening of frog skin as a bioassay system, Lerner and co-workers (1960) identified the hormone responsible for this effect, namely N-acetyl-5-methoxytryptamine, also called melatonin. Several years later, it was demonstrated that melatonin is produced by the pineal gland from serotonin (Figure 9) (Weissbach et al., 1960, 1961; Quay, 1963; Fiske, 1964; Axelrod, 1974). The levels of both compounds vary on a daily basis and in opposite directions; serotonin content is high during day and low at night whereas melatonin levels are high at night and low during day (Quay, 1963). Klein and Weller (1970, 1972) found that the melatonin rhythm results from the rhythmic activity of the arylalkylamine N-acetytransferase (AANAT). The AANAT catalyses the conversion of serotonin into N-acetylserotonin; its activity increases about 100-fold at night in the rat pineal. Hence, this enzyme is considered as the rate limiting enzyme for melatonin biosynthesis.

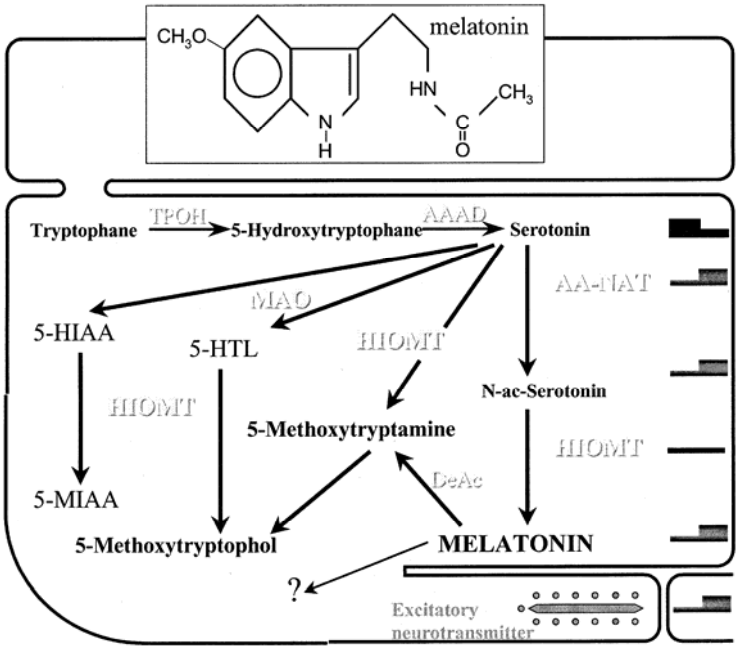

Figure 9. Indole metabolism pathways in the pineal cell. The biosynthetic pathway of melatonin starts with the amino acid tryptophan. The tryptophan is hydroxyled on position 5 by the Tryptophan hydroxylase (TPOH). Then, the carboxyl group of the hydroxytryptophan neo-formed is removed from the amino terminal by the activity of the L-aromatic amino acid decarboxylase (AAAD) leading to the formation of serotonin. The next step is the acetylation of the N-terminal part of the serotonin by the activity of the Arylalkylamine N-acetyltransferase (AANAT) leading to the formation of N-acetyl serotonin. Finally, the Hydoxyindole-O-methyltransferase (HIOMT) adds a methyl group on position 5 of the N-acetylserotonin to form melatonin. DeAc, deacetylase; 5-HIAA, 5-hydoxyindole acetic acid; 5-HTL, 5-hydroxytryptophole; MAO, monoamine oxidase; 5-MIAA; 5-methoxyindole acetic acid. From Falcon, 1999.

In vertebrates, pineal melatonin is released into the blood and cerebrospinal fluid as it biosynthetized, and thus appears as a signal of darkness (Cassone et al., 1993; Falcon, 1999). In addition, the rhythmic pattern in melatonin biosynthesis changes according to season. The rhythm allows synchronization of several physiological, biochemical and behavioural rhythms to the prevailing daily and annual photoperiod. These include locomotor activity, hibernation, release of pituitary homones, metamorphosis in amphibians and the reproduction (Reiter et al., 1987; Pevet, 1988; Zachmann et al., 1992; Mayer et al., 1997; Vanecek, 1998; Lincoln et al., 2003; Wright, 2002). Moreover, it has been shown that melatonin is able to reset the central circadian clock and to play a role of relay to the periphical oscillators (Gauer et al., 1993; McArthur et al., 1991; Weaver et al., 1993).

2.2.4 The two major sites of melatonin biosynthesis, the pineal gland and the retina

The two major sites for melatonin biosynthesis in vertebrates are the pineal gland and the retina, although other sites have also been described such as the lacrimal gland of the eye, the ciliary body, the gastrointestinal tract and the lymphocytes (Falcon, 1999; Wikström, 1996 in Isorna, 2004). In vertebrates, melatonin produced by the retina acts as an auto and paracrine neurohormone in the regulation of the adaptative process of vision (Wiechmann and Wirsig-Wiechmann, 1993), whereas the melatonin produced by the pineal gland is released into the blood and acts principaly as an endocrine neurohormone (Falcon, 1999). It plays a role in the synchronization of the periodical daily and seasonal functions (Falcon, 1999). Hence, pinealectomy generally results in a decrease or a loss of the melatonin levels into the blood (Underwood and Siopes, 1984; Lewy et al., 1980). In contrast, in amphibians and in some avian species the melatonin plasmatic levels originate mainly from the retina (Isorna, 2004; Iuvone et al., 2005).

The cellular localization of melatonin biosynthesis in both the pineal gland and the retina is primarily in the photoreceptor cells or pinealocytes (Cahill and Besharse, 1993; Guerlotte et al., 1988; Voisin et al., 1988; Kuwano et al., 1983; Sato et al., 1991; Greve et al., 1993; Wiechmann, 1996; Wiechmann and Craft, 1993; Besseau et al., 2006; Zilberman-Peled et al., 2006; for review see Falcon, 1999).

3. Development of the photoreceptives organes in vertebrates

3.1 Development of the eye

Eye development in vertebrate is an excellent model system to study several processes including tissue induction and highly specialized structure formation. The formation of this complex system starts during gastrulation. At the end of gastrulation, the endoderm and mesoderm interact with the prospective head surface ectoderm to give it a lens forming bias. Latter, during neurulation, the optic vesicles (OV) evaginating from the diencephalon, contact the overlying ectoderm and induce the specification of these small regions to become thicker giving rise to the lens placodes (Figure 10A, F). In most vertebrates, ablation of the OV or arrest of OV development prevents the formation of lens structures indicating that the lens specification is dependent on the contact between the OV with the surface head ectoderm. The lens palcodes then invaginate to form the lens vesicles and induce the invagination of the OV to become the optic cups (OC) (Figure 10B, C, G). At this stage, the formation of the optic cup is completely dependent on the development of a lens placode since a mutant without a lens placode fails to develop an OC (Ashery-Padan et al., 2000). Instead, several neuroretina folds separated by patches of retinal pigment epithelium (RPE) developed from the OV. Thus, the early lens structures are providing the molecular and mechanical cues required for the formation of the OC from the OV. When an OC is formed, it differentiates into two main layers. The cells of the outer layer produce melanin pigments to form the RPE, the cells of the inner layer differentiate rapidly in generating the different cells types including photoreceptors, ganglion cells, glia, interneurons forming the neural retina (Figure 10D, E, H). The axons of the retinal ganglion cells meet at the base of the eye to form the optic nerve innervating the brain (Figure 10D, E).

3.1.1 Genetic control of eye development

The control of eye development in eumetazoa is triggered by a complex genetic cascade estimated to be composed of about 3,000 genes. At the top of this cascade are located several genes encoding signaling molecules and transcription factors acting in a complex network (Gehring and Ikeo, 1999).

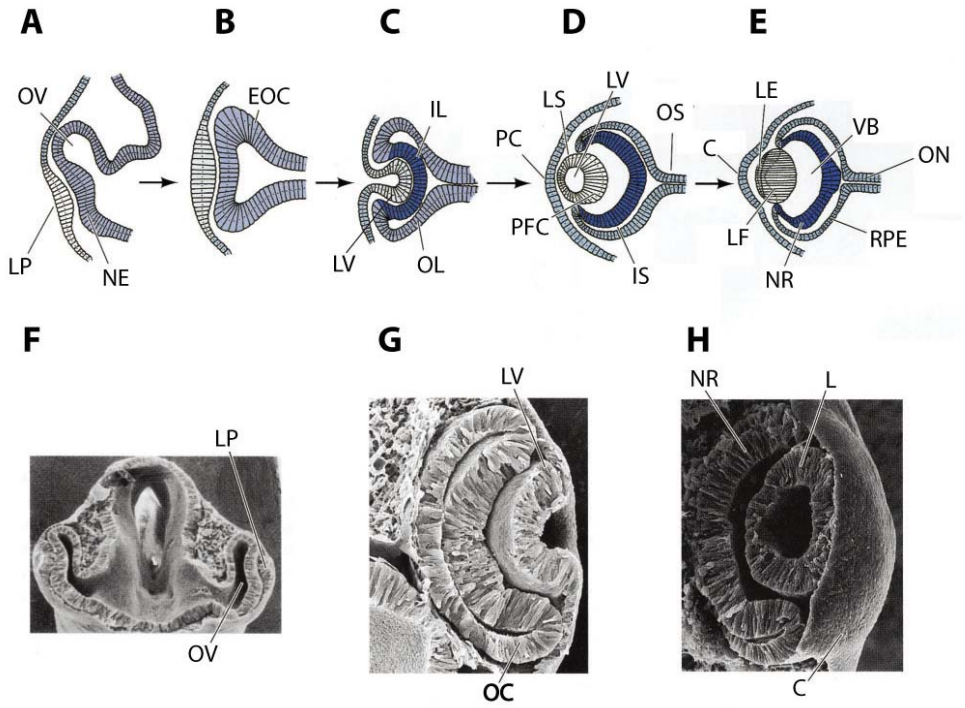

Figure 10. Development of the eye in vertebrates. (A-E) Schematic representation of the different steps leading to eye development from an optic vesicle (A) throughout an optic cup (C,D) to a mature eye (E). (F-H) Photographs showing the development of the eye in a chick embryo at (F) optic vesicle stage, (G) optic cup stage and (H) mature eye. C, cornea; EOC, early optic cup; IL, prospective retina; IS, intraretinal space; L, lens; LE, lens epithelium; LF, lens fibers; LP, lens placode; LS, lens capsule; LV, lens vesicle; NE, neural ectoderm; NR, neural retina; OC, optic cup; OL, prospective pigmented epithelium; ON, optic nerve; OS, optic stalk; OV, optic vesicle; PC, prospective cornea; PFC, primary fiber cells; RPE, retinal pigmented epithelium; VB, vitreous body. From Gilbert, 2003.

Generally, these genes are recruited several times during eye development playing a role at different stages such as the formation of the optic vesicles, invagination of the optic cups, retinogenesis. The two last decades, it has been shown that the proteins encoded by these genes are, with *Pax6* on the top of the hierarchy, structurally and functionally highly conserved and are found in almost all metazoans studied so far. These discoveries led to the hypothesis that the eyes may have a monophyletic origin (for review see Gehring and Ikeo, 1999; Gehring, 2004). A traditional example of such conserved genes involved in eye development are the *Paired box 6* (*Pax6*), *Sine oculis homeobox homolog 3* (*Six3*), *Eye absent* (*Eya*), *Sonic hedgehog* (*Shh*) and *Bone morphogenetic protein* (*Bmp2/4*) genes having at least one homologue in the fruitfly genome which are the *eyeless* (*ey*)/*twin of eyeless* (*toy*), *sine oculis* (*so*)/*optix* (*optix*), *eye absent* (*eya*), *hedgehog* (*hh*) and *decapentaplegic* (*dpp*) genes, respectively

(Wawersik and Maas, 2000). In the following sections, we will focus on the *Pax6* gene whose functions have been studied in details in mouse and fruitfly eyes development.

3.1.2 General informations on the Pax genes and their highly conserved domains

The *Pax* genes encode transcription factors characterized by the presence of a highly conserved amino acid sequence allowing the protein to bind DNA, namely the paired domain (PD) (Figure 11).

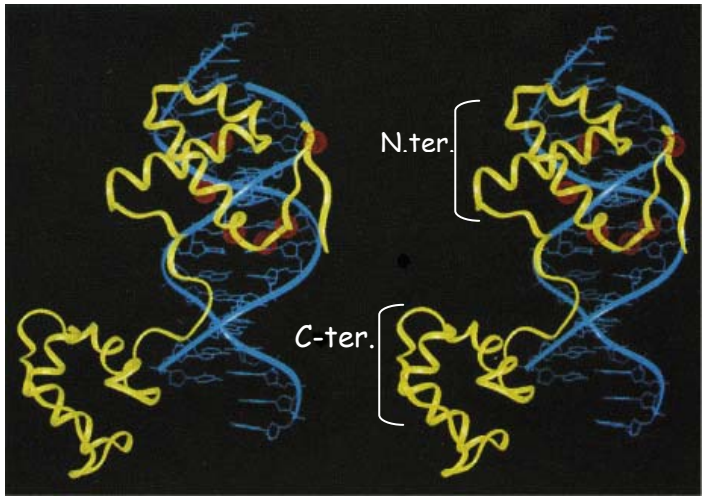

Figure 11. Schematic representation of the paired domain of PAX6. Interaction of the N-terminal subdomain of the paired domain (yellow) with the double stranded DNA (blue). The red dots indicates the sites of loss-of-function mutations in the Pax6 gene giving rise to a non functional protein. From Xu et al., 1995.

The PD was initially discovered in *Drosophila* for the segmentation gene *Paired* (Bopp et al., 1986). The PD is a 125-128 amino acids bipartite domain containing an N- and C-terminal subdomain each containing a helix-turn-helix motif (Czerny et al., 1993; Xu et al., 1995). This domain was then found in 8 other developmental genes in fly (Callaerts et al., 1997; Fu and Noll, 1997). In human and rodents, nine members (*Pax1-Pax9*) have been described and classified in four groups according to their primary structure (Figure 12) (For review see Strachan and Read, 1994). The first group contains the *Pax4* and *Pax6* genes. They are principaly characterized by the presence of a PD and an other highly conserved DNA binding domain, the paired-like homeodomain (HD) (Frigerio et al., 1986). The second group

including *Pax2*, *Pax5* and *Pax8* is characterized by the presence of a PD, a truncated HD and a third conserved domain, the octapeptide (O). It has been shown that the octapeptide of PAX5 directly interacts with a member of the Groucho corepressor family, in order to exert its transcriptional repression activity (Eberhard et al., 2000; Lechner and Dressler, 1996). The third group including *Pax3* and *Pax7* is principaly characterized by the presence of a PD, a HD and an octapeptide. Finally, the fourth group including *Pax1* and *Pax9* is principaly characterized by the presence of a PD, an octapeptide and abscence of HD.

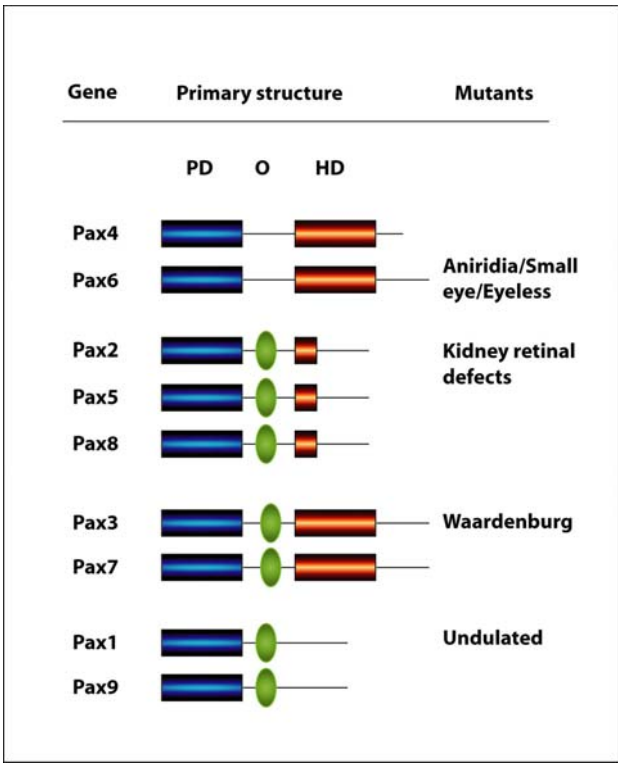

Figure 12. Classification of the different Pax genes found in vertebrates according to their primary structure. PD, paired domain; O, octapeptide; HD, homeodomain.

3.1.3 General informations on Pax6 and eyeless

The *Pax6* gene encodes a highly conserved transcription factor containing a paired and paired-like homeodomain separated by a flexible, acidic linker region (Krauss et al., 1991; Wilson et al., 1995). The C-terminal end of the protein acts as the transctivation domain (Glaser et al., 1994; Carriere et al., 1995; Czerny and Busslinger, 1995; Tang et al., 1998). The *Pax6* gene was initially discovered in human (Ton et al., 1991), mouse (Walther and Gruss,

1991) and zebrafish (Krauss et al., 1991). Three years after, the cloning of one of the fruitfly *Pax6* homologue, namely *eye*less (*ey*), was reported (Quiring et al., 1994). Subsequently, *Pax6* homologues were described in other vertebrates such as lamprey (*Lampetra japonica*), medaka (*Oryzias latipes*), pufferfish (*Fugu rubripes*), frog (*Xenopus laevis*), newt (*Cynops pyrrogaster*), chicken (*Gallus gallus*) and rat (*Rattus norvegicus*) and invertebrates such as ribbonworm (*Lineus sanguineus*), planarian (*Dugesia tigrina*), squid (*Loligo opalescens*), sea urchin (*Paracentrotus lividus*), nematode (*Caenorhabditis elegans*), ascidian (*Phallusia mammilata*) and amphioxus (*Branchiostoma floridae*) (reviewed in Callaerts et al., 1997; Callaerts et al., 1999; Czerny and Busslinger, 1995; Glardon et al., 1998; Glardon et al., 1997; Loosli et al., 1996; Tomarev et al., 1997; Murakami et al., 2001; Mizuno et al., 1999). In vertebrate embryos, *Pax6* is expressed in the eye, nose, CNS and pancreas where it plays a crucial role for the development of these organs (Krauss et al., 1991; Turque et al., 1994; Walther and Gruss, 1991). The expression of *Pax6* in the eye and the CNS is also found in invertebrates (Quiring et al., 1994; Tomarev et al., 1997; Gonzalez-Estevez et al., 2003; Callaerts et al., 1999; Loosli et al., 1996) suggesting a surprising conservation of the gene function among the different animal phyla. The regulation of *Pax6* in space and time in vertebrate is controlled by several enhancers located in the promotor and introns of the gene. The critical role of PAX6 played in development is highlighted by the studies of its mutants. While the heterozygous loss-of-function Pax6 mutants lead to known phenotypes as Aniridia, Peter's anomaly and congenital cataracts in human and to a microphtalmia phenotype in rodents called Small eye (Sey) (Ton et al., 1991; Hanson et al., 1995; Hill et al., 1991; Matsuo, 1993), the homozygous mutation of the gene in mammals leads to an absence of eye structure, nasal cavities and severe brain abnormalities causing postnatal lethality (Hogan et al., 1986; Glaser et al., 1994) (Figure 13). In testing this hypothesis with a *Pax6* gain-of-function approach, Halder and co-workers (1995) succeeded to induce ectopic eyes on legs, antennae and wings of flies by targeted expression of *ey* or *Sey* in the larval imaginal discs with the UAS/Gal4 system (Brand and Perrimon, 1993). Reciprocally, partial vertebrate eyes structures can be induced by the ectopic expression of *ey* and *toy* in *Xenopus* (Onuma et al., 2002).

3.1.4 Pax6 and eye development

Until today, most studies investigating *Pax6* function during eye and brain development were carried out in rodents and fruitflies.

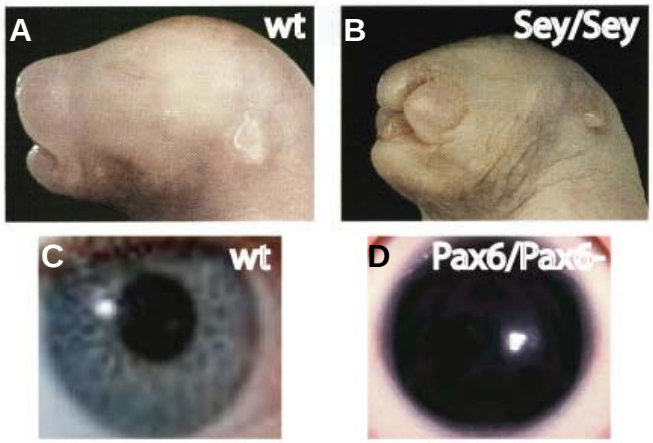

Figure 13. Photographs showing the dramatic effects caused by Pax6 mutation on vertebrate eye development. (A) Newborn wild-type rat presents two closed eyes and a nose. (B) Newborn homozygous Pax6 rat mutant presents an abscence of eyes and nose. (C) Wild-type human eye displays the presence of an iris. (D) Heterozygous Pax6 mutant human eye displays an abscence of iris namely aniridia.

These two models were privileged because they present major advantages in comparison with other vertebrate and invertebrate models as the availability of mutants and genetic tools such as the Cre/loxP and UAS/Gal4 systems, respectively.

In the following section, we will emphasize the different functions of PAX6 and others interacting factors during the successive stages of vertebrate eye development especially in the rodent model system (for review see Ashery-Padan and Gruss, 2001; Lang, 2004; Pichaud and Desplan, 2002) .

3.1.4.1 Function of PAX6 in lens formation in rodents and Xenopus

Several studies have suggested a crucial role of PAX6 in the lens induction process. In the first of these, tissue recombination experiments between optic vesicles (OV) and surface ectoderm (SE) from wild-type and *Pax6-/Pax6-* rat embryos suggested that *Pax6* is not essential for the inductive activity of the OV, rather, it has a cell autonomous function in the SE (Fujiwara et al., 1994). In two other experiments, it has been shown that *Pax6-/Pax6-* cells in chimeric mice embryos are excluded from the SE and did not contribute to the lens placode or subsequently to the differentiating lens (Quinn et al., 1996; Collinson et al., 2000). In addition, the lens specification marker *Sox2* fails to be expressed in *Pax6-/Pax6-* embryos

(Furuta and Hogan, 1998; Wawersik et al., 1999). Finally, Ashery-Padan and colleagues in 2000 succeeded to dissect the molecular function of *Pax6* in lens development after deleting PAX6 in the SE using the Cre/loxP system. The strong advantage of this technique allows to knock out the target gene somatically at the desired place and time. They showed that initially, PAX6 activity is essential for the competence of the SE to respond to the inductive signal produced by the OV, including a secreted factor of the BMP family, in activating *Sox2* transcription in the ectoderm (Figure 14). Then, during the specification process, PAX6 activity is dispensable to maintain the expression of *Sox2*.

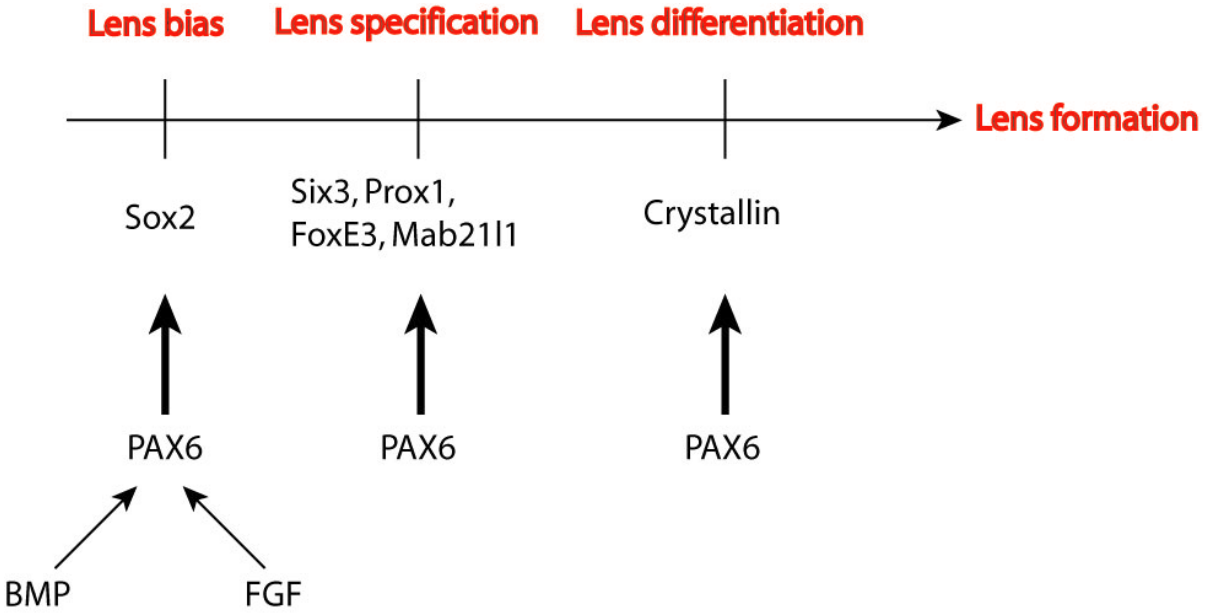

Figure 14. Summary of the different functions of Pax6 during lens development. Adapted from Ashery-Padan and Gruss, 2001 and Lang, 2004.

Hence, a Pax6 Cre/lox mutant mice embryo, of which PAX6 was removed from the SE during the lens specification stage, showed a normal *Sox2* expression in the SE. However, in the absence of PAX6 during differentiation, SOX2 is not sufficient to activate the crystallin genes. PAX6 binds cooperatively with SOX2 on the delta-crystallin enhancer to activate crystallin expression during initiation of lens differentiation in chicken (Kamachi et al., 2001). In addition, PAX6 activates the expression of other homeobox genes involved in lens differentiation such as *Six3*, *Prox1*, *Mab21l1* and *FoxE3* during the specification stage (for review see Ashery-Padan and Gruss, 2001; Lang, 2004; Ogino and Yasuda, 2000).

In *Xenopus*, gain-of-function experiments have also revealed a central role of PAX6 in lens development; overexpression of PAX6 induced ectopic eyes formation. However, it was

also possible to obtain ectopic lenses at a high frequency in the absence of any retinal tissue (Altmann et al., 1997; Chow et al., 1999). Taken together, these results indicate that PAX6 is needed and sufficient for lens development in *Xenopus*.

3.1.4.2 Function of PAX6 in early retina development of mice

Although *Pax6* is expressed in the anterior neural plate in the cells that will give rise to the optic vesicle (OV), its function seems to be dispensable for the formation of the OV (Lee et al., 2005; Grindley et al., 1995). Accordingly, in the homozygous Pax6 mutant mouse embryo the OV form and the eye morphogenesis is arrested at this stage. However, it is important to note that the OV formed in homozygous *Pax6-/-* mouse embryo are misshapened (Grindley et al., 1995). This is in agreement with the study of *Pax6-/Pax6-* cells in chimeric mice embryos carried out by Collinson et al. (2000) who showed that PAX6 plays a role in proximo-distal patterning of the optic vesicles. Recently, it has been suggested that HES1, a mammalian basic helix-loop-helix (bHLH) transcription factor homologous of the *Drosophila Hairy* and *Enhancer of split* genes, participates with PAX6 in OV formation (Lee et al., 2005). While the homozygous Hes1 or Pax6 mutant mouse embryos develop an OV, the double mutant for both genes fails to do it. One plausible explanation is that both genes act redondantly in OV development. Accordingly, when both gene products are absent, the OV morphogenesis fails to be initiated. A second function of PAX6 for OV development is that this gene is required for the maintenance of the contact between the OV and the lens placode. Hence, if *Pax6* expression is deleted in the OV cells and not in the LP cells, the contact between both is lost (Collinson et al., 2000) suggesting a role for PAX6 in controlling the expression of extracellular adhesion molecules. Cadherins could be good candidates because they were described as being controlled by *Pax6* in other developmental processes (Andrews and Mastick, 2003; Estivill-Torrus et al., 2001; Liu et al., 2001; Stoykova et al., 1997).

During the optic cup (OC) stage, *Pax6* is required for cell proliferation and differentiation, since both processes are affected in *Pax6-/-* mice embryos. In addition, it has been shown that PAX6 activity is required in the late optic vesicle and early optic cup to establish the dorsoventral boundary of the developing eye in mice and chicken (Figure 15) (Leconte et al., 2004; Schwarz et al., 2000; Canto-Soler and Adler, 2006). PAX6 activity in this territory restricts *Vax1*, *Vax2* and *Pax2* expression to the ventral part of the early optic cup (Leconte et al., 2004; Schwarz et al., 2000).

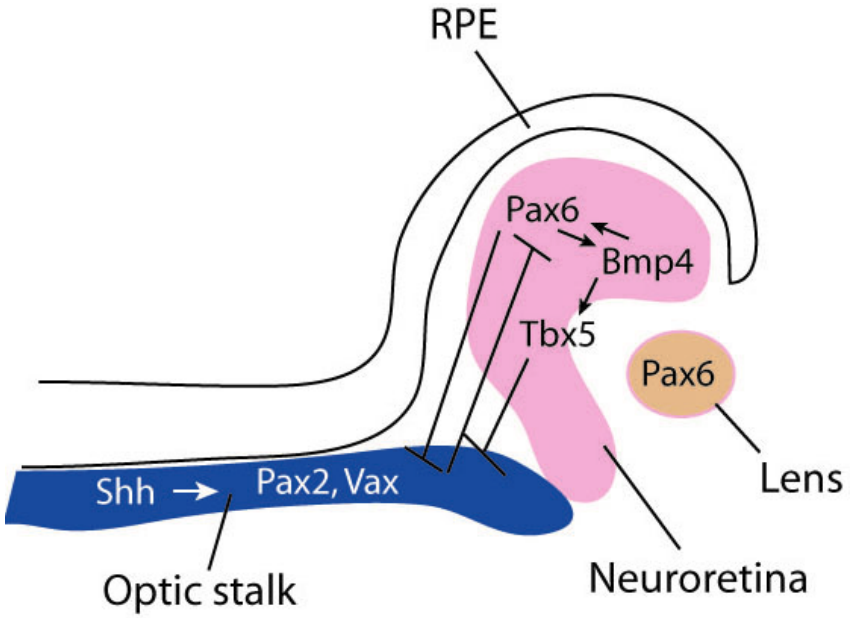

Figure 15. Dorsoventral patterning of the early optic cup during vertebrate development. BMP4 and PAX6 in the dorsal side of the eye cup induces *Tbx5* expression. TBX5 and PAX6 repress in the dorsal retina the expression of the *Pax2* and *Vax* genes, two transcription factors whose expression is induced in the optic stalk and ventral retina by sonic hedgehog (SHH). Similarly, PAX2 and VAX repress the expression of *Pax6* and *Tbx5* in the ventral retina. This inhibitory effect establishes the mutually exclusive patterns of the dorsal and ventral markers.

This is in agreement with the observation that murine Pax6-/- mutant embryos showed their *Vax1* and *Vax2* expression domains expanded to the entire OV. This is also true for *Pax2* expression which expands to the dorsal OC in the homozygous Pax6 mutant (Schwarz et al., 2000). Following optic cup formation, *Pax6* expression is down-regulated in the optic stalk and the retinal pigment epithelium, and maintained in the neural retina (NR). Expression in the NR is maintained in the retinal progenitor cells and down-regulated in most cells upon differentiation. In the mature mice retina, *Pax6* expression is confined to bipolar and amacrine cells.

3.1.4.3 Function of PAX6 in retinogenesis and RPE formation

During the differentiation of the retina, all six different cell types including retinal ganglion, amacrine, bipolar, horizontal, cone photoreceptor and müller glial cells are generated from the retinal progenitor cells (RPC) residing in the inner nuclear layer of the mouse retina or the ciliary marginal zone of ectothermic vertebrates retinae. Several homeodomain transcription factors such as *Pax6*, *Six3*, *Rx*, *Chx10* are expressed in the RPC

underlining their potential function in the proliferation and differentiation processes of retinal cells (Perron et al., 1998). Gruss and colleagues (2001) have shown by conditional knock out that mouse PAX6 activity is required for their normal proliferation and in order to maintain the retinal progenitor cells multipotents. In its abscence, there is reduced proliferation of the RPC, which did not acquire early and late neuronal cell fates but differentiated only into amacrine interneurons (Marquardt et al., 2001). Recently, Collinson and colleagues (2003) have shown in Pax6-/- chimeric mice embryos that PAX6 also contributes to the retinal ganglion cell layer formation. Indeed, mutant cells in the retinal ganglion cell layer appeared abnormal, either in forming tight clusters or having a vesicular appearence indicating perhaps that these cells were not correctly differentiated (Collinson et al., 2003).

The retinal pigment epithelium (RPE) domain is initially defined during OV formation by the *microphtalmia-associated bHLH transcription factor* (*Mitf*). *Mitf* starts to be expressed throughout the entire OV and subsequently, its expression is down-regulated in the distal part of the OV and maintained in the proximal part defining the presumptive RPE. Because Pax6-/- mutant embryos develop RPE, PAX6 activity seems to be dispensable for the formation of this domain. However, it was shown in Pax6-/-; Pax2-/- mice double mutant embryos that the RPE is transformed in neural retina indicating that PAX6 acts redondantly with PAX2 to direct the determination of RPE by directly controlling the *Mitf* epression (Baumer et al., 2003).

3.2 Development of the pineal gland

3.2.1 Genetic control of pineal gland development, an overview

In contrast to the retina, the pineal gland develops from an evagination of the roof of the diencephalon to form an epiphysial vesicle located just underneath the skin of the embryo. This organ differentiates early during embryonic development as for instance in zebrafish in which neurons of the epiphysis are among the first ones to differentiate and initiate axogenesis into the forebrain (Wilson and Easter, 1991). Although the genetic control of pineal gland development has been less studied compared to the eye, the central actors triggering this process appear to be quite different between both organs.

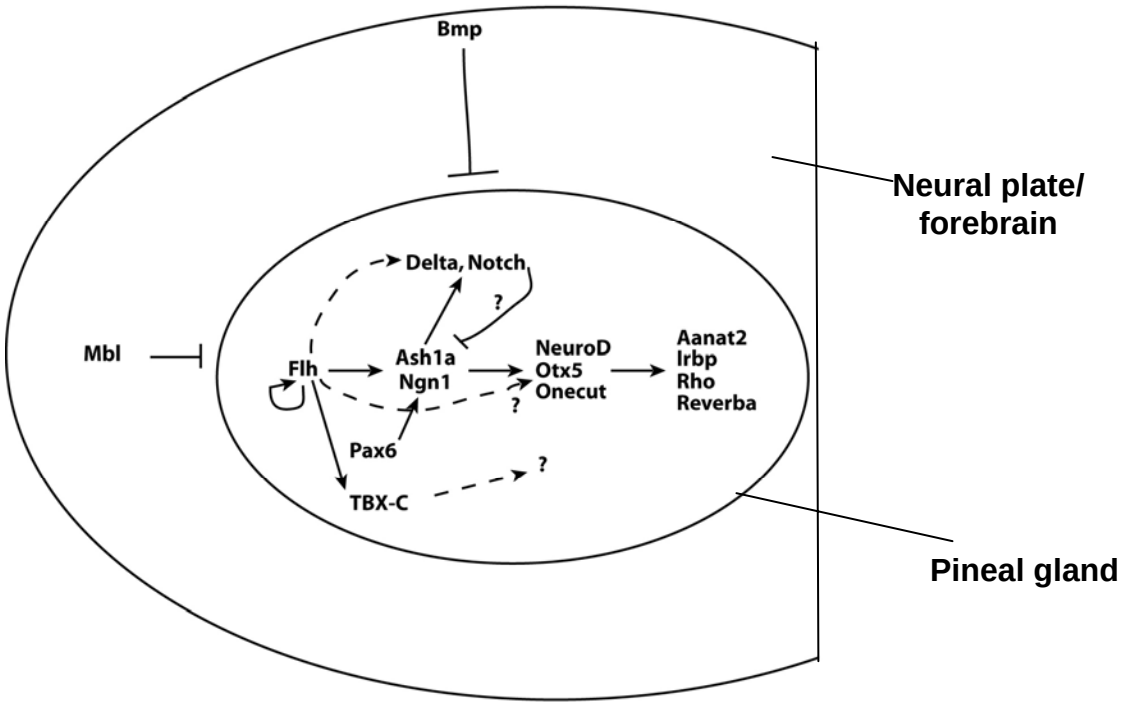

Figure 16. Schematic representation of the interactions of the different known genetic factors involved in zebrafish pineal gland development. Anterior is left.

Figure 16 displays a recent model for zebrafish pineal gland development where the homeobox transcription factor *Floating head* (*Flh*) regulates the epiphysial neurogenesis throughout the regulation of proneural bHLH transcription factors including *Ash1a* and *Ngn1* (Cau and Wilson, 2003). The products of these genes activate the expression of differentiation factors such as *Otx5*, *Onecut* and *NeuroD*; OTX5 regulates directly the expression of pineal opsins and several circadian clock genes such as *Reverba*, and clock controlled genes such as *Aanat2* and *Irbp* (Gamse et al., 2002; Cau and Wilson, 2003). The spatial restriction of *Flh* expression on the anterio-posterior (AP) and DV axis of the pineal gland anlage is controlled by the bone morphogenetic protein (Bmp) and wingless-type (Wnt) signaling pathways. For instance, in the *Master blind* (*Mbl*) mutant, the activity of WNT is increased in the neural plate leading to an expansion of *Flh* expression into regions of the anterior forebrain (Masai et al., 1997; Heisenberg et al., 2001). In contrast, when the BMP activity was reduced in the Swirl (swr) mutant, the Flh expression domain expanded into more ectodermal cells (Barth et al., 1999).

3.2.2 Pax6 function in pineal gland development

The very few data available suggest that *Pax6* plays a critical role also in pineal gland development. In mice and zebrafish, the pineal gland expresses its mRNA and protein during pineal gland development (Estivill-Torrus et al., 2001; Wullimann and Rink, 2001; Masai et al., 1997). In addition, the analysis of Pax6 mutants in human and mice has revealed that this gene is essential for the formation of the epiphysis and in its absence the pineal gland is absent (Mitchell et al., 2003; Estivill-Torrus et al., 2001). However, despite of these strong evidences for a role of *Pax6* in pineal gland development, its role in the genetic cascade is still not understood. It has been proposed that PAX6 may act directly on *Ngn1* expression to generate second order neurons in zebrafish (Blader et al., 2004; Masai et al., 1997).

4. Brain development

The transcription factor PAX6 was shown to be involved not only in the development of the photoreceptive organs in vertebrates and invertebrates but also in the formation of the central nervous system as revealed by the study of the Sey and Ey mutants (Stoykova et al., 1996; Callaerts et al., 2001).

In this section, the basis of brain development and the role of *Pax6* in this process will be summarized.

4.1 General informations on brain formation and patterning

The brain of vertebrates starts to develop during neurulation of the neural plate, which is converted into a neural tube. The neural tube is then subdivided into three vesicle promordia corresponding to the forebrain, midbrain and hindbrain. Later in development, these regions are subdivided by transverse constrictions into neural segments called neuromeres. At this stage, the antero-posterior (AP) patterning of the brain is established. Neuromeres are present in the forebrain and hindbrain where they are called prosomeres and rhombomeres, respectively. Brain patterning occurs later in development in specifying the different neuronal cell types according to their position along the AP and dorso-ventral (DV) axis in the brain. Brain patterning also functions by the guidance for neuronal cell

migration and axonal extension. The precise location in the brain of the different neuronal subtypes are determined by fine molecular mechanisms. Several of the factors and pathways involved have been identified including the *Bmps*, *Sonic hedgehog* (*Shh*), and the nodal and retinoic acid pathways. The best known example is the control of the DV axis of the neural tube by the activities of BMP4 and SHH. BMP4 acts as a dorsalizing morphogen to induce dorsal characteristics to the neuroepithelial cells of the developing neural tube. Conversely, SHH released from the notochord acts as a morphogen to induce ventral characteristics of the epithelial cells of the neural tube (for review see Osumi, 2001; Manuel and Price, 2005; Guillemot, 2005).

4.2 Pax6 and brain development

In addition to affecting the development of the photoreceptive organs, *Pax6* also affects the formation of the brain as shown by loss-of-function mutations. During vertebrate development, *Pax6* starts to be expressed during the neural plate stage in the neuroectoderm domains, which will give rise to the forebrain, hindbrain and spinal cord. Later at the neuromere stage, *Pax6* is expressed in the dorsal part of the telencephalon and diencephalon as well as in the latero-ventral part of the rhombencephalon and spinal cord (Stoykova and Gruss, 1994; Osumi, 2001; Inoue et al., 2000).

4.3 Function of PAX6 in mice forebrain development

The forebrain is subdivided into two majors regions : the telencephalon where the cortex develops and the diencephalon which gives rise mainly to the thalamus.

4.3.1 The telencephalon

The telencephalon including the cerebral cortex and basal ganglia is the seat of motor coordination, emotions, higher cognition and consciousness in human. While it is one of the more complex region of the adult mammalian brain, the anatomical structure is relatively simple. It comprises large subdivisions with distinct cell populations (for review see Guillemot, 2005). The two main subdivisions separeted by a dorsoventral boundary, namely the pallium-subpallium boundary (PSB), are the dorsal telencephalon and ventral

telencephalon, namely pallium and subpallium, respectively. The germinal zone of the pallium generates the excitatory glutaminergic projection neurons of the cerebral cortex whereas the progenitors of the subpallium give rise in part to the GABA-ergic inhibitory neurons (for review see Manuel and Price, 2005).

4.3.2 Function of Pax6 in mice telencephalon development

During neurogenesis of the mouse telencephalon, *Pax6* expression is detected in the neuroepithelium of the ventral pallium where the mitotically active ventricular zone of the dorsal telencephalon is located. This zone corresponds to the intermediate region located just dorsal to the PSB. The function of PAX6 in the telecephalon is supported by the study of molecular markers in homozygous Small eye embryos displaying a ventralization phenotype of the dorsal regions at the PSB (for review see Manuel and Price, 2005) (Figure 17).

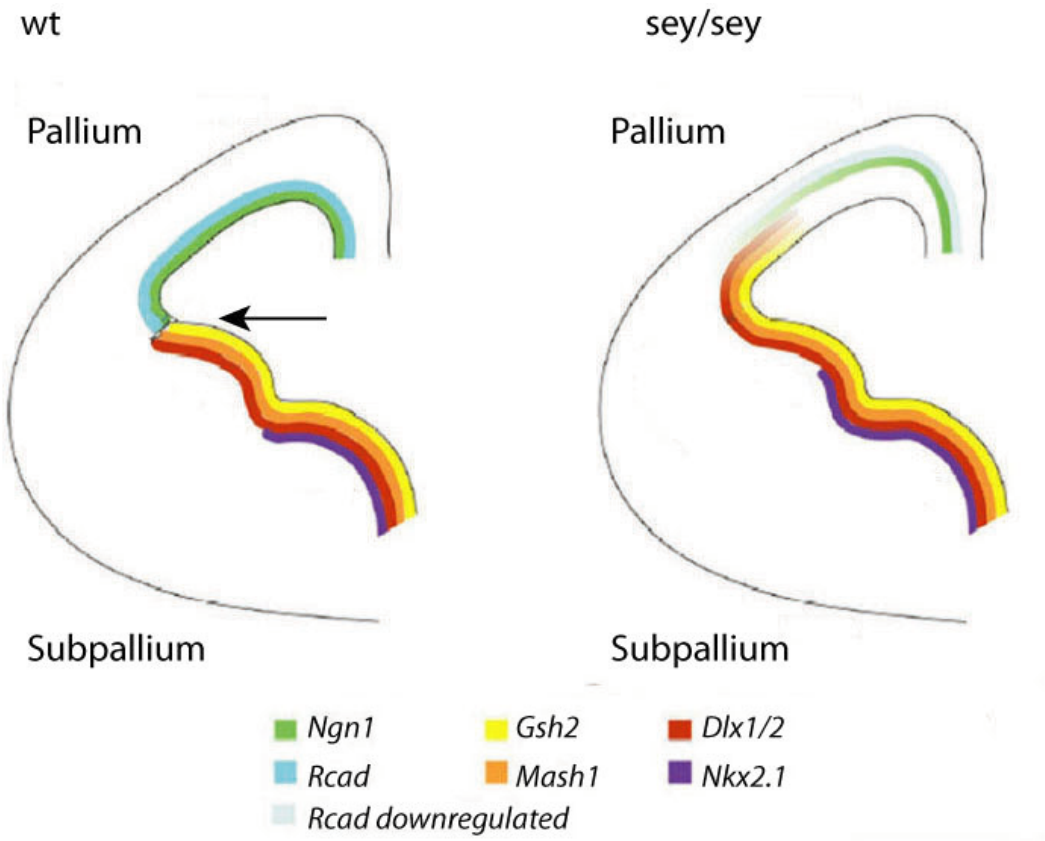

Figure 17. Schematic representation of a transverse section of a wild type and *Sey/Sey* mice telencephalon and expression domains of several dorsoventral molecular markers. The black arrow shows the pallium/subpallium boundary. From Manuel and Price, 2005.

Therefore, if PAX6 is absent at the PSB boundary, this leads to a down-regulation or a dorsal retraction of the expression of pallial markers such as *Emx1*, *Ngn1*, and to the dorsal extension of the expression of subpallial markers such as *Dlx2*, *Vax1* and *Six3* to the pallium. Hence, PAX6 acts in the telencephalon as a dorsalizing factor through the activities of the transcription factors *Ngn1* and *Ngn2* in repressing subpallial markers (Blader et al., 2004; Scardigli et al., 2003).

Besides its critical role played in telencephalon development, PAX6 is required for the proper formation of the diencephalon, olfactory epithelium, hindbrain and spinal cord. (For review see Manuel and Price, 2005; Osumi, 2001).

4.3.3 The hypothalamus

An other part of the forebrain is the hypothalamus ensuring a connection between the central nervous sytem and the endocrine system. The hypothalamus transmits nervous signals into the posterior lobe of the hypophysis with a part of its axons to regulate body homeostasis and control secretion of hormones which in turn act on target tissus. As a consequence, the hypothalamus controls many different functions such as thermoregulation, cardiac rhythms, vasoconstriction and emotions and rhythmic production of melatonin (Demuro and Obici, 2006; Guyenet, 2006; Falcon, 1999; Saper, 2006; Gainotti, 2001).

4.3.4 Pax6 function in hypothalamus development in mice

Pax6 expression is also detected in the hypothalamus during neurogenesis indicating that it may play a role during the formation of this area (Vitalis et al., 2000; Stoykova et al., 1996). For instance, in homozygous mutant Sey mice, the ventricular part of the hypothalamus is greatly disjointed and abnormally shaped suggesting that *Pax6* is required to keep the adhesive properties between both lobes of the hypothalamus (Vitalis et al., 2000; Stoykova et al., 1996).

5. Regulation of PAX6 activity by alternative mRNA splicing, the exon 5a as an example

Notably, the formation of the eye during development is not only triggered by the correct dosage of the PAX6 protein but also by the ratio between the different alternative PAX6 splice variants (Pinson et al., 2005; Chauhan et al., 2004). Therefore, it is essential to introduce the notion of alternative splicing and to illustrate it by a relevant example.

In contrast to the constitutive splicing which is involved excising the introns of most pre-mRNAs (for review see Stamm et al., 2005), the alternative splicing is a mechanism excising the exons differentially according to the state or type of the cell. It is an extensively used process in eucaryotes allowing the biosynthesis of several proteins from only one single gene. The advantage of having such a mechanism is to regulate the translation of the mRNAs and to increase protein diversity and hence, the number of functions of the gene (Graveley, 2001; for review see Maniatis and Tasic, 2002).

Several alternative splice isoforms of *Pax6* were found in almost all chordate species studied to date (Glardon et al., 1998; Nornes et al., 1998; Kleinjan et al., 2004; Gorlov and Saunders, 2002; Mishra et al., 2002; Carriere et al., 1993). However, the specific function(s) for the majority of them were not examined *in vivo* because of either the difficulty presented by the model organism studied or redundant functions of the different isoforms. Until today the majority of the studies was focussed on the functions of one alternative PAX6 splice variant. This PAX6 isoform protein found to be conserved from fish to human, but it is absent in amphioxus. It is characterized by the presence of an alternative 42 bp exon (exon 5a) encoding a 14 amino acids sequence in the N-terminal subdomain of its paired domain (PD) (Epstein et al., 1994a; Epstein et al., 1994b; Azuma et al., 1999; Singh et al., 2002). The insertion of this exon in the PD acts in unmasking the DNA binding potential of the C-terminal subdomain and thus giving the possibility to the protein to bind other DNA binding sites different form the canonical ones (Epstein et al., 1994a; Epstein et al., 1994b; Kozmik et al., 1997). Interestingly, the deletion of this exon 5a in mice by the Cre/*lox*P technique led to eye defects in the iris, cornea, lens, and retina (Singh et al., 2002). It was also reported in humans that a single base mutation in the exon 5a at the 20th nucleotide position resulting in a valine to asparagine substitution leads to severe eye defects (Azuma et al., 1999).

6. Metamorphosis of the vertebrate eye

6.1 Definition of the metamorphosis

In most species of animals, embryonic development leads to a larval stage mostly different from the adult organism. During metamorphosis, developmental processes are reactivated by specific hormones and the entire larval organism changes its morphology, physiology and behavior to prepare itself for its new mode of adult existence. Hence, the metamorphosis is often a time of dramatic developmental changes affecting the entire organism. The best known examples are the transformation of a caterpillar into a butterfly or the transformation of a tadpole into a frog. In teleost fish, this phenomenon is characteristic of flatfish.

6.2 The metamorphosis in amphibians and flatfish

Amphibian metamorphosis is associated to several morphological, physiological and biochemical changes that prepare an aquatic organism for a primarily terestrial existence. During metamorphosis of anurans (frogs and toads) tadpoles, several regressive changes occur including the resorption of the tail, the loss of the internal gills and horny teeth. At the same time, constructive changes such as limb development are observed. In addition, the tadpole cartilaginous skull is replaced by the bony skull of the frog, the long intestine characteristic of herbivores is remodeled to acquire short gut characterisitics of carnivores, the lungs enlarge allowing the frog to breath atmospheric oxygen, the eyes move forward from their originally lateral position allowing binocular vision, etc. In summary, almost all the components of the body change radically during metamorphosis. Interestingly, several morphogen factors such as BMPs and SHH known to be involved in embryonic development, are recruited again for the remodeling of the organs during metamorphosis (Stolow and Shi, 1995; Ishizuya-Oka et al., 2001).

Metamorphosis in flatfish transforms a pelagic symmetric larva into a benthic asymmetric one. During this transformation, the eye and the nostril migrate from one side of the head to the other side (this process is described more in details below). In parallel to these modifications, several other morphological, anatomical, biochemical and physiological changes occur in the whole organism (Evans and Fernald, 1993; Graf and Baker, 1983; Schreiber, 2001). Like metamorphosis in amphibians, the catilaginous skull of the flatfish

larva is replaced progressively by a bonny skull, the long intestine is remodelled to a short one, and the digestive enzymes are replaced by others more adapted to the new feeding regime. In addition, during the metamorphic process, the pigmentation of the body radically changes with the blind (under) side becoming entirely white, the telencephalon becomes asymmetric, the vestibulo-ocular pathways are radically reorganized allowing the animal to orientate in space, the opercular orifices change allowing the animal to be adapted to stay on the ground of the sea floor, etc (Medina et al., 1993; Brinon et al., 1993, Graf and Baker, 1983). Therefore, as in amphibians, almost all the components of the flatfish body change during metamorphosis.

6.3 Hormonal control of metamorphosis

The control of metamorphosis in amphibian and flatsfish is triggered by the thyroid hormones (THs). In 1912, Gudernatsch showed that tadpoles feeded with horse tyroid gland metamorphosed prematuraly. Four years later, Allen (1916) discovered that thyroidectomy of early tadpoles inhibited them to metamorphose and they grew into giant tadpoles in a complementary experiment. Subsequent studies gave rise to the treshold model postulating that the different events of metamorphosis are controlled by different concentrations of thyroid hormones (Saxen et al., 1957; Kollros, 1961; Hanken and Hall, 1988). For instance, the development of the limbs occurs early when the concentration of thyroid hormones are low. In contrast, the resorption of the tail, the remodelling of the intestine and the regression of the gills occur at the end of metamorphosis when the concentration of thyroid hormones are high. The process of metamorphosis is triggered by two thyroid hormones produced mainly in two different places. The thyroxine (T4) is secreted into the blood by the thyroid gland and is converted in the target tissue or into the blood in a more active form, the tri-iodothyronine (T3) (Figure 18). The conversion of T4 into T3 is triggered by the activity of the type II deiodinase which removes an iodine atom from outer ring of the precursor T4. Thyroid hormones, principally T3, act by binding to the thyroid hormone receptors (TRs) and cause them to become transcriptional activators. Two types of TR genes have been discovered and named thyroid hormone receptor alpha (TRα) and thyroid hormone receptor beta (TRβ). In Xenopus, TRα is widely expressed in all the tissues of the organism and is present before the apparition of a thyroid gland. In contrast, TRβ expression is directly activated by THs.

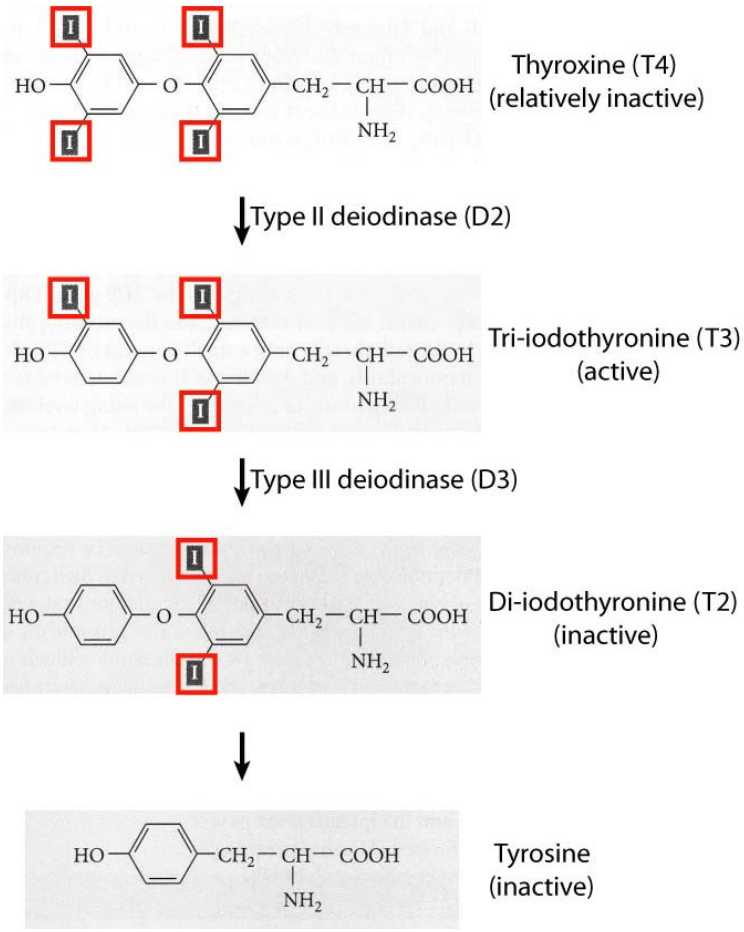

Figure 18. Metabolism of the thyroid hormones during metamorphosis. The iodine atoms are indicated in red. From Gilbert, 2003.

Hence, TRβ expression level is low before metamorphosis and increases as the metamorphosis process progresses (Yaoita and Brown, 1990; Eliceiri and Brown, 1994). TRs form heterodimers with the retinoic acid receptor (RXR) and bind to the thyroid response elements (TREs). These sequences generally consist of two half sites arranged as a direct repeat spaced by four nucleotides (DR4) (Umesono et al., 1991). They can also be palindromic elements (HREpal) (Glass et al., 1988; for review see Desvergne, 1994). It has been shown that in absence of the THs the TR-RXR heterodimer binds to co-repressors and represses transcription (Chen and Evans, 1995; Horlein et al., 1995). If THs are present, the TRs undergo a conformational change that induces the release of the co-repressors and the recruitment of co-activators (for review see McKenna et al., 1999). The T3–TR-RXR-co-activators complex is thought to bind to the chromatin of its target genes and to activate these genes through a process involving histone acetylation (Sachs et al., 2001).

Metamorphosis is often divided into two stages:

- During premetamorphosis, the thyroid gland starts to mature and secrets low levels of T4 and very low levels of tri-iodothyronine (T3) into the blood. The initiation of thyroid secretion of T4 is brought by corticotropin releasing hormone (CRH) which direcly acts on the larvae pituitary gland in instructing it to release thyroid stimulating hormone (TSH) or renders the cells of the target tissues to be responsive to low level of T3 (Denver, 1993). In frogs, the limb rudiments have high levels of type II deiodinase so that TRα can convert T4 into T3 and use this hormone directly to initiate leg growth (Becker et al., 1997; Huang et al., 2001; Schreiber, 2001).
- During the prometamorphosis stage, the T4 concentration in the blood increases dramatically and the TRβ expression levels insides the cells follow this increase until they reach a maximum at the metamorphic climax. At this stage, the TRβ is the principal TR that mediates the effects of the THs. At metamorphic climax, in the tail, TRβ expression is high and type II deiodinase is expressed leading to the beginning of the tail resorbtion process.

Interestingly, the hormonal mechanisms of metamorphosis seem to be conserved between amphibians and flatfish (flounder and turbot). As in amphibians, this process is triggered by the THs and accordingly, these hormones are able to induce metamorphosis prematurely in young larvae (Inui and Miwa, 1985). In flounder, three TH receptors genes have been found : two TR alpha (TRαA and TRαB) and one TR beta (TRβ). The presence of two TRα in several Teleost genomes is thought to be the consequence of a genome duplication event which occured within the Teleost lineage (Jaillon et al., 2004). During flatfish metamorphosis, when the level of T3 increases dramatically, TRαA and TRβ are strongly expressed whereas TRαB expression levels remains low. In contrast to Xenopus, TRαA shows the strongest induction of mRNA expression and not TRβ (Yamano et al., 1994; Yamano and Inui, 1995; Yamano and Miwa, 1998; Marchand et al., 2004).

6.4 Metamorphosis of the eye in amphibians and flatfish

As the majority of the other tissues of the body, the visual system of anurans and flatfish undergo dramatic changes during metamorphosis (for review see Hoskins, 1986). In anuran tadpoles, the eyes are located laterally on the head allowing them to benefit of a panoramic vision, a case typical of animals with a herbivore regime. During metamorphosis, the eyes move forward from their originally lateral position allowing the animal to see in

three dimensions and hence, to be adapted to a more predatory lifestyle. Thus, the animal acquires a binocular vision wherein the input of both eyes converges into the brain. In the tadpole, the right eye innervates the left side of the brain whereas the left eye innervates the right side. During metamorphosis, ipsilateral projections of the retinal neurons into the brain emerges, enabling both eyes to reach the same area of the brain (Hoskins and Grobstein, 1985c; Hoskins and Grobstein, 1985b; Hoskins and Grobstein, 1985a).

An other interesting modification observed during metamorphosis of the Xenopus eye is the patterning of retinal proliferation. The premetamorphic tadpole retina grows by proliferating symmetrically at the ciliary marginal zone (CMZ). During metamorphosis, the CMZ of the retina grows in size ventrally but not dorsally and remains asymmetric until adulthood (Beach and Jacobson, 1979b; for review see Mann and Holt, 2001). Therefore, the adult frog retina is derived from ventral CMZ cells. Since this process is blocked by chemicals inhibiting the production of THs and induced by the addition of exogenous THs, the shift from symmetric to asymmetric growth is THs dependent (Hoskins and Grobstein, 1984; Beach and Jacobson, 1979a). Interestingly, Beach and Jacobson (1979) have shown by eye inversion studies that the growth pattern of the retina at metamorphosis is determined during embryogenesis before the development of a functional thyroid gland. This suggests the presence of a factor involved in metamorphosis already at this early stage. Twenty years later, Brown and colleagues (1999) discovered that this factor is type 3 deiodinase (D3). This enzyme removes a iodine atom from the inner ring of the T3 (Figure 18) to convert it into an inactive coumpound that will be eventually be metabolized to tyrosine (Becker et al., 1997). Thus, the tissues diplaying a D3 activity are protected from the THs effects. In *Xenopus*, the D3 gene is expressed in the dorsal CMZ at early stages of development until metamorphosis. In contrast, the D3 activity in the eye is low before and after metamorphosis and becomes high only at metamorphic climax protecting the dorsal CMZ from the proliferative effect of the T3 (Marsh-Armstrong et al., 1999).

In flatfish, the process of metamorphosis at the level of the eye is still more dramatic. At the beginning of metamorphosis, one eye starts to migrate from one side along (or across) the back to the other side of the body (Figure 19). Hence, the pelagic symmetric larva (figure 19A) transforms into a benthic asymmetric juvenile (Figure 19C). In addition, during metamorphosis the structure of the retina radically changes. Before this process, the larval retina contains only cone photoreceptor cells whereas afterwards, rod and double cone photoreceptor cells appear (Evans and Fernald, 1993; Mader and Cameron, 2004).

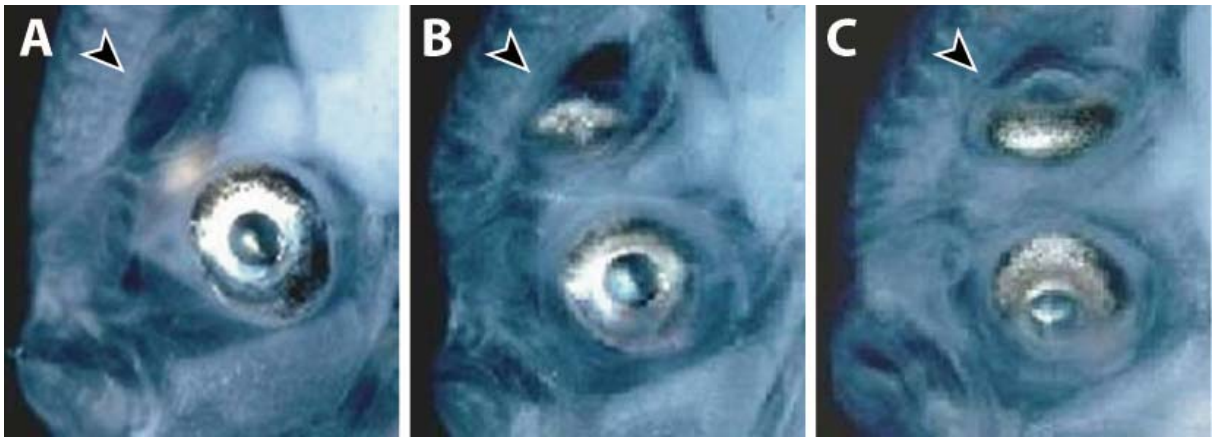

Figure 19. Metamorphosis of the eye in *Bothus ocellatus*. (A) Before metamorphosis, there is one eye on each side of the body. (B) During metamorphosis, a hole is formed between the dorsal fin and the back where the right eye pass throughout to go to the left side. (C) After the eye has finished to migrate, the hole is closed.
From http://www.nmnh.si.edu/vert/fishes/larval/pleur.html

7. Presentation of the models used during this study

7.1 Why to study fish ?

The fish belong to the oldest and most important group of vertebrates appearing about 470 million years (Myr) ago, and comprising about 23,800 known currently living species distributed over about 4,265 genera. The diversity of the fish taxon is therefore exceptional at all levels of organisation (from the anatomical, functional and behavioural point of view). In comparison, mammals count only 5,500 species distributed over about 1,200 genera.

Part of the wide variability that fish exihibit has been attributed to a whole genome duplication event which is thought to have occured at the emergence of the Teleost lineage about 250 Myr ago (Jaillon et al., 2004). After this event, the genomes of the different Teleost lineages have evolved independently due to different environmental pressures. The selective pressure has induced several changes which are thought to have principally occured in the cis-regulatory elements of the pre-existing genes and also resulted in the formation of new chimeric genes acquiring new functions (Levine, 2002).

The comparison of divergent Teleosts will provide insights into the evolution of the genetic and biochemical networks controlling development, hormone biosynthesis, etc. and the plasticity of these regulatory networks.

7.2 The zebrafish as a model

The zebrafish (*Danio rerio*) is a fresh water teleost fish species described by Hamilton in 1822 belonging to the Cyprinid family belonging to the class of ray-finned fishes (Actinopterygii) (Figures 20 and 21). The cyprinids appeared about 160-110 Myr at the beginning of the Euteleost lineage indicating that the last common ancestor of cyprinids and mammals existed about 450 Myr ago (Wittbrodt et al., 2002). The haploid zebrafish genome is about 1.7 gigabases in size, divided into 25 chromosomes. The zebrafish is currently the most studied Teleost species in laboratories. The advantages are: a small size allowing to raise them in a great number in relatively small tanks. In addition, its sexual maturity is reached after three months and a female can lay up to 200 eggs every two weeks. Furthermore, the observation of its rapid embryonic development is largely facilited through its transparency until the end of the first day of development (Figure 20B).

7.3 The turbot as a model

The turbot (*Scophthalmus maximus*) is a seawater flatfish species described by Linneus in 1758 belonging to the order of pleuronectiforms and the Scophthalmidae family. Its geographic distribution extends from 68°N in Europe to 30°N Morocco. This species is absent in the black sea. The pleuronectiform order gathers Teleosts displaying a "true" metamorphosis transforming a symmetric larva into an asymmetric juvenile, an unique case among vertebrates (Figure 22).

B

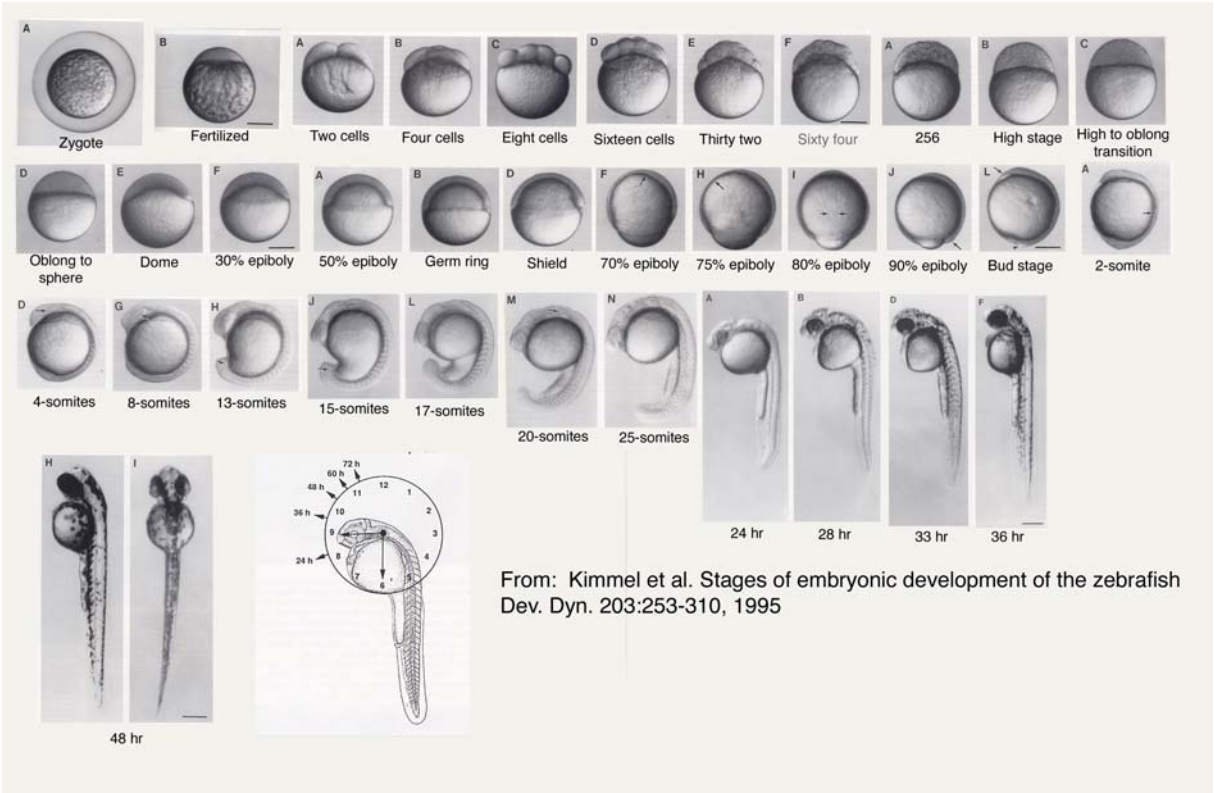

Figure 20. Photographs of zebrafish. (A) A small group of adult zebrafish is shown. From www.openscience.it/ opendanio.htm. (B) Embryonic development in the zebrafish. In this species, the neurulation starts at 9 hpf (90% epiboly stage) and the optic vesicles develop at 12 hpf (9-10 somites stage). At 24 hpf (Prim-5 stage), the optic cups are already formed.

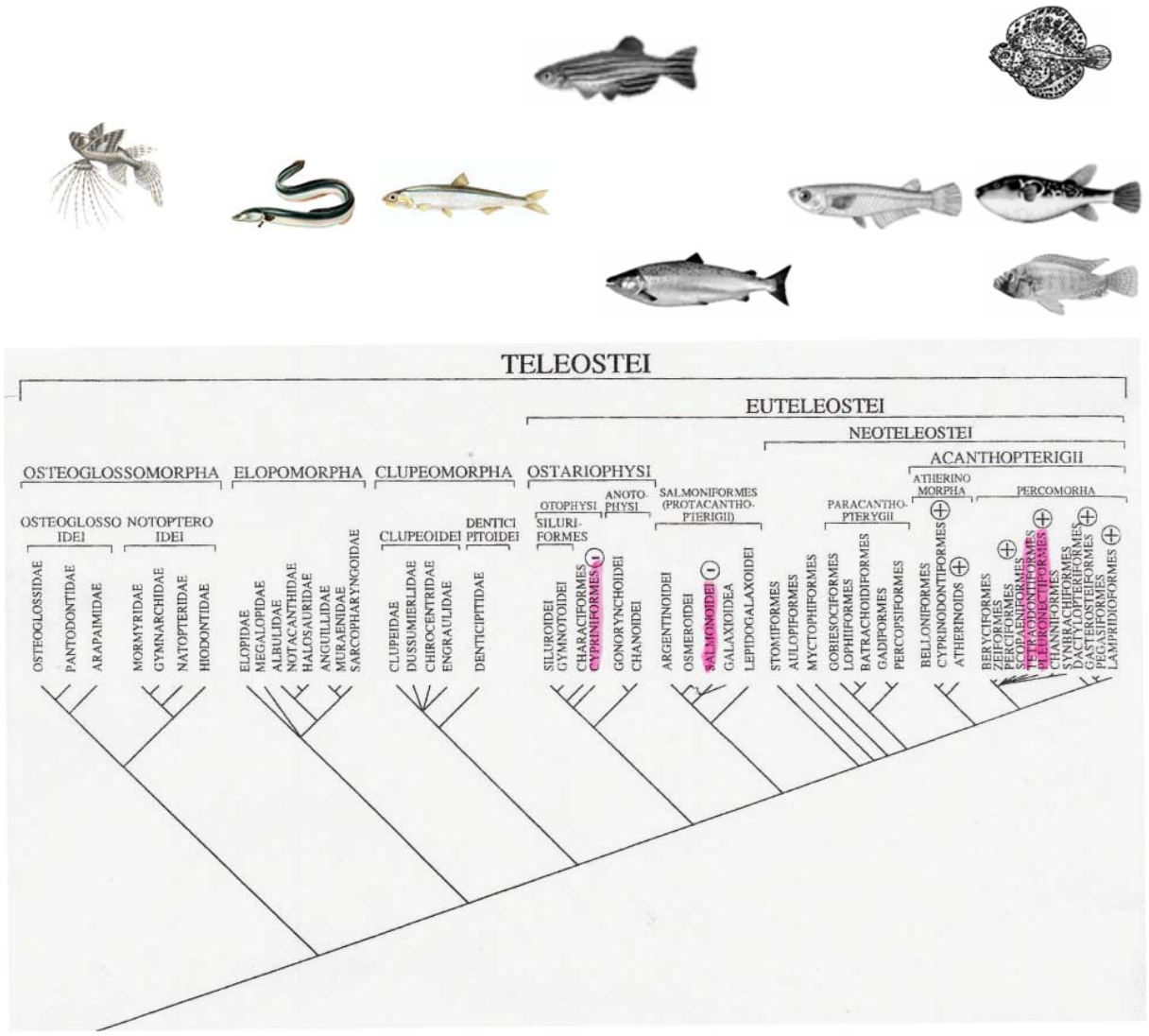

Figure 21. Phylogenetic tree of the Teleost group. From Lauder and Liem, 1983.

In addition, these species are very interesting because of their phylogenetic position (Figure 21). Their last common ancestor with other Teleosts appeared recently at about 50 Myr ago and they are classified as sister group of Tetraodontiforms, a group including the pufferfish (Lauder and Liem, 1983). In addition to the proper characteristics of the flatfish group mentionned before, the turbot was choosen as a model for this thesis for several additional reasons. First, the turbot embryos, larvae, juveniles and adults are available almost all the year around at "France Turbot" in Noirmoutier. Second, the metamorphosis in turbot starts earlier (at 20 days post-hatching) and is quicker (around 15 days) compared to other flatfish species such as flounder (Appendix 1). Third, the turbot displays a high fertility averaging about 430,000 eggs per kilo of female allowing to dispose of a large quantity of biological material to carry out experiments.

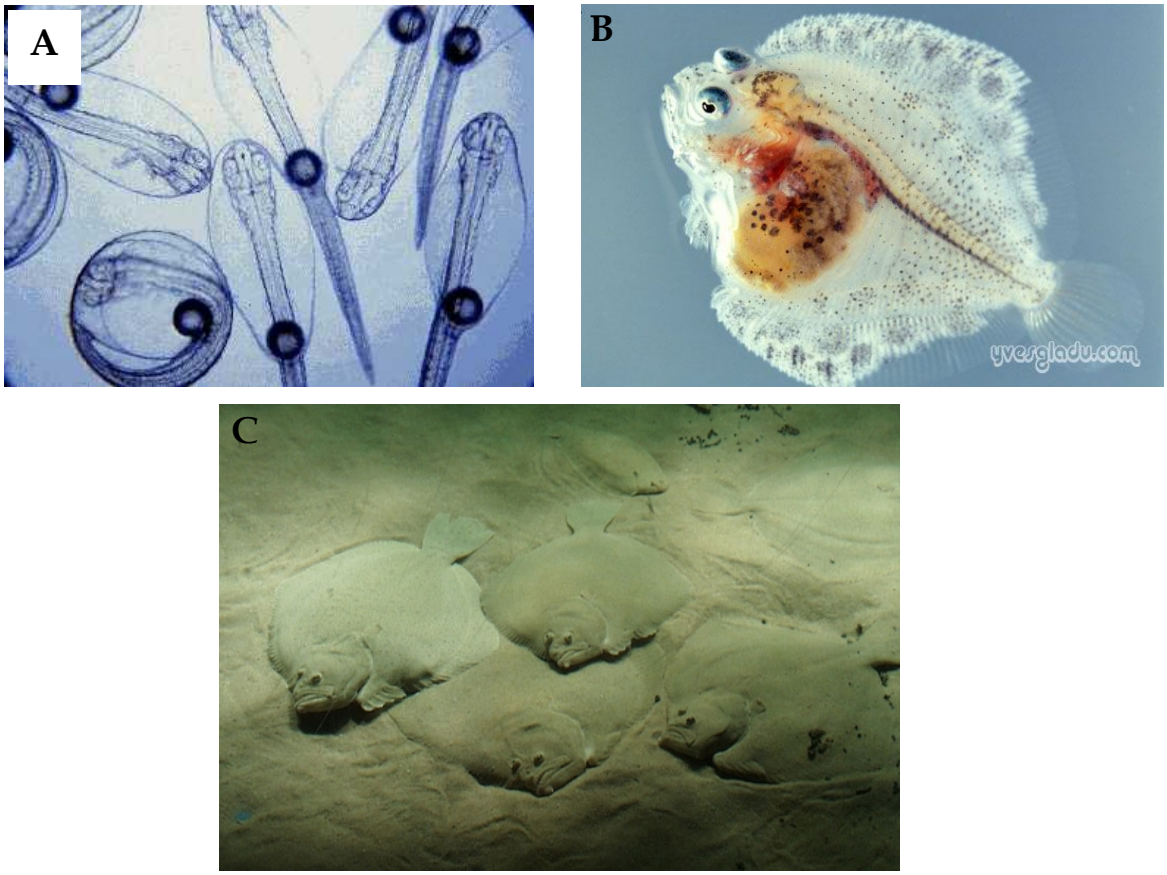

Figure 22. Photographs showing premetamorphic larvae (*A*), a metamorphic larva (B) and adults (*C*) of turbot. Note that in (*A*), the larvae are symmetric with an eye on each side of the body. In (B) the right eye has started to migrate and is located on the back of the metamorphic larva. In (*C*) the adult turbots are asymmetric with both eyes on the left side of the body. (*A*) From www.uncw.edu/cmsr/aqf/larval.htm and (*C*) from www.ridder.punt.nl/index.php.

8. Aims of this PhD thesis

As discussed before, the majority of the studies that have been conducted on the development of the central nervous system (CNS) and photoreceptive organs in vertebrates were performed in rodents. Indeed, these mammalian models display a close genetic relationship with human as well as several technical advantages. However, the study of ectotherms including Teleost fish species should not be omitted because they represent model systems allowing to better understand the genetic mechanisms patterning the CNS and photoreceptive organs and to study how they have evolved among the vertebrates. Moreover, the retina and the pineal gland in these species represent a comparative paradigm

to study the molecular and cellular mechanisms controlling the formation and the functions of the photoreceptive organs in vertebrates.

Therefore, during this thesis, we were interested particularly in the development of the epiphysis and retina in two phylogenetically distant Teleost fish species, namely the zebrafish and the turbot, and we investigated mainly the following three questions:

- How are the photoreceptive and melatonin biosynthesis functions in the fish pineal gland and retina established during development?
- Is the establishement of the mechanisms triggering these functions conserved during Teleost evolution?
- Are the mechanisms controlling CNS and photoreceptive organs development conserved during vertebrates evolution?

To answer these questions, we performed a detailed study of the establishment of the pineal functions during embryonic and larval development in zebrafish and turbot by using a multi-disciplinary approach. We focused especially on the transcriptional regulation of the genes encoding the two last enzymes involved in the melatonin biosynthesis pathway and a specific photopigment molecule of the epiphysis. The results presented in the next section allow us to conclude that the pineal gland rather than the retina mediates photic response during early stages of development in Teleost fish. However, they also suggest that the establishment of the molecular mechanisms controlling the embryonic pineal functions have been modified during evolution of the Teleosts.

Then, we focused on the turbot to examine the retinal metamorphosis. The preliminary results suggest that this process and the one described in *Xenopus*, are convergent.

Finally, we characterized by several *in vivo* and *in vitro* experiments two alternative *Pax6* splice variants in zebrafish and examined their functions in the CNS and in photoreceptive organs by a gene knock down approach. The results suggest that the genetic networks controlling eye and brain patterning are highly conserved between zebrafish and mice.

Chapter 2

9. Materials and Methods

9.1 Materials

9.1.1 Experimental animals

Adult zebrafish were kept at 28.5°C on a 14 hours light/10 hours dark cycle, and embryos were obtained by natural mating (Westerfield, 1993). Embyros destinated to whole mount *in situ* hybridization were raised in 0.2 μM phenylthiocarbamide (PTU) (Sigma) from 12 hpf to prevent pigment formation.

Embryos, larvae and juveniles of turbot (*Scophthalmus maximus*) were obtained from France Turbot (Noirmoûtier, France) where they were reared in seawater at 16°C, as detailed elsewhere (Person-Le-Ruyet, 1989).

Fruitfly (*Drosophila melanogaster*) were reared on standard medium at 25°C for working purpose and kept at 18°C for maintenance.

9.1.2 Degenerated and specific primers

The degenerate primers used to clone the partial cDNA of the *S. maximus Pax6*, *Bmp4*, *Bmp2*, *Aanat1*, *Aanat2*, *Hiomt* and *D3* genes are indicated in Appendix 2. All the specific primers used to clone the full-length of these genes can be found in the research articles presented in chapter 3.

The specific primers used for the quantitative PCRs were designed with the Primer3 software (Rozen and Skaletsky, 2000) and are presented in Appendix 3.

9.1.3 Constructs

- *In vitro* translation constructs:

Pax6.1c: the full-length sequence of zebrafish *Pax6.1c* cDNA was subcloned into pBluescript II SK (Stratagene) (kindly provided by Dr. Krauss).

Pax6.2c: the full-length sequence of zebrafish *Pax6.2c* cDNA was subcloned into pBluescript II SK (Stratagene) (kindly provided by Dr. Krauss).
Pax6.2(2a): the full-length sequence of zebrafish *Pax6.2(2a)* cDNA was subcloned EcoRI/XhoI into pBluescript II KS (Stratagene).

- Cell transfection constructs :

pcDNA3-Pax6.2c: the full-length zebrafish *Pax6.2c* cDNA in pBSII SK was subcloned EcoRI/XhoI into pcDNA3 (vector kindly provided by Dr. Geneviève).
pcDNA3-Pax6.2(2a): the full-length zebrafish *Pax6.2(2a)* cDNA in pBSII KS was subcloned EcoRI/XhoI into pcDNA3.

- Fly constructs:

UAS-Pax6.2c: the full-length zebrafish *Pax6.2c* cDNA in pBSII SK was subcloned EcoRI/XhoI into pUAST (vector kindly provided by Dr. Seimya).
UAS-Pax6.2(2a): the full-length zebrafish *Pax6.2(2a)* cDNA in pBSII KS was subcloned EcoRI/XhoI into pUAST.

- *In vivo* translation constructs:

T7N2eGFP: the T7 promotor from pBSII KS was inserted into the NheI/SacI restriction sites of N2eGFP (Clontech) (vector kindly provided by Dr. Schwartz).
T7N2eGFP$_{M\rightarrow N}$: the first methionine of eGFP of the T7N2eGFP vector was mutated to asparagine.
***6.2*UTR/eGFP**: the 5'UTR and partial ORF of a *Pax6.2c* (bases 17 to 375) cDNA fragment amplified by PCR was subcloned EcoRI/BamHI into T7N2eGFP.
***6.2(2a)*UTR/eGFP**: the 5'UTR and partial ORF of a *Pax6.2(2a)* (bases 17 to 446) cDNA fragment amplified by PCR was sublconed EcoRI/BamHI into T7N2eGFP.
6.2UTR/T7N2eGFP$_{M\rightarrow N}$: the 5'UTR and partial ORF of a *Pax6.2c* (bases 17-330) cDNA fragment amplified by PCR was subcloned EcoRI/BamHI into T7N2eGFP$_{M\rightarrow N}$.
6.2(2a)UTR/T7N2eGFP$_{M\rightarrow N}$: the 5'UTR and partial ORF of a *Pax6.2(2a)* (bases17-401) cDNA fragment amplified by PCR was subcloned EcoRI/BamHI into T7N2eGFP$_{M\rightarrow N}$.

6.2UTR1mut/T7N2eGFP$_{M\rightarrow N}$: the second putative start codon of the *Pax6.2c* cDNA in 6.2UTR/T7N2eGFP$_{M\rightarrow N}$ was mutated from methionine to asparagine.

6.2UTR2mut/T7N2eGFP$_{M\rightarrow N}$: both putative start codons of the *Pax6.2c* cDNA in 6.2UTR/T7N2eGFP$_{M\rightarrow N}$ were mutated from methionine to asparagine.

6.2(2a)UTR1mut/T7N2eGFP$_{M\rightarrow N}$: the putative start codon of the *Pax6.2(2a)* cDNA in 6.2(2a)UTR/T7N2eGFP$_{M\rightarrow N}$ was mutated from methionine to asparagine.

9.1.4 Details of the RNA probes for in situ hybridization on whole mount and sections

ZfAanat2: the probe corresponds to a partial fragment (990 bp) of the *ZfAanat2* cDNA (kindly provided by Dr. Gothilf)

ZfPax6.1: the probe corresponds to the full-length *Pax6.1* cDNA (kindly provided by Dr. Krauss)

ZfPax6.2: the probe corresponds to the full-length *Pax6.2* cDNA (kindly provided by Dr. Krauss)

ZfOtx5: not detailed (kindly provided by Dr. Gamse)

ZfVax1: the probe corresponds to a partial fragment (450 bp) of the *ZfVax1* cDNA (kindly provided by Dr. Wilson)

ZfVax2: the probe corresponds to a partial fragment (450 bp) of the *ZfVax2* cDNA (kindly provided by Dr. Wilson)

ZfEmx3: the probe corresponds to a partial fragment (bases: 26-810) of the *Emx3* cDNA

ZfDlx2: the probe corresponds to a partial fragment (bases: 681-1620) of the *Dlx2* cDNA

ZfPax2b: the probe corresponds to a partial fragment(bases: 1231-2745) of the *Pax2b* cDNA

ZfSix3b: the probe corresponds to a partial fragment (bases: 381-1520) of the *Six3b* cDNA

ZfNgn1: the probe corresponds to a partial fragment (bases: 131-1220)of the *Ngn1* cDNA

ZfExR: the probe corresponds to a partial fragment (575 bp) of the *ExR* gene cDNA (kindly provided by Dr. Falcon)

ZfFlh: the probe corresponds to a partial fragment (bases: 71-875) of the *Flh* cDNA

SmBmp2: the probe corresponds to a partial fragment (bases: 224-1634)of the *SmBmp2* cDNA

SmBmp4: the probe corresponds to a partial fragment (bases: 46-1170) of the *SmBmp4* cDNA

SmOtx5: the probe corresponds to a partial fragment (bases: 218-1280) of the *SmOtx5* cDNA

SmAanat2: the probe corresponds to a partial fragment (bases: 399-1315) of the *SmAanat2* cDNA

SmHiomt: the probe corresponds to a partial fragment (bases: 202-1027)of the *SmHiomt* cDNA

SmD3: Two probes corresponding to the full-length *D3* cDNA.

9.1.5 Sequence of the morpholinos used to inject zebrafish embryos

- Morpholinos targeting the first putative start codon of zebrafish *Pax6c*:

Mo3 (complementing bases *Pax6.1*: 489-513 ; *Pax6.2*: 261-285): **5′GGTTATAGTATTCTTTTTGAGGCAT 3′**

Pax6.1cMo (complementing bases 481-505): **5′TATTCTTTTTGAGGCATAGTTCCAA3′**

Pax6.2 cMo (complementing bases 254-278): **5′GTATTCTTTTTGAGGCATTCTGCTC3′**

- Morpholinos targeting the putative start codon of Pax6(2a):

MoV (complementing bases *Pax6.1*: 543-567; *Pax6.2*: 315-339): **5′CGCCACTGTGACTGTTTTGCATCAT 3′**

MoV2 (complementing bases *Pax6.1*: 537-561; *Pax6.2*: 309-333): **5′TGTGACTGTTTTGCATCATGGACGC 3′**

- Control morpholinos:

Standard control Mo (StdMoC): **5′CCTCTTACCTCAGTTACAATTTATA 3′**

MoV2 with 5 mutations (MoV25mut): 5′TGTAACTGTTGTGCATTACGGATGC3′

9.2 Methods

Standard molecular methods including standard RT-PCR, DNA purification, PCR fragment cloning, chemically-competent or electro-competent cells transformation, minipreps, *in vitro* transcription of dig-labeled RNA probes and RNA extraction were performed according to the manufacturer protocol and will not be further described. Only protocols less commonly used are described in this section.

9.2.1 RT-PCR and real time quantitative PCR

Reverse transcription of mRNA of turbot and zebrafish was carried out with the Superscript II first strand synthesis kit following the standard protocol (Invitrogen). PCR were performed with the Advantage 2 polymerase mix kit following the standard protocol (Clontech).

The real time quantitative PCR was performed in using a Light Cycler (Roche) and QuantiTect™ SYBR® Green PCR kit (Qiagen). The standard amplification protocol was as follows: 15 minutes at 95°C, 15 seconds at 94°C, 20 seconds at 56-58°C, 10 seconds at 72°C over 50 cycles. The fluorescence of the amplified products was detected 5 seconds at 76°C after the elongation step.

9.2.2 Bioinformatics sequence analysis

Deduced full-length amino acid sequences of cloned genes were aligned using PipeAlign (Plewniak et al., 2003). The Phylo_win version 2.0 software program was used to infer phylogenetic trees (Galtier et al., 1996). After gaps removing, trees were inferred by the Neighbor Joining method (NJ). The degree of support for internal nodes was assessed using 1000 bootstrap replications. Sequences were analyzed by BLASTP (Altschul et al., 1997) and PROSITE motif search (Bairoch et al., 1997).

9.2.3 In vitro translation of mRNA

In vitro translation was performed with the TNT Coupled Reticulocyte Lysate System (Promega) as described by the manufacturer protocol.

Full-length *Pax6.1c* and *Pax6.2c* cDNAs were transcribed with the T3 polymerase and the full-length *Pax6.2(2a)* cDNA with the T7 polymerase. Synthetized ^{35}S methionine radiolabeled proteins were loaded on a 12% acrylamide gel and detected by autoradiography.

9.2.4 Cell transfection and western blot

HeLa human cells were transfected with 3 µg of the pcDNA3-Pax6.2c and pcDNA3-Pax6.2(2a) constructs with the lipofectamine reagent (Invitrogen) following the manufacturer protocol. Preparation and immunoblotting of protein extracts from transfected HeLa cells was carried out as described previously (Even et al., 2006). To detect zfPAX6s, a rabbit polyclonal antibody targeting the carboxyl terminal end of the protein (Covance) was used at a dilution of 1:2000. Secondary antibodies coupled to horseradish peroxydase and an ECL Plus kit (Amersham) was used for the photodetection.

9.2.5 Preparation of the samples for in situ hybridization and antibody staining

- Whole mount samples for *in situ* hybridization and antibody staining

Embryos and larvae of turbot and zebrafish were fixed in 4% paraformaldehyde (PFA) overnight (O/N) at 4°C. They were then washed three times 5 min. in PBS, dechorionate if needed with forceps in PBS, and washed three times 5 min. in methanol. Finally, they were stored in methanol at -20°C during at least 2 hours.

- BrdU labeling and sections for BrdU histochemistry and *in situ* hybridization

Larvae, metamorphic larvae and juveniles of turbot were soaked in a 100 µM, 1 mM and 10 mM BrdU (Sigma) solution, respectively, during two days. They were then removed and fixed in a 4% PFA solution overnight at 4°C. For larvae older than 17 dph (days post-hatching), the eyeballs were removed from the head. After several washes in PBS, the larvae and eyeballs were dehydrated in graded series of PBS/gylcerol/sucrose solutions (Besseau

et al., 2006), included in Tissue Freezing Medium (Jung) and frozen in dry ice. They were then sectioned (30-40µm) using a Leica CM1900 cryotome and dried at 37°C O/N.

The preparation of the sample sections destinated to the *in* situ hybridization were carried out with the same protocol as above except the BrdU labeling step.

9.2.6 In situ hybridization

The following protocol for the *in situ* hybridization is adapted from (Thisse et al., 2004).

Rehydratation: Samples stored in methanol at -20°C were rehydrated in PBST with 5 gradual washes of methanol/PBST with the two last washes in PBST only.

Permeabilization: For whole mount samples, they were digested in proteinase K (10µg/ml) in PBST at room temperature (RT) during different times according to the developmental stage. For gastrulae 1 min., neurulae 4 min., early somitogenesis 10 min., organogenesis 20-45 min. For sections, the proteinase K (5µg/ml) treatment was carried at 37°C during 15 min.

Fixation: The samples were fixed in 4% PFA during 20 min. at RT.

Washes: Samples were washed 5 times 5 min. in PBST.

Prehybridization: Samples were prehybridized in hybridization buffer (HB) during at least 4 hours at 67°C.

Hybridization: The hybridization was performed in HB O/N at 67°C with 1 µg/ml digoxygenin (dig) labeled riboprobe.

Washes: Samples were washed once at 67°C during 15 min. in each solutions of 75%HB/SSC2x, 50%HB/SSC2x, 25%HB/SSC2x and SSC2x and finally two times 30 min. in SSC0.2x.

Blocking: The samples were washed once 5 min. in blocking solution (BS) before to be blocked in BS during 6 hours at RT.

Immuno: Preabsorbed alkaline phosphatase conjugated anti-dig antibodies (Roche) were added to the samples at a dilution of 1:2000 in BS and incubated O/N at 4°C.

Washes: The samples were then washed 7 times 15 min. in PBST at RT.

Staining buffer: They were incubated in staining buffer (SB) with two washes of 10 min each.

Detection: The substrate (BM purple, Roche) of alkaline phosphatase was added to the samples and the reaction was carried out in the dark. The detection was followed under a microscope.

Solutions

BS: 2 mg/ml BSA and 3% goat serum in PBST, pH 7.4

HB: 50% formamide, SSC5x, Tween20 0.1%, Heparin 50 µg/ml, tRNA 500 µg/ml, pH 6

SB: 0.1M Tris-HCl, 0.1 NaCl, 50mM $MgCl_2$, Tween20 0.1%, pH 9.5

9.2.7 BrdU histochemistry

The following protocol is adapted from (Strickler et al., 2002).

Rehydratation: Dried sections were rehydrated in two washes of PBST during 5 min.

Permeabilization and inactivation of the enzyme: They were then incubated in 0,05% trypsin with 0,05% $CaCl_2$ in PBS at 37°C during 10 minutes. Inactivation of the enzyme was carried out in 10 mg/ml trypsin inhibitor in PBS during 10 minutes.

Denaturation: The denaturation of the DNA was carried out in 4M HCl during 23 min. at RT.

Washes and blocking: The sections were then washed two times 5 min. in PBST and incubated 30 min. in BS.

Immuno: They were incubated in a primary antibody (mouse Anti-BrdU, Sigma) at a 1:1000 dilution in BS during 2 hours at RT.

Washes and blocking: The sections were then washed three times 5 min. and once 1 hour in BS.

Immuno: they were incubated in a secondary antibody (Anti-mouse FITC conjugated, Sigma) at a 1:500 dilution in BS during two hours.

Washes and mounting: After six washes of 10 minutes in PBST and one in PBS they were mounted in 100% glycerol with DABCO (0.3%). Fluorescent staining was examined with an epifluorescence microscope.

9.2.8 Microinjection of zebrafish embryos

Microinjection of the **Mo3**, **Pax6.1 Mo, Pax6.2 Mo, MoV**, **MoV2**, **MoC and MoV25mut** morpholinos and the ***6.2c*UTR/eGFP**, ***6.2(2a)*UTR/eGFP**, **6.2cUTR/T7N2eGFP$_{M\rightarrow N}$**, **6.2(2a)UTR/T7N2eGFP$_{M\rightarrow N}$**, **6.2cUTR1mut/T7N2eGFP$_{M\rightarrow N}$**, **6.2cUTR2mut/T7N2eGFP$_{M\rightarrow N}$** and **6.2(2a)UTR1mut/T7N2eGFP$_{M\rightarrow N}$** mRNA constructs was carried out as described in (Gilmour, 2002). Briefly, 1-4 nl of mRNA and/or Mo were injected

into the cytoplasm of one to four cell stage embryos with an Eppendorf micromanipulator. Injected embryos were then reared with gentamycin (concentration) in an incubator at 28.5°C under a 14/10 LD cycle before to be fixed at different developmental stages.

9.2.9 Antibody staining

The following protocol is adapted from (Schulte-Merker, 2002).

Rehydratation: The mRNA injected zebrafish embryos were rehydrated from methanol as described in the *in situ* hybridization protocol.

Blocking and immuno: Samples were then incubated in BS during 4 hours at RT before to be incubated in preabsorbed primary antibody (rabbit anti-GFP, Torrey Pines Biolabs) at a dilution of 1:1000 in BS O/N at 4°C.

Washes and blocking : Embryos were washes 4 times 10 min. in BS before to be incubated 1 hour in BS at RT.

Immuno: They were then incubated in an alkaline phosphatase conjugated anti-rabbit secondary antibody (Zymed) at a dilution of 1:300 in BS O/N at 4°C.

Washes, staining buffer and detection: The protocol was the same as described for the *in situ* hybridization experiment.

9.2.10 Microinjection of Drosophila embryos

Microinjection of the fruitfly embryos was carried out as described in (Rubin and Spradling, 1982). Briefly, eggs were precollected for 1-2 hours in a dark place. They were discarded and new eggs were collected for 20-30 min. After dechorionation with 3% sodium hypochlorid during 2 min., the eggs were washed with tap water and then with wash solution. They were again washed with tap water and transfered on a grape juice plate where they were aligned. The embryos were then stamped on a slide with a stripe of Scotch double sticky tape and dried under a hairdryer during 4 min. The dried embryos were covered with Voltalef 10S oil to prevent further drying. The pUAS-Pax6.2c and pUAS-Pax6.2(2a) DNA constructs (150 ng/µl) were then coinjected in the posterior part of the embryos with a helper DNA plasmid (100 ng/µl) under constant flow.

Chapter 3

In adult ectothermic vertebrates, the photoreceptive, circadian and endocrine functions of the retina and pineal gland have been previously well studied (reviewed in Falcon, 1999) whereas their establishment during embryonic development remains relatively unknown. In addition, the few studies which have been carried out on this subject are contradictory (Kazimi and Cahill, 1999; Delaunay et al., 2000; Ziv et al., 2005).

In order to resolve these conflicting results and to get insights concerning the establishment of the different pineal functions, we examined the expression pattern of two marker genes of this organ during zebrafish development.

In the next section, the results of this study are presented.

10. Starting the Zebrafish Pineal Circadian Clock with a Single Photic Transition

10.1 Abstract

The issue of what starts the circadian clock 'ticking' was addressed by studying the developmental appearance of the daily rhythm in the expression of two genes in the zebrafish pineal gland that are part of the circadian clock system. One encodes the photopigment exorhodopsin (ExR) and the other the melatonin synthesizing enzyme arylalkylamine *N*-acetyltransferase (AANAT2). Significant daily rhythms in *Aanat2* mRNA abundance were detectable for several days following fertilization in animals maintained in a normal or reversed lighting cycle providing 12 h of light and 12 h of dark. In contrast, these rhythms do not develop if animals are maintained in constant lighting or constant darkness from fertilization. In contrast to *ExR*, rhythmicity of *Aanat2* can be initiated by a pulse of light against a background of constant darkness, by a pulse of darkness against a background of constant lighting, or by single light-to-dark or dark-to-light transitions. Accordingly, these studies indicate that circadian clock function in the zebrafish pineal gland can be initiated by minimal photic cues, and that single photic transitions can be used as an experimental tool to dissect the mechanism which starts the circadian clock in the pineal gland.

10.2 Introduction

Life on earth is characterized by a 24-hour pattern of activity, reflecting the solar day. In essentially all forms, these rhythms are not directly controlled by the light/dark cycle, but reflect the action of an endogenous timing mechanism - the circadian clock - which exhibits a ~24 hour period. In addition, mechanisms exist through which the environmental lighting cycle synchronizes circadian rhythms with light-to-dark and dark-to-light transitions.

In contrast to the significant progress made in understanding the molecular basis of circadian clocks and how light acts on the clock (Vallone et al., 2004; Sato et al., 2004), scant progress has been made in understanding the fundamental question of what initially starts the clock 'ticking' - as defined by producing a coordinated output signal - and whether a

photic perturbation is required. This issue is of interest and importance in view of the fundamental role that circadian rhythms play in biology.

The question of whether the vertebrate circadian clock function develops autonomously or requires an external trigger has been investigated in zebrafish, at the molecular, physiological and behavioral levels. This has generated conflicting results. For example, studies on the transcription factor z*Per3,* a component of the circadian clock machinery, are at odds: expression was reported to oscillate under constant darkness (DD) by one group (Delaunay et al., 2000) but not by another using transgenic embryos expressing luciferase under control of the *zPer3* promoter (Kaneko and Cahill, 2005). It is clear that conclusions regarding clock function can not be based on observations of *zPer3* expression alone, because zPER3 is just one among other components of the clock machinery; accordingly it may not be a reliable indicator of the functional state of the clock. Other approaches in which physiological and behavioral endpoints have been used are also problematical because the endpoints are a reflection of factors other than clock development, including downstream processes and the mechanisms linking the two (Kazimi and Cahill, 1999; Hurd and Cahill, 2002). Accordingly, studies using these systems may not provide an entirely reliable indication of clock function.

An experimental approach which circumvents these limitations is the measurement of *Aanat2* mRNA in the fish pineal organ. The pineal organ is generally considered a master circadian clock in fish, and is of special experimental value because each pinealocyte contains all elements of a circadian system - a photoreceptor, a clock, and an output (Falcon, 2006), *i.e.*, mRNA encoded by the arylalkylamine *N*-acetyltransferase-2 (*Aanat2*) gene. *Aanat* encodes the next-to-last enzyme in vertebrate melatonin synthesis and *Aanat2* expression in the adult is controlled by integral elements of the molecular circadian clock, thereby providing a reliable marker of clock function (Appelbaum et al., 2005; Chen and Baler, 2000; Chong et al., 2000; Gothilf et al., 1999). In addition, measurement of *Aanat2* mRNA, is superior to the measurement of melatonin release from intact embryonic zebrafish, which has been used to study clock function (Kazimi and Cahill, 1999), because melatonin synthesis is regulated not only by the clock, but also by a downstream gating mechanism through which light acts to rapidly switch off melatonin production, without necessarily having immediate effects on clock function. As a result, it is not possible to study clock function in constant light, because light masks the output. However, measurement of *Aanat2* mRNA eliminates this limitation because light does not have an immediate effect on this parameter.

In the current study, we have examined the relationship between lighting and the rhythmic expression of zebrafish *Aanat2* and of another clock related gene, *exorhodopsin* (*ExR*), which encodes the photopigment thought to mediate photic control of the pineal clock (Mano et al., 1999). Our experiments addressed the issue of whether minimal photic perturbations can initiate circadian expression of each of these genes in the embryonic zebrafish pineal gland. Previous studies raised this possibility, because *Aanat2* mRNA transiently increased after exposure to a single 1 hour light pulse against a background of constant darkness (Ziv et al., 2005). The nature of the controlling mechanism was investigated here, to determine whether this increase was a transient one-time response to the light pulse (Ziv et al., 2005) or represented the initiation of a circadian rhythm. The results establish that circadian rhythmicity is initiated by a single light pulse and extend this finding by revealing that rhythmicity can also be initiated by a single dark pulse or by single photic transitions (light-to-dark: L→D, or dark-to-light: D→L). Moreover, our findings indicate that clock function is initiated before the retina can detect light and at a time when the pinealocyte is anatomically immature.

10.3 Materials and methods

10.3.1 Animals

Adult zebrafish were kept at 28.5°C on a 12/12 light/dark (LD) cycle. Light was provided by fluorescent lamps (λ = 400-700 nm; Nominal TX Universal aquarium lamps (IRC70-Lumen/W70), Actizoo, Beaufort La Vallée, France); the intensity at tank level was 5000 lux. Fertilized eggs were usually obtained in the morning shortly after lights on. They were incubated at the same temperature and under the indicated photoperiodic conditions (see Results section and legends of the figures). Embryos were collected at different developmental stages. Dark samples were maintained in the dark until time of collection; dim red light used for night collections was provided by 230V/15W red bulbs (PF712E, Philips, Suresnes, France), with an intensity not exceeding 6 lux at the level of the embryos.

For the whole-mount *in situ* hybridization, pigmentation of the embryos was prevented by addition of 0.2 mM phenylthiourea to the egg water at 24 h post-fertilization (hpf).

Animal experimentation was conducted in accord with accepted standards of humane

animal care (principles set out in the Declaration of Helsinki).

10.3.2 Whole-mount in situ hybridization

At the end of the incubation time, embryos were fixed overnight in 4% paraformaldehyde (PFA) in phosphate buffer saline (PBS) at 4°C, transferred to 100% methanol and stored at -20°C.

Whole-mount ISH was done using commercially available kits according to the manufacturer's instructions (Roche, Meylan, France). Sense and antisense digoxygenin (Dig)-labeled *zfAANAT2* riboprobes corresponding to a 900 bp cDNA of *Aanat2* (accession number: AF124756) were generated as described (Gothilf et al., 1999). The Dig-labeled *ExR* probes were generated from a fragment corresponding to bp 28-602 from *ExR* (accession number: AB025312) inserted in the Topo vector (Invitrogen, Meylan, France). All probes (1 µg/ml) were hybridized at a temperature of 68°C, and detection was performed using alkaline phosphatase (AP)-conjugated anti-digoxigenin antibodies, and AP substrate (Roche, Meylan, France). For each embryo, intensity of the staining was submitted to triple evaluation by three independent observers, within a scale of 0 (no staining at all) to 4 (highest signal intensity) (Delaunay et al., 2000)). Preliminary studies indicated that densitometry measurements on black and white photomicrographs gave similar results as also shown elsewhere (Gothilf et al., 1999)).

Statistics and data plotting were performed using the Instat-3 and PRISM-4 softwares (GraphPad™). Each time point included 5 to 10 individuals, and all embryos from a given experiment were treated simultaneously. Data are presented as the mean ± S.E.M.; they were analyzed by one-way or two-ways ANOVA. One-way ANOVA was followed, when significant, by Tukey's post comparison of means (for convenience, only a comparison of the higher and lower means are reported in the legend of the figures). Experiments were repeated at least twice, each on different days. Pictures were obtained using a C-35AD-2 Olympus camera on a BH-2 Olympus microscope.

10.3.3 Electron microscopy

Embryos and larvae were sampled at 22, 48, 72 hours post fertilization (hpf) and 11 days pf, and fixed for 2 hours in 4% glutaraldehyde/2% PFA, in 0.1 M phosphate buffer (PB)

pH 7.4. After a brief rinsing in PB, they were post-fixed in 1% osmium tetroxide for 1 h at room temperature. After rinsing in PB, all specimens were dehydrated in a graded ethanol series and embedded in araldite. Ultra-thin (50-70 nm thick) sections made on the pineal area were stained with 7% uranyl acetate in methanol, and contrasted with lead citrate (Reynolds, 1963). Sections were viewed and photographed on a Hitachi 7500 transmission electron microscope.

10.4 Results

10.4.1 Appearance of photoreceptor characteristics in developing pinealocytes

The embryonic pineal organ expresses *ExR* starting at 18 hpf (Figure 23A). The area of *ExR* expression becomes larger at 24 hpf (Figure 23B).

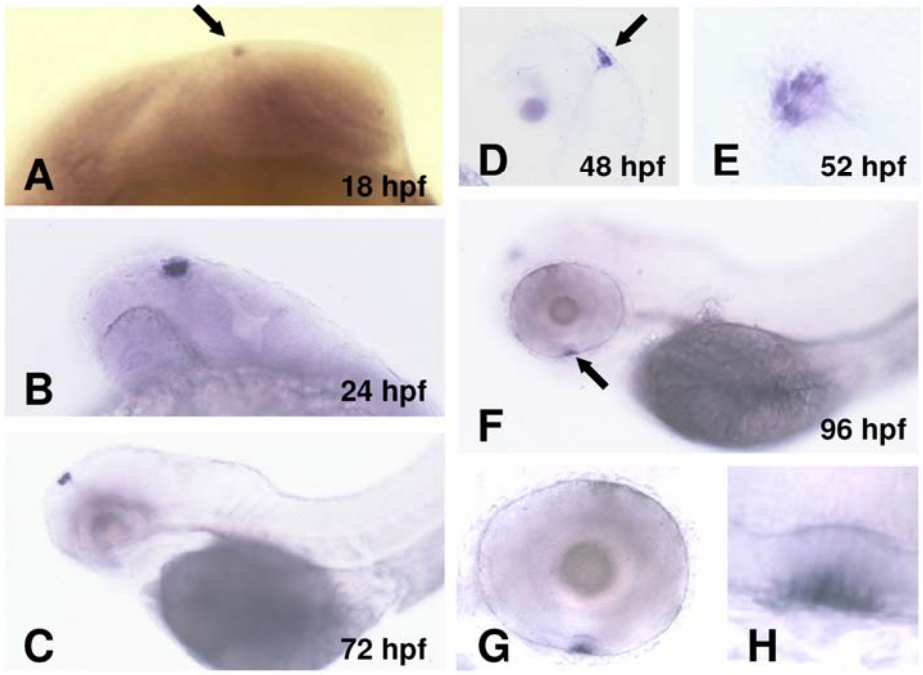

Figure 23. Localization of *Exorhodopsin* (*ExR*) expression in the developing zebrafish embryo. *ExR* mRNA was visualized using *in situ* hybridization (see Materials and Methods). (A-E) With the anti-sense riboprobe, a specific expression is evidenced in the pineal organ, which appears as a spot located dorsally of the embryo's head as early as 18 hpf (arrow in A). At higher stages, *i.e.*, from 24 (B) to 72 (C) hpf, the spot appears located dorsally (D) in the midline of the head, between the eyes. (E) shows a dorsal view of an embryo's pineal spot at 52 hpf; a few individual labeled cells are seen. (F-H) At later stages, some expression also appears in the ventral retina as shown by the arrow in (F). (G, H) are higher magnifications of the labeled retina in (F).

Expression is limited to the pineal organ until 72 hpf (Figure 23C-E); at 96 hpf weak expression occurs in the ventral retina (Figure 23F) at the level of the photoreceptor layer (Figure 23G, H).

Electron microscopic examination revealed that the initial *ExR* expression (18 hpf) is accompanied by the appearance of two defining structural characteristics of photoreceptors, centrosomes and [2x9+0] ciliary structures (Figure 24A); a third feature of photoreceptors, the extensive infoldings of plasma membranes, first becomes obvious at 48 hpf (Figure 24B).

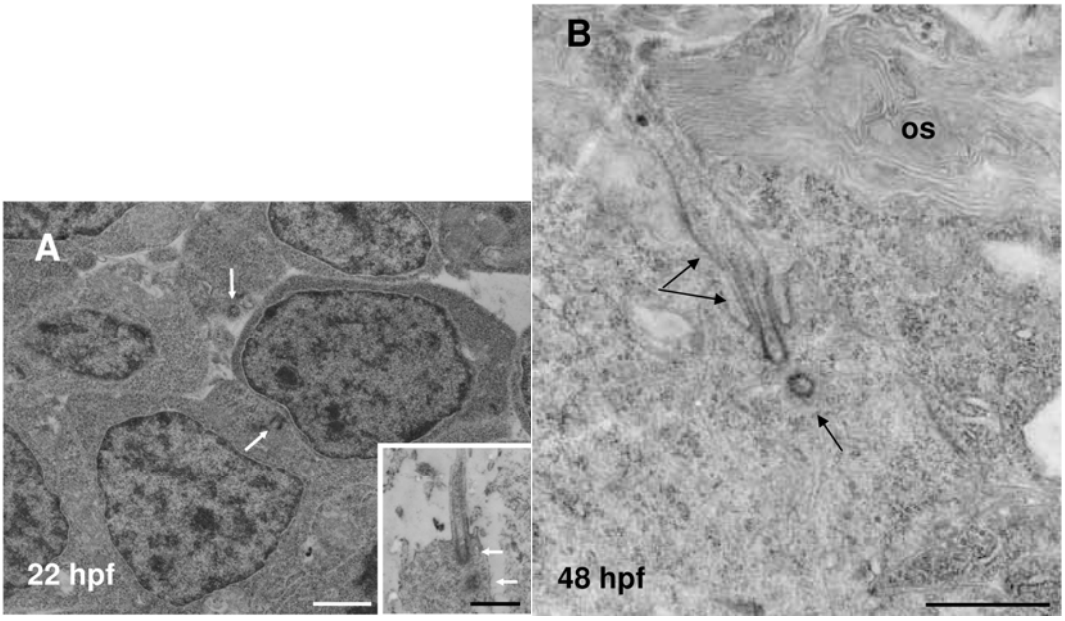

Figure 24. Ultrastructure of zebrafish pineal photoreceptor cells at early stages of development. (A) At 22 hpf the pineal cells show little signs of differentiation, except the cilia of the 9x2+0 type and the associated centrosome (arrows, and inset). (B) At 48 hpf photoreceptors are fully differentiated, and the well developed outer segment (os) arises from the cilia (arrows). Bars = 1 μm.

10.4.2 Rhythmic expression of ExR and Aanat2 develops in LD but not in LL or DD

ExR and *Aanat2* mRNAs were studied in parallel as a function of environmental lighting. Daily rhythms in both were detected in LD, but were only statistically significant for *Aanat2*; rhythmic changes in these mRNAs were not apparent in LL or DD (Figure 25).

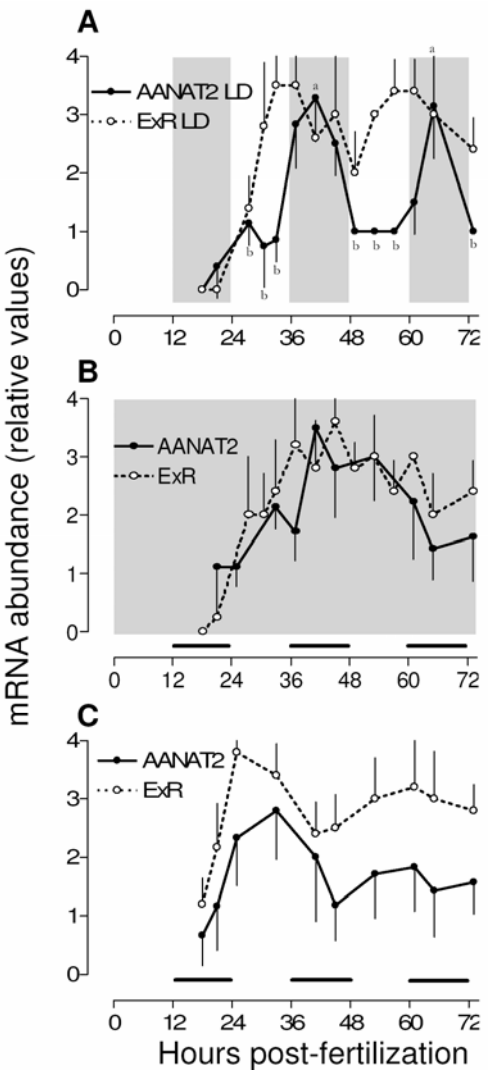

Figure 25. *ExR* and *Aanat2* mRNA abundance under light/dark (LD) and constant (DD, LL) conditions. Embryos were kept at 28.5 °C under either a 12:12 LD cycle (A), DD (B) or LL (C). The grey boxes correspond to the dark phases (which are the same as those of the embryos genitors in A). The black bars at the bottom (B, C) indicate the subjective dark phases (dark phases of the genitors). Embryos were collected at the times indicated and processed for the *in situ* hybridization; mRNA abundance was estimated as indicated in Materials and Methods. Mean ± S.E.M. (n = 7-10). '0' in the abscissa corresponds to 8 a.m. (time of fertilization). One-way ANOVA indicated that *Aanat2* mRNA abundance did not vary significantly under DD or LL. However, significant changes occurred under LD ($P<0.0003$); 'a' significantly different from 'b' (Tukey's post comparison of means, $P<0.05$). Differences in *ExR* mRNA abundance were not statistically significant under any of the conditions tested. Similar results were obtained in two other experiments.

10.4.3 Circadian rhythmicity of Aanat2 is maintained following LD cycles or a single dark pulse

Aanat2 was expressed rhythmically for at least 24 h in LL, if animals were first exposed to either two 12:12 LD (not shown) or two DL cycles (Figure 26).

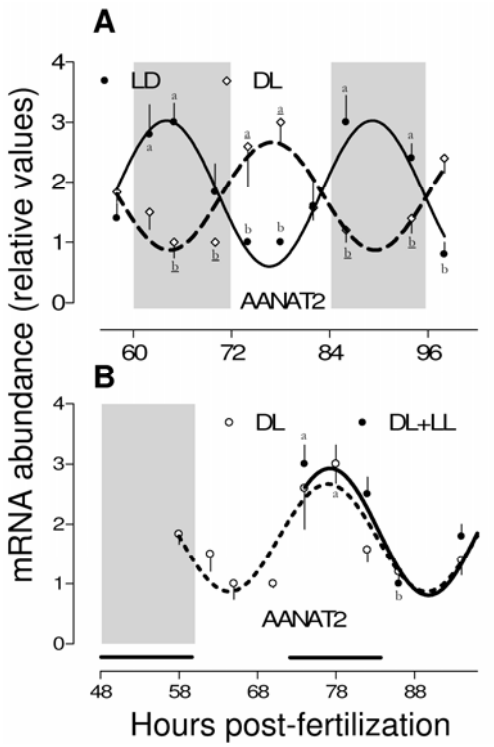

Figure 26. *Aanat2* mRNA abundance under a reversed DL cycle (A) followed by constant light (B). (A) Embryos were placed under a LD cycle (controls; 'solid' line) or a reversed DL cycle (DL; dashed line) from fertilization. (B) An initial DL cycle was followed by constant light (LL) at 60 hpf (solid line); the controls (dashed line) were maintained under DL. The grey panels correspond to the dark phases. Embryos were collected at the times indicated and processed as in Figure 25. Mean ± S.E.M. (n = 7-10). The data fitted a sinusoidal; in each curve the variations in mRNA abundance were statistically significant (one-way ANOVA: P<0.005 or below). 'a' significantly different from 'b', and 'a' significantly different from 'b' (Tukey's post comparison of means, P<0.05) Similar results were obtained in two other experiments.

It was also found that rhythmicity was induced in LL following a single dark pulse applied at 24 hpf, and that the phase of the circadian rhythm was a function of pulse duration (Figure 27). The finding that the *Aanat2* mRNA rhythm persists for two cycles, and with similar amplitude, strengthens the idea that this represents a true circadian rhythm, rather than a one-time transient response.

10.4.4 Photic pulses initiate circadian rhythmicity of Aanat2

The above experiment used a dark pulse against an LL background. Similarly, a light pulse (1 to 8 hours) against a DD background induced circadian expression of *Aanat2* (Figure 28): the phases of the subsequent oscillations were similar, independent of the pulse duration.

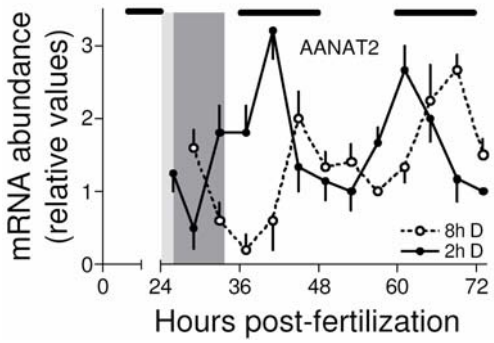

Figure 27. Effects of dark stimuli of different durations on *Aanat2* mRNA abundance in embryos maintained under constant light (LL). Embryos were maintained under LL from fertilization; a dark stimulus of 2 (light grey, solid line) or 8 h (dark grey, dashed line) duration was applied at 24 hpf, as indicated. Embryos were then processed as indicated in Figure 25. The black bars at the top of each column indicate the subjective dark phases (dark phases of the genitors). Mean ± S.E.M. (n = 7-10). In each curve the observed variations in mRNA abundance were statistically significant as indicated by the one-way ANOVA analysis ($P<0.005$); Tukey's post-comparison of individual means indicated that peak and nadir values differed from each other ($P<0.05$). Pulse duration affected significantly the shape of the oscillations, as indicated by a two-ways ANOVA comparison of the data ($P<0.0008$). '0' in the abscissa indicates time of fertilization (8 a.m.). Similar results were obtained in a second experiment.

However, variations induced by the 1 h pulse were not significant and of lower amplitude than those obtained with the 2 or 8 h pulses.

Thus, 4 hour pulses of light applied at successive points during the 20- to 46-hpf period induced corresponding delays in peak appearance (Figure 29). Conversely, the appearance of the peak in *Aanat2* mRNA abundance depended on the time at which the pulse was applied.

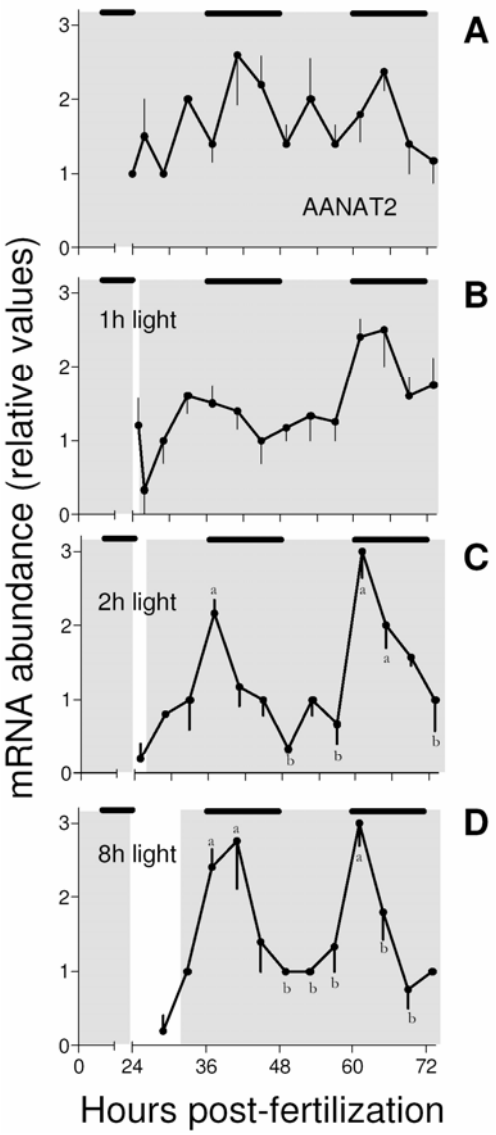

Figure 28. Effects of light pulses of different duration on *Aanat2* mRNA abundance in embryos maintained under constant darkness (DD). Embryos were maintained under DD (A) from fertilization and a light pulse of 1 (B), 2 (C) or 8 (D) h was applied at 24 hpf, as indicated. They were then processed as indicated in Figure 25. The black bars at the top indicate the subjective dark phases (dark phases of the genitors). The grey panels indicate darkness for the embryos. Mean ± S.E.M. (n = 7-10). '0' in the abscissa indicates time of fertilization (8 a.m.). One-way ANOVA indicated that the variations in mRNA abundance were statistically significant only in (C) (2h light pulse) and (D) (8h light pulse) ($P<0.0001$). 'a' significantly different from 'b' (Tukey's post comparison of means, $P<0.05$). Two-ways ANOVA indicated that the 2 h and 8 h light pulses curves were significantly different from the DD curves ($P<0.01$), but the duration of the pulse (2 h *vs*. 8 h) had no significant effect ($P<0.7$). Similar results were obtained in another experiment.

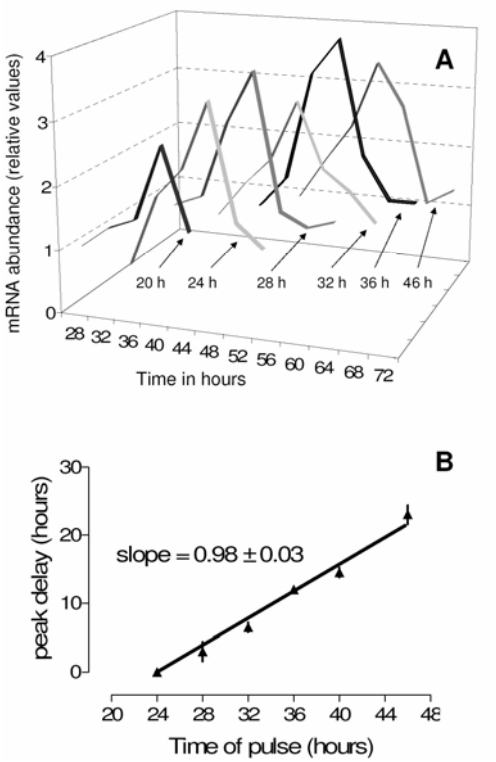

Figure 29. Effects of light pulses applied at different post-fertilization times on the circadian expression of *Aanat2* mRNA abundance in embryos maintained under constant darkness (DD). (A) Embryos were maintained under DD from fertilization. A 4 h light pulse was applied at 24, 28, 32, 36, 40 or 46 hpf as indicated; embryos were collected shortly after at different time intervals and processed as indicated in Figure 25. Mean ± S.E.M. (n = 5-10); error bars are not shown for clarity of the graph. ANOVA indicated that the variations in mRNA abundance differ significantly in all curves ($P<0.0001$); in each curve, Tukey's post comparison of means indicated that the peak values were different from the nadir values ($P<0.001$). (B) Data are replotted from those presented in (A). There is strict correlation between the times at which the light pulses are applied (abscissa) and the corresponding phase delays in peak appearance reported in the ordinates (time of peak appearance minus time of peak obtained with the first pulse of light).

10.4.5 Single photic transitions (D→L or L→D) initiate circadian rhythmicity of Aanat2

The above photic perturbations involve two photic transitions, L→D at the start and D→L at the end of the dark pulse. It was also found that a single cue initiated clock function when the D→L transition occurred at 21 hpf or later (Figure 30A-E). In a reversed experiment, embryos were raised under LL and then switched to DD; this initiated circadian oscillations when the L→D transition occurred at 21 hpf or later (Figure 30A'-E').

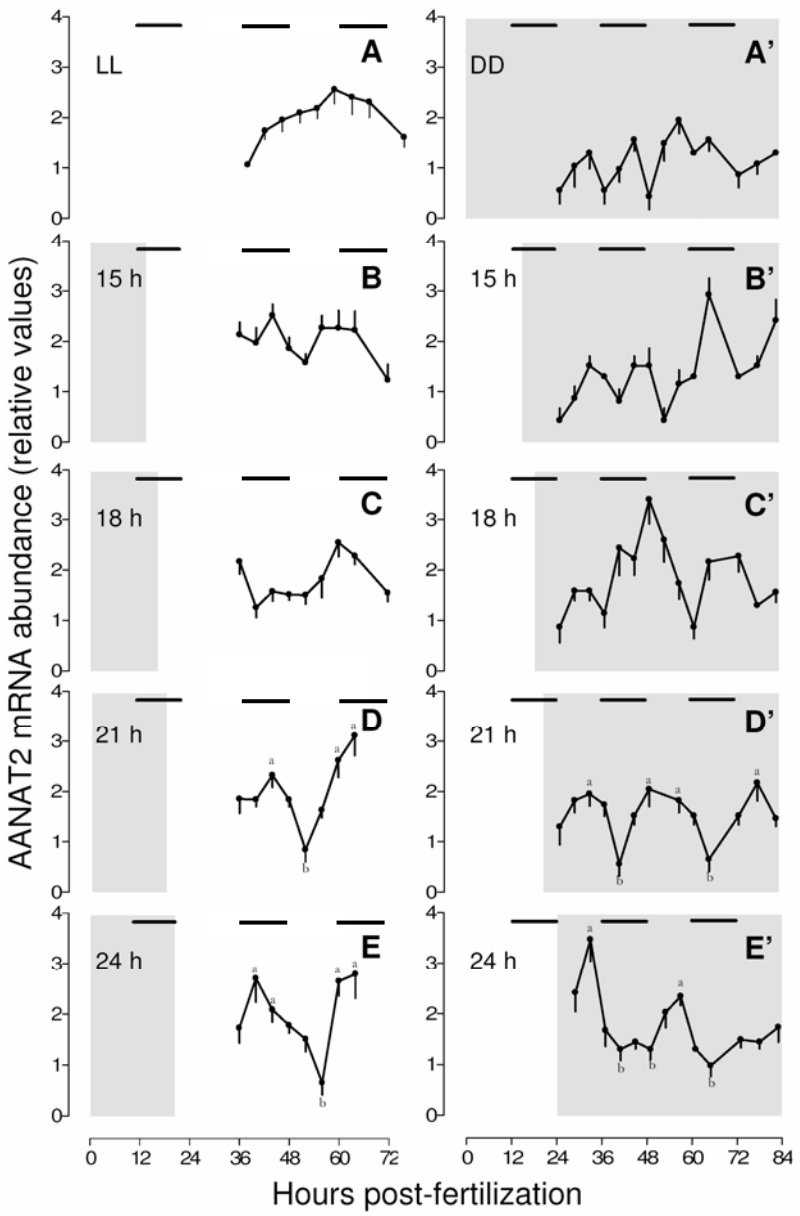

Figure 30. Effects of dark-to-light and light-to-dark transitions on *Aanat2* mRNA abundance. (A-E) Embryos were maintained under constant light from fertilization (A: LL), or first exposed to darkness for 15 (B), 18 (C), 21 (D) or 24 (E) hours, before being released under LL. A'-E'. Embryos were first placed under constant darkness (A': DD) from fertilization or exposed to light for 15 (B'), 18 (C'), 21 (D') or 24 (E') hours before being released under DD. They were then processed as indicated in Figure 25. The black bars at the top of graph indicate the dark phases of the genitors, and the grey boxes indicate darkness for the embryos. Mean ± S.E.M. (n = 7-10). Two-ways ANOVA indicated that the curves in D and E were not different from each other, but differed from the others (A-C) ($P<0.0001$). Similarly, the curves in (D') and (E') were not different from each other, but differed from the (A'-C') curves ($P<0.0001$). 'a' significantly different from 'b' (Tukey's post comparison of means, $P<0.05$) '0' in the abscissa indicates time of fertilization (8 a.m.). Similar results were obtained in an independent experiment.

10.5 Discussion

One of the advances of this study is finding that elements of the three functional components of circadian clock system in the zebrafish pineal organ - photodetection, clock function and output – appear to be in place at the end of day 1 pf. This is coincident with the appearance of the first pinealofugal nerve fibers (19 hpf) (Wilson and Easter, 1991). It is of interest to note that at this point in development, pinealocytes appear to be anatomically immature compared to those observed day 2 (this study) or day 6 pf (Allwardt and Dowling, 2001). At 24 hpf they lack the defining feature which characterizes the adult pinealocyte – distinct photoreceptor outer segments – while containing the characteristic 2x9+0 cilia from which the outer segments develop (Allwardt and Dowling, 2001; Falcon, 1999; Tsujikawa and Malicki, 2004). The expression of *ExR* at day 1 pf is likely to explain pinealocyte photosensitivity at this stage. Accordingly, it appears that at day 1 pf, when the pinealocyte is not anatomically mature, it is fully capable of functioning as a complete circadian system, capable of responding to light. The interpretation that at this stage of development light acts indirectly on the pineal gland through another structure is less attractive because it assumes a developmental extrinsic→intrinsic switch in how light regulates the pineal circadian clock.

Our results also provide additional support to the view that fish pineal photoreceptors develop before retinal photoreceptors (Forsell et al., 2002). Specifically, at 24 and 48 hpf, photodetector features were not evident in the zebrafish retina (data not shown). The first rudiments of retinal photoreceptor outer segments are not observable before 54 hpf (Schmitt and Dowling, 1999), whereas the initial retinal expression of an opsin gene is not seen before 40 hpf (Takechi and Kawamura, 2005). It is however not impossible that other pigments function during this period of time in the retina. We also detected *ExR* expression at day 4 pf in the ventral retina, as has been described for *Aanat2* (detectable at day 3 pf) (Gothilf et al., 1999), indicating that retinal *ExR* expression is developmentally transient. In contrast to the day 4 pf retinal expression of *ExR*, pineal expression was detectable at 24 hpf, when structural features of photoreceptors were also apparent. Earlier development of pineal photoreceptors relative to that of retinal photoreceptors is intriguing, because similar transcription factors control expression of the same or closely related genes in each tissue. It will be of interest to determine the molecular basis of this temporal difference.

Previous observations have been interpreted to indicate that the nocturnal increase in *Aanat2* mRNA abundance is itself triggered by light-induced expression of *Per2* (Ziv et al., 2005). If this was the only condition, however, one would expect an increase in *Aanat2*

expression to occur under LL once the pineal becomes activated, *i.e.*, between 18 and 24 hpf. This was not observed, *i.e,.* neither a surge, nor endogenous oscillations in *Aanat2* expression was observed in embryos raised under LL from birth. Accordingly, it would appear more accurate to conclude that the embryos also needed to experience both dark and a photic transition. This is supported by the finding that circadian oscillations in *Aanat2* expression occurred under LL providing that the embryos were previously exposed to an LD or DL cycle. Moreover, a single transition from DD to LL, or LL to DD, initiated circadian oscillations in *Aanat2*, providing that this transition occurred at 21 hpf or later. This is consistent with the proposal that exposure to both light and darkness is necessary to initiate pineal clock function. However, it is not yet clear whether this initiation of pineal clock function reflects the start of the circadian clocks in individual pinealocytes or the synchronization of active clocks in these cells, or both.

Synchronization of the clocks in individual pinealocytes may involve light-dependent induction of *Per2* (Ziv et al., 2005), and dark-dependent induction of a yet-unidentified factor, both of which could interact with components of the transcriptional/translational feedback loop which constitutes the circadian clock (Iuvone et al., 2005; Reppert and Weaver, 2002). From the effects of dark pulses under LL and light pulses under DD, it appears that the timing of light onset, not duration, determines the phase of the resulting circadian rhythm. The results of these studies provide clear indication that *Aanat2* is under circadian control. This is likely to reflect the presence of E-Box elements (Appelbaum et al., 2005), which mediate circadian control of many genes through interactions with protein components of the clock (Appelbaum et al., 2005; Hardin, 2004; Munoz and Baler, 2003). The mechanism underlying the non-circadian photic control of *ExR* expression in LD lighting cycles remains unknown.

In summary, the present study provides evidence that the circadian system in the zebrafish pineal organ is potentially functional as early as 18-21 hpf, *i.e.*, two days before the retina. Anatomically immature pinealocytes are capable of transducing light signals and generating circadian oscillations in *Aanat2* expression. Accordingly, it appears that light sensitivity, circadian clock function and output are present early in embryonic development and that the pineal gland - not the retina - mediates photic responses at this stage. Our results also provide further support to the interpretation that minimal photic cues are sufficient to initiate pineal circadian clock function during development. Finally, it appears that light perception *per se*, as provided by LL, is not sufficient to initiate the circadian oscillations; rather, a photic transition is required, with the time of light onset determining

the subsequent phase of the oscillations. This and previous studies (Ziv et al., 2005) suggest that the onset and entrainment of the pineal circadian clocks need both light and darkness, *i.e.*, light acting through induction of *Per2* expression, and darkness acting through a yet unknown mechanism. It remains to be determined whether the photic transitions (L→D or D→L) start the clock 'ticking' in each cell or synchronizes circadian activity of individual cells, or does both. These questions may be asked, using the paradigm established here, in which single photic transitions are sufficient to generate a circadian output, *i.e., Aanat2* mRNA.

We examined in a previous study the establishment of the pineal and retinal functions during zebrafish development. To get significant insights concerning the evolution of the molecular mechanisms triggering it among the Teleost group, we examined the situation in a Teleost species phylogenetically far away from zebrafish , namely the turbot.

The following work presents the characterization and expression pattern of three relevant marker genes of the photoreceptive organs during turbot development.

11. Characterization, transcriptional regulation and evolution of two melatonin biosynthesis enzymes during development of the turbot (Scophthalmus maximus), a flatfish.

11.1 Abstract

In the pineal gland, melatonin biosynthesis from serotonin involves the sequential activity of the Arylalkylamine *N*-acetyltransferase (AANAT) and the Hydroxyindole-*O*-methyltransferase (HIOMT). In all vertebrate species studied to date, photoperiod synchronizes a daily rhythm in melatonin secretion, through controlling AANAT activity, which is higher at night than during day. Although several studies have carried on the modalities of this photoperiodic control in adult Teleost, the establishment of this function during embryonic development remains relatively unknown. In addition, the majority of the studies focused on Teleost phylogenetically far away from representatives displaying more recent phenotypical characters such as flatfish including the turbot.

In this study, we report the cloning of the full-length cDNA of an Arylalkylamine N-acetyltransferase gene (Sm*Aanat2*) and, for the first time in an ectothermic vertebrate, the full-length cDNA of a Hydroxyindole-O-methyltransferase gene (Sm*Hiomt*), in the turbot. We then examined the expression pattern of both genes during embryogenesis and larval stages and we found that the expression of *SmAanat2* is pineal gland specific whereas the *SmHiomt* gene is expressed in both the photoreceptors of the retina and the pineal gland. In contrast to zebrafish, turbot embryos and larvae kept in a 12h Light/Dark cycle from fertilization onward display no cyclic accumulation of the two messengers. This result suggests that the molecular mechanisms controlling the establishment of the pineal functions during embryonic development have been modified during Teleosts' evolution.

11.2 Introduction

In vertebrates, melatonin is a major synchronizer of physiological and behavioural processes to the daily and seasonal variations of photoperiod (Zachmann et al., 1992; Pevet, 2003; Arendt and Skene, 2005; Barrenetxe et al., 2004). Melatonin is biosynthesized by two neural organs, the retina and the pineal gland. However, it is generally admitted that retinal melatonin acts and is metabolized *in situ*, whereas pineal melatonin is released into the blood and cerebrospinal fluid. Melatonin biosynthesis from serotonin is mediated by the sequential activity of two enzymes (Klein et al., 1981; Klein et al., 1997). The Arylalkylamine *N*-acetyltransferase (AANAT; EC 2.3.1.87) first catalyses the conversion of serotonin to *N*-acetylserotonin; then, the Hydroxyindole-*O*-methyltransferase (HIOMT; EC 2.1.1.4) allows formation of melatonin from *N*-acetylserotonin (Klein et al., 1997). In the pineal gland and retina of most species, a nocturnal rise in AANAT protein amount and AANAT activity is responsible for the increase in melatonin; light turns off the system by inducing AANAT protein degradation by proteasome proteolysis (Gastel et al., 1998; Falcon et al., 2001). In most Teleost species studied so far, in chicken and in rodents, the nocturnal rise in AANAT protein and activity amount is due to an increase in *Aanat* gene expression (Schomerus and Korf, 2005; Gothilf et al., 1999; Begay et al., 1998). In contrast, in rainbow trout, ungulates and primates, there is no rhythmic changes in *Aanat* gene expression during the Light/Dark (LD) cycle and therefore the rhythmic AANAT activity in these species is only dependent of post-transcriptional controls of the protein (Schomerus and Korf, 2005; Begay et al., 1998). *Hiomt* gene expression may also vary on a daily basis in several endotherms studied to date, although HIOMT activity in these species displays a rhythm of weak amplitude throughout the LD cycle (Falcon, 1999; Ribelayga et al., 1999).

In vertebrates, levels of the circulating hormone are high at night and low during the day reflecting the photoperiodic control of melatonin secretion by the pineal gland. In most vertebrate species investigated so far, this control results from the action of light on circadian clocks, which in turn impact on the melatonin production machinery (Falcon, 1999, Klein et al., 1997). In ectotherms, all three elements - *i.e.*, light detection, circadian clock activity and melatonin biosynthesis - operate within one cell type, the pineal and retinal photoreceptors (Falcon, 1999). In mammals, the three components are located in distinct areas: light is detected by the retina and the photoperiodic signals synchronize and entrain the autonomous activity of circadian clocks located in the suprachiasmatic nuclei (SCN) of the hypothalamus. In turn, the rhythmic signals from the SCN are transmitted to the pineal

gland, through a complex multisynaptic pathway (Klein et al., 1981). Intermediate situations are found in birds (Falcon, 1999). Despite these profound anatomic modifications in the ways melatonin secretion is controlled, similar processes contribute to control melatonin biosynthesis within the pineal gland; the nocturnal pattern has been preserved, emphasizing its importance in vertebrates.

Teleost fish represent the largest group of vertebrates and their last common ancestor (LCA) appeared about 250 million years (Myr) ago. One of the first group that diverged at about 110 Myr ago from the Euteleostei was the Ostariophysi including zebrafish, and the LCA evolved about more than 60 Myr until the Percomorpha including pufferfish and flatfish appeared (Wittbrodt et al., 2002; Lauder and Liem, 1983). Hence, regarding evolution of the melatonin system, Teleost fish are of special interest. In addition, they display specific features such as the presence of two *Aanat* genes, *Aanat1* expressed in the retina, and *Aanat2* mostly expressed in the pineal organ with no orthologue in other vertebrates investigated so far (Coon et al., 1999; Gothilf et al., 1999; Benyassi et al., 2000). Moreover, there is a great variability at the morphological, physiological, biochemical and molecular levels among the different species studied (Falcon, 2006). For instance, the rhythm in melatonin production is under circadian control in most examined Teleost including zebrafish, pike and turbot (Cahill, 1996; Bolliet et al., 1996; Rebollar et al., 1999) but not in rainbow trout in which it is under direct photoperiodic control (Gern and Greenhouse, 1988). In order to decide whether these variabilities reflect specific adaptation in a given family of fish, or an evolutionary trend among Teleost, more Teleost fish species have to be examined. This is particulary the case for representatives displaying more recent phenotypical characters such as the Percomorpha for which embryonic and larval data are still missing. In this regard, flatfish are relevant because they are sister group of pufferfish (Nelson, 1995). In addition, they undergo a "true" metamorphic process in the course of their development (Evans and Fernald, 1993; Graf and Baker, 1983; Schreiber, 2001) allowing to examine the events triggering cell proliferation and differentiation over a longer period compared with other Teleosts.

In this study, we focus on the turbot and report the full-length cDNA cloning of the *Aanat2* and *Hiomt* genes, protein characterization and expression patterns during embryonic and larval stages. Furthermore, we also cloned the full-length cDNA encoding the orthodenticle homeodomain protein 5 (*Otx5*), a circadian regulator of the *Aanat* and *Hiomt* genes (Gamse et al., 2002; Appelbaum et al., 2005) and compare its expression pattern with both downstream genes cited above. The data presented here provide entirely new evolutive

insights concerning the establishment of the molecular mechanisms controlling the expression of the enzymes involved in the melatonin biosynthesis by the pineal gland.

11.3 Materials and methods

11.3.1 Experimental animals

Embryos and larvae of turbot (*Scophthalmus maximus*) were obtained from France Turbot (Noirmoutier, France) where they were reared in seawater at 16°C, as detailed elsewhere (Person-Le-Ruyet, 1989). Embryos and larvae of zebrafish were reared in fresh water at 28,5°C as detailed elsewhere (Westerfield, 1993). Embryos and larvae were collected at different developmental stages during day and night; night samples were collected under dim red light. They were frozen in dry ice for RNA or DNA extraction, or fixed overnight in 4% paraformaldehyde (PFA) in PBS at 4°C, washed in PBS, and finally stored in methanol at -20°C for whole mount *in situ* hybridization.

11.3.2 Cloning of full-length cDNAs

Fragments of *S. maximus Aanat2* and *Hiomt* genes were isolated by nested PCR after reverse transcription of mRNA, extracted from a pool of embryos (48, 72, 96 and 120 hours post-fertilization; hpf) and larvae (20 days post-hatching; dph). The degenerated primers indicated in table 1 were used for the cloning of the *Aanat2* and *Hiomt* genes:

Primer	Sequence (5'→ 3')
SmAanat2 forward	GTTTGA(A/G)ATCGAGAGAGA(A/G)GC
SmAanat2 reverse	CTA(A/G)CA(G/T)CC(A/G)CTGTT(C/G/T)CG(C/T)CG
SmAanat2 nested reverse	TTCTGGTAGAAGGG(A/C/G)ACCAG
SmHiomt forward	TAC(C/G/T)(G/T)GTGCTGG(C/G)GCCACCTG
SmHiomt reverse	AGGTC(A/G)CA(A/C/G)AT(A/C/G)AGTG(G/T)GAA
SmHiomt nested forward	GGC(A/T)GA(C/T)GC(A/C/T)GT(C/G)AGAGAAGG
SmHiomt nested reverse	GAAC(A/G)(C/G)(C/G/T)GA(A/C)AGGTCAAAGGC

Table 1. Degenerated primers used to clone *SmAanat2* and *SmHiomt*.

The PCR amplification was as follows: 2 minutes at 95°C, 15x (20 seconds at 94°C, 1 minute at 37°C, 1 minute at 68°C) then 25x (20 seconds at 94°C, 1 minute at 42°C, 1 minute at 68°C) followed by 7 minutes at 68°C. The conditions for the nested PCR were : 2 minutes at 95°C, 30x (20 seconds at 94°C, 1 minute at 48°C, 1 minute at 68°C) followed by 7 minutes at 68°C. Full-length sequences were obtained by 5′ and 3′-RACE (Rapid Amplification cDNA Ends) PCR following the standard protocol (Clontech, BD Bioscience).

Specific primers were designed from fragments of *S. maximus Aanat2*, *Hiomt* and *Otx5* genes (Sm*Aanat2*: forward, 5′AGCAGTGGTATCAACGCAGAGTAC3′; nested forward, 5′GATGGCACAGCAGGTCAGCGGCTCACCGT3′; reverse, 5′CGCAGGTACTGCAAGTAG CGCCACAG3′; nested reverse, 5′GAGGATGGAGCCCTTGCCCTGCTGGCG3′; *SmHiomt*: forward, 5′GACCGACGCTGTCAGAGAGGGAAGAAACC3′; nested forward, 5′GCTCTCT ACAGGTGTGACGAGGAGATGG3′; reverse, 5′CGTGACCACGTCTTTACCACAGATGTT CC3′; nested reverse, 5′CCATCTCCTCGTCACACCTGTAGAGAGC3′; *SmOtx5*: forward, 5′AGAATGATGTCCTACATAAAGCAGCCCCA3′; nested forward, 5′CCGAGGAAGCAGC GTCGAGAGCGCACCAC3′; reverse, 5′CCGCTGGTCTGCTGCTGCTGCTGGCGGCA3′; nested reverse: 5′TTAGCACGACGGTTCTTA AACCACACCTG3′) and used in nested PCR.

For *Aanat2*, 5′-RACE was done first and the amplified fragment was used to design forward primers for the 3′-RACE. The conditions for the first round of PCR were 2 minutes at 95°C, 30x (13 seconds at 94°C, 1 minute at 66°C(*Aanat*) or 64°C(*Hiomt*) or 63°C(*Otx5*), 3 minutes at 68°C) followed by 7 minutes at 68°C. Same conditions were used for the nested PCR except that the number of cycles was 25.

11.3.3 Proteins alignments, inference of phylogenetic trees and sequence analysis

Deduced full-length amino acid sequences of AANAT and HIOMT were aligned using PipeAlign (Plewniak et al., 2003). The Phylo_win version 2.0 software program was used to infer phylogenetic trees (Galtier et al., 1996). After gaps removing, trees were inferred by the Neighbor Joining method (NJ). The degree of support for internal nodes was assessed using 1000 bootstrap replications. Sequences were analyzed by BLASTP (Altschul et al., 1997) and PROSITE motif search (Bairoch et al., 1997).

11.3.4 In situ hybridization

The same *in situ* hybridization procedure was used for whole mount embryos and larvae. *In vitro* synthesis of the riboprobes (*SmAanat2*: bases 399-1315 in Figure 31; *SmHiomt*: bases 202-1027 in Figure 33; *SmOtx5*: bases 218-1280 in Appendix 7) and the high stringency *in situ* hybridization protocol were as detailed elsewhere (Thisse et al., 2004). After staining embryos and larvae were post-fixed in 4% PFA in PBS. For embyos and larvae, intensity of the pineal staining was evaluated independantly by two observers within a scale of 0 (no staining at all) to 3 (highest signal intensity) (Delaunay et al., 2000). At some occasions, stained larvae were dehydrated in PBS/10% glycerol/20% sucrose overnight at 4 °C; they were then included in Tissue Freezing Medium (Jung), frozen in dry ice, and cut (30 µm) using a Leica CM1900 cryotome. Embryos, larvae and sections were mounted in 100% glycerol prior to being photographed (Canon Powershot S45 digital camera).

11.3.5 Genomic Southern blot analysis

Southern blots of genomic turbot DNA were prepared according to Sambrook and Russel (2001). Ten micrograms of genomic DNA extracted with a DNeasy tissue kit (Qiagen) from juvenile turbots were digested with either BglII, EcoRI or SacI and loaded on a 0.7% agarose gel. After electrophoresis, DNA fragments were blotted overnight and UV-crosslinked to a positive charged nylon membrane (Nytran, Schleicher & Schuell). The blot was then hybridized with a 123 bp SmHiomt PCR α^{32}P radiolabeled DNA probe (bases 901-1024 in Figure 33). The moderate-stringency hybridization was performed in 6x SSC, 10x Denhardt's, 1mM EDTA, 0.2% SDS and 0.1 mg/ml tRNA at 62 °C, followed by washes in 1x SSC, 0.1% SDS at 58 °C. The images were generated from a PhosphorImager.

11.3.6 Reverse Transcription (RT) and quantitative real time PCR

Total RNA extractions were performed from *S. maximus* embryos and larvae sampled at 51, 57, 63, 69, 75, 81, 87, 93, 99, 105 and 111 hpf and from *D. rerio* embryos at 28, 34, 40, 46 and 52 hpf according to the standard protocol (TRIzol reageant, Invitrogen). After digestion of residual genomic DNA with 2 units of DNAse I (Promega) during one hour at 37 °C, 500 ng of total RNA of each stage were used as a template for first strand cDNAs synthesis using oligo-dT primer and the Superscript III reverse transcriptase kit (Invitrogen). The reaction

proceeded for 1 hour at 50°C followed by the inactivation of the enzyme at 94°C during three minutes. Real time PCR amplification of cDNAs was then carried out in a LightCycler (Roche) using a QuantiTect™ SYBR® Green PCR kit (Qiagen) as described in the standard protocol. The reaction mixture included 2 µl of cDNA, 1x SYBR Green mix and 0.5 µM of each specific forward and reverse primers. Real time PCR amplification of cDNAs conditions were as follows : 15 minutes at 95°C, 15 seconds at 94°C, 20 seconds at 57°C, 10 seconds at 72°C over 50 cycles. The fluorescence of the amplified products was detected 5 seconds at 76°C after the elongation step. For each sample point, a melting curve was obtained at the end of the PCR amplification allowing us to verify the specificity of the amplificon. In each experiment and for each gene, a standard curve generated by four dilutions from one cDNA sample was included in the PCR amplification to determine an expression value for each samples. Experiments were realized two times in triplicates and normalized with *Elongation factor 1 alpha* (*Ef1a*), a housekeeping gene. The following specific primers used in the experiment were designed with the Primer3 software (Rosen and Skaletsky, 2000) from the *SmAanat2* , *SmHiomt* , *SmEf1a* (GenBank accession number AF467776), *ZfAanat2* (GenBank accession number NM131411) and *ZfEf1a* (GenBank accession number NM131263) genes :

SmAanat2 forward : 5'ATTCCACGAGATGGAGTACACG3'
SmAanat2 reverse : 5'TGGTGAGTAAGTCGGAGTGTAAGG3'
SmHiomt forward : 5'GAGGGCAGGGAGAGGACAG3'
SmHiomt reverse : 5'TCTTGATACATGAGTAGCCGAGGT3'
SmEf1a forward : 5'CTCACATCGCCTGCAAGTTC3'
SmEf1a reverse : 5'GACACACATGGGCTTTCCAG3'
ZfAanat2 forward : 5'CGACGAAACAGCGGATGTTAG3'
ZfAanat2 reverse : 5'GAACCTTTGAGCCTGTGATCG3'
ZfEf1a forward : 5'TCCCAACCTCTTGGAATTTCTC3'
ZfEf1a reverse : 5'TGAAAGAGGCACTATCAGTCAAT3'

11.4 Results

11.4.1 Isolation of S. maximus Arylalkylamine N-acetyltransferase-2 (SmAanat2) cDNA

The first round of PCR using degenerated primers allowed isolating a 258 bp fragment displaying similarity with the N-acetyltransferase domain of *Aanat2* from other species. From this sequence we designed specific primers that allowed amplification of a 440 bp fragment by 5′ RACE PCR. This 5′ DNA fragment was used to design specific primers that were used for the 3′ RACE PCR; a fragment of 1309 bp was amplified. Put together, the two fragments corresponded to the entire full-length cDNA of *SmAanat2* gene. The *Sm*A*anat2* cDNA contains a deduced 624 bp open reading frame (ORF) encoding 208 amino acids flanked by a 7 bp 5′ UTR and a 684 bp 3′ UTR which is terminated by a 30 bp poly(A) tail (Figure 31). One putative poly(A) addition signal is located immediately upstream of the poly(A) tail (underlined in Figure 31). The deduced protein contains an acetyltransferase domain of 93 amino acids (shaded in Figure 31), two putative acetyl coenzyme A binding motifs namely Motif A and B, two phosphorylation sites for protein kinase A (PKA) critical for the activation and the stabilization of the protein (Ganguly et al., 2001; Ganguly et al., 2005), three highly conserved regions found in vertebrates, namely C/c-1, D/c-1 and D/c-2, four highly conserved histidine residues and four highly conserved cystein residues which are important for disulfide bond formation in AANAT (Figure 31) (Klein et al., 1997; Craft and Zhan-Poe, 2000). The alignment of the deduced *Sm*AANAT2 amino acid sequence with other AANAT sequences indicated strong similarity with Teleost fish AANAT2 (rainbow trout, 84%; zebrafish, 83%; pike, 82%, sea bream, 72%), and less similarity with vertebrates' AANAT1 (zebrafish, 68%; pike, 66%) (Appendix 4). A phylogenetic tree was inferred using the different AANAT sequences available in the NCBI databank (Figure 32) allowing to conclude that the cloned gene corresponds to the *S. maximus Aanat2* gene (*SmAanat2*).

This approach also allowed us to obtain the full-length *SmAanat1* gene (Appendix 5). Phylogenetic anaylsis of the deduced *Sm*AANAT1 amino acid sequence showed that it shares a high similarity with the rainbow trout AANAT1, medaka AANAT1b and pufferfish AANAT1b characterized by an extension of 21 amino acids at the carboxyl terminal end of the protein compared with other AANAT1 (Figure 32; Appendix 5). The expression pattern of this gene is not detailed here because it is beyond the scope of this study.

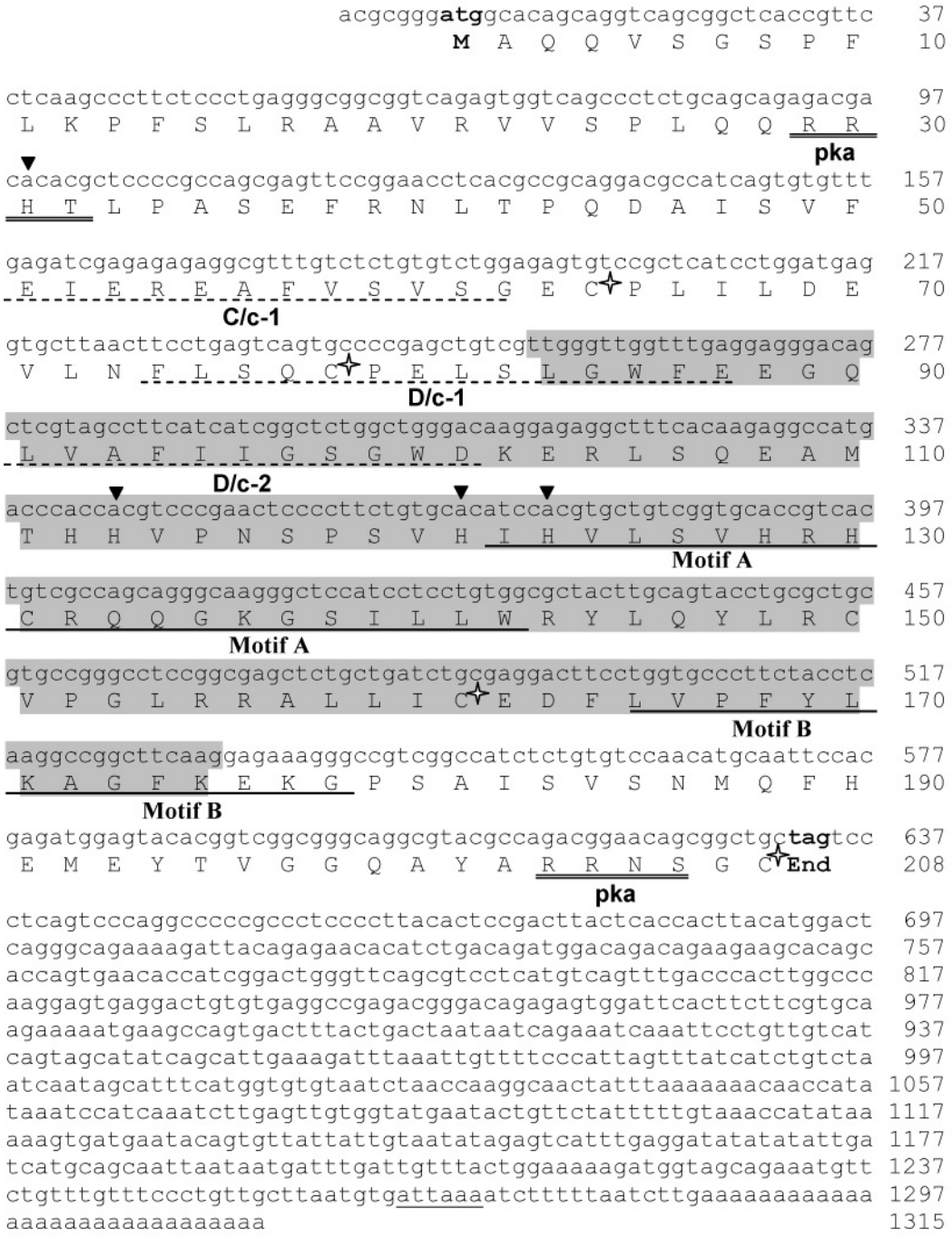

Figure 31. Nucleotide and deduced amino acid sequence of the turbot *Aanat2* cDNA. The nucleotide and amino acid positions are numbered and indicated on the right. The start and stop codons are indicated in bold letters. The acetyltransferase domain is shaded while the two putative acetyl coenzyme A binding motives and the two phosphorylation sites for PKA are indicated by simple and double underlining, respectively. The three highly conserved regions C/c-1, D/c-1 and D/c-2 found in vertebrates are indicated by dashed underligning. The four highly conserved cystein residues important for disulfide bond formation are indicated by a star. The four histidine residues are indicated by a black arrowhead. The putative polyadenylation signal is underlined.

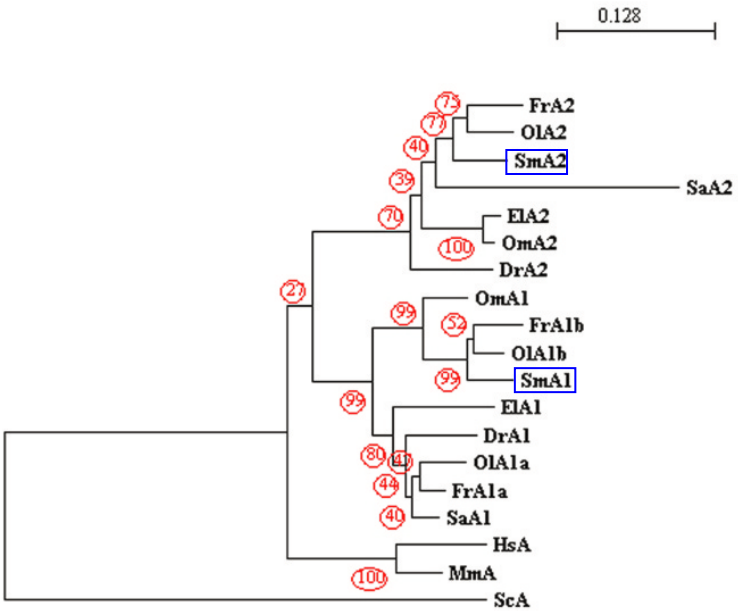

Figure 32. Phylogenetic tree of AANAT inferred by the Neighbor Joining method. The length of branches is proportional to the phylogenetic distance. The scale bar represents an evolutionary distance of 0.128 amino acid substitutions per site. 1000 bootstrap replications were used to test the robustness of each internal node (see Mat. & Meth.). Accessions numbers of the sequences used for the tree inference are as follows : (A) AANAT of yeast (ScA) (AAS55998), AANAT2 of turbot (SmA2) (ND), AANAT2 of zebrafish (DrA2) (AAF01140), AANAT2 of rainbow trout (OmA2) (AAD25333), AANAT2 of pike (ElA2) (AAD21317), AANAT2 of sea bream (SaA2) (AAT02160), AANAT2 of medaka (OlA2) (BAE78762), AANAT2 of pufferfish (FrA2) (NEWSINFRUP00000147708), AANAT1 of rainbow trout (OmA1) (BAA34809), AANAT1 of turbot (SmA1) (ND), AANAT1 of pike (ElA1) (AAD21316), AANAT1 of zebrafish (DrA1) (AAH59448), AANAT1a of medaka (OlA1a) (BAE78760), AANAT1b of medaka (OlA1b) (BAE78761), AANAT1a of pufferfish (FrA1a) (NEWSINFRUP00000130562), AANAT1b of pufferfish (FrA1b) (NEWSINFRUP00000152865), AANAT1 of seabream (SaA1) (AY533402), mice (MmA) (AAD09408) and human (HsA) (Q16613). ND, not deposited.

11.4.2 Isolation of S. maximus Hydroxyindole-O-methyltranferase (SmHiomt) cDNA

We used a similar strategy to identify a *SmHiomt* gene. A 179 bp fragment was amplified by RT-PCR using degenerated primers and sequenced. The sequence encodes part of the methyltransferase domain typical of the HIOMT family. The full-length *SmHiomt* cDNA was obtained by 5' and 3' RACE PCR with specific primers; two fragments of 487 and 888 bp, respectively, were amplified, which appeared to correspond to the entire *SmHiomt* full-length cDNA. It contains a deduced ORF of 996 bp encoding 332 amino acids, flanked by a 59 bp 5'UTR and a 276 bp 3'UTR ending by a poly(A) tail of 26 bp (Figure 33). One putative

polyadenylation signal is present upstream of the poly(A) tail (underlined in Figure 33). The deduced protein sequence encodes a methyltransferase domain (shaded in Figure 33), eight highly conserved cysteine residues and a putative casein kinase II phosphorylation site (ckII) (Figure 33). The complete deduced *Sm*HIOMT protein sequence was aligned with other available vertebrate HIOMT protein sequences, and a phylogenetic tree was inferred (Figure 34; Appendix 6) allowing to conclude that the cloned gene corresponds to the *SmHiomt*. *Sm*HIOMT displays similarity with chicken (62%), bovine (56%), apes (55%) and human (54%) HIOMT.

In order to determine if one or several *SmHiomt* genes exist in the turbot genome, we performed a Southern blot analysis at moderate hybridization stringency. The radio-labeled DNA probe recognized a single band, independent of the restriction enzymes used to cut the genomic DNA (Figure 35).

11.4.3 Isolation of S. maximus orthodenticle homeobox-5 (SmOtx5) cDNA

Parallel to the cloning of the *SmAanat2* and *SmHiomt* genes, we also have cloned the full-length cDNA of *SmOtx5*. The *Otx5* gene encodes a homeodomain transcription factor which is a relevant marker of the differentiation and maintenance of the photoreceptor cells, and expression of several pineal circadian genes including *Aanat2* and *Hiomt* (Gamse et al., 2002; Plouhinec et al., 2003; Furukawa et al., 1997; Furukawa et al., 1999; Chen et al., 1997). PCR amplification of the full-length *S. maximus Otx5* cDNA was carried out with specific primers designed from conserved regions of the gene. The full-length cDNA obtained corresponds to a 1479 bp sequence containing a deduced ORF of 885 bp. This ORF encoding a 295 amino acids protein is flanked by a 69 bp 5'UTR and a 525 bp 3'UTR, which ends with a poly(A) tail of 29 bp (Appendix 7). One putative polyadenylation signal is present upstream of the poly(A) tail (underlined in Appendix 7). The deduced protein sequence encodes a homeodomain (shaded in Appendix 7), a polybasic region (dashed lines in Appendix 7) and two repeats of the "Otx tail" motif typical of OTX proteins (single black line in Appendix 7) (Gamse et al., 2002). The complete *Sm*OTX5 protein sequence has similarity with the OTX5 sequences from frog (68%), shark (67%) and zebrafish (62%) and with the Crx sequences from zebrafish (67%) and chicken (58%). Altogether, our data allow concluding that the sequence we have obtained corresponds to *S. maximus Otx5* gene.

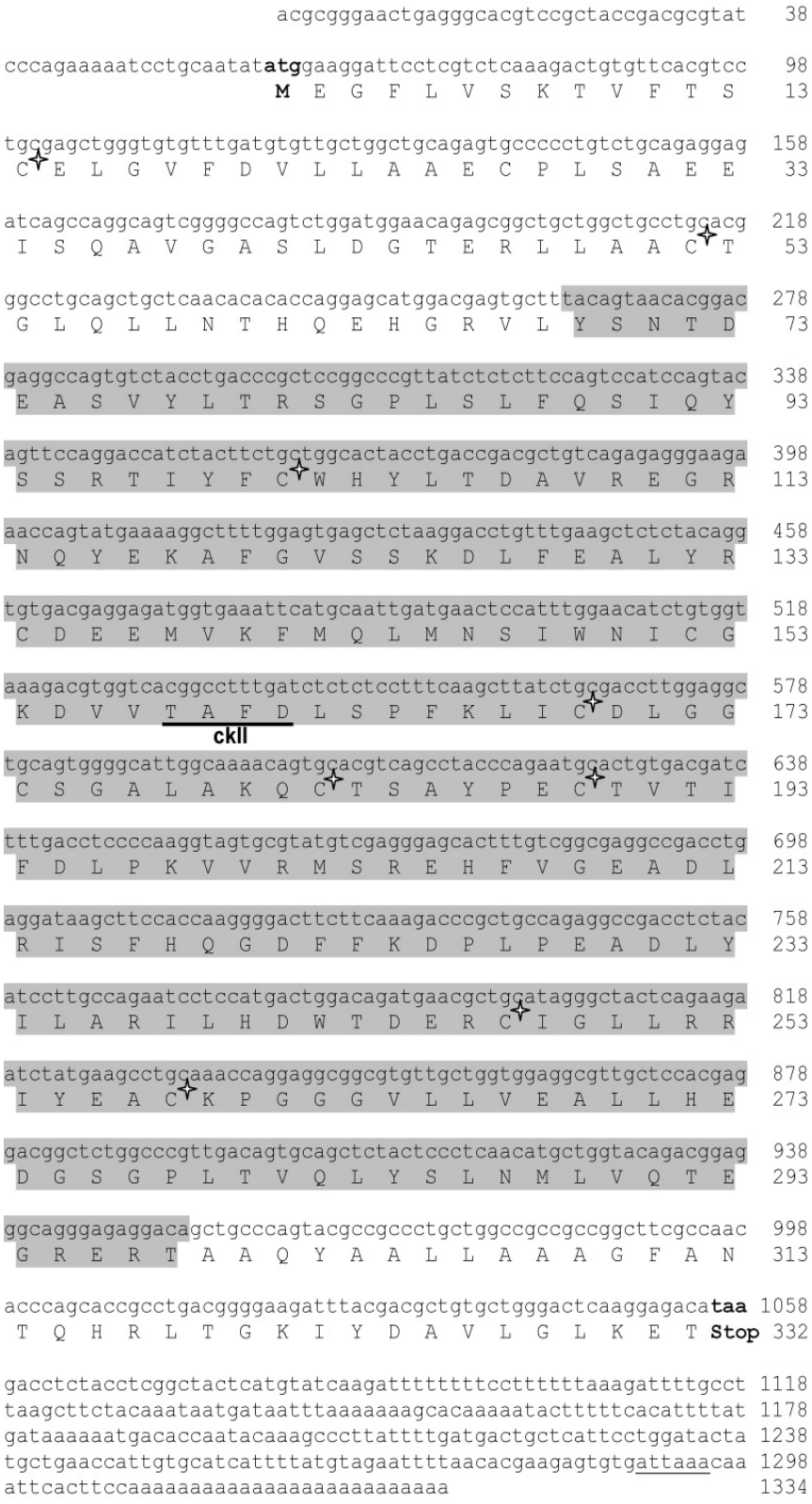

Figure 33. Nucleotide and deduced amino acid sequence of the turbot *Hiomt* cDNA. The nucleotide and amino acid positions are numbered and indicated on the right. The methyltransferase domain is shaded. The start and stop codons are indicated in bold letters. The putative casein kinase II phosphorylation site is indicated by strong underlining. The eight highly conserved cystein residues important for disulfide bond formation are indicated by a star. The putative poly (A) addition signal is underlined.

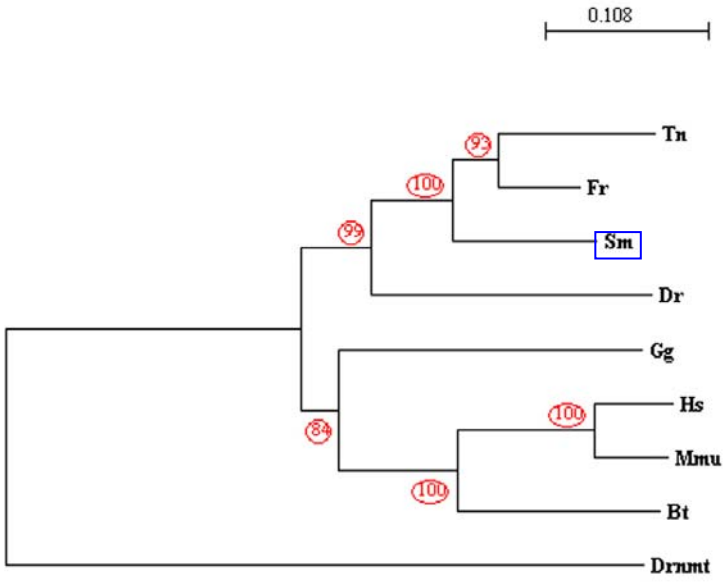

Figure 34. Phylogenetic tree of HIOMT inferred by the Neighbor Joining method. The length of branches is proportional to the phylogenetic distance. The scale bar represents an evolutionary distance of 0.108 amino acid substitutions per site. 1000 bootstrap replications were used to test the robustness of each internal node (see Mat. & Meth.). Accessions numbers of the sequences used for the tree inference are as follows : HIOMT of chicken (Gg) (NP_990674), bovin (Bt) (P10950), apes (Mmu) (AAL49966) and human (Hs) (CAI41503), turbot (Sm) (ND), zebrafish (Dr) (ENSDARP00000033596), Fugu (Fr) (NEWSINFRUP00000145608), Tetraodon (Tn) (GSTENT00030451001). ND, not deposited.

11.4.4 Embryonic and larval expression pattern of S. maximus Aanat2, Hiomt and Otx5

Both *SmAanat2* and *SmHiomt* mRNAs were first detected at 3 days pf. The labeling appeared as a single spot located in a frontal and media-dorsal position of the embryo, in a position likely to correspond to that of the pineal organ (Figure 36A-E, H-I). This was confirmed after observation of ultrathin sections of 3 dpf embryos previously hybridized with a *SmHiomt* mRNA riboprobe; expression was seen in cells lying around a lumen at the top of the brain (data not shown).

SmAanat2 was specifically expressed in the pineal organ at least until day 7 pf (data not shown). In contrast, from day 4 pf, *SmHiomt* expression was seen in the pineal organ as well as in the retina (Figure 36D-G). In the retina, the labeling was seen in the outer nuclear layer exclusively.

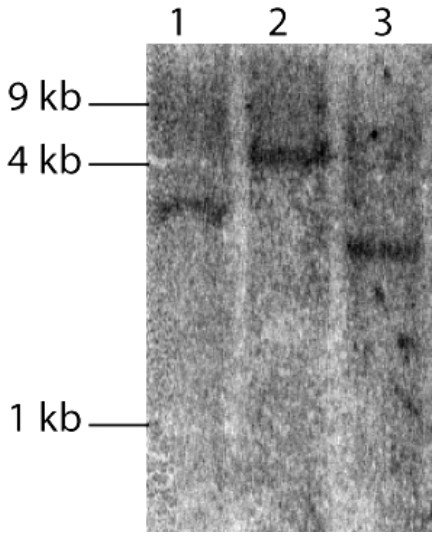

Figure 35. Genomic Southern blot analysis of turbot genomic DNA. 10 µg of genomic DNA extracted from turbot juveniles were digested with three different restriction enzymes: *Lane 1, Bgl II; 2, EcoR I; 3, Sac I.* The blot was probed at moderate-stringency with a DNA α^{32}P probe (see Mat. & Meth.). Size markers are on the left.

It was intense in the apical part corresponding to the inner segment; a thin labeling was also seen in the layer corresponding to the photoreceptor end pedicles, close to the outer plexiform layer (Figure 36G).

SmOtx5 expression starts first in the pineal gland anlage at day 2 pf, before the optic cups form (Figure 36 J, K). Later, at 3 dpf, expression starts being seen in the temporal part of the retina (Figure 36L). At 4 dpf, the SmOtx5 expression is detected to the full outer plexiform layer of the retina (Figure 36M).

Independent of the gene considered, no labeling was seen with the sense probes used as negative controls (Figure 36C and data not shown).

11.4.5 Daily expression of Aanat2 and Hiomt in the embryonic and larval S. maximus and D. rerio

In order to determine whether the expression of *SmAanat2* and *SmHiomt* follows a daily rhythm in the developing pineal gland, turbot embryos and larvae were maintained under a 12L/12D cycle, and sampled at midday and midnight from day 3 to day 6 pf, *i.e.* one day after hatching, before to be processed to whole mount *in situ* hybridization (see Materials and Methods).

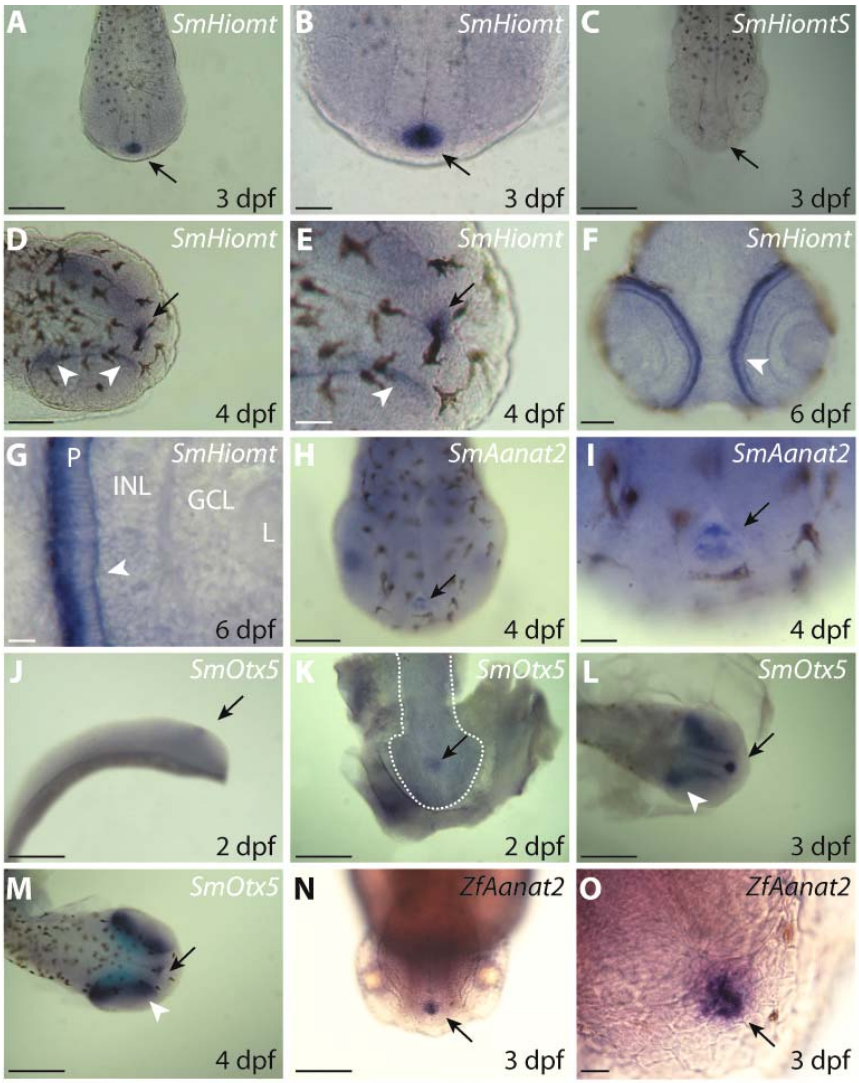

Figure 36. Localization of *Aanat2* and Sm*Hiomt* expression in embryos and larvae of turbot and zebrafish by *in situ* hybridization. *Aanat2* and *SmHiomt* gene expression was localized by whole mount *in situ* hybridization (see Mat. & Meth. for details). (A-C) 3 dpf turbot embryos dark adapted hybridized with an anti-sense (A-B) or sense (C) digoxygenin *SmHiomt* riboprobe. (D-E) 4 dpf turbot embryo and 6 dpf turbot larva (F-G) light adapted were hybridized with an anti-sense digoxygenin *SmHiomt* riboprobe. (H-I) 4 dpf light adapted turbot embryo hybridized with an anti-sense digoxygenin *SmAanat2* riboprobe. (J-K) 2 dpf (L) 3 dpf and (M) 4 dpf light adapted turbot embryos hybridized with an anti-sense digoxygenin *SmOtx5* riboprobe. (N-O) 3 dpf dark adapted zebrafish larva hybridized with an anti-sense digoxygenin *ZfAanat2* riboprobe. The black arrow and white arrowheads show the pineal gland and the photoreceptors of the retina, respectively. GCL, retinal ganglion cell layer; INL, inner nuclear layer; L, lens; P, photoreceptors layer. Scale bars: (A, C, J, K, L, M, N) 100 µm; (D, F, H) 50 µm; (B, E, I) 25 µm; (G, I, O) 10 µm.

Under these conditions, we found no daily variations in the expression of either gene (Figure 37A, C); in contrast, under similar conditions, embryonic and larval pineal expression of zebrafish *Aanat2 (ZfAanat2)* was low during day and high at night (Figures 36N-O, 37E) as previously shown (Gothilf et al., 1999; Vuilleumier et al., 2006).

Three dpf embryos to five dpf larvae of turbot were also collected every 6 h starting at 5 am one hour before the light switch on and until midnight of the fifth day, and assayed using a real time quantitative PCR approach (Figure 37B, D). No significant daily variations in the expression of either gene was seen under these conditions. In contrast, a significant rhythm in Zf*Aanat2* expression in two dpf embryos was detected in using this approach (Figure 37F). This rhythm is characterized by a maximum at 6 am.

11.5 Discussion

The present study reports, for the first time, the full-length cDNA cloning of *Aanat2*, *Aanat1*, *Hiomt* and *Otx5* genes in the turbot, a percomorph Teleost. The first three genes encode, the penultimate and ultimate enzymes in the melatonin biosynthesis pathway, respectively (Klein et al., 1981). They are of interest because they are markers not only of the melatonin function, but also, at least for *Aanat2* and *Hiomt*, of pineal clock function. Indeed, in zebrafish, transcription factors of the circadian clock machinery act directly on regulatory sequences of *ZfAanat2* to direct its circadian expression (Appelbaum et al., 2005). In chicken, pineal *Hiomt* expression is controlled by a circadian oscillator *in vitro* and *in vivo* (Greve et al., 1996). Whereas much attention has focussed on *Aanat*, which has now been cloned in a important number of vertebrates including Teleost fish, little information is available on *Hiomt*. This is the first study reporting the full-length cDNA cloning, tissue distribution and regulation of the *Hiomt* gene expression in an ectothermic vertebrate.

Multiple alignment and phylogenetic analysis of the complete putative protein sequences deduced from the three genes cloned from turbot clearly indicate that they belong to the AANAT and HIOMT protein families. As far as *Sm*AANAT2 is concerned, the deduced amino acid sequence of the putative coding region indicates similarities with conserved sequences from AANAT cloned in other species. For *Sm*AANAT2, this corresponds to the regulatory and catalytic sites previously described in the literature (Coon and Klein, 2006; Obsil et al., 2001; Hickman et al., 1999a; Hickman et al., 1999b).

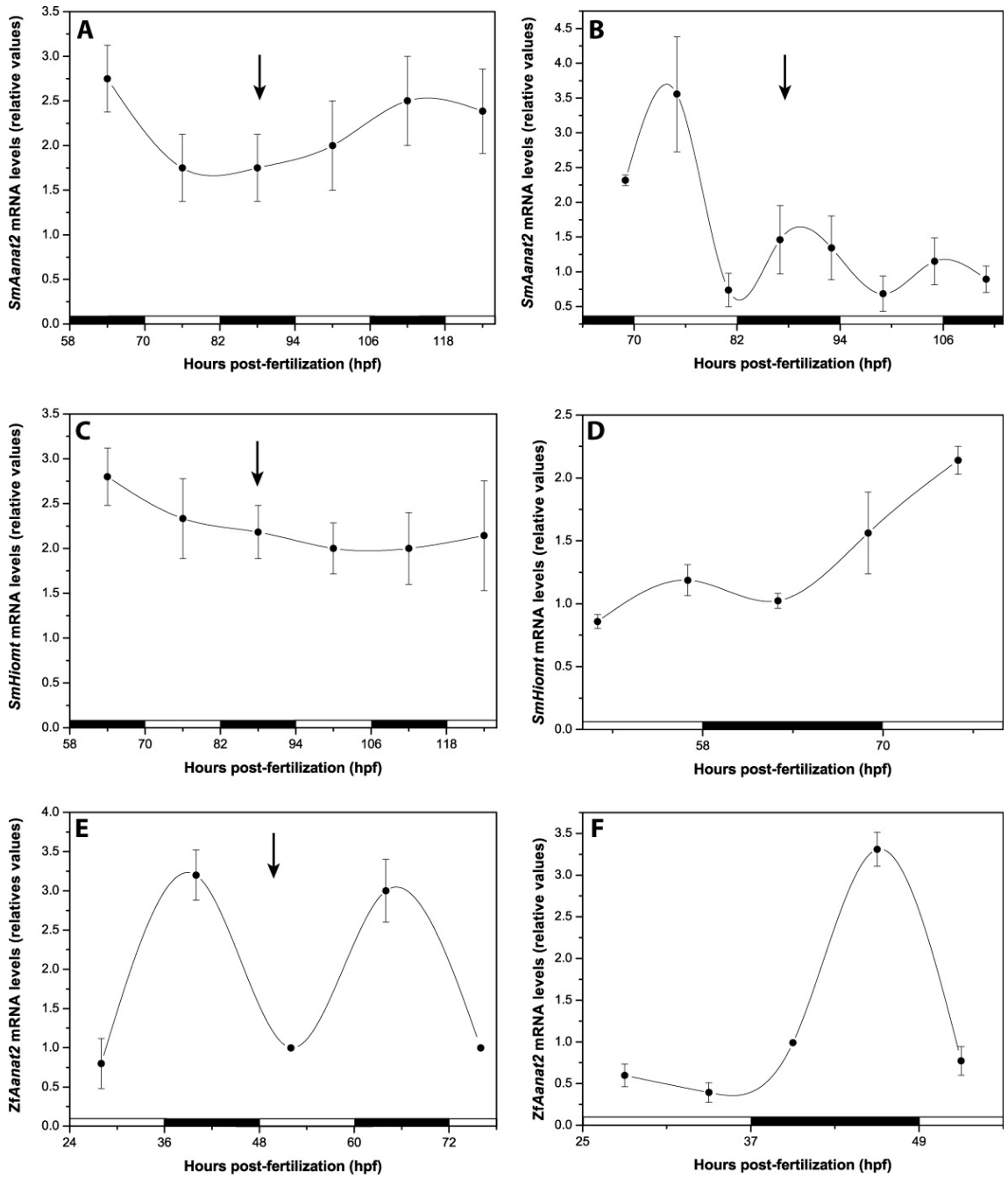

Figure 37. Variation of *SmAanat2*, *SmHiomt*, *ZfAanat2* expression levels during the first days of development under Light/Dark (LD) cycles. Embryos and larvae were kept at 16 °C for turbot or 28.5 °C for zebrafish under a 12h LD cycle. They were collected at different days post-fertilization and subjected to whole mount *in situ* hybridization (A, C, E) or extracted for a real time quantitative PCR analysis (B, D, F). *SmAanat2* (A, B), *SmHiomt* (C, D) and *ZfAanat2* (E, F) mRNAs levels were quantified as indicated in Materials and Methods. Analysis of the variance indicated a significant daily rhythm only for *ZfAanat2* using both approaches cited above (by one way ANOVA and Tukey's test, $p<0.001$ for (E) and by one way ANOVA $p<0.001$ and Tukey's test : between 46 and 28 hpf $p<0.01$ and 40 and 34 hpf $p<0.05$ for (F)). The black bars indicate the dark phases. The black arrow indicates the hatching period.

The turbot HIOMT deduced amino acid sequence displays a high similarity with the few HIOMT sequences available (Donohue et al., 1993; Ishida et al., 1987; Klein et al., 1997; Voisin et al., 1992). Also, the *Sm*HIOMT harbors several highly conserved domains corresponding to the catalytic as well as to non-catalytic sites of the protein, *e.g.* a putative casein kinase II phosphorylation site. The functional significance of these last domains will have to be investigated in further studies.

In an *in silico* recent study of several vertebrate genomes, it has been predicted that percomorph Teleosts may contain three *Aanat* genes : one *Aanat2* and two *Aanat1*, namely *Aanat1a* and *Aanat1b* (Coon and Klein, 2006). The predicted protein of *Aanat1a* is similar at the carboxyl terminal end to zebrafish, pike and seabream AANAT1 and to all AANAT of other vertebrates described so far. In contrast, the predicted carboxyl terminal end of the AANAT1b protein of pufferfish and medaka is 21 amino acids longer. This extension shares some similarities with rainbow trout AANAT1 suggesting that they derived from a common ancestor (Coon and Klein, 2006). It is therefore not surprising that beside *SmAanat2*, we also succeeded in cloning another turbot *Aanat*. After phylogenetic analysis of its deduced protein sequence, it appeared belonging to the *Aanat1b* gene family. Further studies will aim at examining the specific functions of both isoforms.

The specific expression of *SmAanat2* in the pineal organ agrees with previous biochemical and molecular studies indicating that (i) AANAT2 is mainly the pineal enzyme and AANAT1 is the retinal one (Benyassi et al., 2000; Coon et al., 1999; Gothilf et al., 1999), and (ii) that regulatory elements of the zebrafish *Aanat2* gene direct specific expression in the pineal organ and repress expression in the retina (Appelbaum et al., 2004).

More generally, it appears that in Teleost several photoreceptor specific genes have been duplicated and express tissue-specific distribution; this is the case for *Aanat*, but also for several genes of the phototransduction cascade (Mano et al., 1999; Decressac et al., 2002). This is thought to be in part a result of a whole genome duplication that occurred early at the emergence of the Teleost fish lineage (Hoegg et al., 2004; Jaillon et al., 2004). In contrast, we found that (i) our cloning strategy using degenerated primers allowed amplification of only one *Hiomt* cDNA type; (ii) hybridization of genomic DNA with an *Hiomt* probe chosen in a conserved sequence of the gene labeled a single band, (iii) identical sequences were obtained after partial cloning of a 200 bp fragment of the *Hiomt* gene from retinal and pineal gland extracts in trout and pike (data not shown) and (iv) only one putative *Hiomt* gene can be found in the zebrafish genome in blasting the cDNA and peptide databanks (Ensembl). Hence, we conclude that the turbot genome may contain only one *Hiomt* gene, although an

other, *e.g.* highly divergent, cannot totally be ruled out. For instance, two putative *Hiomt* genes may be found in the pufferfish genomes, although one of both seems to have a highly divergent amino acid sequence and is expressed in the muscle. In the future, it will be primordial to determine if this paralogous gene has kept its function to biosynthesize melatonin in these species.

The result concerning the *SmHiomt* expression pattern in turbot is of special interest because it shows that the mRNA appear first in the pineal gland in 3 days old embryos and, one day later, in the retina. Thus, it strongly suggests that the photoreceptors of the pineal gland biosynthesize melatonin before those of the retina implying an important role for pineal melatonin during development such it has been shown in zebrafish (Danilova et al., 2004). In the retina of turbot embryos and larvae, we found *SmHiomt* mRNA only the in inner segments and pedicles of photoreceptors corroborating what was found by *in situ* hybridization in retina of chicken (Wiechmann, 1996; Wiechmann et al., 1985). One interesting conclusion from this observation is that at early stages of development the melatonin pathway is a cone specific property because the pre-metamorphic retina of flatfish contains only cones (Evans and Fernald, 1993; Helvik et al., 2001) and the larval and adult pineal organ contains only cone-like photoreceptors (Falcon, 2006). In order to know if the rod photoreceptors may also biosynthesize melatonin, it will be primordial to examine Teleost species displaying an "only rod" retina as for instance in the eels' leptocephal larva retina (Evans and Fernald, 1993).

The observation that the transcription factor *Sm*OTX5 is expressed in the photoreceptor cells one day before *SmAanat2* and *SmHiomt* is in agreement with that the former controls the expression of the latter by binding to their transcriptional regulatory elements (Gamse et al., 2002; Bernard et al., 2001; Appelbaum et al., 2005). As it was the case for *SmHiomt*, *SmOtx5* - but not *SmAanat2* - started to be expressed in the retina one day after the expression in the pineal gland. The difference in the temporal pattern of expression of *SmOtx5* in the pineal organ and retina at initial stages of development supports the idea that in Teleost fish the former differentiates before the latter (Vuilleumier et al., 2006; Forsell et al., 2002).

Previous results and those obtained here suggest that the pineal gland rather than the retina mediates photic responses during embryonic development of Teleost (Gothilf et al., 1999; Vuilleumier et al., 2006; Forsell et al., 2002). Although this feature seems to be conserved between zebrafish and turbot, the establishment of the pineal functions during embryonic development is different between both species. Indeed, whereas in zebrafish the

expression of *ZfAanat2* displays a robust circadian rhythm in the pineal gland as early as the second day of development, *i.e.* one day before hatching, the expression of this gene in turbot does not show any rhythm in the epiphysis at least one day after this process. This suggests that during evolution of the Teleost lineage, at least two mechanisms controlling *Aanat2* expression during early development have evolved.

The rhythm in the melatonin biosynthesis in all studied vertebrates is primarily driven by a rhythm in AANAT activity (Klein et al., 1997). This rhythm is generated by post-transcriptional controls of the enzyme (Coon et al., 2001; Falcon et al., 2001; Ganguly et al., 2001; Ganguly et al., 2005; Gastel et al., 1998) or by both transcriptional and post-trancriptional control mechanisms (Falcon, 1999; Klein et al., 1997), depending of the examined species. The absence of any rhythm in the *SmAanat2* expression during turbot embryonic development suggests that pineal melatonin biosynthesis at these early stages is mainly controlled at the post-transcriptional level although further studies on the *SmAanat2* expression pattern in larva, juvenile and adult of turbot will be necessary to conclude on the regulation of this enzyme.

Until now, data concerning the regulation of the expression of the HIOMT gene during LD cycles were available only in mammals and birds (Falcon, 1999; Ribelayga et al., 1999). In chicken and quail, which are diurnally active animals, maxima and minima of expression were observed during the middle of light and dark phase, respectively, whereas in rat, a nocturnal animal, the expression is reversed (Fu et al., 2001; Greve et al., 1996; Ribelayga et al., 1999). Because all these rhythms are maintained under constant illumination, this indicates that the *Hiomt* gene expression is controlled by a circadian oscillator in chicken and mammals (Greve et al., 1996; Ribelayga et al., 1999). In contrast, in the turbot, we were not able to show significant variations in the levels of the *SmHiomt* mRNAs during the LD cycle indicating that the circadian control of *SmHiomt* expression does not occur in the embryos and larvae of turbot, a case already observed for adult primates (Coon et al., 2002; Ackermann et al., 2006)).

In summary, in this study, we cloned the full-length cDNAs encoding *Sm*HIOMT, *Sm*AANAT2 and *Sm*OTX5, which the former has only been described so far in birds and mammals. We showed that in contrast to *SmAanat2*, *SmOtx5* and *SmHiomt* are expressed in both major sites of melatonin biosynthesis, the cone photoreceptors of the pineal gland and retina. Finally, we found that the molecular mechanisms involved in the regulation of the *Aanat2* expression during embryonic development are different between zebrafish and turbot. Further studies examining other fish species at different developmental stages will

allow to better understand the role of the pineal organ during embryonic development and how were established its different functions during evolution of vertebrates.

Previously, we examined the early ontogeny of the two main photoreceptive organs in the zebrafish and turbot. The turbot belongs to the flatfish group characterized by an indirect development, a process also called metamorphosis, which is protracted compared with other Teleost groups. Hence, the flatfish retina appears as a relevant model to study the mechanisms leading to cell proliferation and differentiation.

The following study reports the characterization of cellular changes during metamorphosis of the tubot retina and presents evidence that this visual remodelling process is convergent with the one previously observed in frog.

12. Characterization of the asymmetric retinal changes occuring during turbot (Scophthalmus maximus) metamorphosis

12.1 Abstract

The metamorphosis in amphibians and flatfish is a complex process triggered by the thyroid homones including the tri-iodothyronine (T_3) and thyroxine (T_4). Whereas this body transformation has been already well studied in frogs, little has been done concerning flatfish. In these animals, the symmetric pelagic larva is transformed into a benthic asymmetric juvenile during the metamorphic process. This change is characterized by dorsal migration of either the right or the left eye to the other side of the body. In addition, during this transformation, several other anatomical, physiological and biochemical changes occur in the whole organism.

In this study, we focused on the turbot (*Scophthalmus maximus*), a senestral flatfish, and examined the retinal changes which occur during metamorphosis. Among them, we found that the photoreceptors of the premetamorphic retina do not display any rhodopsin expression whereas during metamorphosis, this photopigment molecule appears in the ventral retina. This suggests that in turbot the scotopic vision is acquired in the same time that the animal is changing its habitat. Also we found that the growth at the ciliary marginal zone (CMZ) of the retina becomes asymmetric during turbot metamorphosis and that this shift may be controlled by a type 3 deiodinase gene (*SmD3*). Because a similar case of asymmetric growth was already described in *Xenopus*, the hypothesis of an evolutionary convergence between both visual systems is discussed here.

12.2 Introduction

In the animal kingdom, development of an adult organism from a larva can be described as either direct or indirect. Direct development indicates that the larva of an organism displays the same phenotype as the adult and the growth until adulthood is accompagnied by relatively few phenotypic transformations. In contrast, indirect

development indicates that dramatic transformations of the body, namely metamorphosis, occur. Although this process is often observed in invertebrates, "true" metamorphosis in vertebrates occurs in amphibians and flatfish.

In frog, the metamorphosis transforming a swimming herbivore tadpole into a carnivore tetrapod vertebrate is triggered by the thyroid hormones (THs) mostly the tri-iodothyronine (T_3) (Brown et al., 1995). According to these multiple body modifications, the adult frog has to reorganize the existing larval visual system in order to see overlapping visuals fields adapted to its predatory lifestyle (Grant and Keating, 1986). This is realized by the migration of the lateral eyes typical of tadpoles to a new dorso-frontal position, by the formation of new retinal projections to the ipsilateral thalamus and by a shift from a symmetric to an asymmetric growth pattern of the retina from stem cells located at the ciliary marginal zone (CMZ) (Hoskins and Grobstein, 1984; Mann and Holt, 2001). This shift is controlled by the asymmetric expression of a type 3 deiodinase (D3), a selenocystein containing enzyme, in the retina. In this tissue, the *D3* gene is only expressed in the stem cells located in the dorsal CMZ and acts by protecting them from the proliferative effect of the THs (Marsh-Armstrong et al., 1999). Accordingly, during metamorphosis, only the stem cells located in the ventral CMZ which do not express D3 increase their mitotic divisions, resulting in the asymmetric cell growth pattern of the retina (Marsh-Armstrong et al., 1999). Moreover, it has been proposed that these dramatic modifications occuring during amphibian metamorphosis are triggered by the same genetic actors, namely *Bmp* and *Shh*, playing a role during early development (Stolow and Shi, 1995; Ishizuya-Oka et al., 2001).

Although the molecular and cellular processes triggering metamorphosis in amphibians have been well studied, very little has been done concerning flatfish metamorphosis. Metamorphosis in flatfish transforms a pelagic symmetric larva into a benthic asymmetric one. During this transformation triggered also by the THs (Power et al., 2001), the eye and the nostril migrate from one side across the back to the other side of the body. In parallel of these modifications, several other morphological, anatomical, biochemical and physiological changes occur in the whole organism (Evans and Fernald, 1993; Graf and Baker, 1983; Schreiber, 2001). In addition, during flatfish metamorphosis the retina radically changes with the appearance of rod and double cone photoreceptors and a new ratio between neuronal connections (Evans and Fernald, 1993). This extremly protracted development in flatfish provides a unique opportunity to study sequentially the events leading to cell proliferation and differentiation in the retina. However, few molecular studies concerning retinal development and metamorphosis in flatfish have been carried out to date.

In order to characterize the complex process occuring in the flatfish retina during metamorphosis, we looked at the cellular level with a marker of cell division and two retinal marker genes. In this study, we first show that cell proliferation in the photoreceptors layer of the turbot retina is activated during metamorphosis preceeding the appearence of rhodopsin expression suggesting that the scotopic vision in flatfish is acquired during this process. We also found in turbot that cell proliferation at the CMZ during and after metamorphosis is higher in the ventral retina than in the dorsal one, a process which may be controlled by the retinal asymmetric expression of the turbot type 3 deiodinase gene (*SmD3*). Finally, because the asymmetric growth at the CMZ of the retina also occurs in *Xenopus*, these results suggest an evolutionary convergence between these two visual systems.

12.3 Materials and methods

12.3.1 Experimental animals

Embryos, larvae and juveniles of turbot (*Scophthalmus maximus*) were obtained at the France Turbot company in Noirmoutier (France) where they were reared in sea water at 16 °C following the protocol of (Person-Le-Ruyet, 1989). They were collected at different developmental stages and frozen in dry ice for RNA extraction, or fixed overnight in 4% paraformaldehyde (PFA) in PBS at 4°C, washed in PBS, and finally stored in methanol at -20°C for whole mount *in situ* hybridization. The preparation of the eye sections used for *in situ* hybridization was carried out as described below (see Cell Proliferation assay with BrdU and histochemistry).

12.3.2 Cloning of the full-length SmD3 cDNAs

A *Scophthalmus maximus* fragment of the *type 3 Deiodinase* (*D3*) gene was isolated by nested PCR after reverse transcription of mRNA extracted from a pool of embryos (48, 72, 96 and 120 hours post-fertilization; hpf) and larvae (20 days post-hatching; dph). Nested degenerated primers for *SmD3* (forward: 5'CCGYTGGTKSTCAATTTYGGCAGCTG3'; nested forward: 5'GCTGYACCTGACCMCCGTTCATGGC3'; reverse: 5'TCSGGSCCMCGRCCBCCCTGGTACA3') were used for PCR with the following conditions: 2 minutes at 95°C, 15x(20 seconds at 94°C, 1 minute at 37°C, 1 minute at 68°C)

then 25x(20 seconds at 94°C, 1 minute at 42°C, 1 minute at 68°C) followed by 7 minutes at 68°C. The conditions for the nested PCR were : 2 minutes at 95°C, 30x(20 seconds at 94°C, 1 minute at 48°C, 1 minute at 68°C) followed by 7 minutes at 68°C.

Full-length sequence of *SmD3* was obtained by 5′ and 3′ RACE PCR using the standard protocol (Clontech). Nested forward and reverse specific primers were designed from fragments of *S. maximus D3* (forward: 5′CCGTATCAGATCCCCAAGCACCGCTGC3′; nested forward: 5′GCAGCAGCGTGGTGGTGGACGACATGG3′ ; reverse: 5′CCATGTCGTCCACCACCACGCTGCTGC3′; nested reverse: 5′GCAGCGGTGCTTGGGGATCTGATACGG3′) and used in PCR with the following conditions: 2 minutes at 95°C, 30x (13 seconds at 94°C, 1 minute at 63°C, 3 minutes at 68°C) followed by 7 minutes at 68°C. Same conditions were used for the nested PCR except that the number of cycles was 25.

12.3.3 Protein alignment, inference of phylogenetic tree and sequence analysis

Deduced full-length amino acid sequence of D3 was aligned using PipeAlign (Plewniak et al., 2003). The Phylo_win version 2.0 software program was used to infer phylogenetic trees (Galtier et al., 1996). After removing gaps, trees were inferred by the Neighbor Joining method (NJ). The degree of support for internal nodes was assessed using 1000 bootstrap replications. Sequences were analyzed by BLASTP (Altschul et al., 1997).

12.3.4 In situ hybridization

The *in situ* hybridization on whole mount and sections were carried out as described elsewhere (Thisse et al., 2004; Besseau et al., 2006) except the hybridization and washing temperatures which were 67°C. Details of the SmPax6, SmOtx5, SmBmp4 and SmD3 riboprobes are available upon request.

12.3.5 Cell Proliferation assay with BrdU and histochemistry

Larvae, metamorphic larvae and juveniles of turbot were soaked in a 100 µM, 1 mM and 10 mM BrdU (Sigma) solution, respectively, during two days. They were then removed

and fixed in a 4% PFA solution overnight at 4°C. For larvae older than 17 dph (days post-hatching), the two eyeballs were removed from the head. After several washes in PBS, the larvae and eyeballs were dehydrated in graded series of PBS/glycerol/sucrose solutions (Besseau et al., 2006), embedded in Tissue Freezing Medium (Jung) and frozen in dry ice. They were then cut (30 µm) using a Leica CM1900 cryotome and dried at 37°C overnight. To detect BrdU, sections were rehydrated in two washes of 5 minutes in PBST and incubated in 0,05% trypsin with 0,05% $CaCl_2$ in PBS at 37°C during 10 minutes. Inactivation of the enzyme was carried out in 10 mg/ml trypsin inhibitor in PBS during 10 minutes and the DNA was denatured in 4M HCl during 23 minutes at room temperature (RT). The sections were then washed twice for 5 minutes in PBST and incubated for 30 minutes in blocking solution (BS) (2 mg/ml BSA; 3% sheep serum) before incubation in the primary antibody (mouse anti-BrdU, Sigma) at a 1:1000 dilution in BS during 2 hours at RT. The sections were then washed three times for 5 minutes and once for 1 hour in BS and incubated in secondary antibody (goat anti-mouse FITC, Sigma) at a 1:500 dilution during two hours. After six washes of 10 minutes in PBST and one more in PBS they were mounted in 100% glycerol with DABCO (0.3%). Fluorescent staining was examined with an epifluorescence microscope.

Immunodetection of rhodopsin on cryosections was carried out as described elsewhere (). The primary antibody (rabbit anti-rhodopsin) was used at a 1:200 dilution in BS during two hours. The secondary antibody (goat anti-rabbit AP, Sigma) was used at a 1:500 dilution during two hours.

12.4 Results

12.4.1 The rhodopsin appears in the retina during metamorphosis

Previous studies have shown that the flounder retina contains only cone photoreceptors before metamorphosis and that during this process double cones and rods appear (Evans and Fernald, 1993; Mader and Cameron, 2004). In order to determine if this retinal change also occurs in turbot, we tried to detect the rod specific photopigment molecule in retinae of different developmental stages using a polyclonal anti-rhodopsin antibody. Before metamorphosis, at about 14 dph, the turbot larval retina did not show any labeling even in the photoreceptor layer (PL) (Figure 38A). In contrast, at the end of

metamorphosis, at about 60 dph, a labeling was seen specifically in the PL of the ventral retina (black arrowhead) but not in the dorsal one (white arrowhead) (Figure 38B-D).

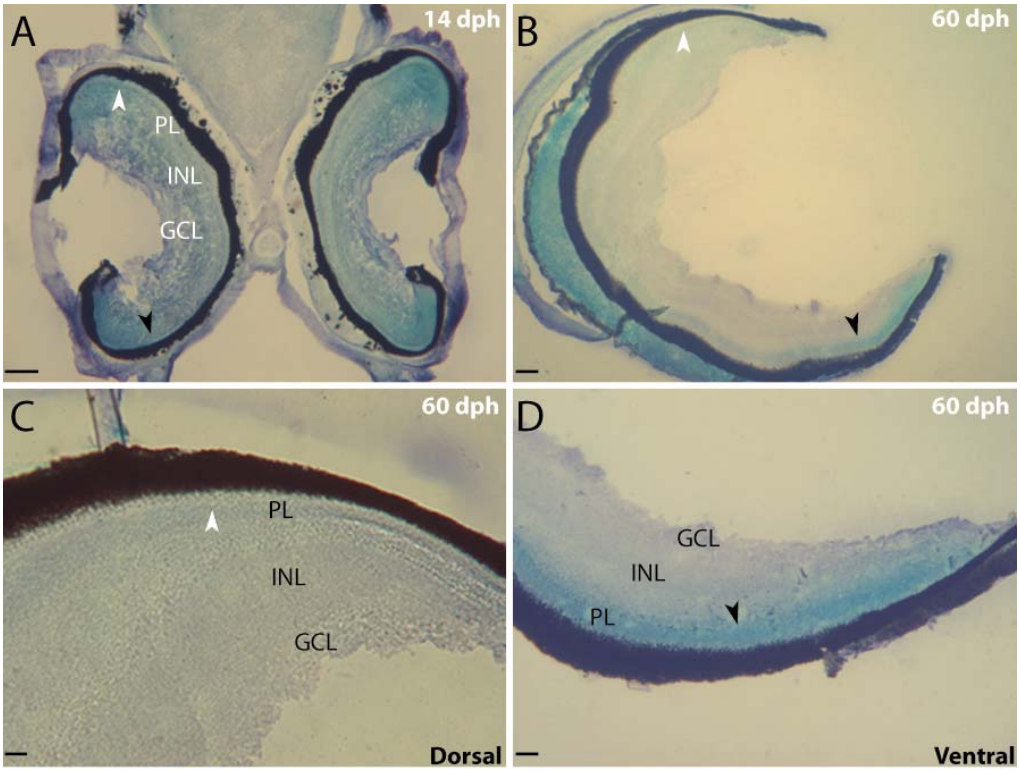

Figure 38. Immunodetection of rhodopsin in the retina of larvae and juveniles of turbot. (A-D) Cryosections of a 14 dph larva (A) and an eyeball of a 60 dph juvenile (B-D) of turbot labeled with a primary anti-rhodopsin antibody and a secondary antibody coupled to alkaline phosphatase (see materials and methods for details). (C) and (D) show at a higher magnification the dorsal and ventral retina in (B), respectively. The white and black arrowheads show the dorsal and ventral PL, respectively. GCL, ganglion cell layer; INL, inner nuclear layer; PL, photoreceptors layer. Scale bar: (A, B) 200 µm; (C, D) 50 µm.

In Teleost fish, in contrast of the other retinal cell types which are generated by the CMZ, the rod photoreceptor cells are generated from dividing rod precursors located in the PL and circumferential larval zone (CLZ) (Otteson et al., 2001). In order to determine if such putative rod precursors are present in the retina of turbot larvae and early juveniles, we incorporated Bromodeoxyuridine (BrdU) in DNA of dividing retina cells in premetamorphic and metamorphic fish. Before metamorphosis, the larval retina displayed dividing cells labeling only in the CMZ (Figure 39A, B). During metamorphosis, retinal BrdU positive cells were detected in the CMZ but also in the PL (dashed white arrow), the retinal ganglion cell layer (GCL) and a ventral zone corresponding probably to the CLZ (white arrow) (Fig. 39G, H; data not shown).

Taken together, these results suggest that before metamorphosis, the turbot retina contains only cone photoreceptors and during the metamorphic process, the generation of rod photoreceptors from rod precursors located into the photoreceptor layer and ventral CLZ, begins.

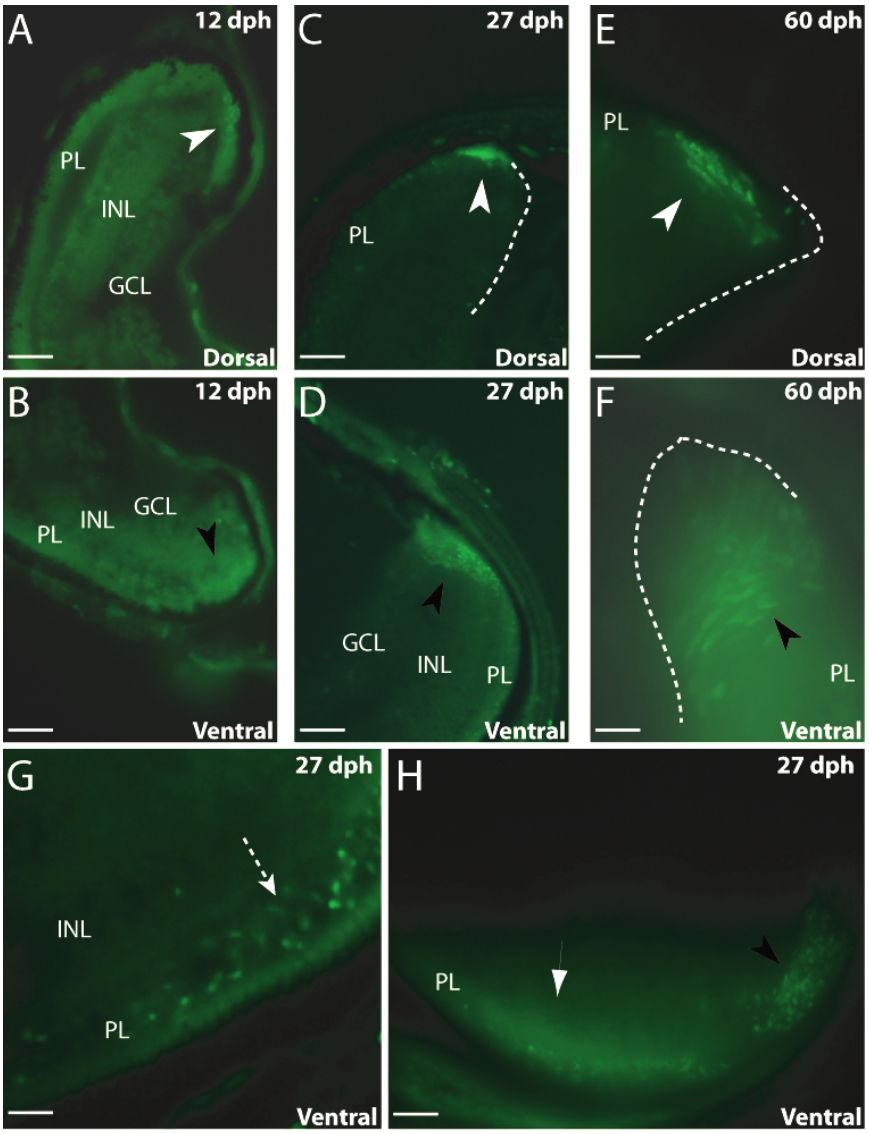

Figure 39. Immunolocalization of dividing cells in pre-metamorphic, metamorphic and post-metamorphic turbot retina. (A-H) Cryosections of a 12 dph larval (A, B), 27 dph metamorphic (C, D, G, H) and 60 dph juvenile (E, F) turbot retina labeled with a primary anti-BrdU antibody and a secondary antibody coupled to FITC (see materials and methods for details). The photographs in (A, C, E) and (B, D, F) show the dorsal and ventral retinae, respectively. The white and black arrowheads show the dividing cells at the dorsal and ventral CMZ, respectively. The dashed white arrow in (G) shows dividing cells in the ventral ONL. The white arrow in (H) shows dividing cells at the ventral CLZ. The white dashed line (C, E, F) displays the most apical part of the retina. GCL, ganglion cell layer; INL, inner nuclear layer; PL, photoreceptors layer. Scale bar: (A, B, H) 75 μm, (C, D) 150 μm, (E, F) 250 μm and (G) 30 μm.

Accordingly, at the end of the metamorphic process, rods are mostly found in the ventral flatfish retina.

12.4.2 The cell growth pattern at the ciliary margin zone of the turbot retina becomes asymmetric during metamorphosis

In ectothermic vertebrates, stem cells and retinoblasts located in the apical and more central part of the ciliary marginal zone (CMZ) of the retina, respectively, contribute to the continuous growth of this organ throughout the life of these organisms. To examine the process of cell growth in the CMZ during turbot metamorphosis, we performed BrdU incorporation in dividing cells at pre-metamorphic, metamorphic and post-metamorphic stages.

Before metamorphosis, at about 12 days post-hatching (dph), BrdU incorporation in both the dorsal (Figure 39A) and ventral (Figure 39B) CMZ of the larval retina was symmetric as indicated by the number of BrdU positive cells. During metamorphic climax, at about 27 dph, the cell proliferation became asymmetric in the CMZ as indicated by an increase of the number of BrdU positive cells in the ventral retina (Figure 39C, D). At the end of metamorphosis, at about 60 dph, the CMZ of the turbot retina has kept the pattern of asymmetric cell growth as indicated by the number of positive BrdU cells (Figure 39E, F). No difference in BrdU incorporation was observed between both eyes (data not shown). To further characterize the retinal changes occuring during metamorphosis, we next compared the expression pattern of two retinal molecular markers between the dorsal and ventral retina, before metamorphosis and during end of metamorphic climax. The first one, *Pax6*, encodes a highly conserved transcription factor involved in the formation of the eye and is expressed strongly in the amacrine cells of the inner nuclear layer (INL), ganglion cells of the ganglion cell layer (GCL) and at a lower level in the stem cells and retinoblasts of the CMZ of the mature retina in mice and frogs (Marquardt et al., 2001; Perron et al., 1998). The second one, *Otx5*, is expressed in the differentiated photoreceptors and horizontal cells of the mature retina but not in the CMZ (Shen and Raymond, 2004). Whereas before metamorphosis, *Pax6* expression in turbot was mainly located to the inner nuclear layer (INL) (Figure 40A), after metamorphic climax, *Pax6* was strongly expressed in the amacrine cells and more weakly in the retinal ganglion cells (Figure 40G). In addition, after metamorphic climax, a low *Pax6* expression was detected in cells of both the ventral (black arrowhead) and dorsal (white arrowhead) CMZ (Figure 40C, E). The number of *Pax6* positive cells in the ventral CMZ (black arrowhead) was higher than in the dorsal one (white arrowhead) (Figure 40C, E). In

examining the expression of *Otx5* in different developmental stages turbot retina, we could detect the expression of the gene only in photoreceptors before metamorphosis and in horizontal and photoreceptors cells after climax of metamorphosis (Figure 40B, H).

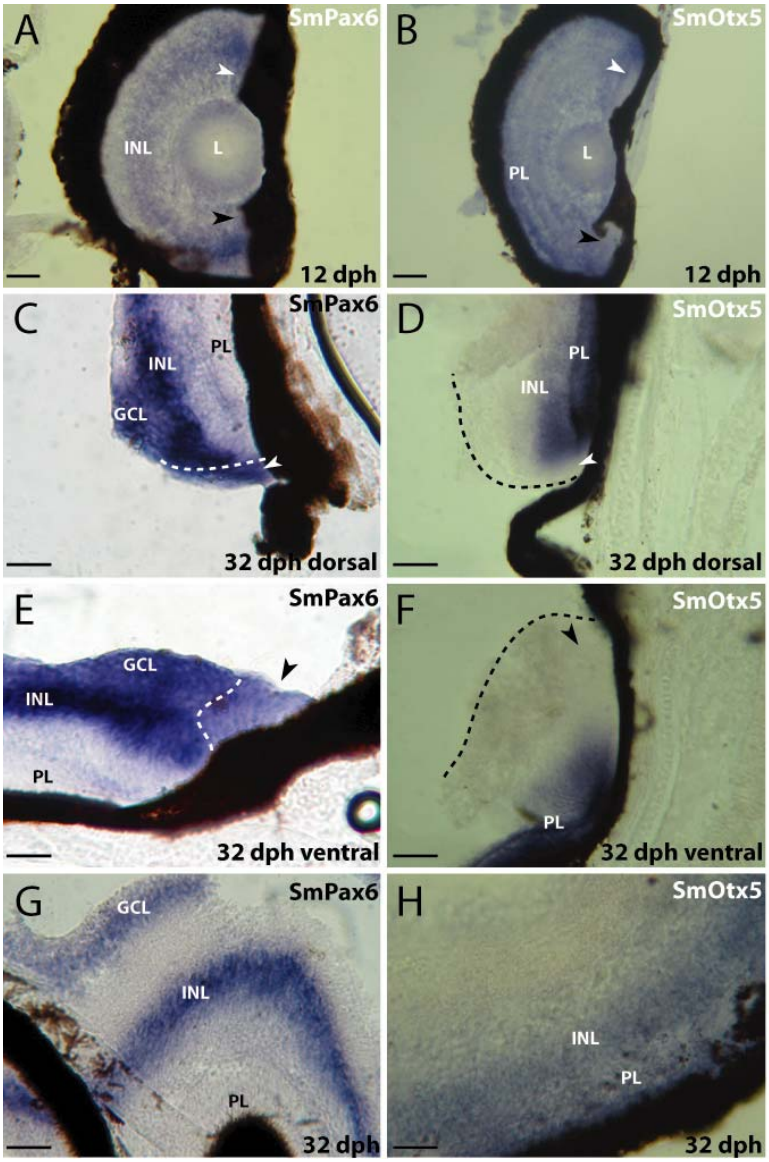

Figure 40. Symmetric and asymmetric expression of *SmPax6* and *SmOtx5* in the pre-metamorphic and metamorphic turbot retina, respectively. (A-H) The expression of *SmPax6* (A, C, E, G) and *SmOtx5* (B, D, F, H) was localized by *in situ* hybridization on retinal cryosections (see materials and methods for details). (A, B) Eye sections of a 12 dph turbot larva hybridized with an anti-sense digoxygenin labeled SmPax6 (A) or SmOtx5 (B) riboprobe. In (A, B) the dorsal part of the eye is up. (C-H) Retinal sections of a 32 dph turbot juvenile hybridized with an anti-sense digoxygenin labeled *SmPax6* (C, E, G) or *SmOtx5* (D, F, H) riboprobe. (G, H) show the center of the retina. The white (A-D) and black (A-B, E-F) arrowheads show the dorsal and ventral CMZ, respectively. The white dashed line in (C, E) show the border between the differentiated cells of the retina and the CMZ. GCL, ganglion cell layer; INL, inner nuclear layer; PL, photoreceptors layer. Scale bar: (A, B) 200 μm, (C-H) 150 μm.

In contrast to *Pax6*, no expression of *Otx5* was detected in cells of the CMZ before and during metamorphosis (Figure 40B, D, F). Whereas the number of *Otx5* negative cells was equal between the ventral (black arrowhead) and dorsal (white arrowhead) CMZ before metamorphosis, it was higher in the ventral CMZ (black arrowhead) than in the dorsal one (white arrowhead) after this process (Figure 40B, D, F).

Taken together, these results indicate that the retinal stems cells and/or retinoblasts of the CMZ of turbot undergo a shift from a symmetric to an asymmetric proliferative pattern during metamorphosis and that this pattern is kept after this process.

12.4.3 The type 3 deiodinase (SmD3) is expressed in the dorsal CMZ in premetamorphic turbot

To find out the molecular actors involved in the process of asymmetric growth at the CMZ, we investigated a candidate gene encoding a type 3 deiodinase (D3). Indeed, this phenomenon of asymmetric growth at the CMZ was already observed during metamorphosis in the *Xenopus* retina (Beach and Jacobson, 1979b)). In this species, it was shown that the shift in the growth pattern of the CMZ was controlled by the thyroid hormones (THs) and a type 3 deiodinase (D3) which transforms the active hormones T_4 and T_3 into inactive forms (Marsh-Armstrong et al., 1999). During embryogenesis, the mRNA of *D3* is accumulated in the dorsal CMZ of the frog retina until metamorphosis begins (Marsh-Armstrong et al., 1999). At this stage, D3 activity increases dramatically in the retina protecting the cells in the dorsal CMZ of the THs proliferative effect. In contrast, the cells of the ventral CMZ where *D3* is not expressed respond to the THs in increasing the number of mitotic divisions (Marsh-Armstrong et al., 1999).

To examine whether a similar molecular mechanism triggers the metamorphosis of the turbot retina, we cloned *D3* from the turbot and examined its expression pattern during embryonic and metamorphic stages. The first round of PCR using degenerated primers allowed isolating a 336 bp fragment displaying similarity with the deiodinase domain of *type 3 deiodinase* (*D3*) from other species. From this sequence we designed nested reverse and forward specific primers allowing amplification of a 618 bp and 964 bp fragment by 5' and 3' RACE PCR, respectively. Put together, the two fragments correspond to the entire full-length cDNA of the *SmD3* gene.

A

```
acgcggggatgggtaaaggtgactaaataccagttgtgtgtctttcgccggctcggtcgc  60

atcccgccggtgatgcacgactcgggcagtgtccagatggcgcgggcgctgaagcacgcc 120
            M  H  D  S  G  S  V  Q  M  A  R  A  L  K  H  A  16

gccctgtgcctgatgctgctgccccggttcctcctggccgcggtcatgctgtggctcctg 180
 A  L  C  L  M  L  L  P  R  F  L  L  A  A  V  M  L  W  L  L  36

gatttcttgtgcatcaggaaaaaagtgctgctgaacatgggagaccggcaggacagcgcg 240
 D  F  L  C  I  R  K  K  V  L  L  N  M  G  D  R  Q  D  S  A  56

gacgacccgccggtgtgcgtctccgactccaacaagatgttcaccttggagtccctcagg 300
 D  D  P  P  V  C  V  S  D  S  N  K  M  F  T  L  E  S  L  R  76

gccgtgtggtacggacagaaattggacttttcaaatccgcgcacctcgggcgcagtgcg 360
 A  V  W  Y  G  Q  K  L  D  F  F  K  S  A  H  L  G  R  S  A  96

cccaacaccgaggtggtgctggtccaggagcagcggcgggtccggatcctggactgcatg 420
 P  N  T  E  V  V  L  V  Q  E  Q  R  R  V  R  I  L  D  C  M 116

agggggaagaggccgctcattctcaacttcggcagctgctcttgaccgccgttcatgacg 480
 R  G  K  R  P  L  I  L  N  F  G  S  C  S  U  P  P  F  M  T 136

cgcctggcggcgttccagcgcgtcgtgagccagtacgcggacattgcggactttgtagtt 540
 R  L  A  A  F  Q  R  V  V  S  Q  Y  A  D  I  A  D  F  V  V 156

gtatatatcgaggaggcgcatccgtccgacggctgggtgagctcggacgcgccgtatcag 600
 V  Y  I  E  E  A  H  P  S  D  G  W  V  S  S  D  A  P  Y  Q 176

atccccaagcaccgctgcctggaggaccggctcagagccgcccagctgatgctcgccgag 660
 I  P  K  H  R  C  L  E  D  R  L  R  A  A  Q  L  M  L  A  E 196

gtgcccggcagcagcgtggtggtggacgacatggacaactcgtccaacgccgcgtacgga 720
 V  P  G  S  S  V  V  V  D  D  M  D  N  S  S  N  A  A  Y  G 216

gcctacttcgagaggctctacatcgtcagggacgagcgcgtggtgtaccaggggggccgg 780
 A  Y  F  E  R  L  Y  I  V  R  D  E  R  V  V  Y  Q  G  G  R 236

ggtccggagggataccggatctccggcctcagaagctggctggagcagtacagggacgat 840
 G  P  E  G  Y  R  I  S  G  L  R  S  W  L  E  Q  Y  R  D  D 256

ctggagacttcccagaccgcggtgctccatgtgtagttggggaagatgccgagcccgcct 900
 L  E  T  S  Q  T  A  V  L  H  V Stop                       267

gccacttcagtgcaaaatattaaaaagctgctatcaaatgttcacacatggtacattatg 960
ttgtgtccccccccgcatcgacgatggactggactctgtgacagatagcctgaagccttg 1020
ccgaagccccatccccaggctggataggctggcacgttgtgctcgtctcaccttcactga 1080
ttgctcatggaccgatttttctttattattatttttttttttttgtatggaaaagtcttg 1140
gatccgtttaaactggattcaattagtggtcgctctatttttctacagtgtgtgtgtgag 1200
tgtgtgtgtgtgtgtgtgtgcgtgcgtgcgtaaaagcgcgtgcgctgttcgcgttaat 1260
atctcgatccgctcgggtgtgtctatgaagttcggtttttaaaaggcgcagccagagaac 1320
cgacactgatgtttctgacgtcgcgagcgggtcgatattagcaggatcgggcgccaaacg 1380
atgtgatgttggtcatgaaacgaggaagatgtaactgaacaaatgtttgtaataaatgtc 1440
agtcatccctcactggtgattcactgtcgactgtggaacaaacgccgtaaacttcctcct 1500
tcgggtccttctgtggtttgatggttggtaacgtgatgagctcatcggtcatactctcag 1560
gtttgaggacaataataataaaaaaaaaaaaagtttgatgtaaaaaaaaaaaaaaaaaaa 1620
aaaaaaaaa                                                    1629
```

B

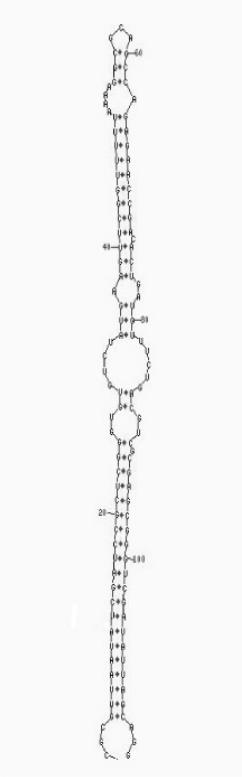

Figure 41. Nucleotide and deduced amino acid sequence of the *S. maximus D3* cDNA and secondary structure of SECIS. (A) The nucleotide and amino acid positions are numbered and indicated on the right. The start and stop codons are indicated in bold letters. The deiodinase domain is shaded with the highly conserved selenocystein (U) amino acid indicated in bold letter. The Selenocystein Insertion Sequence (SECIS) is located in the 3'UTR and is indicated in bold letters. The putative polyadenylation signal is underlined. (B) Representation of the secondary structure of the SECIS RNA element.

The *SmD3* cDNA contains a deduced 801 bp open reading frame (ORF) encoding 267 amino acids flanked by a 72 bp 5′ UTR and a 753 bp 3′ UTR which is terminated by a 29 bp poly(A) tail (Figure 41A). In addition, the 3′UTR contains a Selenocystein Insertion Sequence (SECIS) of 114 bp allowing the translation of a premature stop codon located in position 463 into the rare selenocystein amino acid (Figure 41B). The deduced *Sm*D3 protein contains a deiodinase domain of 242 amino acids (shaded in Figure 41A) and a selenocystein amino acid in position 131 (Figure 41A). The complete deduced protein sequence was aligned with other vertebrate deiodinase proteins sequences available in the NCBI databank, and a phylogenetic tree was inferred allowing the conclusion that we cloned a *SmD3* gene (Figure 42). We next investigated the expression pattern of *SmD3* in turbot embryos and larvae by *in situ* hybridization on whole mounts and sections with *SmD3* digoxygenin labeled anti-sense riboprobes. At the early stages examined until 6 dpf, we did not detect any expression of *SmD3* in the eye (data not shown), whereas *SmBmp4* and *SmBmp2*, two marker genes of the dorsal CMZ in vertebrates (Papalopulu and Kintner, 1996), used as positive controls, were expressed in the dorsal CMZ of turbot retina of 4 dpf embryos (Figure 43B-D; data not shown).

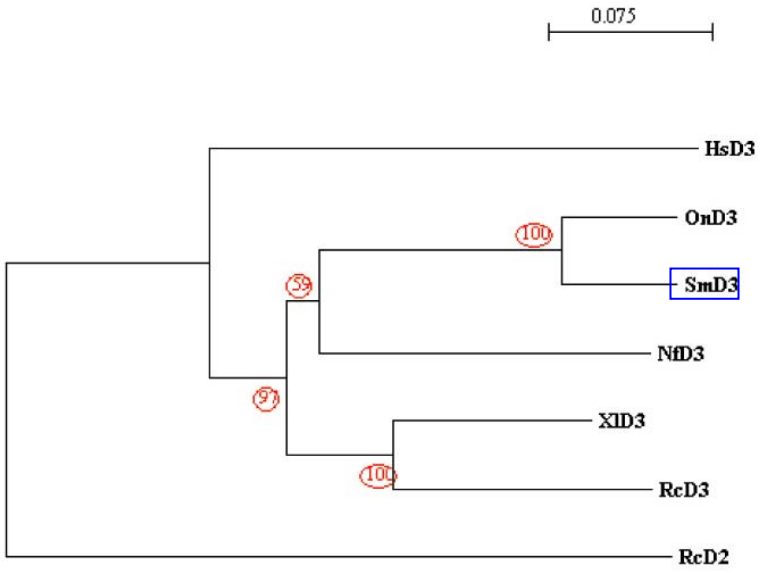

Figure 42. Phylogenetic tree of D3 inferred by the Neighbor Joining method. The length of branches is proportional to the phylogenetic distance. The scale bar represents an evolutionary distance of 0.075 amino acid substitutions per site. 1000 bootstrap replications were used to test the robustness of each internal node (see materials and methods for details.). Accessions numbers of the sequences used for the tree inference are as follows : D3 of nile tilapia (OnD3) (CAA71997), D3 of african clawed frog (XlD3) (AAA49971), D3 of human (HsD3) (P55073), D3 of turbot (SmD3) (ND), D3 of australian lungfish (NfD3) D3 of bullfrog (RcD3) (L41731) and D2 of bullfrog as outgroup (Rc) (L42815). ND, not deposited.

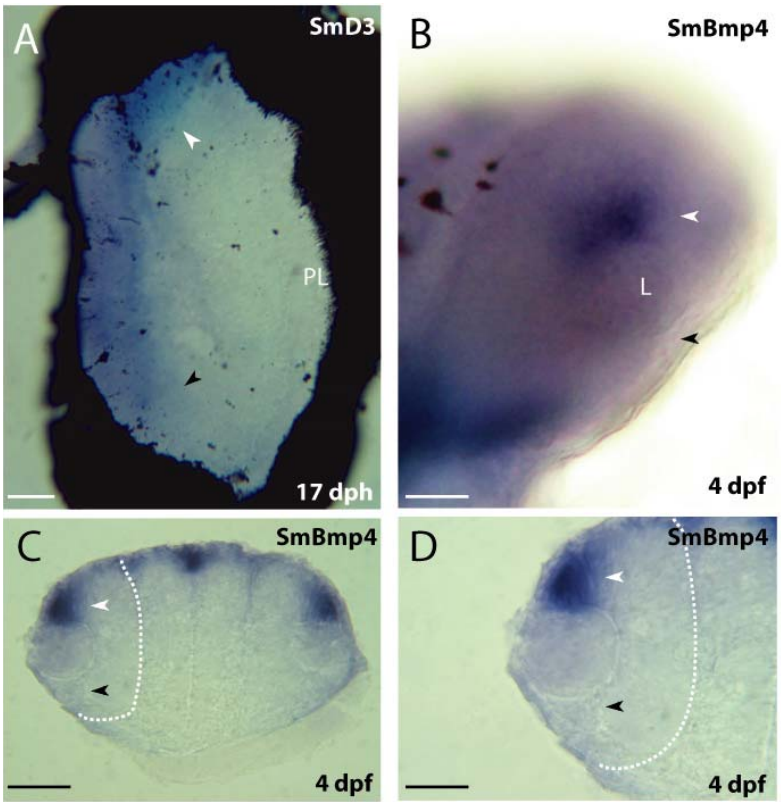

Figure 43. Asymmetric expression of *SmD3* and *SmBmp4* into the CMZ of premetamorphic turbot retina. (A-D) The expression of *SmD3* (A) and *SmBmp4* (B, C, D) was localized by *in situ* hybridization on whole mount and retinal cryosections (see materials and methods for details). (A) Eye section of a 17 dph turbot larva hybridized with an anti-sense SmD3 digoxygenin labeled riboprobe. The distal part of the eye is toward the left. (B) 4 dpf turbot embryo hybridized with an anti-sense *SmBmp4* digoxygenin labeled riboprobe. The anterior part of the embryo is toward the right. (C-D) Cryosections of the turbot embryo shown in (B). The white and black arrowheads in (A-D) show the dorsal and ventral CMZ, respectively. L, lens; PL, photoreceptors layer. Scale bar: (A) 200 µm, (C) 50 µm, (B, D) 25 µm.

At later stages before metamorphosis, at about 17 dph, we found *SmD3* expression in the dorsal CMZ (white arrowhead) and not in the ventral one (black arrowhead) (Figure 43A). At later stages, the expression of both genes was undetectable in this organ (data not shown). Independent of the gene considered, no labeling was seen with the sense probes used as negative controls (data not shown). These results suggest that the shift from a symmetric to an asymmetric growth of the CMZ during turbot metamorphosis may be controlled by the asymmetric expression of the *SmD3* gene.

12.5 Discussion

Whereas the changes occuring during amphibians metamorphosis have been now well studied (Marsh-Armstrong et al., 1999; Mann and Holt, 2001), little is known concerning

flatfish metamorphosis. The present study is the first one examining the retinal changes occuring during this process in turbot. We found that the principal photopigment molecule of the rod photoreceptors, namely rhodopsin, appears during metamorphosis, but not before, suggesting that the rod photoreceptor cell type is generated only after the larval life. This agrees well with what was found in halibut and flounder, two other flatfish species in which rods and rhodopsin were found only after the metamorphic process (Kvenseth, 1996; Evans and Fernald, 1993; Mader and Cameron, 2004). Interestingly enough, a cone-to-rod differentiation sequence was also reported in nonmetamorphic Teleost fish, as for instance in goldfish (Raymond, 1985). In larvae of this species, the PL of the retina is constituted of only cones (Johns, 1982; Raymond and Rivlin, 1987) and during maturation of this organ rod photoreceptors are generated mostly from precursors located into the CLZ and to a lesser degree from precursors located into the PL (Otteson et al., 2001). In contrast to goldfish, we found that during metamorphosis of turbot a zone of positive BrdU cells close to the CMZ, likely the CLZ, was only localized in the ventral part of the retina. According to this result, the rhodopsin was only found in the ventral postmetamorphic retina of turbot, respectively. Therefore, the appearance of rod photoreceptor cells in the flatfish juvenile retina, contributes to the acquisition of a scotopic vision allowing these animals to be adapted to their new habitat characterized by weak light conditions.

An other asymmetric cellular process occuring in the turbot retina during and after metamorphosis is the asymmetric growth pattern at the CMZ. Interestingly, this difference of growth between the ventral and dorsal retina was already described in metamorphic and postmetamorphic *Xenopus*. In this species, due to an increase number of progenitors in the ventral CMZ compared with the dorsal CMZ, more cells are added to the ventral part of the retina than to the dorsal one. The increase of proliferation in the ventral CMZ is believed to allow the production of neurons in the portion of the retina viewing the new binocular visual field (Mann and Holt, 2001). In addition, this change is thought to compensate for the change in eye position observed during metamorphosis (Mann and Holt, 2001). This may also be the case for turbot which displays an important remodelling of the larval visual system during metamorphosis allowing the juvenile to acquire a new binocular visual field. Previous work in frogs and this study in turbot suggest that the asymmetric growth in the CMZ of both species may be controlled by the asymmetric expression of the type 3 deiodinase (Marsh-Armstrong et al., 1999). This selenocystein containing enzyme acts in removing an iodine atom from the inner ring of the T_3 and T_4 hormones to convert them into inactive compounds that will be eventually metabolized to tyrosine (Becker et al., 1997). It was shown that the

mRNA of this enzyme are expressed in the retinal progenitor cells of the dorsal CMZ in the *Xenopus* embryo as early as stage 22 before any functional thyroid gland is developed. However, altough this gene is expressed very early, the D3 activity in the frog retina peaks much later only at metamorphic climax at stage 62. It acts in preventing the dorsal CMZ from responding to the THs signal which controls the metamorphic process. In contrast, the retinal progenitors of the ventral CMZ where the *D3* is not expressed respond to the THs in increasing their proliferation. Although in our study we found *SmD3* expression in the dorsal pre-metamorphic retina, a zone corresponding likely to the CMZ, we could not examine the functionality of this enzyme *in vivo* because of the technical limitations of the turbot model system.

Eye inversion studies in frog embryos showed that the growth pattern in the metamorphic retina is determined during embryogenesis (Beach and Jacobson, 1979b). Therefore, an unknown factor expressed during embryogenesis would be directly involved in the regulation of metamorphosis through the regulation of *D3* expression. Two good candidates for the unknown factor would be the *Bmp2* and *Bmp4* genes involved in the BMP signaling pathway. They encode secreted molecules containing a TGFβ domain acting as morphogens and are known to control cell growth and development (for review see Schier and Talbot, 2005; Varga and Wrana, 2005). In frog and turbot, both genes are expressed transiently into the embryonic retina specifically into the cells of the dorsal CMZ, but not in the ventral ones (Papalopulu and Kintner, 1996; this study). In the future, the hypothesis of a regulation of *D3* expression by the BMP signaling pathway will have to be tested.

In conclusion, this study suggests that the metamorphosis of the turbot visual system displays an evolutionary convergence with the one of *Xenopus*. In both ectothermic vertebrates, this process transforms a larva harboring a panoramic visual field into a juvenile harboring a binocular one. This is achieved by the migration of the eyes and the asymmetric growth of the retina.

Previously, we have shown that the establishment of the functions between the pineal gland and retina is temporally, spatially and functionally different during Teleost development. To better understand the molecular mechanisms triggering formation of both photoreceptive organs, we examined the functions of the *Paired box 6* (*Pax6)* gene, a master key player for photoreceptors development and evolution (Gehring and Ikeo, 1999), in the zebrafish. In addition, during my master degree, we found a new alternative *Pax6* splice variant containing a new identified exon. Although the functions of *Pax6* during mammalian development have been described in details, the functions of this gene and its splice variants during Teleost development remains poorly documented.

The following work presents the characterization and the functions of two alternative splice variants of *Pax6* during zebrafish development.

13. Characterization and functions of two alternative Pax6.2 splice variants in photoreceptive organs and forebrain development in zebrafish

13.1 Abstract

The development of the central nervous system including the eyes in eumetazoa is triggered by several highly conserved molecules including signaling molecules and transcription factors. Among them, *Pax6* encoding a DNA binding protein was shown to be one of the master controlling gene for eye development in vertebrates and invertebrates. In addition, it has been demonstrated by knock out experiments in mice that the different activities of this transcription factor can be modified by alternative splicing. Unfortunately, whereas several alternative splice variants have been described from amphioxus to human, their functions has not been yet examined *in vivo*.

In this study, we report in zebrafish (*Danio rerio*) the cloning of a new alternative *Pax6.2* splice variant, namely *Pax6.2(2a)*, encoding a truncated protein without its N-terminal 18-19 amino acids compared with the canonical *Pax6.2* (*Pax6.2c*). We studied the expression of both, *Pax6.2c* and *Pax6.2(2a)* splice variants, during zebrafish development and report that both are able to induce ectopic eyes when overexpressed in larval imaginal discs of fly. A PCR screen and an *in silico* study revealed that the *Pax6.2* exon 2a is present from amphioxus to human but not in ascidians. Finally, we provide evidences that the PAX6.2(2a) splice variant is principaly involved in the morphogenesis and patterning of the forebrain, including hypothalamus, whereas PAX6.2c is necessary for both, forebrain development and proper dorso-ventral patterning of the optic cups.

13.2 Introduction

During eumetazoa development, the formation of the central nervous system (CNS) and the photoreceptive organs is triggered by the activity of several conserved proteins including signaling molecules and transcription factors (Gehring and Ikeo, 1999; Sharman and Brand, 1998; Leuzinger et al., 1998; Nagao et al., 1998; Tomarev, 1997; Lupo et al., 2005).

Among them, *Pax6* encodes a highly conserved transcription factor containing two DNA binding domains, the paired domain and paired-like homeodomain, both separated by a flexible, glycin-rich acidic linker region (Krauss et al., 1991; Wilson et al., 1995). PAX6 acts as an activator of gene expression via its transactivation domain enriched in proline, serine and threonine located in the C-terminal end of the protein following the homeodomain (Glaser et al., 1994; Carriere et al., 1995; Czerny and Busslinger, 1995; Tang et al., 1998). In vertebrates, *Pax6* is expressed in the developing CNS including forebrain, hindbrain, eyes, pineal gland, nose and spinal chord of the embryo (Krauss et al., 1991; Turque et al., 1994; Walther and Gruss, 1991; Wullimann and Rink, 2001; Estivill-Torrus et al., 2001), as well as in the endocrine cells of the pancreas where it regulates the biosynthesis of insulin and glucagon (Ashery-Padan et al., 2004; St-Onge et al., 1997; Turque et al., 1994; Beimesche et al., 1999). In the genome of all vertebrates examined to date, only one *Pax6* gene have been found, excepted in zebrafish in which two *Pax6* genes, namely *Pax6.1* and *Pax6.2*, are present (Nornes et al., 1998). In this species, both genes are expressed in overlapping and specific areas in the CNS and the photoreceptive organs (Nornes et al., 1998). In invertebrates, *Pax6* is also expressed in the CNS and the eyes (Hartmann et al., 2003; Kammermeier et al., 2001; Czerny and Busslinger, 1995, Quiring et al., 1994). Heterozygous mutations of *Pax6* lead to severe eye and CNS phenotypes such as Aniridia and Peter's anomaly in human, Small eye (*Sey*) in rodents and Eyeless (*Ey*) in fruit fly, whereas homozygous mutations are lethal (Ton et al., 1991; Hanson et al., 1995; Hill et al., 1991; Matsuo, 1993; Quiring et al., 1994, Hogan et al., 1986; Glaser et al., 1994). Overexpression of *Pax6* leads to the induction of ectopic eyes in frog and fly, indicating that it is one of the master genes in eye development (Halder et al., 1995; Chow et al., 1999; Onuma et al., 2002; Zuber et al., 2003).

The different functions of PAX6 are determined by the specific activities of the paired domain, paired-like homeodomain and transactivation domain of the protein (Haubst et al., 2004; Punzo et al., 2001). These activities can be modified by alternative mRNA splicing. In vertebrates, the best known example is the presence or absence, in the N-terminal subdomain of the paired domain, of an alternative 42 bp exon, namely exon 5a, encoding a 14 amino acids sequence (Epstein et al., 1994a; Epstein et al., 1994b; Azuma et al., 1999; Singh et al., 2002). The exon 5a insertion into the PAX6 paired domain allows unmasking the DNA binding potential of the C-terminal subdomain allowing the PAX6 protein to bind other DNA binding sites (Epstein et al., 1994a; Epstein et al., 1994b; Kozmik et al., 1997). Notably, the targeted exon 5a deletion in mice by the Cre/*lox*P system leads to eye defects in the iris, cornea, lens, and retina (Singh et al., 2002). A single base mutation at the 20th nucleotide

position of exon 5a, which results in a valine to asparagine substitution, leads to severe eye defects in human (Azuma et al., 1999). Besides this well known example, the existence of other *Pax6* splice variants has been reported but their functions have not been examined *in vivo* (Jaworski et al., 1997; Glardon et al., 1998; Mishra et al., 2002).

Here we report the cloning of a new alternative *Pax6.2* splice variant in the zebrafish (*Danio rerio*) which is characterized by the insertion of a 71 bp exon, namely 2a, introducing an internal stop codon into the canonical *Pax6.2* (*Pax6.2c*). This variant called *Pax6.2(2a)* encodes a truncated protein without its 18-19 N-terminal amino acids, compared with the *Pax6.2c*. We studied the expression of both, *Pax6.2c* and *Pax6.2(2a)*, during zebrafish development and show that both induce ectopic eyes when overexpressed in larval imaginal discs of fly. A PCR screen and an *in silico* study revealed that *Pax6.2(2a)* is present from amphioxus to human and is absent in ascidians. Finally, we provide evidences that the PAX6.2(2a) splice variant is principaly involved in the morphogenesis and dorso-ventral (DV) patterning of the forebrain, including hypothalamus, whereas PAX6.2c is necessary for both, forebrain development and DV patterning of the eyes.

13.3 Materials and Methods

13.3.1 Fish lines

Zebrafish (*Danio rerio*) were maintained on a 14h light/10h dark (LD) cycle at 28.5 °C and bred as described previously (Westerfield, 1993). Eggs were obtained as described previously (Westerfield, 1993). For whole mount *in situ* hybridization studies, phenylthiocarbamide (PTU; 0.2 mM) was added to eggs water at 12 hpf to prevent pigmentation .

13.3.2 Cloning and contruction of the full-length Pax6.2(2a) splice variant

A PCR strategy was used on extracts from 78 hours post-fertilization (hpf) old larvae to isolate the *Pax6.2(2a)* splice variant with the following specific primers designed from the 5' UTR (forward: 5'GAGATTTCCACACCGTACGGG3', bases 5-25) and 3' UTR (reverse: 5'GTCTG TGCGCTCAAGTCAAAGGGCGTA3', bases 1585-1611) of *Pax6.2c*. Messenger RNA were extracted with the TRIzol reagent (Invitrogen) and reverse transcribed in cDNA with the Superscript-II (Gibco) before being used for PCR amplification with the Advantage

High Fidelity kit (Clontech): 1 minute 40 seconds at 95 °C, 30x(13 seconds at 94 °C, 1 minute at 63.5 °C, 2 minutes at 68 °C), followed by a final extension time of 7 minutes at 68 °C. A fragment of about 1.5 kb was obtained and cloned into the pCR2.1-TOPO vector. Eighteen clones were sequenced and two corresponded to the *Pax6.2(2a)* cDNA. After verification that only one exon insertion occurs in the *Pax6.2(2a)* compared to the *Pax6.2c* cDNA, we exchanged the first 300 bp of the full-length *Pax6.2c* cDNA (a gift from Dr. Stefan Krauss) with the first 371 bp of the *Pax6.2(2a)* variant in order to obtain a full-length *Pax6.2(2a)* cDNA. For this purpose, we digested the cDNA of *Pax6.2(2a)* with EcoR1 and Pml1 and *Pax6.2c* with Xho1 and Pml1 and we purified two fragments of about 400 and 1400 bp, respectively. Both were then inserted into the vector pBluescript II KS digested with EcoR1 and Xho1. The correct sequence of the full-length *Pax6.2(2a)* cDNA obtained was then controlled by sequencing.

13.3.3 Genomic localization of the new exon 2a

The genomic position of the new exon was located by PCR on a zebrafish genomic DNA template extracted with a PCR extraction buffer (10mM Tris pH8, 2 mM EDTA, 0.2 % Triton X-100, 200 µg/ml Proteinase K) from 78 hpf larvae. The second intron was amplified with the following specific primers designed from the second exon (forward: 5'GGGCTCAGGCGCTGGAGCAGAATGCCT3') and the third exon (reverse: 5'CGCCACTCCTGATTCCCACGTGGGTTG3') and sequenced.

13.3.4 Whole mount in situ hybridization

Whole mount *in situ* hybridization was performed as described in Thisse et al. (2004) except that hybridization temperature and washes were at 67.5 °C. Details on the *Pax2b, Six3b, Emx3, Ngn1, ExR, Flh, Dlx2* riboprobes are available upon request. The *Pax6.1* and *Pax6.2* , *Otx5*, *Vax1* and *Vax2* riboprobes were a gift from Dr. S. Krauss, J. Gamse and S.W. Wilson, respectively.

13.3.5 Constructs, in vitro transcription of messenger RNA and detection of eGFP

To test the specificity of the morpholinos used during this study, we generated two different constructs. The 5'UTR and partial ORF of *Pax6.2c* (bases 17 to 375) or *Pax6.2(2a)* (bases 17 to 446) cDNA were cloned into the EcoRI/BamHI restriction sites of the modified N2eGFP vector (Clontech) (T7N2eGFP). The T7N2eGFP vector was constructed by inserting a T7 promotor taken from the pBluescript KSII (Stratagene) into the NheI/SacI restriction sites of N2eGFP. Both constructs, namely *6.2*UTR/eGFP and *6.2(2a)*UTR/eGFP, are in frame with the enhanced green fluorescent protein (eGFP) and the SV40 polyA signal. *In vitro* synthesis of mRNA from *6.2*UTR/eGFP and *6.2(2a)*UTR/eGFP cDNA was carried out with the mMessage mMachine kit (Ambion) using the standard procedure. Messenger RNA was injected at the one to two cell stages. EGFP was detected at 12 hpf with an epifluorescence binocular.

To examine if both *Pax6.2* splice variants were synthetized *in vivo*, we made five similar constructs as above with some modifications. First, the start codon of eGFP was mutated from methionine to asparagine (M→N) in order to avoid any translational interferences with the other putative start codons of *Pax6.2c* and *Pax6.2(2a)*. Then, the 5'UTR and partial ORF (bases 17-330) of *Pax6.2c* and *Pax6.2(2a)* were inserted into the T7eGFPM→N vector. Mutations of the putative start codons were carried out by PCR with mutated primers. Messenger RNA transcription and injections were carried out as indicated above. Detection of eGFP was performed with a rabbit anti-GFP (Torrey Pines Biolabs) at a 1:1000 dilution and an alkaline phosphatase coupled to an anti-rabbit secondary antibody (Zymed) at a 1:300 dilution.

13.3.6 Injections of morpholinos

Morpholinos (MO) were purchased from Gene Tools, LLC (Oregon) and designed against the first start codon of *Pax6.1c* (Pushel et al., 1992) (GenBank accession number NM_131304) and *Pax6.2c* (Nornes et al., 1998) (GenBank accession number NM_131641) and against the putative start codon of the *Pax6.2(2a)* and *Pax6.1(2a)* transcripts. The sequences of the MOs targeting Pax6.1c/Pax6.2c and Pax6.1(2a)/Pax6.2(2a), namely Mo3 and MoV, are respectively:

Mo3 (complementing bases): 5' GGTTATAGTATTCTTTTTGAGGCAT 3'

MoV (complementing bases): 5′ CGCCACTGTGACTGTTTTGCATCAT 3′

Different controls were used to test the MOs specificity and associated phenotypes:

Fisrt a second set of shifted morpholinos was used to knock down the translation of the *Pax6.1c/Pax6.2c* and *Pax6.1(2a)/Pax6.2(2a)* transcripts:

Pax6.1cMo (complementing bases 481-505): 5′ TATTCTTTTTGAGGCATAGTTCCAA 3′

Pax6.2cMo (complementing bases 254-278): 5′ GTATTCTTTTTGAGGCATTCTGCTC 3′

MoV2 (complementing bases *Pax6.1*:537-561; *Pax6.2*: 309-333): 5′TGTGACTGTTTTGCATCATGGACGC 3′

Second, as negative controls, we used the standard MO control (MoC) provided by Gene Tools, LLC (Oregon) which sequence is 5′CCTCTTACCTCAGTTACAATTTATA3′ and a MoV2 containing five mismatches (MoV2.5mut) which sequence is 5′TGTAACTGTTGTGCATTACGGATGC3′.

MOs were diluted in water (1 mM) and injected (1 to 4 nl) into embryos at the one to four-cells stages and at a concentration of 0.25 mM (Mo3), 0.3 mM (MoV, MoV2, MoV25mut) and 0.5 mM (MoC, Pax6.1c/Pax6.2cMo).

13.3.7 Transient transfection

The full-length *Pax6.2c* and *Pax6.2(2a)* cDNAs were cloned into the EcoR1/Xho1 site of pcDNA3 (Promega), respectively. Each construct was transfected to HeLa cells using the Lipofectamine reagent (Invitrogen) according to the manufacturer's protocol. The cells were grown in Dulbecco's medium (Gibco-Invitrogen) in Petri dishes supplemented with 10% fetal bovine serum, 1 mM sodium pyruvate, penicillin (100 units/ml) and streptomycin (100 µg/ml).

13.3.8 Western blot analyses

Preparation and immunoblotting of extracts from transfected HeLa cells were carried out as reported previously (Even et al., 2006). Zebrafish PAX6s were detected using a rabbit polyclonal antibody (1: 2000 dilution) raised against the carboxyl terminal end of the protein (Covance). Secondary antibodies coupled to horseradish peroxydase and an ECL Plus kit (Amersham LIFE SCIENCE) were used for the photo detection.

13.3.9 Targeted expression of PAX6.2c and PAX6.2(2a) in Drosophila

Ectopic expression of PAX6.2c and PAX6.2(2a) in larval imaginal discs of *D. melanogaster* was performed using the Gal4 system (Brand and Perrimon 1993). Full-length *Pax6.2c* and *Pax6.2(2a)* cDNAs were cloned in the pUAST vector (Brand and Perrimon, 1993) in the EcoR1/Xho1 site. For each constructs, transformant flies from three independant transgenic lines were crossed to the dpp^{blink} /Gal4 line.

13.3.10 In vitro translation

In vitro translation was performed using the TNT Coupled Reticulocyte Lysate Systems (Promega) as described in the manufacturer's protocol. Full-length *Pax6.1c* and *Pax6.2c* cDNAs were transcribed with the T3 polymerase and the full-length *Pax6.2(2a)* cDNA with the T7 polymerase. Synthetized ^{35}S-Met radiolabeled proteins were loaded on a 12% acrylamide gel and detected by autoradiography.

13.3.11 Real time quantitative PCR

Total RNA was extracted from embryos and larvae at different developmental stages with the Trizol Reagents (Invitrogen) and reverse transcribed with SuperScript III (Invitrogen) as described in the kit protocol. A 10-fold dilution of the cDNA obtained was used as a template for quantitative PCR amplification. Real time PCR was performed by means of a Light Cycler (Roche) and QuantiTect™ SYBR® Green PCR kit (Qiagen) under the following conditions: 15 minutes at 95°C, 15 seconds at 94°C, 20 seconds at 56°C, 10 seconds at 72°C over 50 cycles. The fluorescence of the amplified products was detected during 5 seconds at 76°C after the elongation step. For each sample point, a melting curve was obtained at the end of the PCR amplification to verify the specificity of the amplificon. In each experiment and for each gene, a standard curve generated by four dilutions from one cDNA sample was included in the PCR amplification to determine an expression value for each samples. *Elongation factor 1 alpha* (*Ef1a*) was used as a housekeeping gene for normalization of the data. The following specific primers used in the quantitative PCR experiment were designed with the Primer3 software (Rosen and Skaletsky, 2000):

Pax6.2c:

forward: 5'CCATTGGACAGTCATTGTTTATTTC3';

reverse: 5'GGGTTGGTTATGGTATTCTTTTTGA3';
Pax6.2(2a):
forward: 5'AAGAGGGACGCTGGGAAAA3';
reverse: 5'CAGAGTTGACTGTCCGTTTA3';
EF1α:
forward: TCCCAACCTCTTGGAATTTCTC;
reverse: 5'TGAAAGAGGCACTATCAGTCAAT3'.

Each experiment was conducted three times.

13.3.12 Cloning of exon 2a from different animal species

Exons corresponding to zebrafish exon 2a and corresponding introns were amplified by PCR from cDNAs and genomic DNA from different animal species. The following specific primers were used against cDNA of:
zebrafish pax6.1:
forward: 5'GGATATTTTAATAGAGTGAAGCAG3',
nested forward: 5'GTTTTAAGCGGACAGTCAACTCTG3',
reverse: 5'GCGCGCCACTGTGTGCGAGTTCAAC3',
nested reverse: 5'GTCTCGTGGAGTCGGGTTAGCGGTC3';
medaka (*Oryzia latipes*):
forward: 5'GGGAGACATTAAGTAGTGAAAACGGC3',
nested forward: 5'GTGGAC AGTCAACTCTGTTTCCAG3',
reverse: 5'GGGTCGCGCGCCGCTGTGA GCAAGTT CC3',
nested reverse: 5'GTATTCTGGAGATGTCGCAGGGTCGCGC3';
turbot (*Scophthalmus maximus*):
forward: 5'GGGAGACATTAAGTAGTGAAAACGGC3',
nested forward: 5'GTGGACAGTCAACTCTGTTTCCAG3',
reverse: 5'GTCGCA GGGTCGAGCACCACTGTG3',
nested reverse: 5'TGCCTGGTGGAATCCGGCAGCGGTC3';
newt (*Cynops pyrrhogaster*)
forward: 5'AGACTTTAAGTAGAGGCAAGCAGAT3',
nested forward: 5'GTGTGAGCCTTTTAATTGCATGACA3',
reverse: 5'TACCAGCCCGGCCGGGTGCCCCAGG3',

nested reverse: 5'GTCTGTCCGTTCAGCATCCGCAGCT3';

lancelet (*Amphioxus floridae*):

forward: 5'AGTACGGCTCTATGTTATAACGTAG3',

nested forward: 5'GTTGTCGCAGATCAAACCATTTCCC3',

reverse: 5'TGTTCTTCTCTCCGCTCGCCAGGTT3',

nested reverse: 5'GCGGTTAATGGAAGAAACGCTGGGG3'.

The following specific primers were used against genomic DNA of

Newt:

forward: 5'GGGGGCCGACTCCGAGCACCGCAG3',

nested forward: 5'CGAGCACCGCAGACCGGCAGCCATG3',

reverse: 5'CTGCTCCAGCGCGATCCCCTGTGT3',

nested reverse: 5'CAGCGCGATCCCCTGTGTCTCCCTT3';

lancelet:

forward: 5'GGTGGACGTCAAGCCGACCATGCCCC3',

reverse: 5'CCGGGCTGTACTGCGCATGCTCGTCC3';

turbot:

forward: 5'GGACTTTGACAACGACGCAGGATG3',

nested forward: 5'AACGACGCAGGATGCCCCAAAAA3',

reverse: 5'TGCATCATTGAGGCTACTCCAGAC3',

nested reverse: 5'CACGTGGCTTGGTTGTGG3'.

For the genomic *Pax6.1*, *Pax6* of *Ciona intestinalis* (*CiPax6)* and *HsPax6*, the sequences were found in the ensembl database. For the cDNA of *CiPax6* and *HsPax6*, the sequences were found in the ensembl database.

13.4 Results

13.4.1 Isolation of a new zebrafish Pax6.2 splice variant transcript, namely Pax6.2(2a), and genomic localization of the new exon

A specific RT-PCR was used to isolate a cDNA fragment covering the entire open reading frame (ORF) and a part of the 5' and 3' UTR of the *Pax6.2(2a)* transcript from 78 hpf

old larvae mRNA. The full-length *Pax6.2(2a)* cDNA was subsequently obtained by making a construction between the *Pax6.2c* and *Pax6.2(2a)* cDNAs (see materials and methods). The *Pax6.2(2a)* transcript harbors one more 71 bp exon, namely exon 2a, compared with the *Pax6.2c* transcript. It is located in the ORF between exon 2 and 3 and it introduces a premature stop codon six amino acids after the putative first start codon (Figure 44A-B).

To localize the genomic position of the exon 2a on the *Pax6.2* gene, we performed a PCR on zebrafish genomic DNA with specific primers designed from exon 2 and 3 leading to the amplification of a DNA fragment of about 3000 bp. The sequencing of this fragment indicated that it corresponds to intron 2 of *Pax6.2* including exon 2a located about 200 bp before the third exon (Figure 44A).

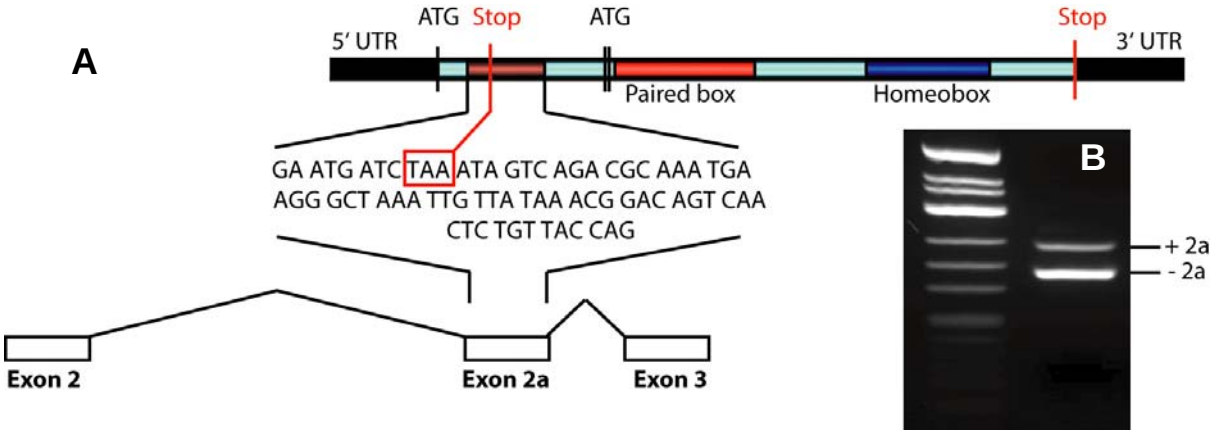

Figure 44. Nucleotide sequence, genomic location and conservation of the zebrafish *Pax6.2* exon 2a transcript. (A) Schematic drawing of the *Pax6.2(2a)* transcript (up) containing an additional exon, namely 2a, compared with the canonical *Pax6.2* (*Pax6.2c*) and genomic location of the exon 2a in the zebrafish *Pax6.2* gene (down). The exon 2a introducing a putative internal stop codon is located after the first putative start codon of *Pax6.2c*. (B) Representative RT-PCR amplification from mRNA of 78 hpf zebrafish larvae with two specific primers of *Pax6.2* located on exon 2 and 3. Presence or absence of the exon 2a in the amplified fragments is indicated by +2a or -2a, respectively.

13.4.2 Conservation of the zebrafish exon 2a sequence in other chordate species

To assess the relevance of the *Pax6.2(2a)* transcript function, we performed a PCR and *in silico* screen to determine whether the exon 2a sequence was also found in other chordate species including urochordates, cephalochordates, Teleosts, amphibians, birds and mammals. First, we examined *in silico* the presence of homologous sequences of exon 2a in the genomes of chordates available at the Ensembl and Japanese databases. It was found in

the *Pax6* gene of medaka, *Pax6.1* of zebrafish and *Pax6* of human with the conservation of the stop codon but not in the genome of the urochordate *Ciona intestinalis* (Table 2; Figure 45). It was also found by PCR in genomic DNA of turbot, newt and amphioxus *Pax6* (Table 2; Figure 45). These genomic sequences allowed designing specific primers that were used to detect the presence of the transcript encoding the putative truncated protein in embryos and larvae of newt, turbot, medaka and zebrafish (Table 2). The exon was also expressed in the canonical *Pax6* transcript of human. The conservation of this exon among chordates suggests that this alternative transcript might play an important role during development.

	B. floridae	*D. rerio 1*	*D. rerio 2*	*O. latipes*	*S. maximus*	*C. pyrrogaster*	*H. sapiens*
gDNA	+	+	+	+	+	+	+
mRNA	ND	+	+	+	+	+	+

Table 2. *In silico* and PCR screening for the *Pax6.2* exon 2a sequence in genomic DNA (gDNA) and mRNA of different animal species. Amphioxus (*B. floridae*), zebrafish (*D. rerio*), medaka (*O. latipes*), turbot (*S. maximus*), newt (*C. pyrogaster*) and human (*H. sapiens*). + : positive. ND, not determined.

```
Hs  GAAGACTTTAA-CTAGGGGCGC---GCAGATGTGT--GAGGCC-TTTTATTGT--GAGAGTGG----ACAGACATCCGAGATTTCAG
Mm  GAAGACTTTAA-CCAAGGGCGGTGAGCAGATGTGT--GAGATC-TTCTATTCT--AGAAGTGG----ACGTATATCCCAGTTCTCAG
Cp  GAAGACTTTAA-GTAGAGGCAA---GCAGATGTGT--GAGCCT-TTTAATTGC--ATGACAAG----ACAGCCACCCCATATTTCAG
Sm  GGAGACATTAA-GTAGTGAGAACG-GCAGATGATT--GACTA--AATTGTTAT--AG-AGTGG----ACAGTCAACTCTGTTTCCAG
Ol  GGAGACATTAA-GTAGTGAAAACG-GCAGATGATT--GACTA--AATTGTATT--AA-AGTGG----ACAGTCAACTCTGTTTCCAG
Dra GGATATTTTAA--TAGAGTGAA---GCAGATGACA--GTCTATAAATTGTTTT--A--AGCGG----ACAGTCAACTCTGTTTCCAG
Drb GAATGATCTAA-ATAGTCAGAC---GCAAATGAAG--GGCTA--AATTGTTAT--A--AACGG----ACAGTCAACTCTGTTACCAG
Bf  CTATGTTATAACGTAGTGGCGC---ACAGTTGTCGCAGATCA--AACCATTTCC--CAAACACCTCCACGGTGCACTTTTCACACAG
    : *:: : ***  :*: :  :    :**::**:    *      ::: :*: :     *  ::    **::  : *:::: :  ***
```

Figure 45. Multiple alignment of *Pax6* exon 2a nucleotide sequence. Human (Hs), mouse (Mm), newt (Cp), turbot (Sm), medaka (Ol), zebrafish (Dr) and amphioxus (Bf). The highly conserved stop codon is shaded.

13.4.3 Embryonic and larval expression of both Pax6.2 transcripts in zebrafish

The expression pattern of both *Pax6.2c* and *Pax6.2(2a)* splice variants was first examined during zebrafish development by real time quantitative PCR. In order to amplify specifically *Pax6.2(2a)* and *Pax6.2c*, specific reverse primers were choosen either in the exon 2a or juxtaposing exon 2 and 3, respectively.

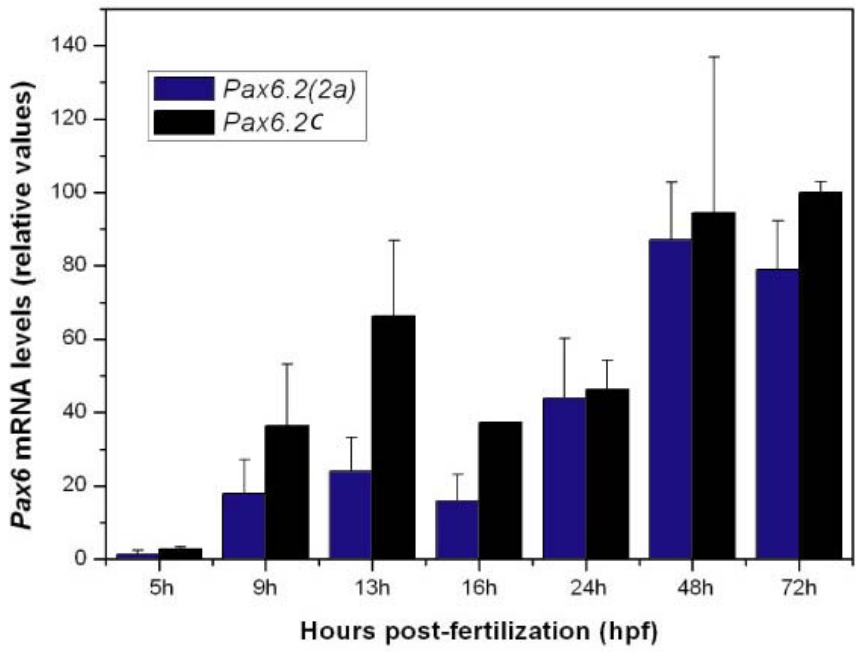

Figure 46. Variation of expression levels of *Pax6.2(2a)* and *Pax6.2c* during zebrafish development. Zebrafish *Pax6.2(2a)* and *Pax6.2c* transcripts abundance was measured by real time quantitative PCR in zebrafish embryos and larvae from 5 to 72 hours post-fertilization (hpf). Means +/- SEM of three independent experiments are represented. The values obtained are not comparable between both splice variants.

Expression of both *Pax6.2* transcripts started at the end of gastrulation (9 hpf; Figure 46); when the eye field and the lens placodes appeared, and was found at all the developmental stages examined until end of day 3 (Figure 46).

Then, the expression pattern of *Pax6.2(2a)* was examined by whole mount *in situ* hybridization. The 100 bp digoxygenin labeled riboprobe used, which targeted specifically exon 2a, did not allow detecting any specific staining. We next decided to perform a whole mount *in situ* hybridization on zebrafish embryos and larvae using a full-length *Pax6.2* digoxygenin labeled riboprobe targeting both variants. As previously shown, we found *Pax6.2* expression in the optic vesicles and diencephalon including the pineal anlage at 12 and 16 hpf (Figure 47A, B) (Nornes et al., 1998). When the optic cups are formed (24 hpf) and until 48 hpf, the expression of *Pax6.2* is still located to the eyes and several nuclei of the forebrain (Figure 47C). At day 3 of development, *Pax6.2* expression became restricted to the ganglion and inner nuclear layer of the retina (Figure 47D, E).

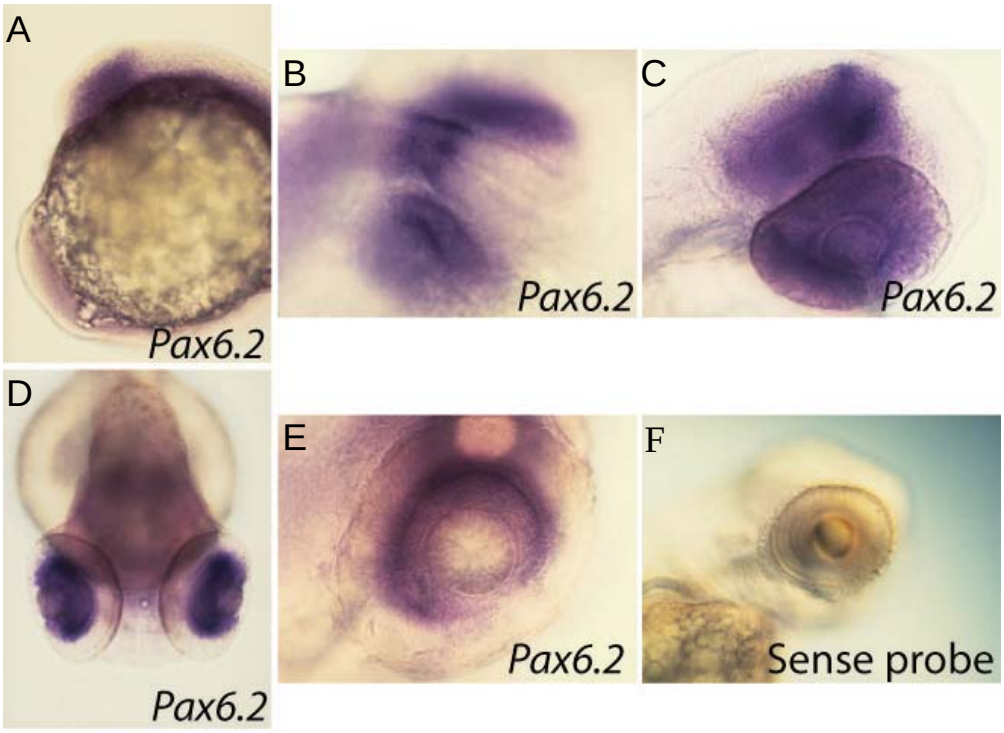

Figure 47. Localization of the general expression of *Pax6.2* in zebrafish embryos and larvae by whole mount *in situ* hybridization with an anti-sense digoxygenin labeled riboprobe at different developmental stages. *Pax6.2* expression is located in the optic vesicles and the diencephalon at 12 (A) and 16 (B) hpf. At later stages, *Pax6.2* expression is located in the retina at 48 (C) and 72 (D-F) hpf. (F) 72 hpf larvae hybridized with a Pax6.2 sense riboprobe used as a negative control.

Taken together, these results suggest that both variants play a role in all developmental stages in zebrafish and they are expressed in the eye at least until end of organogenesis.

13.4.4 In vitro and in vivo characterization of Pax6.2(2a)

Because the *Pax6.2(2a)* transcript is characterized by the presence of a putative internal stop codon, we felt necessary to test the hypothesis that the translation of this transcript leads to a truncated protein without its N-terminal 18-19 amino acids. The *in vitro* translation of the *Pax6.2(2a)* transcript in rabbit reticulocyte lysates or in HeLa cells led to the synthesis of a smaller protein compared with the *Pax6.2c* variant without the exon 2a as indicated by a shift to the down on a denaturing polyacrylamide gel (Figure 48A, B).

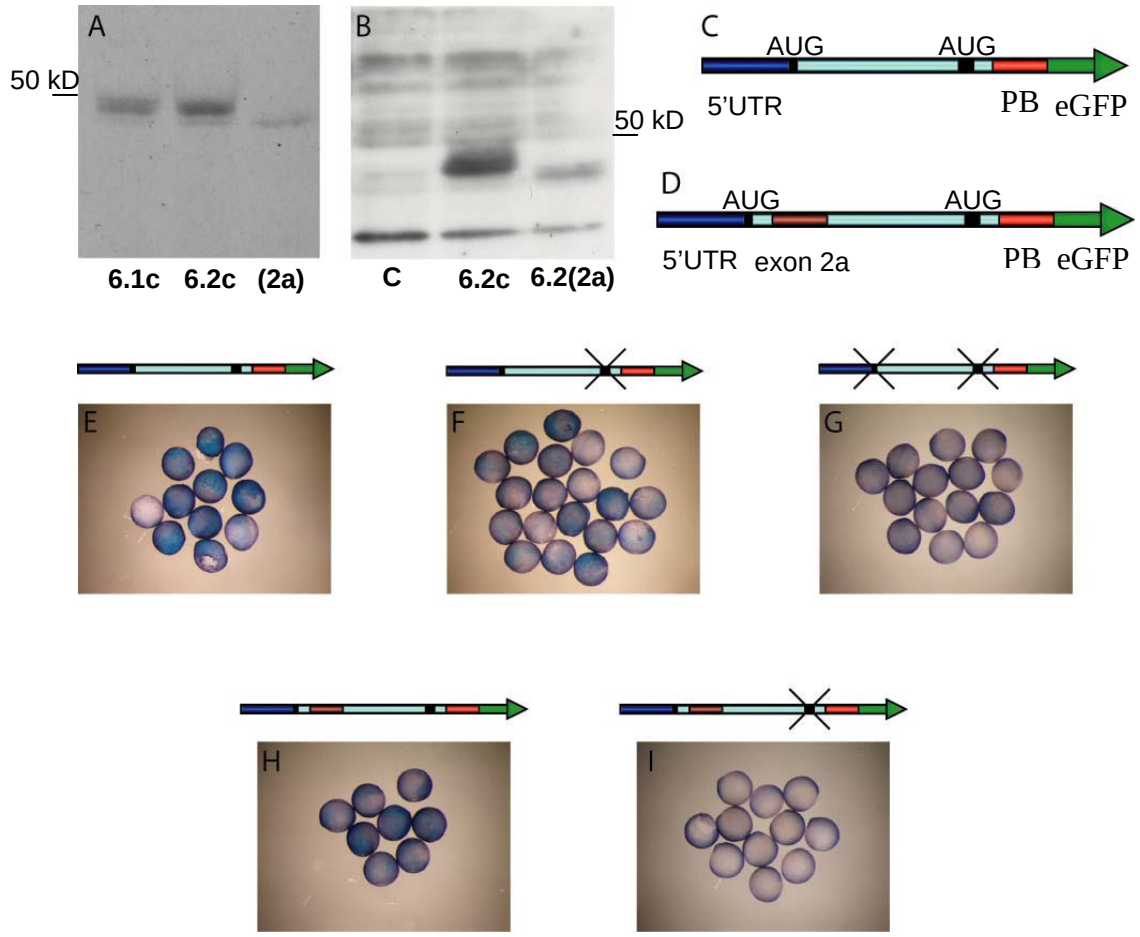

Figure 48. ***In vitro*** **and** ***in vivo*** **translation of both** ***Pax6.2*** **splice variants.** (A) *In vitro* translation of *Pax6.1*, *Pax6.2* and *Pax6.2(2a)* in rabbit reticulocyte lysates. Proteins were labeled with ^{S35}methionine and detected by autoradiography. The *in vitro* translation of the *Pax6.2(2a)* transcript leads to a protein shorter than PAX6.1c and PAX6.2c. (B) Western blot on protein extracts of Hela cells transfected with a *Pax6.2c* or *Pax6.2(2a)* cDNA and detection using a polyclonal antibody raised against the carboxyl terminal end of the PAX6 protein. The translation in human cells of the *Pax6.2(2a)* transcript leads to a shorter protein than PAX6.2c. (C-D) Schematic drawings of two messenger RNA constructs encoding PAX6.2c (C) and PAX6.2(2a) (D) fused to eGFP and used in (E, H). (E-I) Detection of eGFP with a polyclonal anti-eGFP and a secondary antibody fused to alkaline phosphatase in 9 hpf zebrafish embryos injected at the one to four cells stages with different mRNA constructs as indicated above each photographs (see materials and methods). In (E) both putative start codons of *Pax6.2c* are intacts whereas in (F) and (G) the second and both, respectively, are mutated. In (H) and (I) the putative start codon of *Pax6.2(2a)* is intact and mutated, respectively. Alkaline phosphatase staining is detected in (E-F, H) and not in (G, I).

In addition, we show that when two mRNA constructs containing the 5' UTR and a part of the ORF of *Pax6.2c* (Figure 48C) or *Pax6.2(2a)* (Figure 48D) fused to the eGFPmutM→N were injected in zebrafish embryo they are translated *in vivo* (Figure 48E, H). This was also the case when only the second putative start codon was mutated in the *Pax6.2c* trancript (Figure 48F). In contrast, when the two putative start codons were mutated in the *Pax6.2c*

trancript or the second putative start codon in the *Pax6.2(2a)* transcript, the translation did not occur (Figure 48G, I).

Taken together, these results indicate that the exon 2a insertion in *Pax6.2(2a)* leads to the translation of a shorter protein comparing with *Pax6.2c* and that the functional start codon of *Pax6.2(2a)* is located just before the paired box.

13.4.5 Pax6.2(2a) induces ectopic eyes in Drosophila

Because *sey* or *ey* overexpression in imaginal discs of *Drosophila* leads to the formation of ectopic eyes (Halder et al., 1995), we decided to compare the *in vivo* ability of PAX6.2(2a) and PAX6.2c to induce eye structures. In using the UAS/Gal4 system developed by Brand and Perrimon (1993), we targeted expression of both PAX6.2(2a) or PAX6.2c in imaginal discs of antennae, legs and wings of flies leading to the induction of ectopic eyes in these organs (Figure 49A-E, data not shown). No significative difference was observed between the size and frequency of ectopic eyes induced with both PAX6 protein variants.

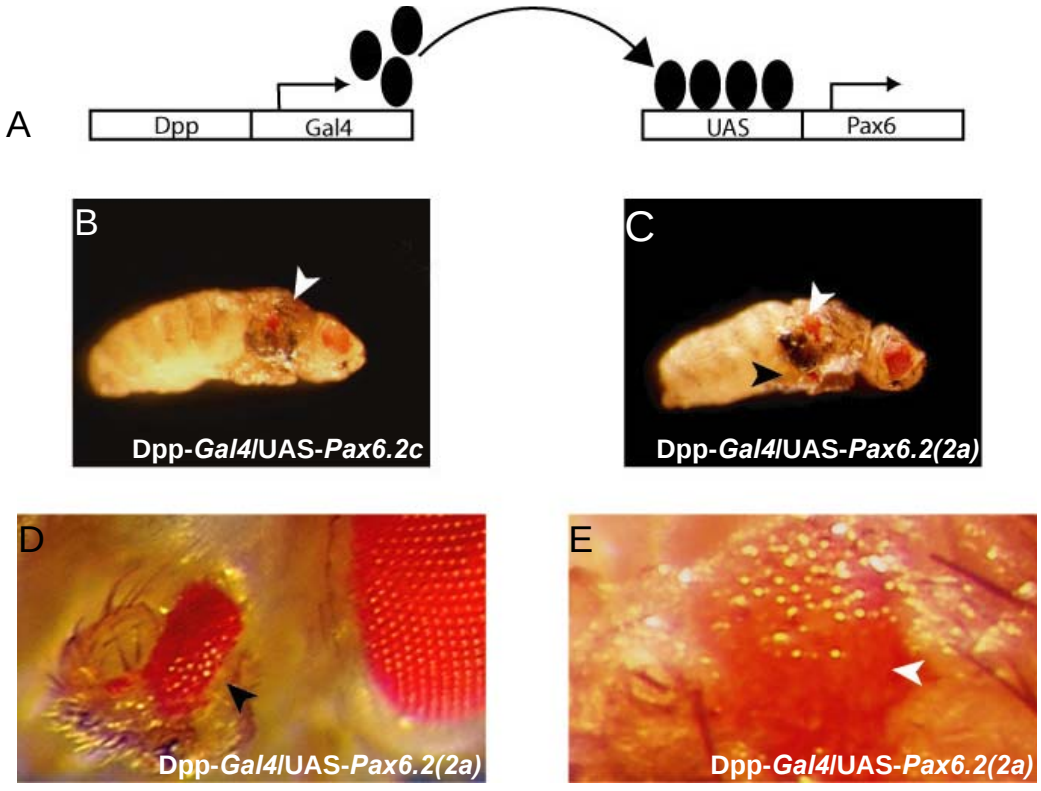

Figure 49. Induction of ectopic eyes in *Drosophila melanogaster*. (A) Schematic drawing of the UAS/GAL4 system used to induce ectopic eyes. (B-E) Ectopic eyes are induced on wings (white arrowhead in B, C, E) and legs (black arrowhead C, D) of *Drosophila* when *Pax6.2c* (B) and *Pax6.2(2a)* (C-E) are overexpressed in larval imaginal discs.

13.4.6 Specific abrogation of Pax6 variants' functions

To dissect the respective functions of the different *Pax6.2* splice variants during embryogenesis, we used the morpholino antisense technology allowing to block translation of the targeted proteins (Nasevicius and Ekker, 2000). For this purpose, two morpholinos, namely Mo3 and MoV, were designed against the first and second start codon of *Pax6.2*, respectively (Figure 50A, F). *In vivo* analysis showed that mRNA of a *Pax6.2c* 5'UTR/eGFP construct co-injected in embryo with a Standard control Morpholino (MoC) or MoV were translated and visualized by eGFP fluoresence under UV (Figure 50C, E).

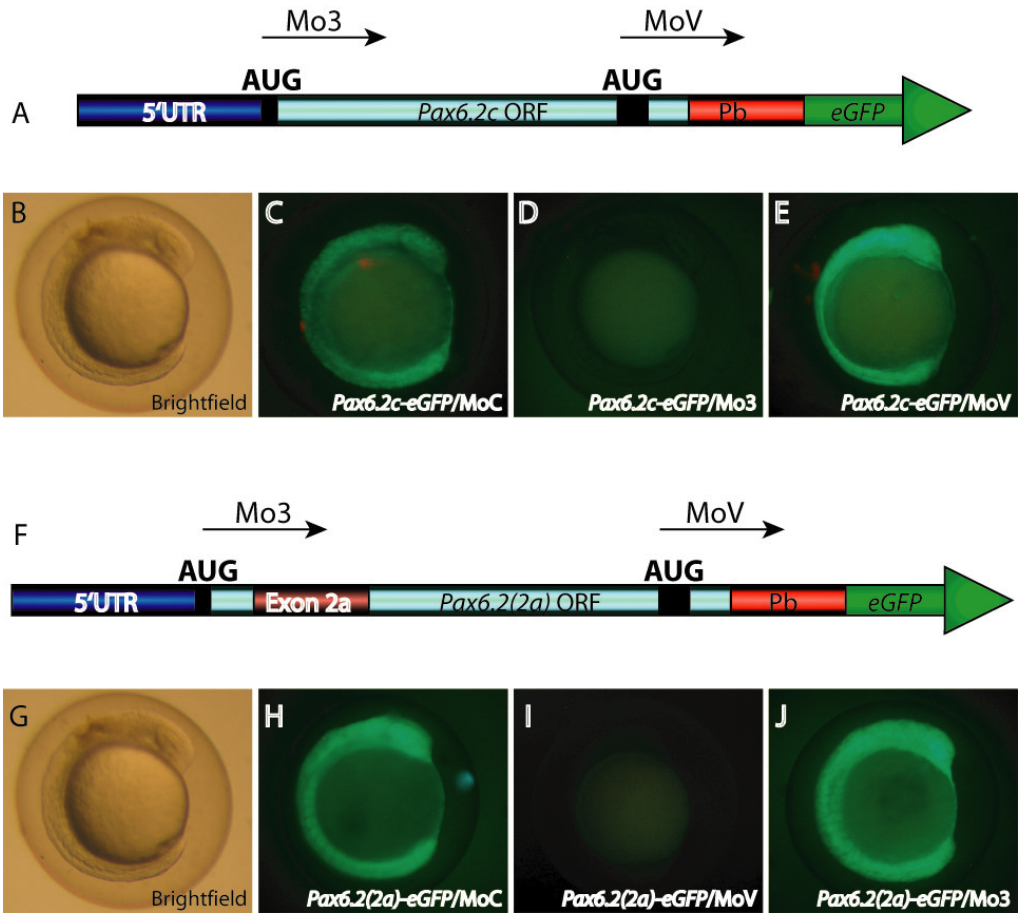

Figure 50. Specific knock down of *Pax6.2c* and *Pax6.2(2a)* translation with morpholino oligos. (B-E) Lateral view of 12 hpf zebrafish embryos co-injected at the one to two cells stages with a Pax6.2c/eGFP mRNA construct as shown in (A) with either a morpholino control (MoC) (B, C), a morpholino targeting the first start codon (Mo3) (D) or the second start codon (MoV) (E). (G-J) Lateral view of 12 hpf embryos co-injected at the one to two cells stages with a Pax6.2(2a)/eGFP mRNA construct as shown in (F) with either a MoC (G, H), a MoV (I) or a Mo3 (J). (B-E, G-J) Anterior is toward the top. The morpholinos used in (D, I) completely block the translation of eGFP when co-injected with the mRNA constructs of (A, F), respectively. In (B-C, E, G-H, J), the translation of eGFP is not blocked by injection of the respective morpholinos. Pb, paired box.

In contrast, when the mRNA were co-injected with Mo3, translation of eGFP was completely blocked (Figure 50D) indicating the specificity of the latter in inhibiting translation. Similarly, co-injection of embryos with a *Pax6.2(2a)* 5'UTR/eGFP mRNA construct with MoC or Mo3 did not inhibit eGFP translation (Figure 50H, J) whereas co-injection with MoV completely blocked it (Figure 50I).

These control experiments demonstrated that both morpholinos interfered specifically with their target mRNA and are therefore suitable for knock down experiments.

13.4.7 Pax6.2c and Pax6.2(2a) splice variants have specific and similar functions during zebrafish development

Injections of either Mo3 or MoV morpholino had no dramatic effect on zebrafish development until the formation of the optic cups (24 hpf). At 28 hpf, specific knock down of *Pax6.2c* with Mo3 induced a small eye phenotype (91%), a reduction of brain size (91%), an outgrowth at the level of the telencephalon (80%), a disruption of the ventral part of the eye (45%) and a small lens phenotype (85%), compared with the standard morpholino control (Figure 51A-F, K). The small eye and brain phenotype was maintained at least until day 3 pf (Figure 51C, F). Similar results were obtained when the Pax6.1cMo and Pax6.2cMo, two shifted morpholinos, were co-injected at the one to four cells stages in zebrafish embryos.
Specific interference of *Pax6.2(2a)* with MoV caused a small eye phenotype (54%) with a reduction in brain size (64%), an outgrowth at the level of the telencephalon (61%) and no closure of the two hypothalamic lobes (58%), compared with the standard or MoV25mut (morpholino similar of MoV2 but containing 5 mismatches) morpholino controls (Figure 51A-C, G-K). In addition, a small percentage (14%) of the injected embryos displayed a slight coloboma of the ventral part of their eye (Figure 51H). The lens remained unaffected under the different conditions mentioned above (Figure 51H). The brain and small eye phenotypes observed in MoV injected embryos were maintained at least until day 3 pf (data not shown). Similar results were obtained when a MoV2, a shifted morpholino, was injected at the one to four cells stages in zebrafish embryos.

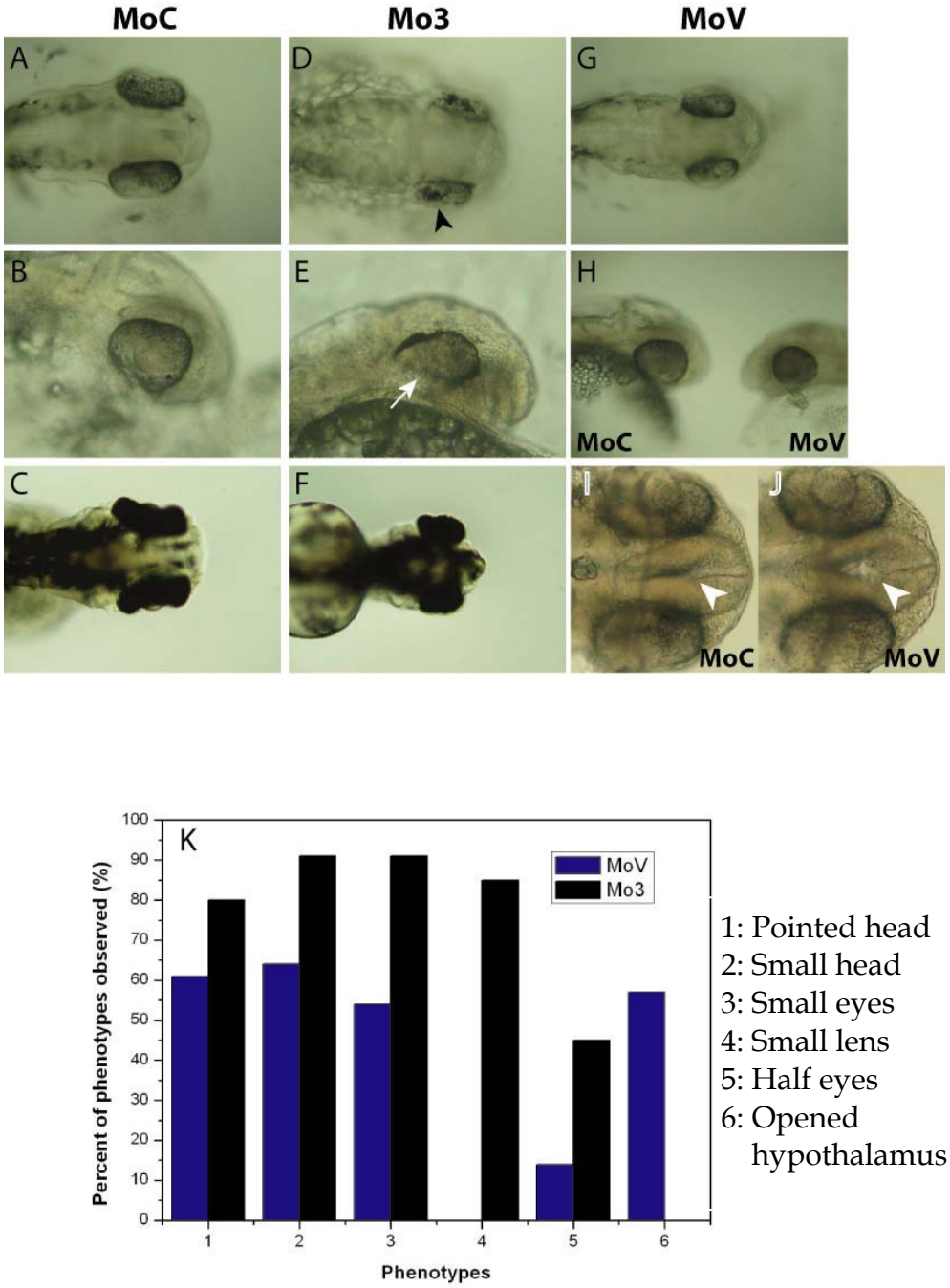

Figure 51. ***Pax6.2c*** **and** ***Pax6.2(2a)*** **are required for eye and forebrain development.** Dorsal (A, C, D, F, G), lateral (B, E, H) and ventral (I, J) views of 28 hpf embryos (A, B, D, E, G, H) and 72 hpf larvae (C-F) injected with either a MoC (A-C, I), a Mo3 (D-F) or a MoV (G, H, J). (K) Effects of Mo3 and MoV on the development of the eye and forebrain in 28 hpf zebrafish embryos. The injection of MoV causes dramatic effects on forebrain development including hypothalamus whereas Mo3 causes dramatic effects on both forebrain and eye development. The black (D) and white (I-J) arrowheads shows patches of retinal pigmented epithelium and the hypothalamus, respectively. The white arrow in (E) shows the ventral optic cup.

13.4.8 Autoregulation of Pax6.2 expression at the pallium/subpallium boundary but not in the optic cups

We next asked whether the inhibition of the translation of either *Pax6.2c* or *Pax6.2(2a)* splice variants had an effect on the general expression of both *Pax6* genes as reported in other species (Pinson et al., 2006; Aota et al., 2003). Hence, we analyzed the *Pax6.1* and *Pax6.2* gene expression pattern at the *Prim-5* stage in morpholino injected zebrafish embryos (Figure 52).

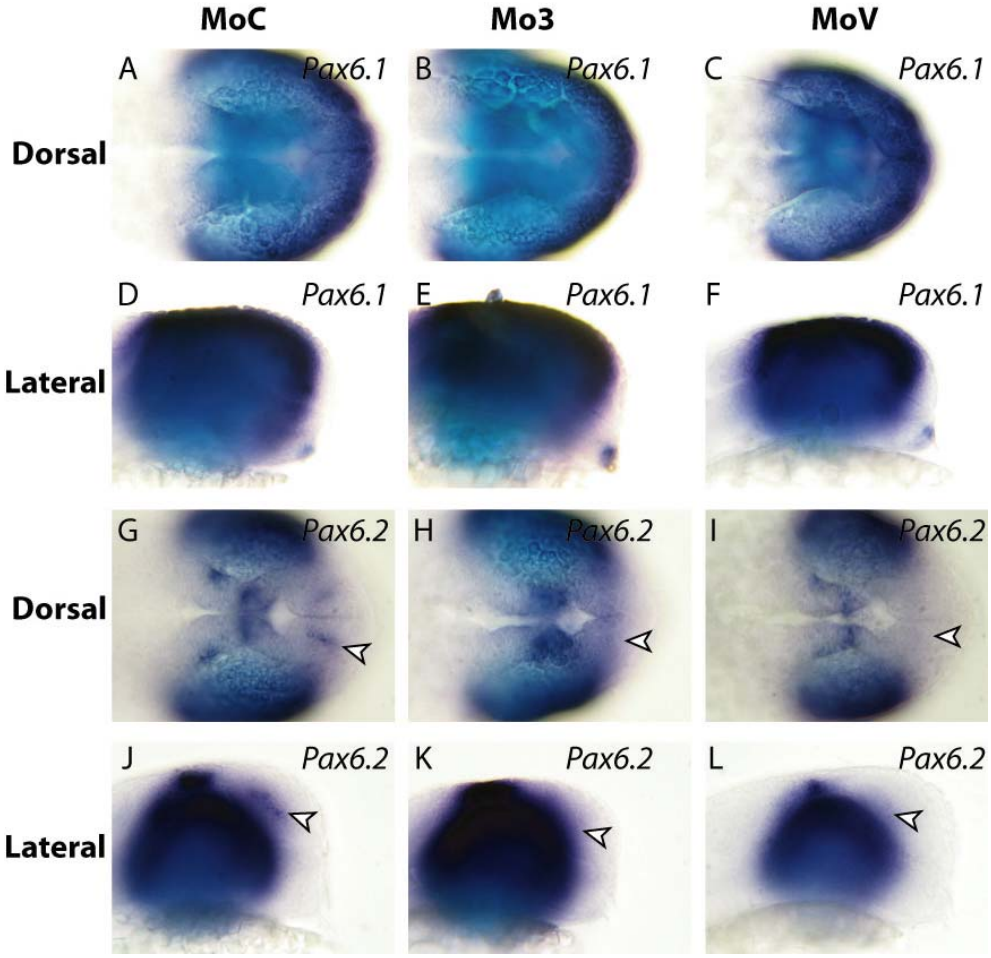

Figure 52. Effects of Mo3 and MoV in injected zebrafish embryos on *Pax6.1* and *Pax6.2* expression. Dorsal (A-C, G-I) and lateral (D-F, J-L) views of 25 hpf embryos; anterior is toward the right. One to four cells stages zebrafish embryos were injected with either a MoC (A, D, G, J), a Mo3 (B, E, H, K) or a MoV (C, F, I, L) and raised at 28.5°C until being processed for whole mount *in situ* hybridization with a full-length *Pax6.1* (A-F) or *Pax6.2* (G-L) digoxygenin labeled riboprobe (see materials and methods). In MoC injected embryos, the expression of *Pax6.1* is detected to the entire dorsal forebrain and the optic cups whereas *Pax6.2* expression is located to the optic cups and several specific nuclei of the forebrain including the pallium/subpallium boundary. The injections of Mo3 or MoV have mainly no effects on *Pax6.1* and *Pax6.2* expression excepted in the pallium/subpallium boundary where the *Pax6.2* expression is lost. The white arrowhead in (G-I, J-L) shows the pallium/subpallium boundary.

At this stage, *Pax6.1* expression was located in the entire dorsal forebrain and optic cups (Figure 52A-F) whereas the *Pax6.2* expression was located in the optic cups and some discrete forebrain nuclei, including the dorsal diencephalon and the pallium/subpallium boundary (Figure 52G-L). Neither Mo3 nor MoV affected the pattern of *Pax6.1* expression (Figure 52A-F). This was also mainly the case when we examined *Pax6.2* expression (Figure 52G-L). However, *Pax6.2* expression was completely lost in the pallium/subpallium boundary in either Mo3 or MoV injected embryos (Figure 52H, I, K, L).

13.4.9 Ventralization of the optic cups in Pax6.2 morphants

Twenty five hpf embryos injected with either Mo3 or MoV displayed a ventralization phenotype as revealed by the analysis of the *Pax2b* expression pattern (Figure 53A-F). In the optic cups of control embryos, *Pax2b* expression is located in the glial cells of the optic stalk extending from the ventral anterior forebrain to the ventral part of the eye (Figure 53A, D). In Mo3 or to a lesser degree in MoV injected embryos, the expression domain of *Pax2b* extends dorsally into the eye (Figure 53B-C, E-F). This is strongly the case for Mo3 where *Pax2b* expression was located to the two thirds of the optic cups (Figure 53E). In addition, when we inhibited the translation of the *Pax6.2c* message, an ectopic expression of *Pax2b* was observed in the telencephalon (Figure 53B).

In contrast to *Pax2b* expression, we observed that *Vax1* and *Vax2* expression in the eye was slighly affected in both Mo3 or MoV injected embryos (Figure 53G-I; data not shown).

13.4.10 The specific activity of both PAX6.2 splice variants is not required for pineal gland development

Because PAX6 plays a crucial role in the development of the eye, we asked whether the zebrafish *Pax6.2* splice variants are also involved in the formation of the pineal gland, a photoreceptive organ involved in the regulation of circadian rhythms in ectothermic vertebrates (Falcon, 2006). To test this hypothesis, we chose three pineal marker genes, namely *Floating head* (*Flh*), *Orthodenticle 5* (*Otx5*) and *Exo-Rhodopsin* (*ExR*). *Flh* encodes a homeodomain prepattern transcription factor which is expressed early in the pineal gland anlage and is required to mediate epiphysial neurogenesis (Masai et al., 1997).

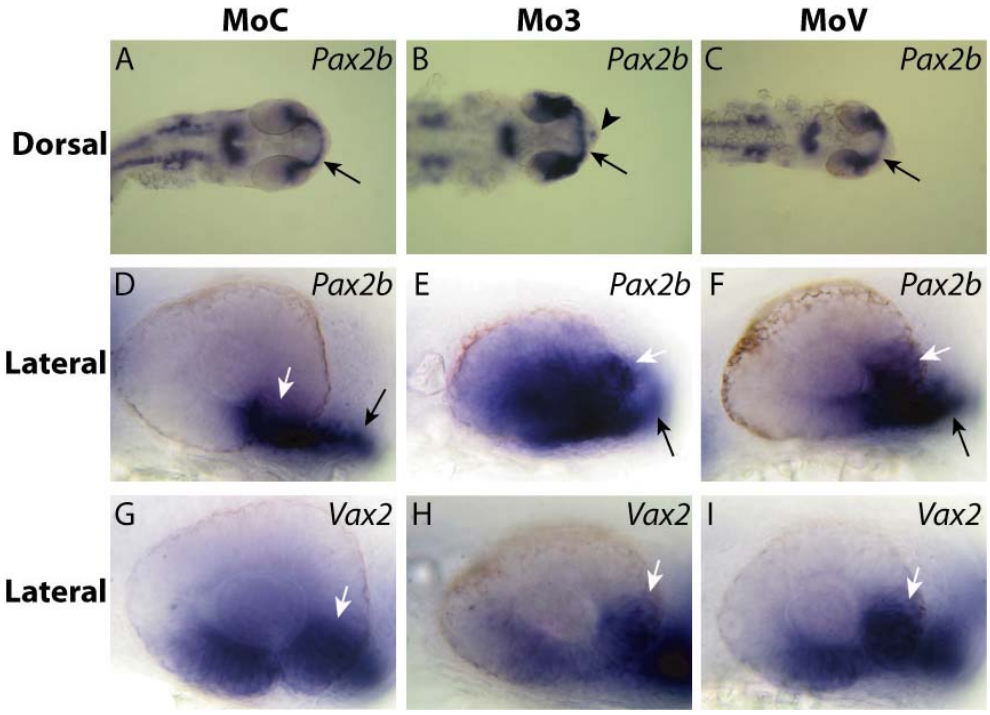

Figure 53. Effects of Mo3 and MoV in injected zebrafish embryos on the *Pax2b* and *Vax2* expression into the eye. Dorsal (A-C) and lateral (D-I) views of 25 hpf embryos; anterior is toward the right. One to four cells stages zebrafish embryos were injected with either a MoC (A, D, G), a Mo3 (B, E, H) or a MoV (C, F, I) and raised at 28.5°C until being processed for whole mount *in situ* hybridization with a *Pax2b* (A-F) or *Vax2* (G-I) digoxygenin labeled riboprobe (see materials and methods). (A, D) In MoC injected embryos, *Pax2b* expression is located in the optic stalks and ventral optic cups. (B, E) In Mo3 injected embryos, the *Pax2b* expression domain is expanded to the two thirds of the optic cups and ectopic expression of the gene is induced at the tip of the telencephalon (black arrowhead). (C, F) The injection of MoV induces a slight expansion of the *Pax2b* expression domain in the retina compared with control. Black and white arrows show *Pax2b* expression in the optic stalk and ventral retina, respectively. (G-I) No difference of *Vax2* expression was observed between Mo3 and MoV injected embryos compared with control.

The second one, encodes a photoreceptor specific transcription factor (Gamse et al., 2002) involved in the differentiation and maintenance of the photoreceptors and the regulation of pineal circadian genes (Gamse et al., 2002; Appelbaum et al., 2005). The third one encodes a specific photopigment of the pineal photoreceptor which expression appears as early as 18 hpf (Vuilleumier et al., 2006).

No difference in the pineal expression pattern of the three genes was found between MoC, Mo3 or MoV injected embryos (Figure 54A-I). This suggests that both *Pax6.2c* and *Pax6.2(2a)* variants are dispensable for the formation of this photoreceptive organ in zebrafish.

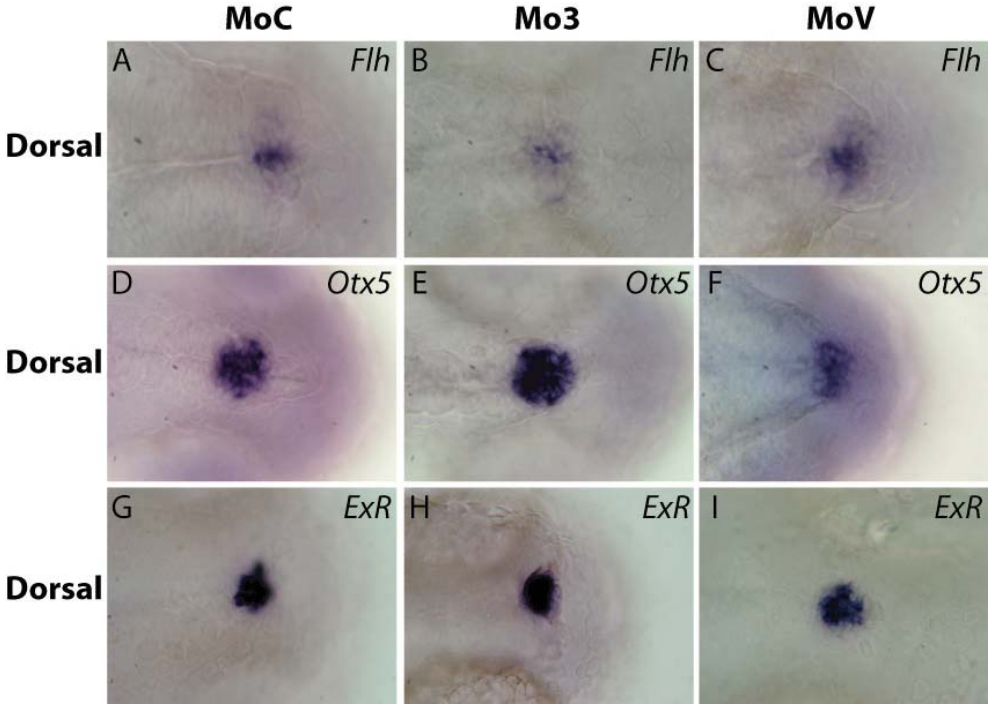

Figure 54. Effects of Mo3 and MoV in injected zebrafish embryos on the development of the pineal gland. (A-I) Dorsal views of 25 (A-F) and 28 (G-I) hpf embryos; anterior is toward the right. One to four cells stages zebrafish embryos were injected with either a MoC (A, D, G), a Mo3 (B, E, H) or a MoV (C, F, I) and raised at 28.5°C until being processed for whole mount *in situ* hybridization with a *Flh* (A-C), *Otx5* (D-F) or *ExR* (G-I) digoxygenin labeled riboprobe (see materials and methods). The three genes are expressed in the pineal gland where they act as a prepattern factor, a circadian regulator and a photopigment molecule, respectively. No difference was observed in the expression of the three molecular markers between Mo3 and MoV injected embryos compared with control.

13.4.11 The specific activity of both Pax6.2 splice variants is required for normal forebrain development

Molecular markers of the patterning of the forebrain include *Vax1*, *Vax2*, *Six3b*, *Dlx2*, *Emx3* and *Ngn1* (Manuel and Price, 2005). We examined the expression pattern of these different genes in morpholino injected embryos in order to determine which one could be responsible for the dramatic phenotypes described above (Figures 55, 56). *Emx3* was the only gene, from the six examined at the *Prim-5* stage, which expression remained unaffected in the forebrain after injection of either morpholino (Figure 55A-F). In contrast, the dorsal marker *Ngn1* displayed a retraction of its expression domain in the diencephalon but not in the telencephalon in *Pax6.2c* and *Pax6.2(2a)* morphants (Figure 55G-L).

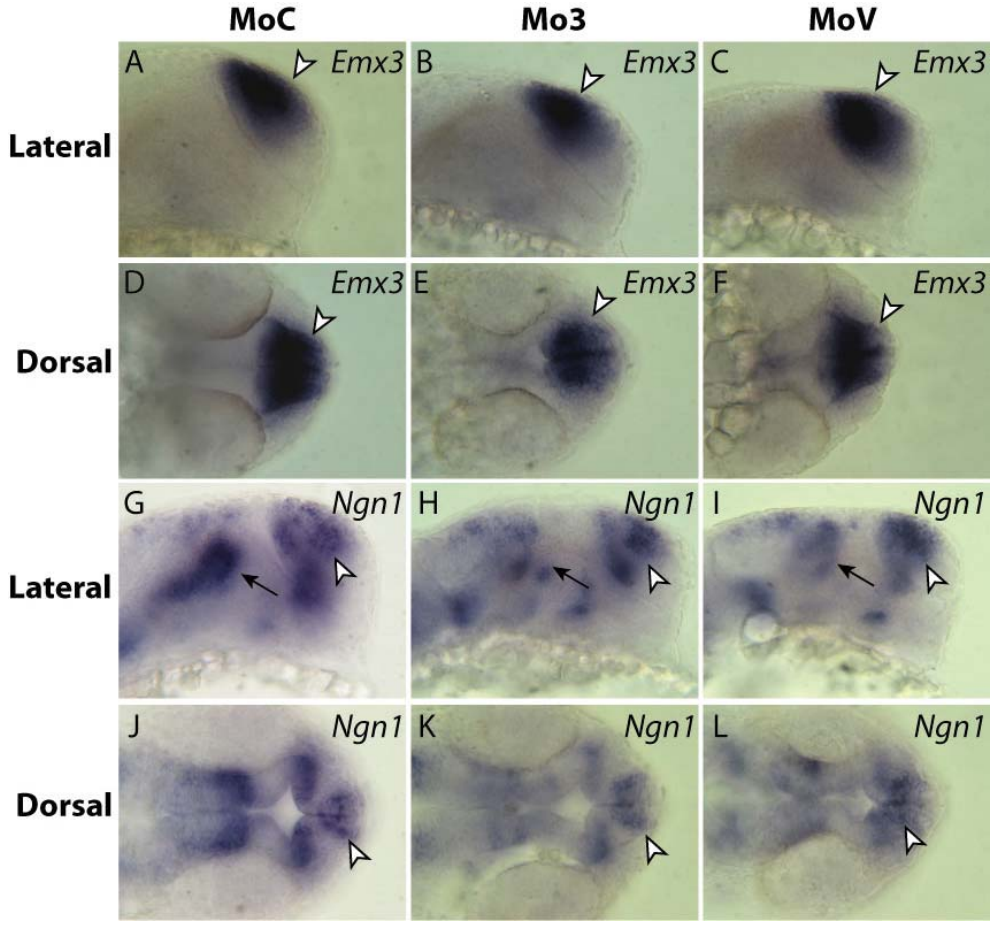

Figure 55. Effects of Mo3 and MoV in injected zebrafish embryos on the expression of dorsal molecular markers of the forebrain. Lateral (A-C, G-I) and dorsal (D-F, J-L) views of 25 hpf embryos; anterior is toward the right. One to four cells stages zebrafish embryos were injected with either a MoC (A, D, G, J), a Mo3 (B, E, H, K) or a MoV (C, F, I, L) and raised at 28.5°C until to be processed for whole mount *in situ* hybridization with an *Emx3* (A-F) or *Ngn1* (G-L) digoxygenin labeled riboprobe (see materials and methods). In MoC injected embryos, the expression of both genes is located to the pallium with an additional domain of expression into the dorsal diencephalon for *Ngn1*. In Mo3 or MoV injected embryos, the pallial expression of *Emx3* and *Ngn1* was not changed as compared with control. In the diencephalon, *Ngn1* expression was strongly decreased in Mo3 and MoV injected embryos. The black arrow in (G-I) shows the dorsal diencephalon. The white arrowhead in (A-L) shows the pallium.

In the telencephalon of both *Pax6.2* splice variants morphants, all the ventral markers examined showed an expansion of their expression domains. Thus, *Vax1* -but not *Vax2*- expression expanded from the diencephalon to the telencephalon in both *Pax6.2* splice variant morphants (Figure 56A-C, G-I). In addition, *Vax2* and *Six3b* telencephalic expression was increased and expanded compared to the control (Figure 56G-L, M-O). Interestingly enough, *Dlx2* expression was slightly increased in the pallium of zebrafish embryos after Mo3 injection (Figure 56P-R).

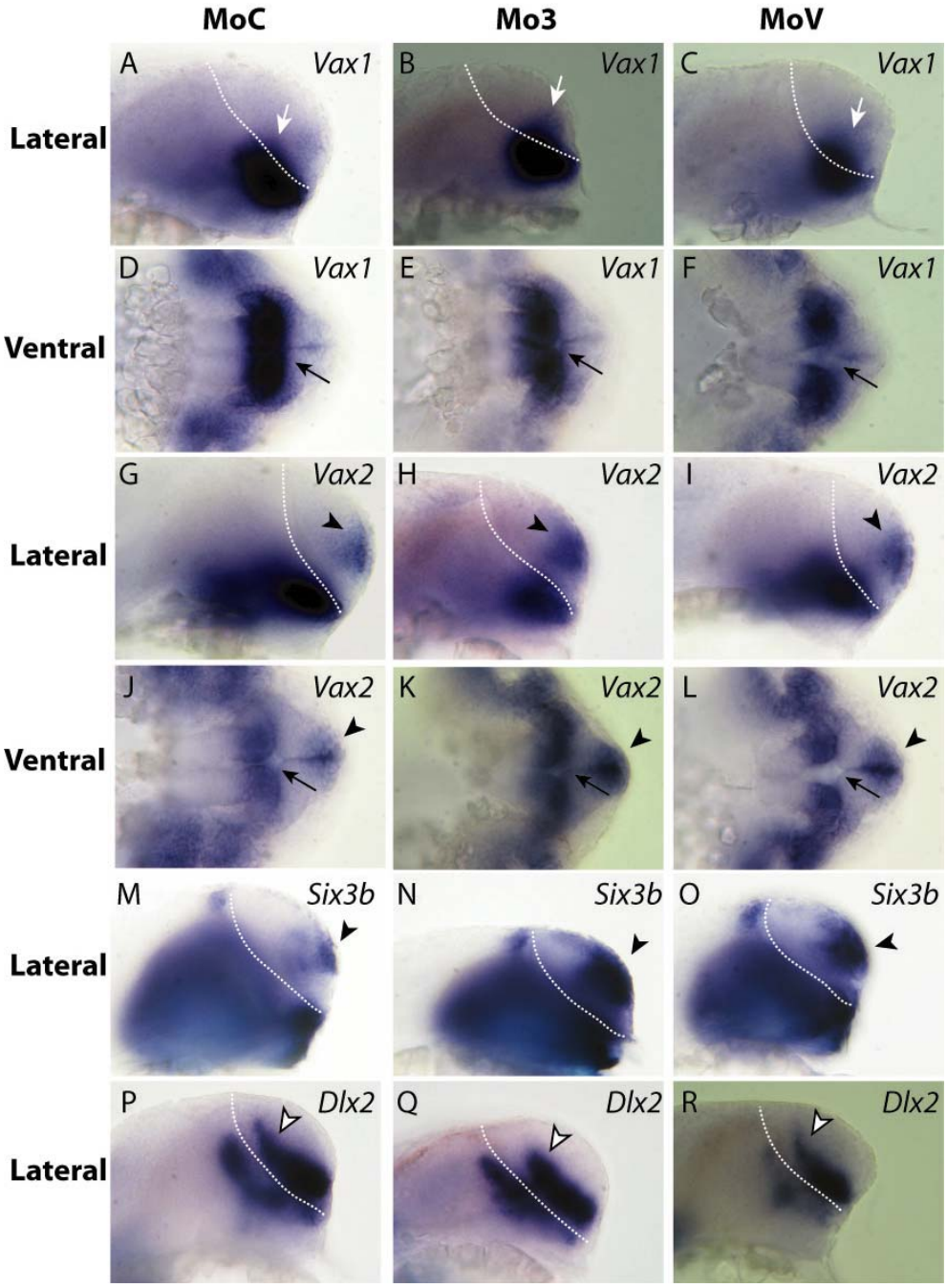

Figure 56. Effects of Mo3 and MoV in injected zebrafish embryos on the expression of ventral molecular markers of the forebrain. Lateral (A-C, G-I, M-R) and ventral (D-F, J-L) views of 25 hpf embryos; anterior is toward the right. One to four cells stages zebrafish embryos were injected with either a MoC (A, D, G, J, M, P), a Mo3 (B, E, H, K, N, Q) or a MoV (C, F, I, L, O, R) and raised at 28.5°C until to be processed for whole mount *in situ* hybridization with a *Vax1* (A-F), *Vax2* (G-L), *Six3b* (M-O) or *Dlx2* (P-R) digoxygenin labeled riboprobe (see materials and methods). In MoC injected embryos, the *Vax1*, *Vax2* and *Six3b* expression domains are located to the ventral forebrain including the hypothalamus. *Vax2* and *Six3b* are also expressed at the tip of the telencephalon. In Mo3 and MoV injected embryos, the *Vax1* expression domain expands from the ventral diencephalon to the telencephalon (white arrow). These embryos show also an increase of *Vax2* and *Six3b* expression at the tip of their telencephalon compared with the controls (black arrowhead). *Legend continues next page.*

In MoC and MoV injected embryos, the telencephalic *Dlx2* expression domain extends as a gradient from the subpallium to the pallium with higher expression levels in the subpallium. In Mo3 injected embryos, the *Dlx2* expression in the pallium is slighly expanded. The dashed white line in (A-C, G-I, M-R) shows the diencephalon/telencephalon boundary. The white arrowhead in (P-R) shows the *Dlx2* expression at the level of the pallium/subpallium boundary. The black arrow in (D-F, J-L) shows the anterior hypothalamus.

13.5 Discussion

The results reported in this study bring entirely new insights on zebrafish eye and forebrain development. Indeed, we describe a novel splice variant of *Pax6.2*, and provide informations concerning the respective functions of the alternative *Pax6.2c* and *Pax6.2(2a)* splice variants in this ectothermic vertebrate. Alternative splicing of transcripts from a single gene is often observed; this mechanism generates protein variants with diverse functions (Maniatis and Tasic, 2002; Essner et al., 2000; Stamm et al., 2005). In the case of genes encoding transcription factors, the isoforms have often specific and sometimes opposite activities (Essner et al., 2000; Foulkes and Sassone-Corsi, 1992; Maniatis and Tasic, 2002). In metazoans, this mechanism is thought to increase protein diversity from a relatively small number of genes (Maniatis and Tasic, 2002). For instance, the human genome counts about 35,000 genes (Lander et al., 2001) but the proteome is estimated to be more than 100,000 different proteins, as a result, in most cases, of alternative splicing (Kalnina et al., 2005).

Until now, several different *Pax6* transcripts generated by alternative splicing have been found in different animal species (Glardon et al., 1998; Gorlov and Saunders, 2002; Carriere et al., 1993; Epstein et al., 1994b; Kim and Lauderdale, 2006; Anderson et al., 2002). However, the expression pattern and the *in vivo* functions of these isoforms have not been extensively studied. Here, we found a new *Pax6.2* splice variant in zebrafish embryos and larvae, which is characterized by the insertion of a 71 bp exon located just downstream of the first start codon. We provide *in vitro* and *in vivo* evidences that the insertion of this exon, which introduces an internal stop codon in the coding sequence, leads to the translation of a N-terminal 19-20 amino acids truncated PAX6.2 protein. Although the PAX6.2(2a) amino acid sequence is shorter than the canonical PAX6.2, the deduced primary structure of the paired domain, paired-like homeodomain and transactivation domain are not affected. This was supported by the results of the overexpression of both *Pax6.2* transcripts in larval imaginal discs of fly, because they induced formation of ectopic eyes in a similar manner.

This suggests that the DNA binding activities of the paired domain were not affected by the presence of exon 2a into the canonical *Pax6.2* transcript. This is in contrast with the situation observed when the PAX6 of human containing the exon 5a into the paired domain was overexpressed in fly; in this case, the ectopic eyes were smaller compared with the mammalian canonical PAX6 (Dominguez et al., 2004).

Expression of the *Pax6.2c* and *Pax6.2(2a)* variants was found at all stages examined from 9 hpf, when the eye field and optic placodes appear, until later stages when the eye is completely differentiated, at 3 dpf. Notably, the general expression of *Pax6.2(2a* and *c)* revealed here by *in situ* hybridization at 72 hpf, and the fact that we found exon 2a in an adult zebrafish EST databank, indicate that both variants are specifically expressed in the mature eye. Future investigations will aim at determining where are expressed the two variants and what are their respective functions in the mature retina.

In vertebrates, the establishment of the dorso-ventral (DV) axis of the eye starts when the optic primordium is forming. At this stage, *Pax6* expression defines the region of the optic primordium that will become the neural retina whereas the *Pax2* expression defines the region that will form the optic stalk (Chow and Lang, 2001). In rodents and chicken, it has been shown that both genes control the expression domains of the other by reciprocal transcriptional repression, thus contributing to establish the boundary between the optic stalk and the neuroretina (Schwarz et al., 2000; Canto-Soler and Adler, 2006). This also holds true in ectothermic vertebrates as shown by the experiments using morpholinos directed against either *Pax6.2* transcript. Therefore, the specific knock down of either *Pax6.2c* or *Pax6.2(2a)* led to a ventralization of the optic cups as revealed by the expansion of the *Pax2b* expression domain from the optic stalk to the medial part of the eye. In both cases, the expansion of the *Pax2b* expression domain observed here strinkingly resembles that observed after *Six3* overexpression in zebrafish embryos (Kobayashi et al., 1998). These results indicate that the transcriptional repression between *Pax6* and *Pax2* during DV patterning of the eye is a conserved feature among vertebrates. Interestingly, the eye phenotype induced by the injection of the morpholino targeting the *Pax6.2c* transcript was much more severe than with the morpholino targeting the *Pax6.2(2a)* transcript. This suggests that the canonical variant is the principal *Pax6.2* isoform necessary for the normal DV patterning of the optic cup in zebrafish.

Our results agree with previous studies in mice, rat and chicken showing that *Pax6* was directly involved in the formation of the lens and retinal pigmented epithelium (Ashery-Padan et al., 2000; Lang, 2004; Kamachi et al., 2001; Baumer et al., 2003). Indeed, most of the

other zebrafish eye defects (small eyes, small lens, dark patches of retinal pigmented epithelium into the dorsal optic cup) were also observed after blocking translation of the *Pax6.2c* transcript.

We found that both *Pax6.2* transcripts are dispensable for the formation of the optic vesicles at earlier stages of zebrafish eye development as previously shown in endotherms (Grindley et al., 1995). In addition, in both zebrafish *Pax6.2* and *Pax6.2(2a)* morphants, the optic vesicles formed optic cups. This is in contrast with the situation found in *Pax6-/Pax6-* mice embryos (Grindley et al., 1995), where the homozygous mutant displayed misshapen evaginations of the optic vesicles from the diencephalon, and eye morphogenesis was arrested (Grindley et al., 1995). These differences might result from the different experimental approaches used.

In ectothermic vertebrates, the pineal gland which is a direct light sensor and a major component of the circadian system, expresses the *Pax6* gene (Falcon, 2006; Wullimann and Rink, 2001). Studies in human and mice indicated that PAX6 proteins are required for the formation of the epiphysis (Mitchell et al., 2003; Estivill-Torrus et al., 2001). For these reasons, it has been suspected that *Pax6* might play a critical role in zebrafish pineal gland development. Here, we found that three marker genes of pineal photoreceptor cells function were still expressed after injection of morpholinos targeting either the *Pax6.2c* or the *Pax6.2(2a)* splice variant. This suggests either that both *Pax6.2* variants (or a product of an other gene) act redundantly in pineal gland development or that (an) other(s) alternative *Pax6* splice variant(s), not targeted by our morpholinos, is involved in this process.

In zebrafish, the *Pax6.2* gene is expressed in restricted domains of the forebrain as early as 12 hpf, but also into the mature brain (Wullimann and Rink, 2001; Wullimann and Rink, 2002). We investigated the respective functions of both alternative *Pax6.2* splice variants on the regional specification of the zebrafish forebrain. For this purpose, we compared the morphology and the patterning of several molecular markers of the telencephalon and diencephalon in control, Mo3 and MoV injected embryos. Inactivation of *Pax6.2c* or *Pax6.2(2a)* variants induced dramatic effects; Mo3 and MoV injected zebrafish displayed a smaller forebrain and a pointed telencephalon compared to controls. In good correlation, we observed that the expression domains of *Vax1* and *Dlx2,* two ventral subpallial markers, were expanded in the dorsal telencephalon, in good agreement with previous results obtained in *Pax6-/Pax6-* mutant mice (Stoykova et al., 2000; Manuel and Price, 2005). In contrast to the situation in Pax6-/- homozygous mice, the expression of two dorsal telencephalic markers, *Emx3* and *Ngn1,* was not affected in zebrafish. However, our

results suggest that there is a high conservation of the molecular events modulating the DV patterning of the vertebrate telencephalon. In addition, in both PAX6.2 morphants, the expression of *Six3b* and *Vax2* at the tip of the telencephalon was much stronger than in controls. Because the correct dosage of SIX3 is required for correct forebrain development (Carl et al., 2002; Del Bene et al., 2004; Gestri et al., 2005), it is plausible to speculate that this localized overexpression explained in part the pointed telencephalon observed at 28 hpf in both *Pax6.2* morphants.

In mice embryos, *Pax6* expression is also located transiently in the hypothalamus from E14.5 to P2 developmental stages, where it plays a crucial role (Vitalis et al., 2000; Stoykova et al., 1996; Stoykova et al., 1997). Indeed, in the Pax6^{-}/Pax6^{-} mutant mice embryo, the ventricular part of the hypothalamus is disjointed and abnormally shaped (Vitalis et al., 2000; Stoykova et al., 1996). Accordingly, it has been shown that in mice lacking PAX6, there is a loss of R-cadherin expression, a gene encoding a cell connective protein, in areas in which this gene is normally coexpressed with PAX6 (Stoykova et al., 1997). The phenotype observed in that case suggested that the adhesive properties between the cells of the two hypothalamic lobes were altered. Interestingly, we found here a similar phenotype but mainly after injection of the morpholino targeting *Pax6.2(2a)* transcript; the effects of the morpholino targeting *Pax6.2(c)* affected the development of the hypothalamus to a much lesser degree. These results would indicate that of both *Pax6*.2 variants described in this study, *Pax6(2a)* is the main one involved in the closure of the hypothalamus.

13.6 Conclusion

The present study reports, for the first time in an ectothermic vertebrate, the analysis of *Pax6* functions during optic cup and forebrain morphogenesis. Furthermore, we characterized a new zebrafish splice variant of *Pax6.2*; we dissected its functions and compared them with the functions of the canonical isoform. We found that both, the *Pax6.2c* and *Pax6.2(2a)* transcripts, are critical for forebrain patterning, whereas the correct formation of the optic cups is principally triggered by *Pax6.2c*. In addition, we found that the *Pax6.2(2a)* transcript is critical for proper closure of the two hypothalamic lobes. This work opens the door to several other studies, which will aim at investigating the proliferation and differentiation of the different neuronal cell types, and understanding how the general gene networks triggering these processes were established during vertebrates' evolution.

Chapter 4

14. Conclusions and Perspectives

14.1 Pineal gland and retina : two different photoreceptive organs

Until recently, the anatomical and functional comparison between the pineal gland and retina of ectothermic vertebrates was essentially carried on adults; only very few data concerned the embryonic development. Here we demonstrate, using electronic microscopy and expression of several molecular markers, that the pineal gland differentiates before the retina during early development in two phylogenetically distant Teleost species. For instance, in zebrafish, the expression of a gene encoding a specific photoreceptive molecule of the epiphysis is activated in this organ before the optic cups start to form. An other relevant example is the presence of *Hiomt* mRNA in the turbot pineal gland one day before the same gene is expressed in the retina. Finally, whereas the zebrafish retina displays photoreceptor characters only after the second day post-fertilization, the pineal gland anlage shows some of them already, one day before. Taken together, the results of this work suggest that the pineal gland rather than the retina mediates photic responses during embryonic development in Teleost fish. Although this feature seems to be conserved during evolution of this vertebrate group, the molecular mechanisms controlling the early different pineal functions are not the same between the zebrafish and the turbot embryos. Indeed, the expression of *Aanat2* displays a robust circadian rhythm in the zebrafish pineal gland as early as the second day of development before hatching, whereas the expression of this gene does not show any rhythm in the epiphysis at least one day after this process in turbot. This suggests that during evolution of the Teleost lineage, the mechanisms controlling the establishment of the melatonin molecular biosynthesis pathway during early development have diverged at least once.

This work opens the door to several other studies concerning the establishment of the pineal functions during embryonic development that will allow determining which molecular system has been privileged during Teleost evolution.

An other crucial difference we found between the pineal gland and retina is that during development both photoreceptive organs are not triggered by the same molecular actors. Indeed, in inhibiting independently the translation of two alternative *Pax6* splice variants, we observed in both cases that the development of the eyes was affected whereas

that of the pineal gland was not. This contrast with the situation observed in human and rodents where the pineal gland was absent when PAX6 functions were lost, thereby indicating that this factor is essential for the development of both, the pineal organ and the eyes (Mitchell et al., 2003; Estivill-Torrus et al., 2001). PAX6 proteins have previously been detected in the zebrafish pineal gland (Wullimann and Rink, 2001), which would suggest that its involvement in pineal gland development is a conserved feature in vertebrates. Three reasons may account for the lack of effect observed here: (1) insufficient amounts of the morpholinos injected; unfortunately, this hypothesis is difficult to test because increasing the morpholinos' concentration would result in several secondary effects such as apoptosis. (2) Both alternative PAX6 splice variants (or the product of an other gene) act **redundantly** during pineal development, and the effects of knocking down one variant are compensated by the other; this hypothesis will be tested in the future by co-injecting both morpholinos. (3) Another **alternative** *Pax6* splice variant, not targeted by our morpholinos, might be specifically responsible for pineal gland development; a good candidate could be a previously described splice variant encoding a PAX6 protein lacking the paired domain and a part of the acidic linker region (Carriere et al., 1993; Kim and Lauderdale, 2006). This transcript which can be generated from an alternative internal promotor (Kleinjan et al., 2004; Kammandel et al., 1999 or by alternative splicing (Gorlov and Saunders, 2002; Mishra et al., 2002) contains only the homeodomain and the carboxyl terminal end of the protein. In Teleost fish, this variant has not been described so far, but the presence of a highly conserved start codon located just upstream of the PAX6 homeodomain in all Teleost species investigated so far, suggests that it may exist. In addition, by using two antibodies targeting the N- and C-terminal end of the PAX6 protein, we could detect by western blot in extracts of three days old zebrafish larvae the presence of a smaller PAX6 protein (data not shown). This shorter PAX6 protein could be a splice variant without the paired domain. In the future, further efforts will aim at cloning this putative splice variant and examining its function *in vivo*.

In summary, we have shown that although the photoreceptive organs in vertebrates may have a monophyletic origin, the molecular pathways involved in their development are not completely identical contributing certainly to their anatomic and functional diversity. Moreover, we show in two different Teleost species that when these organs differentiate, their respective functions are established in a species specific manner; this underlines the plasticity of the genomes and molecular mechanisms during evolution.

14.2 The turbot as a new complementary model for studying eye development and evolution

Since the discovery that PAX6 is needed for eye development and that overexpression of this factor leads to the induction of ectopic eyes in *Xenopus* and *Drosophila*, the different aspects of early eye development have been well studied so far (Gehring and Ikeo, 1999; Tomarev, 1997; Ashery-Padan and Gruss, 2001). Hence, several conserved factors have been found to play a critical role during this process. However, because it is difficult to discern the late from the early molecular events during eye development in "classical" vertebrate model systems, the functions of these key players in the mechanisms leading to proliferation and differentiation of the different retinal cell types are less understood. Excepting some currently technical limitations to use the flatfish as a model, this group of Teleost offers a unique advantage to deal with a vertebrate displaying a such protracted development of the central nervous system (CNS) including the photoreceptive organs. For instance, we found that the photoreceptors layer of the turbot retina displays rhodopsin expression only after metamorphosis, i.e. at 60 days post-hatching, and that this expression is located only in the ventral part of the organ. In comparison, the zebrafish retina displays rhodopsin expression as soon as the third day post-fertilization in the ventronasal outer nuclear layer (Schmitt and Dowling, 1999). In addition, flatfish show several other specific changes occurring during metamorphosis relative to their change of visual field including a reorganization of the vestibulo-ocular pathways (Graf and Baker, 1983) and a change of expression in opsin types (Mader and Cameron, 2004).

In the future, the comparison between flatfish such as turbot and other Teleost species displaying a direct development such as the zebrafish, will allow understanding how the mechanisms patterning the retina have evolved among the different Teleost species. The experimental protocols we developed and the results we found during this work, establish the molecular and comprehensive basis needed for further studies on this new model system, in particular on the development and metamorphosis of the eye. Interestingly, we found a process of asymmetric growth during metamorphosis of turbot at the ciliary marginal zone (CMZ) which is strikingly similar to what was found in *Xenopus*, suggesting an evolutive convergence between these two visual systems. As a perspective, it will be interesting to determine whether this process is triggered by the same genetic cascade in both animals, *i.e.* by the retinal asymmetric expression of the D3 enzyme. Moreover, the

hypothesis of a regulation of the retinal *D3* expression by the BMP signaling pathway will have to be tested in *Xenopus* by gain and loss-of-function experiments.

14.3 Conserved functions of PAX6 in brain formation and patterning among vertebrates

As previously mentioned, *Pax6* is needed for eye development in vertebrates and invertebrates but this is also an essential factor for the correct development of the CNS in both classes of animals. In addition, the comparison of the *Pax6* expression pattern between the developing brain of lamprey, shark, Teleost fish and mammals has suggested that the different functions of this transcription factor in brain morphogenesis and patterning are highly conserved during evolution. The last decade, two teams led by Peter Gruss and David Price have shown in mice that *Pax6* plays a critical role in the dorso-ventral patterning of the telencephalon and the correct development of the hypothalamus (Stoykova et al., 2000; Vitalis et al., 2000). However, until the present work, few data were available concerning the functions of this gene in ectothermic vertebrates. Here we show by a gene knock down approach that PAX6 acts as a dorsalizing factor of the telencephalon in zebrafish, *i.e.* by repressing the expression of several subpallial marker genes including *Vax1*, *Six3* and *Dlx2*; a similar situation as in rodents. This supports the hypothesis that *Pax6* is part of an ancestral genetic network controlling early brain regionalization and which appears to be conserved among all vertebrates. Future studies will aim at examining the functions of *Pax6* in fish species displaying ancestral phenotypical characters such as agnates and chondrichtyans in order to determine if the ancestral function of *Pax6* in the dorso-ventral patterning of the telencephalon correlates with the apparition of this brain subdivision during vertebrates' evolution.

As for the dorso-ventral patterning of the telencephalon, the functions of *Pax6* in hypothalamic development also seems a highly conserved feature of vertebrates' evolution. Interestingly, this function is specifically played by an alternative *Pax6* splice variant in zebrafish, complicating strongly the genetic model of brain morphogenesis. In addition to the study of other model systems, the next steps will aim at examining whether the different functions involved in brain morphogenesis and patterning are triggered by different alternative *Pax6* splice variants also in rodents.

In summary, futures studies in fish using the functional morpholinos designed during this PhD and relevant marker genes, will help elucidating the different functions of *Pax6* and its splice variants in all aspects of brain morphogenesis and patterning during development. The results will bring insights concerning the evolution of brain among the vertebrate class.

In conclusion, this work brings entirely new descriptive, comparative and functional insights on the development of the central nervous system, including the pineal gland and retina of Teleost fish. Furthermore, it opens the door to several more interesting studies concerning the proliferation and differentiation of the different neuronal cell types in vertebrates. The pineal gland and retina of turbot and zebrafish appear as relevant model systems to address these fundamental topics, which interest not only the evo-devo domain, but also the medical field.

15. Appendix

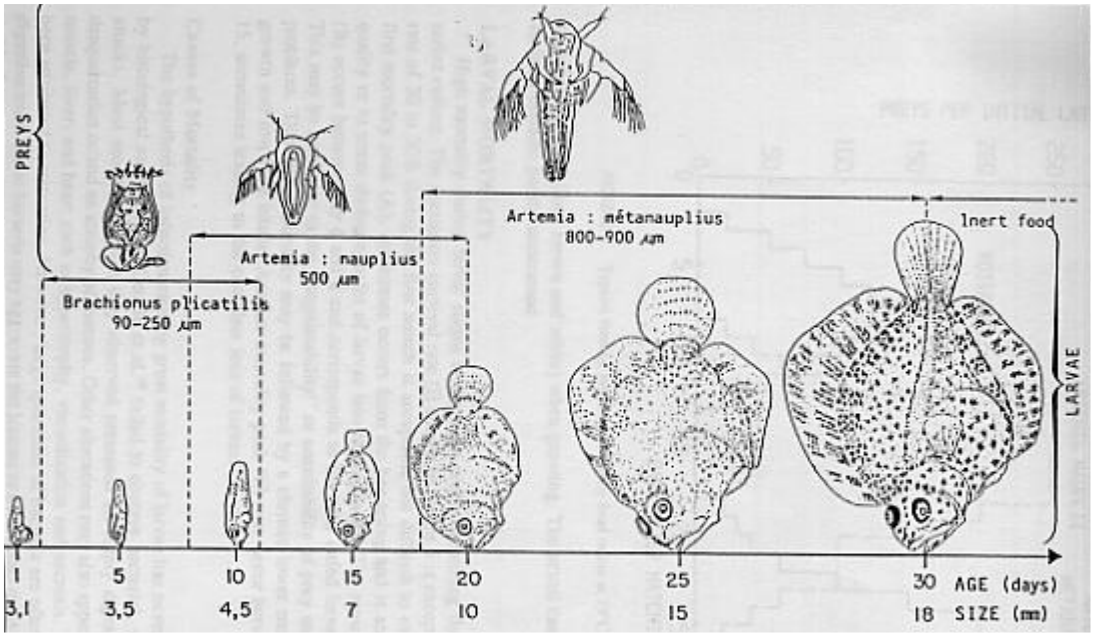

Appendix 1. Schematic drawing of the metamorphic process in turbot at 19 °C. From Person-Le Ruyet, J. 1986.

Degenerated primer	Sequence **5′→3′**
***SmPax6* forward**	**ASGTRTCSAAYGGSTGYGTGAG**
***SmPax6* reverse**	**ACRCTSGGKATRTTRTCGTTKGTGCA**
***SmBmp2/4* forward**	**GAYTTYTCNGAYGTNGGNTGG**
***SmBmp2/4* reverse**	**GTCATNTCYTGRTARTTYTT**
***SmBmp2/4* nested forward**	**AYCAYTGGATHGTNGCNCC**
***SmAanat1/2* forward**	**GTTTGARATCGAGAGAGARGC**
***SmAanat1/2* reverse**	**CTARCAKCCRCTGTTBCGYCG**
***SmAanat1/2* nested reverse**	**TTCTGGTAGAAGGGVACCAG**
***SmHiomt* forward**	**TACBKGTGCTGGSGCCACCTG**
***SmHiomt* reverse**	**AGGTCRCAVATVAGTGKGAA**
***SmHiomt* nested forward**	**GGCWGAYGCHGTSAGAGAAGG**
***SmHiomt* nested reverse**	**GAACRSBGAMAGGTCAAAGGC**
***SmD3* forward**	**CCGYTGGTKSTCAATTTYGGCAGCTG**
***SmD3* reverse**	**TCSGGSCCMCGRCCBCCCTGGTACA**
***SmD3* nested forward**	**GCTGYACCTGACCMCCGTTCATGGC**

Appendix 2. Degenerated primers used to clone the S. maximus *Pax6*, *Bmp2/4*, *Aanat1/2*, *Hiomt* and *D3* genes.

Specific primer	Sequence **5′→3′**
***Pax6.2c* forward**	**CCATTGGACAGTCATTGTTTATTTC**
***Pax6.2c* reverse**	**GGGTTGGTTATGGTATTCTTTTTGA**
***Pax6.2(2a)* forward**	**AAGAGGGACGCTGGGAAAA**
***Pax6.2(2a)* reverse**	**CAGAGTTGACTGTCCGTTTA**
***ZfAanat2* forward**	**CGACGAAACAGCGGATGTTAG**
***ZfAanat2* reverse**	**GAACCTTTGAGCCTGTGATCG**
***Ef1a* forward**	**TCCCAACCTCTTGGAATTTCTC**
***Ef1a* reverse**	**TGAAAGAGGCACTATCAGTCAAT**
***SmAanat2* forward**	**ATTCCACGAGATGGAGTACACG**
***SmAanat2* reverse**	**TGGTGAGTAAGTCGGAGTGTAAGG**
***SmHiomt* forward**	**GAGGGCAGGGAGAGGACAG**
***SmHiomt* reverse**	**TCTTGATACATGAGTAGCCGAGGT**
***SmEf1a* forward**	**CTCACATCGCCTGCAAGTTC**
***SmEf1a* reverse**	**GACACACATGGGCTTTCCAG**

Appendix 3. Specific primers used for the real time PCR quantitative experiments.

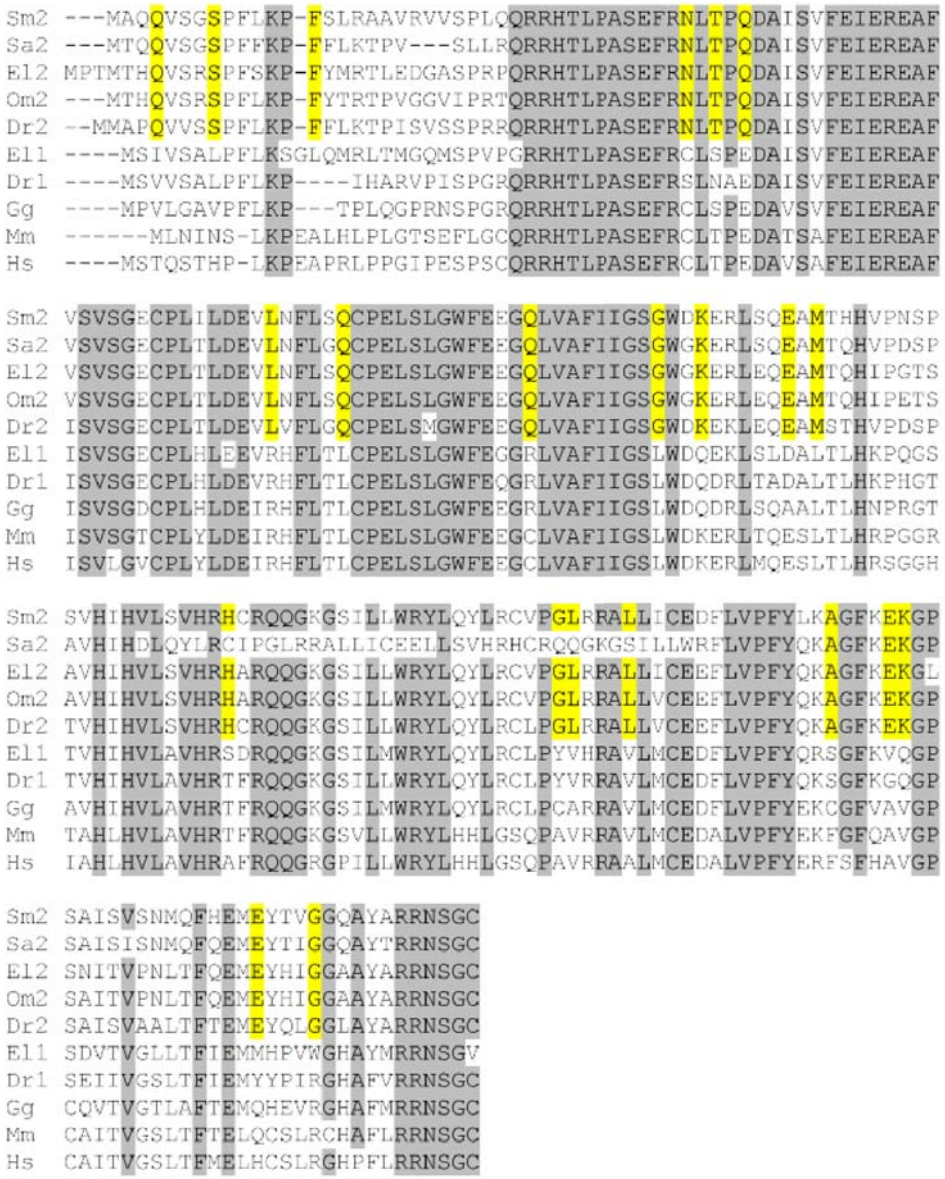

Appendix 4. Amino acid sequence alignment of AANAT. SmAANAT2 (Sm2) amino acid sequence is aligned with AANAT2 of : zebrafish (Dr2) (AAF01140), rainbow trout (Om2) (AAD25333), pike (El2) (AAD21317) and sea bream (Sa2) (AAT02160) and with AANAT1 of : zebrafish (Dr1) (AAQ54582), pike (El1) (AAD21316), chicken (Gg) (NP_990489), mouse (Mm) (AAD09408) and human (Hs) (Q16613). Amino acids shaded in grey indicate that they are conserved in almost all AANAT proteins. Amino acids shaded in yellow indicates that they are specific of AANAT2 proteins.

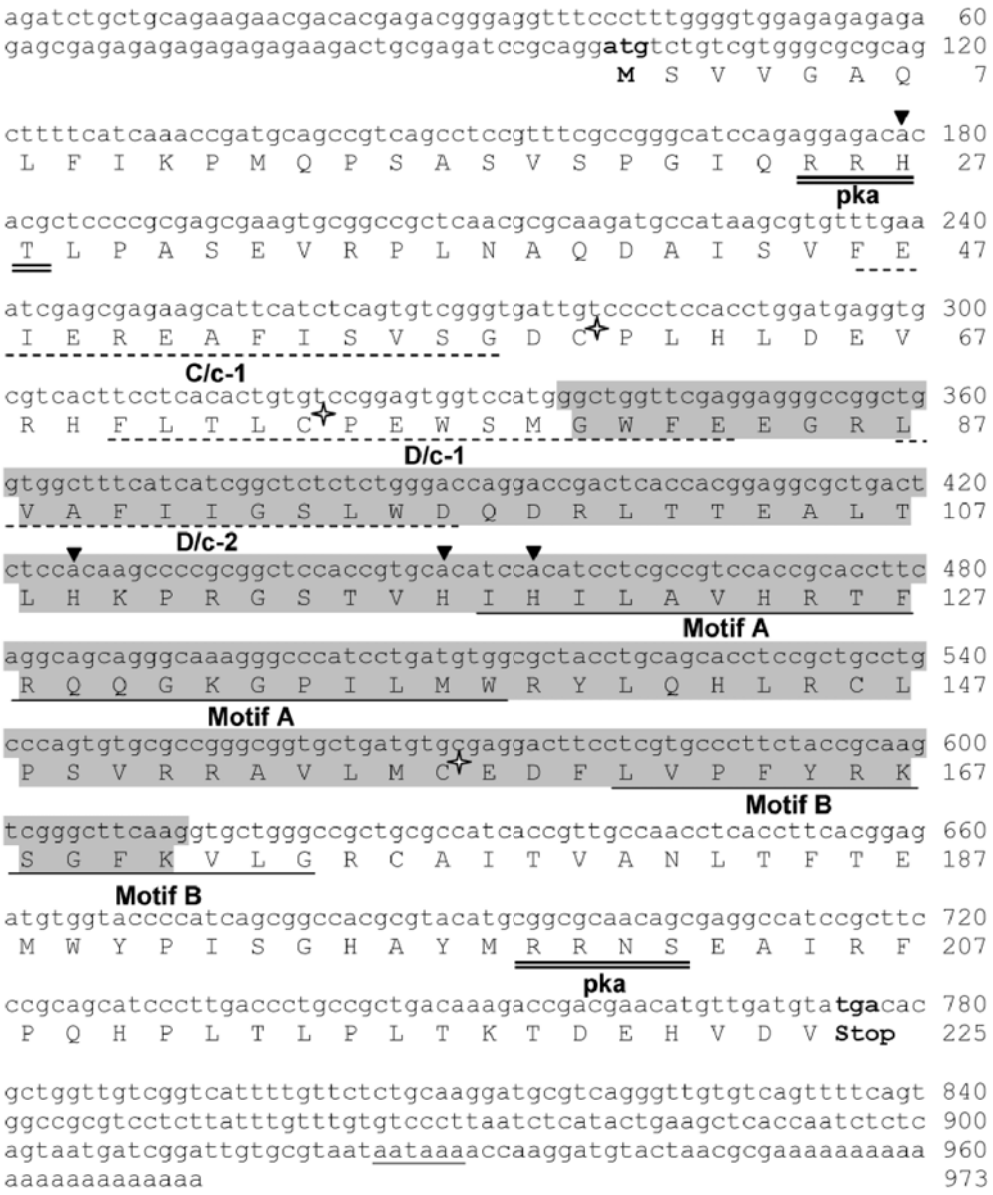

Appendix 5. Nucleotide and deduced amino acid sequence of the turbot *Aanat1* cDNA. The nucleotide and amino acid positions are numbered and indicated on the right. The start and stop codons are indicated in bold letters. The acetyltransferase domain is shaded while the two putative acetyl coenzyme A binding motives and the two phosphorylation sites for PKA are indicated by simple and double underlining, respectively. The three highly conserved regions C/c-1, D/c-1 and D/c-2 found in vertebrates are indicated by dashed underlining. The three highly conserved cystein residues important for disulfide bond formation are indicated by a star. The four histidine residues are indicated by a black arrowhead. The putative polyadenylation signal is underlined.

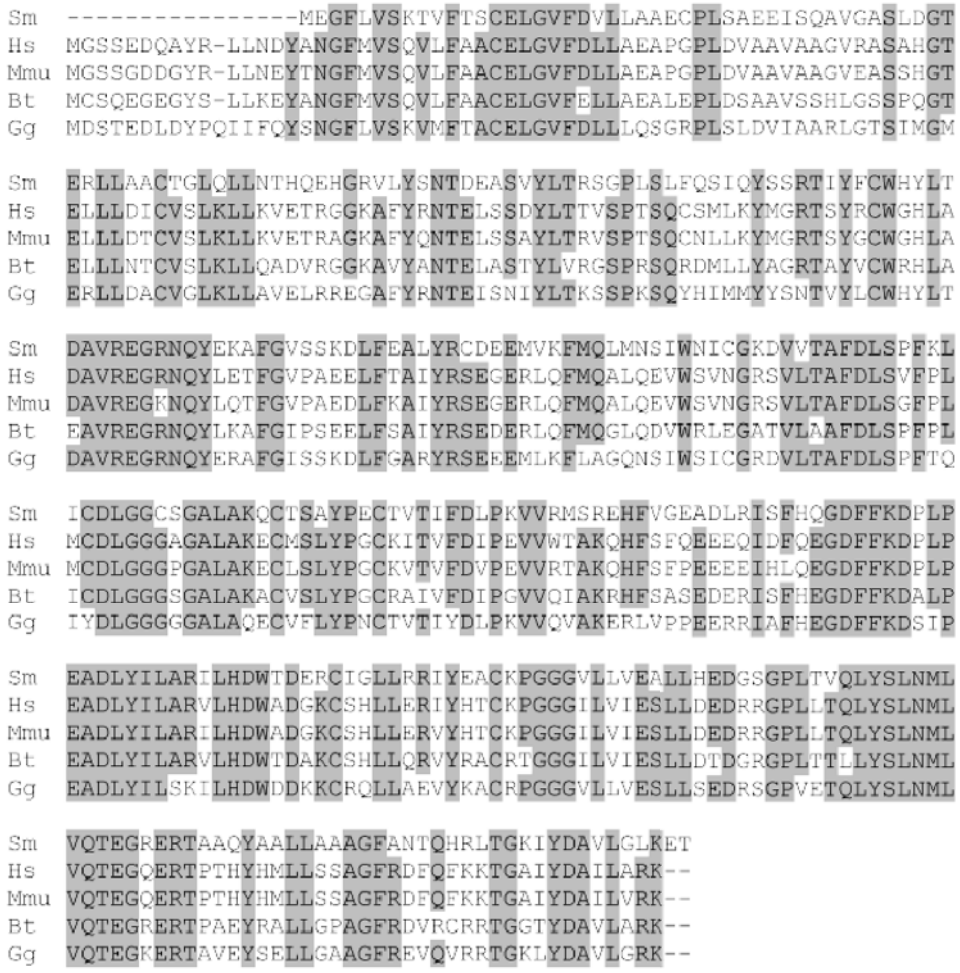

Appendix 6. Amino acid sequence alignment of HIOMT. SmHIOMT (Sm) amino acid sequence is aligned with HIOMT of : chicken (*Gg*) (NP_990674), bovin (Bt) (P10950), apes (Mmu) (*AAL49966*) and human (Hs) (*CAI41503*). Amino acids shaded in grey indicate that they are conserved in almost all HIOMT proteins.

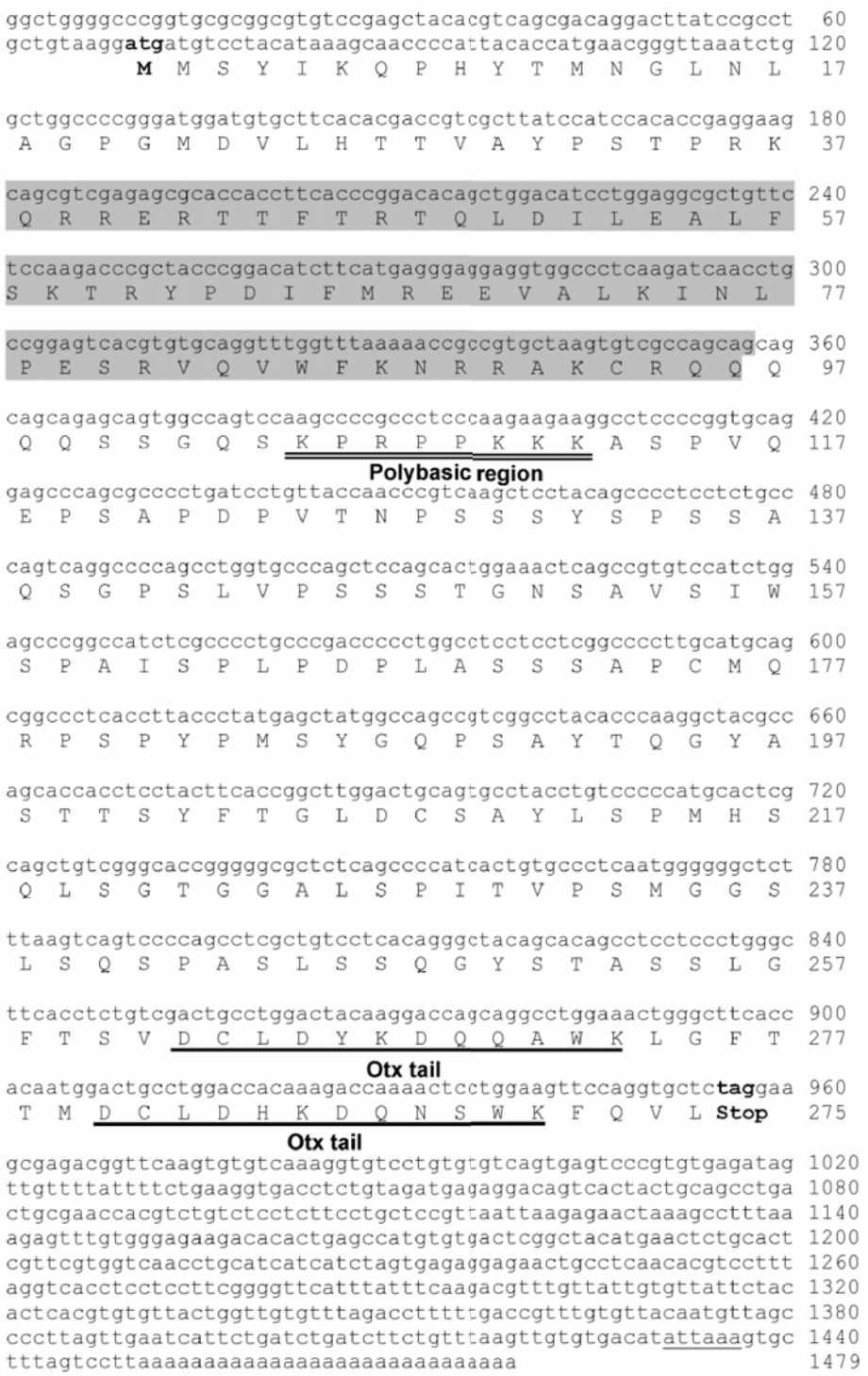

Appendix 7. Nucleotide and deduced amino acid sequence of the turbot *Otx5* cDNA. The nucleotide and amino acid positions are numbered and indicated on the right. The start and stop codons are indicated in bold letters. The homeodomain is shaded while the polybasic region and the two repeats of the Otx tail motif are indicated by double and simple underlining, respectively. The putative polyadenylation signal is underlined.

16. References

Ackermann, K., Bux, R., Rub, U., Korf, H. W., Kauert, G. and Stehle, J. H. (2006). Characterization of human melatonin synthesis using autoptic pineal tissue. Endocrinology 147, 3235-42.

Albrecht, U. and Eichele, G. (2003). The mammalian circadian clock. Curr Opin Genet Dev 13, 271-7.

Allen, B. M. (1916). Extirpation experiments in Rana pipiens larva. Science 44, 755-757.

Allwardt, B. A. and Dowling, J. E. (2001). The pineal gland in wild-type and two zebrafish mutants with retinal defects. J Neurocytol 30, 493-501.

Altmann, C. R., Chow, R. L., Lang, R. A. and Hemmati-Brivanlou, A. (1997). Lens induction by Pax-6 in Xenopus laevis. Dev Biol 185, 119-23.

Altschul, S. F., Madden, T. L., Schaffer, A. A., Zhang, J., Zhang, Z., Miller, W. and Lipman, D. J. (1997). Gapped BLAST and PSI-BLAST: a new generation of protein database search programs. Nucleic Acids Res 25, 3389-402.

Anderson, T. R., Hedlund, E. and Carpenter, E. M. (2002). Differential Pax6 promoter activity and transcript expression during forebrain development. Mech Dev 114, 171-5.

Andrews, G. L. and Mastick, G. S. (2003). R-cadherin is a Pax6-regulated, growth-promoting cue for pioneer axons. J Neurosci 23, 9873-80.

Aota, S., Nakajima, N., Sakamoto, R., Watanabe, S., Ibaraki, N. and Okazaki, K. (2003). Pax6 autoregulation mediated by direct interaction of Pax6 protein with the head surface ectoderm-specific enhancer of the mouse Pax6 gene. Dev Biol 257, 1-13.

Appelbaum, L., Anzulovich, A., Baler, R. and Gothilf, Y. (2005). Homeobox-clock protein interaction in zebrafish. A shared mechanism for pineal-specific and circadian gene expression. J Biol Chem 280, 11544-51.

Appelbaum, L., Toyama, R., Dawid, I. B., Klein, D. C., Baler, R. and Gothilf, Y. (2004). Zebrafish serotonin-N-acetyltransferase-2 gene regulation: pineal-restrictive downstream module contains a functional E-box and three photoreceptor conserved elements. Mol Endocrinol 18, 1210-21.

Arendt, J. and Skene, D. J. (2005). Melatonin as a chronobiotic. Sleep Med Rev 9, 25-39.

Ashery-Padan, R. and Gruss, P. (2001). Pax6 lights-up the way for eye development. Curr Opin Cell Biol 13, 706-14.

Ashery-Padan, R., Marquardt, T., Zhou, X. and Gruss, P. (2000). Pax6 activity in the lens primordium is required for lens formation and for correct placement of a single retina in the eye. Genes Dev 14, 2701-11.

Ashery-Padan, R., Zhou, X., Marquardt, T., Herrera, P., Toube, L., Berry, A. and Gruss, P. (2004). Conditional inactivation of Pax6 in the pancreas causes early onset of diabetes. Dev Biol 269, 479-88.

Axelrod, J. (1974). The pineal gland: a neurochemical transducer. Science 184, 1341-8.

Azuma, N., Yamaguchi, Y., Handa, H., Hayakawa, M., Kanai, A. and Yamada, M. (1999). Missense mutation in the alternative splice region of the PAX6 gene in eye anomalies. Am J Hum Genet 65, 656-63.

Bairoch, A., Bucher, P. and Hofmann, K. (1997). The PROSITE database, its status in 1997. Nucleic Acids Res 25, 217-21.

Barrenetxe, J., Delagrange, P. and Martinez, J. A. (2004). Physiological and metabolic functions of melatonin. J Physiol Biochem 60, 61-72.

Barth, K. A., Kishimoto, Y., Rohr, K. B., Seydler, C., Schulte-Merker, S. and Wilson, S. W. (1999). Bmp activity establishes a gradient of positional information throughout the entire neural plate. Development 126, 4977-87.

Baumer, N., Marquardt, T., Stoykova, A., Spieler, D., Treichel, D., Ashery-Padan, R. and Gruss, P. (2003). Retinal pigmented epithelium determination requires the redundant activities of Pax2 and Pax6. Development 130, 2903-15.

Beach, D. H. and Jacobson, M. (1979a). Influences of thyroxine on cell proliferation in the retina of the clawed frog at different ages. J Comp Neurol 183, 615-23.

Beach, D. H. and Jacobson, M. (1979b). Patterns of cell proliferation in the developing retina of the clawed frog in relation to blood supply and position of the choroidal fissure. J Comp Neurol 183, 625-32.

Becker, K. B., Stephens, K. C., Davey, J. C., Schneider, M. J. and Galton, V. A. (1997). The type 2 and type 3 iodothyronine deiodinases play important roles in coordinating development in Rana catesbeiana tadpoles. Endocrinology 138, 2989-97.

Begay, V., Falcon, J., Cahill, G. M., Klein, D. C. and Coon, S. L. (1998). Transcripts encoding two melatonin synthesis enzymes in the teleost pineal organ: circadian regulation in pike and zebrafish, but not in trout. Endocrinology 139, 905-12.

Beimesche, S., Neubauer, A., Herzig, S., Grzeskowiak, R., Diedrich, T., Cierny, I., Scholz, D., Alejel, T. and Knepel, W. (1999). Tissue-specific transcriptional activity of a pancreatic

islet cell-specific enhancer sequence/Pax6-binding site determined in normal adult tissues in vivo using transgenic mice. Mol Endocrinol 13, 718-28.

Benyassi, A., Schwartz, C., Coon, S. L., Klein, D. C. and Falcon, J. (2000). Melatonin synthesis: arylalkylamine N-acetyltransferases in trout retina and pineal organ are different. Neuroreport 11, 255-8.

Bernard, M., Dinet, V. and Voisin, P. (2001). Transcriptional regulation of the chicken hydroxyindole-O-methyltransferase gene by the cone-rod homeobox-containing protein. J Neurochem 79, 248-57.

Besseau, L., Benyassi, A., Moller, M., Coon, S. L., Weller, J. L., Boeuf, G., Klein, D. C. and Falcon, J. (2006). Melatonin pathway: breaking the 'high-at-night' rule in trout retina. Exp Eye Res 82, 620-7.

Blader, P., Lam, C. S., Rastegar, S., Scardigli, R., Nicod, J. C., Simplicio, N., Plessy, C., Fischer, N., Schuurmans, C., Guillemot, F. et al. (2004). Conserved and acquired features of neurogenin1 regulation. Development 131, 5627-37.

Bok, D. (1993). The retinal pigment epithelium: a versatile partner in vision. J Cell Sci Suppl 17, 189-95.

Bolliet, V., Ali, M. A., Lapointe, F. J. and Falcon, J. (1996). Rhythmic melatonin secretion in different teleost species: an in vitro study. J Comp Physiol [B] 165, 677-83.

Bopp, D., Burri, M., Baumgartner, S., Frigerio, G. and Noll, M. (1986). Conservation of a large protein domain in the segmentation gene paired and in functionally related genes of Drosophila. Cell 47, 1033-40.

Boulton, M. and Dayhaw-Barker, P. (2001). The role of the retinal pigment epithelium: topographical variation and ageing changes. Eye 15, 384-9.

Brand, A. H. and Perrimon, N. (1993). Targeted gene expression as a means of altering cell fates and generating dominant phenotypes. Development 118, 401-15.

Brinon, J. G., Medina, M., Arevalo, R., Alonso, J. R., Lara, J. M. and Aijon, J. (1993). Volumetric analysis of the telencephalon and tectum during metamorphosis in a flatfish, the turbot Scophthalmus maximus. Brain Behav Evol 41, 1-5.

Brown, D. D., Wang, Z., Kanamori, A., Eliceiri, B., Furlow, J. D. and Schwartzman, R. (1995). Amphibian metamorphosis: a complex program of gene expression changes controlled by the thyroid hormone. Recent Prog Horm Res 50, 309-15.

Cahill, G. M. (1996). Circadian regulation of melatonin production in cultured zebrafish pineal and retina. Brain Res 708, 177-81.

Cahill, G. M. and Besharse, J. C. (1993). Circadian clock functions localized in xenopus retinal photoreceptors. Neuron 10, 573-7.

Callaerts, P., Halder, G. and Gehring, W. J. (1997). PAX-6 in development and evolution. Annu Rev Neurosci 20, 483-532.

Callaerts, P., Leng, S., Clements, J., Benassayag, C., Cribbs, D., Kang, Y. Y., Walldorf, U., Fischbach, K. F. and Strauss, R. (2001). Drosophila Pax-6/eyeless is essential for normal adult brain structure and function. J Neurobiol 46, 73-88.

Callaerts, P., Munoz-Marmol, A. M., Glardon, S., Castillo, E., Sun, H., Li, W. H., Gehring, W. J. and Salo, E. (1999). Isolation and expression of a Pax-6 gene in the regenerating and intact Planarian Dugesia(G)tigrina. Proc Natl Acad Sci U S A 96, 558-63.

Canto-Soler, M. V. and Adler, R. (2006). Optic cup and lens development requires Pax6 expression in the early optic vesicle during a narrow time window. Dev Biol 294, 119-32.

Carl, M., Loosli, F. and Wittbrodt, J. (2002). Six3 inactivation reveals its essential role for the formation and patterning of the vertebrate eye. Development 129, 4057-63.

Carriere, C., Plaza, S., Caboche, J., Dozier, C., Bailly, M., Martin, P. and Saule, S. (1995). Nuclear localization signals, DNA binding, and transactivation properties of quail Pax-6 (Pax-QNR) isoforms. Cell Growth Differ 6, 1531-40.

Carriere, C., Plaza, S., Martin, P., Quatannens, B., Bailly, M., Stehelin, D. and Saule, S. (1993). Characterization of quail Pax-6 (Pax-QNR) proteins expressed in the neuroretina. Mol Cell Biol 13, 7257-66.

Cassone, V. M., Warren, W. S., Brooks, D. S. and Lu, J. (1993). Melatonin, the pineal gland, and circadian rhythms. J Biol Rhythms 8 Suppl, S73-81.

Cau, E. and Wilson, S. W. (2003). Ash1a and Neurogenin1 function downstream of Floating head to regulate epiphysial neurogenesis. Development 130, 2455-66.

Chauhan, B. K., Yang, Y., Cveklova, K. and Cvekl, A. (2004). Functional properties of natural human PAX6 and PAX6(5a) mutants. Invest Ophthalmol Vis Sci 45, 385-92.

Chen, J. D. and Evans, R. M. (1995). A transcriptional co-repressor that interacts with nuclear hormone receptors. Nature 377, 454-7.

Chen, S., Wang, Q. L., Nie, Z., Sun, H., Lennon, G., Copeland, N. G., Gilbert, D. J., Jenkins, N. A. and Zack, D. J. (1997). Crx, a novel Otx-like paired-homeodomain protein, binds to and transactivates photoreceptor cell-specific genes. Neuron 19, 1017-30.

Chen, W. and Baler, R. (2000). The rat arylalkylamine N-acetyltransferase E-box: differential use in a master vs. a slave oscillator. Brain Res Mol Brain Res 81, 43-50.

Chong, N. W., Bernard, M. and Klein, D. C. (2000). Characterization of the chicken serotonin N-acetyltransferase gene. Activation via clock gene heterodimer/E box interaction. J Biol Chem 275, 32991-8.

Chow, R. L., Altmann, C. R., Lang, R. A. and Hemmati-Brivanlou, A. (1999). Pax6 induces ectopic eyes in a vertebrate. Development 126, 4213-22.

Chow, R. L. and Lang, R. A. (2001). Early eye development in vertebrates. Annu Rev Cell Dev Biol 17, 255-96.

Collinson, J. M., Hill, R. E. and West, J. D. (2000). Different roles for Pax6 in the optic vesicle and facial epithelium mediate early morphogenesis of the murine eye. Development 127, 945-56.

Collinson, J. M., Quinn, J. C., Hill, R. E. and West, J. D. (2003). The roles of Pax6 in the cornea, retina, and olfactory epithelium of the developing mouse embryo. Dev Biol 255, 303-12.

Coon, S. L., Begay, V., Deurloo, D., Falcon, J. and Klein, D. C. (1999). Two arylalkylamine N-acetyltransferase genes mediate melatonin synthesis in fish. J Biol Chem 274, 9076-82.

Coon, S. L., Del Olmo, E., Young, W. S., 3rd and Klein, D. C. (2002). Melatonin synthesis enzymes in Macaca mulatta: focus on arylalkylamine N-acetyltransferase (EC 2.3.1.87). J Clin Endocrinol Metab 87, 4699-706.

Coon, S. L. and Klein, D. C. (2006). Evolution of arylalkylamine N-acetyltransferase: emergence and divergence. Mol Cell Endocrinol 252, 2-10.

Coon, S. L., Weller, J. L., Korf, H. W., Namboodiri, M. A., Rollag, M. and Klein, D. C. (2001). cAmp regulation of arylalkylamine N-acetyltransferase (AANAT, EC 2.3.1.87): a new cell line (1E7) provides evidence of intracellular AANAT activation. J Biol Chem 276, 24097-107.

Craft, C. M. and Zhan-Poe, X. (2000). Identification of specific histidine residues and the carboxyl terminus are essential for serotonin N-acetyltransferase enzymatic activity. Brain Res Mol Brain Res 75, 198-207.

Czerny, T. and Busslinger, M. (1995). DNA-binding and transactivation properties of Pax-6: three amino acids in the paired domain are responsible for the different sequence recognition of Pax-6 and BSAP (Pax-5). Mol Cell Biol 15, 2858-71.

Czerny, T., Schaffner, G. and Busslinger, M. (1993). DNA sequence recognition by Pax proteins: bipartite structure of the paired domain and its binding site. Genes Dev 7, 2048-61.

Danilova, N., Krupnik, V. E., Sugden, D. and Zhdanova, I. V. (2004). Melatonin stimulates cell proliferation in zebrafish embryo and accelerates its development. Faseb J 18, 751-3.

Decressac, S., Grechez-Cassiau, A., Lenfant, J., Falcon, J. and Bois, P. (2002). Cloning, localization and functional properties of a cGMP-gated channel in photoreceptor cells from fish pineal gland. J Pineal Res 33, 225-33.

Del Bene, F., Tessmar-Raible, K. and Wittbrodt, J. (2004). Direct interaction of geminin and Six3 in eye development. Nature 427, 745-9.

Del Rio-Tsonis, K. and Tsonis, P. A. (2003). Eye regeneration at the molecular age. Dev Dyn 226, 211-24.

Delaunay, F., Thisse, C., Marchand, O., Laudet, V. and Thisse, B. (2000). An inherited functional circadian clock in zebrafish embryos. Science 289, 297-300.

Demuro, G. and Obici, S. (2006). Central nervous system and control of endogenous glucose production. Curr Diab Rep 6, 188-93.

Denver, R. J. (1993). Acceleration of anuran amphibian metamorphosis by corticotropin-releasing hormone-like peptides. Gen Comp Endocrinol 91, 38-51.

Desvergne, B. (1994). How do thyroid hormone receptors bind to structurally diverse response elements? Mol Cell Endocrinol 100, 125-31.

Dominguez, M., Ferres-Marco, D., Gutierrez-Avino, F. J., Speicher, S. A. and Beneyto, M. (2004). Growth and specification of the eye are controlled independently by Eyegone and Eyeless in Drosophila melanogaster. Nat Genet 36, 31-9.

Donohue, S. J., Roseboom, P. H., Illnerova, H., Weller, J. L. and Klein, D. C. (1993). Human hydroxyindole-O-methyltransferase: presence of LINE-1 fragment in a cDNA clone and pineal mRNA. DNA Cell Biol 12, 715-27.

Eberhard, D., Jimenez, G., Heavey, B. and Busslinger, M. (2000). Transcriptional repression by Pax5 (BSAP) through interaction with corepressors of the Groucho family. Embo J 19, 2292-303.

Eliceiri, B. P. and Brown, D. D. (1994). Quantitation of endogenous thyroid hormone receptors alpha and beta during embryogenesis and metamorphosis in Xenopus laevis. J Biol Chem 269, 24459-65.

Epstein, J., Cai, J., Glaser, T., Jepeal, L. and Maas, R. (1994a). Identification of a Pax paired domain recognition sequence and evidence for DNA-dependent conformational changes. J Biol Chem 269, 8355-61.

Epstein, J. A., Glaser, T., Cai, J., Jepeal, L., Walton, D. S. and Maas, R. L. (1994b). Two independent and interactive DNA-binding subdomains of the Pax6 paired domain are regulated by alternative splicing. Genes Dev 8, 2022-34.

Essner, J. J., Branford, W. W., Zhang, J. and Yost, H. J. (2000). Mesendoderm and left-right brain, heart and gut development are differentially regulated by pitx2 isoforms. Development 127, 1081-93.

Estivill-Torrus, G., Vitalis, T., Fernandez-Llebrez, P. and Price, D. J. (2001). The transcription factor Pax6 is required for development of the diencephalic dorsal midline secretory radial glia that form the subcommissural organ. Mech Dev 109, 215-24.

Evans, B. I. and Fernald, R. D. (1993). Retinal transformation at metamorphosis in the winter flounder (Pseudopleuronectes americanus). Vis Neurosci 10, 1055-64.

Even, Y., Durieux, S., Escande, M. L., Lozano, J. C., Peaucellier, G., Weil, D. and Geneviere, A. M. (2006). CDC2L5, a Cdk-like kinase with RS domain, interacts with the ASF/SF2-associated protein p32 and affects splicing in vivo. J Cell Biochem.

Falcon, J. (1999). Cellular circadian clocks in the pineal. Prog Neurobiol 58, 121-62.

Falcon, J., Besseau, L., and Boeuf, G. (2006). Molecular and cellular regulation of pineal organ responses. In: Hara, T. Zielinski, B. eds Fish physiology: sensory systems neuroscience. Amsterdam: Elsevier Science, in press.

Falcon, J., Galarneau, K. M., Weller, J. L., Ron, B., Chen, G., Coon, S. L. and Klein, D. C. (2001). Regulation of arylalkylamine N-acetyltransferase-2 (AANAT2, EC 2.3.1.87) in the fish pineal organ: evidence for a role of proteasomal proteolysis. Endocrinology 142, 1804-13.

Fiske, V. M. (1964). Serotonin Rhythm in the Pineal Organ: Control by the Sympathetic Nervous System. Science 146, 253-4.

Forsell, J., Holmqvist, B. and Ekstrom, P. (2002). Molecular identification and developmental expression of UV and green opsin mRNAs in the pineal organ of the Atlantic halibut. Brain Res Dev Brain Res 136, 51-62.

Foulkes, N. S. and Sassone-Corsi, P. (1992). More is better: activators and repressors from the same gene. Cell 68, 411-4.

Frigerio, G., Burri, M., Bopp, D., Baumgartner, S. and Noll, M. (1986). Structure of the segmentation gene paired and the Drosophila PRD gene set as part of a gene network. Cell 47, 735-46.

Fu, W. and Noll, M. (1997). The Pax2 homolog sparkling is required for development of cone and pigment cells in the Drosophila eye. Genes Dev 11, 2066-78.

Fu, Z., Kato, H., Kotera, N., Noguchi, T., Sugahara, K. and Kubo, T. (2001). Regulation of hydroxyindole-O-methyltransferase gene expression in Japanese quail (Coturnix coturnix japonica). Biosci Biotechnol Biochem 65, 2504-11.

Fujiwara, M., Uchida, T., Osumi-Yamashita, N. and Eto, K. (1994). Uchida rat (rSey): a new mutant rat with craniofacial abnormalities resembling those of the mouse Sey mutant. Differentiation 57, 31-8.

Furukawa, T., Morrow, E. M. and Cepko, C. L. (1997). Crx, a novel otx-like homeobox gene, shows photoreceptor-specific expression and regulates photoreceptor differentiation. Cell 91, 531-41.

Furukawa, T., Morrow, E. M., Li, T., Davis, F. C. and Cepko, C. L. (1999). Retinopathy and attenuated circadian entrainment in Crx-deficient mice. Nat Genet 23, 466-70.

Furuta, Y. and Hogan, B. L. (1998). BMP4 is essential for lens induction in the mouse embryo. Genes Dev 12, 3764-75.

Gachon, F., Nagoshi, E., Brown, S. A., Ripperger, J. and Schibler, U. (2004). The mammalian circadian timing system: from gene expression to physiology. Chromosoma 113, 103-12.

Gainotti, G. (2001). Disorders of emotional behaviour. J Neurol 248, 743-9.

Galtier, N., Gouy, M. and Gautier, C. (1996). SEAVIEW and PHYLO_WIN: two graphic tools for sequence alignment and molecular phylogeny. Comput Appl Biosci 12, 543-8.

Gamse, J. T., Shen, Y. C., Thisse, C., Thisse, B., Raymond, P. A., Halpern, M. E. and Liang, J. O. (2002). Otx5 regulates genes that show circadian expression in the zebrafish pineal complex. Nat Genet 30, 117-21.

Ganguly, S., Gastel, J. A., Weller, J. L., Schwartz, C., Jaffe, H., Namboodiri, M. A., Coon, S. L., Hickman, A. B., Rollag, M., Obsil, T. et al. (2001). Role of a pineal cAMP-operated arylalkylamine N-acetyltransferase/14-3-3-binding switch in melatonin synthesis. Proc Natl Acad Sci U S A 98, 8083-8.

Ganguly, S., Weller, J. L., Ho, A., Chemineau, P., Malpaux, B. and Klein, D. C. (2005). Melatonin synthesis: 14-3-3-dependent activation and inhibition of arylalkylamine N-acetyltransferase mediated by phosphoserine-205. Proc Natl Acad Sci U S A 102, 1222-7.

Gastel, J. A., Roseboom, P. H., Rinaldi, P. A., Weller, J. L. and Klein, D. C. (1998). Melatonin production: proteasomal proteolysis in serotonin N-acetyltransferase regulation. Science 279, 1358-60.

Gauer, F., Masson-Pevet, M., Skene, D. J., Vivien-Roels, B. and Pevet, P. (1993). Daily rhythms of melatonin binding sites in the rat pars tuberalis and suprachiasmatic nuclei; evidence for a regulation of melatonin receptors by melatonin itself. Neuroendocrinology 57, 120-6.

Gehring, W. J. (2002). The genetic control of eye development and its implications for the evolution of the various eye-types. Int J Dev Biol 46, 65-73.

Gehring, W. J. (2004). Historical perspective on the development and evolution of eyes and photoreceptors. Int J Dev Biol 48, 707-17.

Gehring, W. J. and Ikeo, K. (1999). Pax 6: mastering eye morphogenesis and eye evolution. Trends Genet 15, 371-7.

Gern, W. A. and Greenhouse, S. S. (1988). Examination of in vitro melatonin secretion from superfused trout (Salmo gairdneri) pineal organs maintained under diel illumination or continuous darkness. Gen Comp Endocrinol 71, 163-74.

Gestri, G., Carl, M., Appolloni, I., Wilson, S. W., Barsacchi, G. and Andreazzoli, M. (2005). Six3 functions in anterior neural plate specification by promoting cell proliferation and inhibiting Bmp4 expression. Development 132, 2401-13.

Gilmour, D. T., Jessen, J.R. and Lin, S. (2002). Manipulating gene expression in the zebrafish. In: Nüslein-Volhard, C. and Dahm, R. Zebrafish. Practical approach. eds Oxford Press, 121-143.

Glardon, S., Callaerts, P., Halder, G. and Gehring, W. J. (1997). Conservation of Pax-6 in a lower chordate, the ascidian Phallusia mammillata. Development 124, 817-25.

Glardon, S., Holland, L. Z., Gehring, W. J. and Holland, N. D. (1998). Isolation and developmental expression of the amphioxus Pax-6 gene (AmphiPax-6): insights into eye and photoreceptor evolution. Development 125, 2701-10.

Glaser, T., Jepeal, L., Edwards, J. G., Young, S. R., Favor, J. and Maas, R. L. (1994). PAX6 gene dosage effect in a family with congenital cataracts, aniridia, anophthalmia and central nervous system defects. Nat Genet 7, 463-71.

Glass, C. K., Holloway, J. M., Devary, O. V. and Rosenfeld, M. G. (1988). The thyroid hormone receptor binds with opposite transcriptional effects to a common sequence motif in thyroid hormone and estrogen response elements. Cell 54, 313-23.

Gonzalez-Estevez, C., Momose, T., Gehring, W. J. and Salo, E. (2003). Transgenic planarian lines obtained by electroporation using transposon-derived vectors and an eye-specific GFP marker. Proc Natl Acad Sci U S A 100, 14046-51.

Gorlov, I. P. and Saunders, G. F. (2002). A method for isolating alternatively spliced isoforms: isolation of murine Pax6 isoforms. Anal Biochem 308, 401-4.

Gothilf, Y., Coon, S. L., Toyama, R., Chitnis, A., Namboodiri, M. A. and Klein, D. C. (1999). Zebrafish serotonin N-acetyltransferase-2: marker for development of pineal photoreceptors and circadian clock function. Endocrinology 140, 4895-903.

Graf, W. and Baker, R. (1983). Adaptive changes of the vestibulo-ocular reflex in flatfish are achieved by reorganization of central nervous pathways. Science 221, 777-9.

Grant, S. and Keating, M. J. (1986). Ocular migration and the metamorphic and postmetamorphic maturation of the retinotectal system in Xenopus laevis: an autoradiographic and morphometric study. J Embryol Exp Morphol 92, 43-69.

Graveley, B. R. (2001). Alternative splicing: increasing diversity in the proteomic world. Trends Genet 17, 100-7.

Greve, P., Bernard, M., Voisin, P., Cogne, M., Collin, J. P. and Guerlotte, J. (1993). Cellular localization of hydroxyindole-O-methyltransferase mRNA in the chicken pineal gland. Neuroreport 4, 803-6.

Greve, P., Voisin, P., Grechez-Cassiau, A., Bernard, M., Collin, J. P. and Guerlotte, J. (1996). Circadian regulation of hydroxyindole-O-methyltransferase mRNA in the chicken pineal gland in vivo and in vitro. Biochem J 319 (Pt 3), 761-6.

Grindley, J. C., Davidson, D. R. and Hill, R. E. (1995). The role of Pax-6 in eye and nasal development. Development 121, 1433-42.

Guerlotte, J., Voisin, P., Brisson, P., Faure, J. P. and Collin, J. P. (1988). Synthesis of melatonin by the pineal modified photoreceptors of birds immunocytochemical localization of hydroxyindole-O-methyltransferase. Biol Cell 64, 93-6.

Guillemot, F. (2005). Cellular and molecular control of neurogenesis in the mammalian telencephalon. Curr Opin Cell Biol 17, 639-47.

Guyenet, P. G. (2006). The sympathetic control of blood pressure. Nat Rev Neurosci 7, 335-46.

Halder, G., Callaerts, P. and Gehring, W. J. (1995). Induction of ectopic eyes by targeted expression of the eyeless gene in Drosophila. Science 267, 1788-92.

Hanken, J. and Hall, B. K. (1988). Skull development during anuran metamorphosis. II. Role of thyroid hormone in osteogenesis. Anat Embryol (Berl) 178, 219-27.

Hanson, I., Brown, A. and van Heyningen, V. (1995). A new PAX6 mutation in familial aniridia. J Med Genet 32, 488-9.

Hardin, P. E. (2004). Transcription regulation within the circadian clock: the E-box and beyond. J Biol Rhythms 19, 348-60.

Hartmann, B., Lee, P. N., Kang, Y. Y., Tomarev, S., de Couet, H. G. and Callaerts, P. (2003). Pax6 in the sepiolid squid Euprymna scolopes: evidence for a role in eye, sensory organ and brain development. Mech Dev 120, 177-83.

Haubst, N., Berger, J., Radjendirane, V., Graw, J., Favor, J., Saunders, G. F., Stoykova, A. and Gotz, M. (2004). Molecular dissection of Pax6 function: the specific roles of the paired domain and homeodomain in brain development. Development 131, 6131-40.

Heisenberg, C. P., Houart, C., Take-Uchi, M., Rauch, G. J., Young, N., Coutinho, P., Masai, I., Caneparo, L., Concha, M. L., Geisler, R. et al. (2001). A mutation in the Gsk3-binding domain of zebrafish Masterblind/Axin1 leads to a fate transformation of telencephalon and eyes to diencephalon. Genes Dev 15, 1427-34.

Helvik, J. V., Drivenes, O., Naess, T. H., Fjose, A. and Seo, H. C. (2001). Molecular cloning and characterization of five opsin genes from the marine flatfish Atlantic halibut (Hippoglossus hippoglossus). Vis Neurosci 18, 767-80.

Hickman, A. B., Klein, D. C. and Dyda, F. (1999a). Melatonin biosynthesis: the structure of serotonin N-acetyltransferase at 2.5 A resolution suggests a catalytic mechanism. Mol Cell 3, 23-32.

Hickman, A. B., Namboodiri, M. A., Klein, D. C. and Dyda, F. (1999b). The structural basis of ordered substrate binding by serotonin N-acetyltransferase: enzyme complex at 1.8 A resolution with a bisubstrate analog. Cell 97, 361-9.

Hill, R. E., Favor, J., Hogan, B. L., Ton, C. C., Saunders, G. F., Hanson, I. M., Prosser, J., Jordan, T., Hastie, N. D. and van Heyningen, V. (1991). Mouse small eye results from mutations in a paired-like homeobox-containing gene. Nature 354, 522-5.

Hoegg, S., Brinkmann, H., Taylor, J. S. and Meyer, A. (2004). Phylogenetic timing of the fish-specific genome duplication correlates with the diversification of teleost fish. J Mol Evol 59, 190-203.

Hogan, B. L., Horsburgh, G., Cohen, J., Hetherington, C. M., Fisher, G. and Lyon, M. F. (1986). Small eyes (Sey): a homozygous lethal mutation on chromosome 2 which affects the differentiation of both lens and nasal placodes in the mouse. J Embryol Exp Morphol 97, 95-110.

Horlein, A. J., Naar, A. M., Heinzel, T., Torchia, J., Gloss, B., Kurokawa, R., Ryan, A., Kamei, Y., Soderstrom, M., Glass, C. K. et al. (1995). Ligand-independent repression by the thyroid hormone receptor mediated by a nuclear receptor co-repressor. Nature 377, 397-404.

Hoskins, S. G. (1986). Control of the development of the ipsilateral retinothalamic projection in Xenopus laevis by thyroxine: results and speculation. J Neurobiol 17, 203-29.

Hoskins, S. G. and Grobstein, P. (1984). Induction of the ipsilateral retinothalamic projection in Xenopus laevis by thyroxine. Nature 307, 730-3.

Hoskins, S. G. and Grobstein, P. (1985a). Development of the ipsilateral retinothalamic projection in the frog Xenopus laevis. I. Retinal distribution of ipsilaterally projecting cells in normal and experimentally manipulated frogs. J Neurosci 5, 911-9.

Hoskins, S. G. and Grobstein, P. (1985b). Development of the ipsilateral retinothalamic projection in the frog Xenopus laevis. II. Ingrowth of optic nerve fibers and production of ipsilaterally projecting retinal ganglion cells. J Neurosci 5, 920-9.

Hoskins, S. G. and Grobstein, P. (1985c). Development of the ipsilateral retinothalamic projection in the frog Xenopus laevis. III. The role of thyroxine. J Neurosci 5, 930-40.

Huang, H., Cai, L., Remo, B. F. and Brown, D. D. (2001). Timing of metamorphosis and the onset of the negative feedback loop between the thyroid gland and the pituitary is controlled by type II iodothyronine deiodinase in Xenopus laevis. Proc Natl Acad Sci U S A 98, 7348-53.

Hurd, M. W. and Cahill, G. M. (2002). Entraining signals initiate behavioral circadian rhythmicity in larval zebrafish. J Biol Rhythms 17, 307-14.

Inoue, T., Nakamura, S. and Osumi, N. (2000). Fate mapping of the mouse prosencephalic neural plate. Dev Biol 219, 373-83.

Inui, Y. and Miwa, S. (1985). Thyroid hormone induces metamorphosis of flounder larvae. Gen Comp Endocrinol 60, 450-4.

Ishida, I., Obinata, M. and Deguchi, T. (1987). Molecular cloning and nucleotide sequence of cDNA encoding hydroxyindole O-methyltransferase of bovine pineal glands. J Biol Chem 262, 2895-9.

Ishizuya-Oka, A., Ueda, S., Inokuchi, T., Amano, T., Damjanovski, S., Stolow, M. and Shi, Y. B. (2001). Thyroid hormone-induced expression of sonic hedgehog correlates with adult epithelial development during remodeling of the Xenopus stomach and intestine. Differentiation 69, 27-37.

Iuvone, P. M., Tosini, G., Pozdeyev, N., Haque, R., Klein, D. C. and Chaurasia, S. S. (2005). Circadian clocks, clock networks, arylalkylamine N-acetyltransferase, and melatonin in the retina. Prog Retin Eye Res 24, 433-56.

Jaillon, O., Aury, J. M., Brunet, F., Petit, J. L., Stange-Thomann, N., Mauceli, E., Bouneau, L., Fischer, C., Ozouf-Costaz, C., Bernot, A. et al. (2004). Genome duplication in the teleost fish Tetraodon nigroviridis reveals the early vertebrate proto-karyotype. Nature 431, 946-57.

Jaworski, C., Sperbeck, S., Graham, C. and Wistow, G. (1997). Alternative splicing of Pax6 in bovine eye and evolutionary conservation of intron sequences. Biochem Biophys Res Commun 240, 196-202.

Johns, P. R. (1982). Formation of photoreceptors in larval and adult goldfish. J Neurosci 2, 178-98.

Kalnina, Z., Zayakin, P., Silina, K. and Line, A. (2005). Alterations of pre-mRNA splicing in cancer. Genes Chromosomes Cancer 42, 342-57.

Kamachi, Y., Uchikawa, M., Tanouchi, A., Sekido, R. and Kondoh, H. (2001). Pax6 and SOX2 form a co-DNA-binding partner complex that regulates initiation of lens development. Genes Dev 15, 1272-86.

Kammandel, B., Chowdhury, K., Stoykova, A., Aparicio, S., Brenner, S. and Gruss, P. (1999). Distinct cis-essential modules direct the time-space pattern of the Pax6 gene activity. Dev Biol 205, 79-97.

Kammermeier, L., Leemans, R., Hirth, F., Flister, S., Wenger, U., Walldorf, U., Gehring, W. J. and Reichert, H. (2001). Differential expression and function of the Drosophila Pax6 genes eyeless and twin of eyeless in embryonic central nervous system development. Mech Dev 103, 71-8.

Kaneko, M. and Cahill, G. M. (2005). Light-dependent development of circadian gene expression in transgenic zebrafish. PLoS Biol 3, e34.

Kazimi, N. and Cahill, G. M. (1999). Development of a circadian melatonin rhythm in embryonic zebrafish. Brain Res Dev Brain Res 117, 47-52.

Kim, J. and Lauderdale, J. D. (2006). Analysis of Pax6 expression using a BAC transgene reveals the presence of a paired-less isoform of Pax6 in the eye and olfactory bulb. Dev Biol 292, 486-505.

Klein, D. C., Coon, S. L., Roseboom, P. H., Weller, J. L., Bernard, M., Gastel, J. A., Zatz, M., Iuvone, P. M., Rodriguez, I. R., Begay, V. et al. (1997). The melatonin rhythm-generating enzyme: molecular regulation of serotonin N-acetyltransferase in the pineal gland. Recent Prog Horm Res 52, 307-57; discussion 357-8.

Klein, D. C., Namboodiri, M. A. and Auerbach, D. A. (1981). The melatonin rhythm generating system: developmental aspects. Life Sci 28, 1975-86.

Klein, D. C. and Weller, J. L. (1970). Indole metabolism in the pineal gland: a circadian rhythm in N-acetyltransferase. Science 169, 1093-5.

Klein, D. C. and Weller, J. L. (1972). Rapid light-induced decrease in pineal serotonin N-acetyltransferase activity. Science 177, 532-3.

Kleinjan, D. A., Seawright, A., Childs, A. J. and van Heyningen, V. (2004). Conserved elements in Pax6 intron 7 involved in (auto)regulation and alternative transcription. Dev Biol 265, 462-77.

Kobayashi, M., Toyama, R., Takeda, H., Dawid, I. B. and Kawakami, K. (1998). Overexpression of the forebrain-specific homeobox gene six3 induces rostral forebrain enlargement in zebrafish. Development 125, 2973-82.

Kollros. (1961). Mechanisms of amphibian metamorphosis: Hormones. Am. Zool. 1, 107-114.

Kozmik, Z., Czerny, T. and Busslinger, M. (1997). Alternatively spliced insertions in the paired domain restrict the DNA sequence specificity of Pax6 and Pax8. Embo J 16, 6793-803.

Krauss, S., Johansen, T., Korzh, V., Moens, U., Ericson, J. U. and Fjose, A. (1991). Zebrafish pax[zf-a]: a paired box-containing gene expressed in the neural tube. Embo J 10, 3609-19.

Kubota, R., Hokoc, J. N., Moshiri, A., McGuire, C. and Reh, T. A. (2002). A comparative study of neurogenesis in the retinal ciliary marginal zone of homeothermic vertebrates. Brain Res Dev Brain Res 134, 31-41.

Kuwano, R., Iwanaga, T., Nakajima, T., Masuda, T. and Takahashi, Y. (1983). Immunocytochemical demonstration of hydroxyindole O-methyltransferase (HIOMT), neuron-specific enolase (NSE) and S-100 protein in the bovine pineal gland. Brain Res 274, 171-5.

Kvenseth, A. M., Pittman, K. and Helvik, J.V. (1996). Eye development in Atlantic halibut (Hippoglossus hippoglossus): differentiation and development of the retina from early yolk sac stages through metamorphosis. Can. J. Aquat. Sci 53, 2524-2532.

Lander, E. S. Linton, L. M. Birren, B. Nusbaum, C. Zody, M. C. Baldwin, J. Devon, K. Dewar, K. Doyle, M. FitzHugh, W. et al. (2001). Initial sequencing and analysis of the human genome. Nature 409, 860-921.

Lang, R. A. (2004). Pathways regulating lens induction in the mouse. Int J Dev Biol 48, 783-91.

Lauder, G. V. and Liem, K.F. (1983). The evolution and interrelationships of the actinopterygian fishes. Bull. Mus. Com. Zool. 150, 95-197.

Lechner, M. S. and Dressler, G. R. (1996). Mapping of Pax-2 transcription activation domains. J Biol Chem 271, 21088-93.

Leconte, L., Lecoin, L., Martin, P. and Saule, S. (2004). Pax6 interacts with cVax and Tbx5 to establish the dorsoventral boundary of the developing eye. J Biol Chem 279, 47272-7.

Lee, H. Y., Wroblewski, E., Philips, G. T., Stair, C. N., Conley, K., Reedy, M., Mastick, G. S. and Brown, N. L. (2005). Multiple requirements for Hes 1 during early eye formation. Dev Biol 284, 464-78.

Lerner, A. B. and Case, J. D. (1959). Pigment cell regulatory factors. J Invest Dermatol 32, 211-21.

Leuzinger, S., Hirth, F., Gerlich, D., Acampora, D., Simeone, A., Gehring, W. J., Finkelstein, R., Furukubo-Tokunaga, K. and Reichert, H. (1998). Equivalence of the fly orthodenticle gene and the human OTX genes in embryonic brain development of Drosophila. Development 125, 1703-10.

Levine, M. (2002). How insects lose their limbs. Nature 415, 848-9.

Lewy, A. J., Tetsuo, M., Markey, S. P., Goodwin, F. K. and Kopin, I. J. (1980). Pinealectomy abolishes plasma melatonin in the rat. J Clin Endocrinol Metab 50, 204-5.

Lichtneckert, R. and Reichert, H. (2005). Insights into the urbilaterian brain: conserved genetic patterning mechanisms in insect and vertebrate brain development. Heredity 94, 465-77.

Lincoln, G. A., Andersson, H. and Loudon, A. (2003). Clock genes in calendar cells as the basis of annual timekeeping in mammals--a unifying hypothesis. J Endocrinol 179, 1-13.

Liu, Q., Marrs, J. A., Chuang, J. C. and Raymond, P. A. (2001). Cadherin-4 expression in the zebrafish central nervous system and regulation by ventral midline signaling. Brain Res Dev Brain Res 131, 17-29.

Loosli, F., Kmita-Cunisse, M. and Gehring, W. J. (1996). Isolation of a Pax-6 homolog from the ribbonworm Lineus sanguineus. Proc Natl Acad Sci U S A 93, 2658-63.

Lupo, G., Liu, Y., Qiu, R., Chandraratna, R. A., Barsacchi, G., He, R. Q. and Harris, W. A. (2005). Dorsoventral patterning of the Xenopus eye: a collaboration of Retinoid, Hedgehog and FGF receptor signaling. Development 132, 1737-48.

Mader, M. M. and Cameron, D. A. (2004). Photoreceptor differentiation during retinal development, growth, and regeneration in a metamorphic vertebrate. J Neurosci 24, 11463-72.

Maniatis, T. and Tasic, B. (2002). Alternative pre-mRNA splicing and proteome expansion in metazoans. Nature 418, 236-43.

Mann, F. and Holt, C. E. (2001). Control of retinal growth and axon divergence at the chiasm: lessons from Xenopus. Bioessays 23, 319-26.

Mano, H., Kojima, D. and Fukada, Y. (1999). Exo-rhodopsin: a novel rhodopsin expressed in the zebrafish pineal gland. Brain Res Mol Brain Res 73, 110-8.

Manuel, M. and Price, D. J. (2005). Role of Pax6 in forebrain regionalization. Brain Res Bull 66, 387-93.

Marchand, O., Duffraisse, M., Triqueneaux, G., Safi, R. and Laudet, V. (2004). Molecular cloning and developmental expression patterns of thyroid hormone receptors and T3 target genes in the turbot (Scophtalmus maximus) during post-embryonic development. Gen Comp Endocrinol 135, 345-57.

Marquardt, T., Ashery-Padan, R., Andrejewski, N., Scardigli, R., Guillemot, F. and Gruss, P. (2001). Pax6 is required for the multipotent state of retinal progenitor cells. Cell 105, 43-55.

Marsh-Armstrong, N., Huang, H., Remo, B. F., Liu, T. T. and Brown, D. D. (1999). Asymmetric growth and development of the Xenopus laevis retina during metamorphosis is controlled by type III deiodinase. Neuron 24, 871-8.

Martinez-Morales, J. R., Rodrigo, I. and Bovolenta, P. (2004). Eye development: a view from the retina pigmented epithelium. Bioessays 26, 766-77.

Masai, I., Heisenberg, C. P., Barth, K. A., Macdonald, R., Adamek, S. and Wilson, S. W. (1997). floating head and masterblind regulate neuronal patterning in the roof of the forebrain. Neuron 18, 43-57.

Matsuo, T. (1993). The genes involved in the morphogenesis of the eye. Jpn J Ophthalmol 37, 215-51.

Mayer, I., Bornestaf, C., Wetterberg, L. and Borg, B. (1997). Melatonin does not prevent long photoperiod stimulation of secondary sexual characters in the male three-spined stickleback Gasterosteus aculeatus. Gen Comp Endocrinol 108, 386-94.

McArthur, A. J., Gillette, M. U. and Prosser, R. A. (1991). Melatonin directly resets the rat suprachiasmatic circadian clock in vitro. Brain Res 565, 158-61.

McKenna, N. J., Xu, J., Nawaz, Z., Tsai, S. Y., Tsai, M. J. and O'Malley, B. W. (1999). Nuclear receptor coactivators: multiple enzymes, multiple complexes, multiple functions. J Steroid Biochem Mol Biol 69, 3-12.

Medina, M., Reperant, J., Ward, R., Rio, J. P. and Lemire, M. (1993). The primary visual system of flatfish: an evolutionary perspective. Anat Embryol (Berl) 187, 167-91.

Michaelides, M., Hardcastle, A. J., Hunt, D. M. and Moore, A. T. (2006). Progressive cone and cone-rod dystrophies: phenotypes and underlying molecular genetic basis. Surv Ophthalmol 51, 232-58.

Mishra, R., Gorlov, I. P., Chao, L. Y., Singh, S. and Saunders, G. F. (2002). PAX6, paired domain influences sequence recognition by the homeodomain. J Biol Chem 277, 49488-94.

Mitchell, T. N., Free, S. L., Williamson, K. A., Stevens, J. M., Churchill, A. J., Hanson, I. M., Shorvon, S. D., Moore, A. T., van Heyningen, V. and Sisodiya, S. M. (2003). Polymicrogyria and absence of pineal gland due to PAX6 mutation. Ann Neurol 53, 658-63.

Mizuno, N., Mochii, M., Yamamoto, T. S., Takahashi, T. C., Eguchi, G. and Okada, T. S. (1999). Pax-6 and Prox 1 expression during lens regeneration from Cynops iris and Xenopus cornea: evidence for a genetic program common to embryonic lens development. Differentiation 65, 141-9.

Munoz, E. and Baler, R. (2003). The circadian E-box: when perfect is not good enough. Chronobiol Int 20, 371-88.

Murakami, Y., Ogasawara, M., Sugahara, F., Hirano, S., Satoh, N. and Kuratani, S. (2001). Identification and expression of the lamprey Pax6 gene: evolutionary origin of the segmented brain of vertebrates. Development 128, 3521-31.

Nagao, T., Leuzinger, S., Acampora, D., Simeone, A., Finkelstein, R., Reichert, H. and Furukubo-Tokunaga, K. (1998). Developmental rescue of Drosophila cephalic defects by the human Otx genes. Proc Natl Acad Sci U S A 95, 3737-42.

Nasevicius, A. and Ekker, S. C. (2000). Effective targeted gene 'knockdown' in zebrafish. Nat Genet 26, 216-20.

Nelson, J. S. (1995). Book Review. Interrelationships of fishes. Copeia 1997 3, 647-649.

Nornes, S., Clarkson, M., Mikkola, I., Pedersen, M., Bardsley, A., Martinez, J. P., Krauss, S. and Johansen, T. (1998). Zebrafish contains two pax6 genes involved in eye development. Mech Dev 77, 185-96.

Obsil, T., Ghirlando, R., Klein, D. C., Ganguly, S. and Dyda, F. (2001). Crystal structure of the 14-3-3zeta:serotonin N-acetyltransferase complex. a role for scaffolding in enzyme regulation. Cell 105, 257-67.

Ogino, H. and Yasuda, K. (2000). Sequential activation of transcription factors in lens induction. Dev Growth Differ 42, 437-48.

Onuma, Y., Takahashi, S., Asashima, M., Kurata, S. and Gehring, W. J. (2002). Conservation of Pax 6 function and upstream activation by Notch signaling in eye development of frogs and flies. Proc Natl Acad Sci U S A 99, 2020-5.

Osumi, N. (2001). The role of Pax6 in brain patterning. Tohoku J Exp Med 193, 163-74.

Otteson, D. C., D'Costa, A. R. and Hitchcock, P. F. (2001). Putative stem cells and the lineage of rod photoreceptors in the mature retina of the goldfish. Dev Biol 232, 62-76.

Papalopulu, N. and Kintner, C. (1996). A Xenopus gene, Xbr-1, defines a novel class of homeobox genes and is expressed in the dorsal ciliary margin of the eye. Dev Biol 174, 104-14.

Perron, M., Kanekar, S., Vetter, M. L. and Harris, W. A. (1998). The genetic sequence of retinal development in the ciliary margin of the Xenopus eye. Dev Biol 199, 185-200.

Person-Le-Ruyet, J., Lahaye, J., Deniel, C., Metayer, R., Devauchelle, N., Menu, B., Noel, T., Baudin-Laurencin, F. (1989). L'élevage des poissons plats: sole turbot.

Pevet, P. (1988). The role of the pineal gland in the photoperiodic control of reproduction in different hamster species. Reprod Nutr Dev 28, 443-58.

Pevet, P. (2003). Melatonin: from seasonal to circadian signal. J Neuroendocrinol 15, 422-6.

Pichaud, F. and Desplan, C. (2002). Pax genes and eye organogenesis. Curr Opin Genet Dev 12, 430-4.

Pinson, J., Mason, J. O., Simpson, T. I. and Price, D. J. (2005). Regulation of the Pax6 : Pax6(5a) mRNA ratio in the developing mammalian brain. BMC Dev Biol 5, 13.

Pinson, J., Simpson, T. I., Mason, J. O. and Price, D. J. (2006). Positive autoregulation of the transcription factor Pax6 in response to increased levels of either of its major isoforms, Pax6 or Pax6(5a), in cultured cells. BMC Dev Biol 6, 25.

Plewniak, F., Bianchetti, L., Brelivet, Y., Carles, A., Chalmel, F., Lecompte, O., Mochel, T., Moulinier, L., Muller, A., Muller, J. et al. (2003). PipeAlign: A new toolkit for protein family analysis. Nucleic Acids Res 31, 3829-32.

Plouhinec, J. L., Sauka-Spengler, T., Germot, A., Le Mentec, C., Cabana, T., Harrison, G., Pieau, C., Sire, J. Y., Veron, G. and Mazan, S. (2003). The mammalian Crx genes are highly divergent representatives of the Otx5 gene family, a gnathostome orthology class of orthodenticle-related homeogenes involved in the differentiation of retinal photoreceptors and circadian entrainment. Mol Biol Evol 20, 513-21.

Power, D. M., Llewellyn, L., Faustino, M., Nowell, M. A., Bjornsson, B. T., Einarsdottir, I. E., Canario, A. V. and Sweeney, G. E. (2001). Thyroid hormones in growth and development of fish. Comp Biochem Physiol C Toxicol Pharmacol 130, 447-59.

Punzo, C., Kurata, S. and Gehring, W. J. (2001). The eyeless homeodomain is dispensable for eye development in Drosophila. Genes Dev 15, 1716-23.

Quay, W. B. (1963). Circadian Rhythm in Rat Pineal Serotonin and Its Modifications by Estrous Cycle and Photoperiod. Gen Comp Endocrinol 14, 473-9.

Quinn, J. C., West, J. D. and Hill, R. E. (1996). Multiple functions for Pax6 in mouse eye and nasal development. Genes Dev 10, 435-46.

Quiring, R., Walldorf, U., Kloter, U. and Gehring, W. J. (1994). Homology of the eyeless gene of Drosophila to the Small eye gene in mice and Aniridia in humans. Science 265, 785-9.

Raymond, P. A. (1985). Cytodifferentiation of photoreceptors in larval goldfish: delayed maturation of rods. J Comp Neurol 236, 90-105.

Raymond, P. A. and Rivlin, P. K. (1987). Germinal cells in the goldfish retina that produce rod photoreceptors. Dev Biol 122, 120-38.

Rebollar, P. G., Ubilla, E., Peleteiro, J. B., Agapito, M. T. and Alvarino, J. M. (1999). Determination of plasma melatonin levels by enzyme-linked immunosorbent assay (EIA) in turbot (Scophtalmus maximus L.) and tench (Tinca tinca L.). J Physiol Biochem 55, 341-7.

Reiter, R. J., Britt, J. H. and Armstrong, J. D. (1987). Absence of a nocturnal rise in either norepinephrine, N-acetyltransferase, hydroxyindole-O-methyltransferase or melatonin in the pineal gland of the domestic pig kept under natural environment photoperiods. Neurosci Lett 81, 171-6.

Reppert, S. M. and Weaver, D. R. (2002). Coordination of circadian timing in mammals. Nature 418, 935-41.

Reynolds, E. S. (1963). The use of lead citrate at high pH as an electron-opaque stain in electron microscopy. J Cell Biol 17, 208-12.

Ribelayga, C., Gauer, F., Calgari, C., Pevet, P. and Simonneaux, V. (1999). Photoneural regulation of rat pineal hydroxyindole-O-methyltransferase (HIOMT) messenger ribonucleic acid expression: an analysis of its complex relationship with HIOMT activity. Endocrinology 140, 1375-84.

Rozen, S. and Skaletsky, H.J. (2000). Primer3 on the WWW for general users and for biologist programmers. . In: Krawetz S, Misener S (eds) Bioinformatics Methods and Protocols: Methods in Molecular Biology. Humana Press, Totowa, NJ, pp 365-386. Available online (http://frodo.wi.mit.edu/cgi-bin/primer3/primer3_www.cgi).

Rubin, G. M. and and Spradling, A. C. (1982). Genetic transformation of Drosophila with transposable element vectors. Science 218, 348-53.

Sachs, L. M., Amano, T. and Shi, Y. B. (2001). An essential role of histone deacetylases in postembryonic organ transformations in Xenopus laevis. Int J Mol Med 8, 595-601.

Sambrook, J. and Russel, D.W. (2001). Molecular cloning. Cold Spring Harbor Laboratory Press (3 eds) 1.

Saper, C. B. (2006). Chapter 14: Staying awake for dinner: hypothalamic integration of sleep, feeding, and circadian rhythms. Prog Brain Res 153, 243-52.

Sato, F., Kawamoto, T., Fujimoto, K., Noshiro, M., Honda, K. K., Honma, S., Honma, K. and Kato, Y. (2004). Functional analysis of the basic helix-loop-helix transcription factor DEC1 in circadian regulation. Interaction with BMAL1. Eur J Biochem 271, 4409-19.

Sato, T., Deguchi, T., Ichikawa, T., Fujieda, H. and Wake, K. (1991). Localization of hydroxyindole O-methyltransferase-synthesizing cells in bovine epithalamus: immunocytochemistry and in-situ hybridization. Cell Tissue Res 263, 413-8.

Saxen, L., Saxen, E., Toivonen, S. and Salimaki, K. (1957). Quantitative investigation on the anterior pituitary-thyroid mechanism during frog metamorphosis. Endocrinology 61, 35-44.

Scardigli, R., Baumer, N., Gruss, P., Guillemot, F. and Le Roux, I. (2003). Direct and concentration-dependent regulation of the proneural gene Neurogenin2 by Pax6. Development 130, 3269-81.

Schier, A. F. and Talbot, W. S. (2005). Molecular genetics of axis formation in zebrafish. Annu Rev Genet 39, 561-613.

Schmitt, E. A. and Dowling, J. E. (1999). Early retinal development in the zebrafish, Danio rerio: light and electron microscopic analyses. J Comp Neurol 404, 515-36.

Schomerus, C. and Korf, H. W. (2005). Mechanisms regulating melatonin synthesis in the Mammalian pineal organ. Ann N Y Acad Sci 1057, 372-83.

Schreiber, A. M. (2001). Metamorphosis and early larval development of the flatfishes (Pleuronectiformes): an osmoregulatory perspective. Comp Biochem Physiol B Biochem Mol Biol 129, 587-95.

Schulte-Merker, S. (2002). Looking at embryos. In: Nüslein-Volhard, C. and Dahm, R. Zebrafish. Practical approach. eds Oxford Press39-58.

Schwarz, M., Cecconi, F., Bernier, G., Andrejewski, N., Kammandel, B., Wagner, M. and Gruss, P. (2000). Spatial specification of mammalian eye territories by reciprocal transcriptional repression of Pax2 and Pax6. Development 127, 4325-34.

Sharman, A. C. and Brand, M. (1998). Evolution and homology of the nervous system: cross-phylum rescues of otd/Otx genes. Trends Genet 14, 211-4.

Shen, Y. C. and Raymond, P. A. (2004). Zebrafish cone-rod (crx) homeobox gene promotes retinogenesis. Dev Biol 269, 237-51.

Singh, S., Mishra, R., Arango, N. A., Deng, J. M., Behringer, R. R. and Saunders, G. F. (2002). Iris hypoplasia in mice that lack the alternatively spliced Pax6(5a) isoform. Proc Natl Acad Sci U S A 99, 6812-5.

St-Onge, L., Sosa-Pineda, B., Chowdhury, K., Mansouri, A. and Gruss, P. (1997). Pax6 is required for differentiation of glucagon-producing alpha-cells in mouse pancreas. Nature 387, 406-9.

Stamm, S., Ben-Ari, S., Rafalska, I., Tang, Y., Zhang, Z., Toiber, D., Thanaraj, T. A. and Soreq, H. (2005). Function of alternative splicing. Gene 344, 1-20.

Stolow, M. A. and Shi, Y. B. (1995). Xenopus sonic hedgehog as a potential morphogen during embryogenesis and thyroid hormone-dependent metamorphosis. Nucleic Acids Res 23, 2555-62.

Stoykova, A., Fritsch, R., Walther, C. and Gruss, P. (1996). Forebrain patterning defects in Small eye mutant mice. Development 122, 3453-65.

Stoykova, A., Gotz, M., Gruss, P. and Price, J. (1997). Pax6-dependent regulation of adhesive patterning, R-cadherin expression and boundary formation in developing forebrain. Development 124, 3765-77.

Stoykova, A. and Gruss, P. (1994). Roles of Pax-genes in developing and adult brain as suggested by expression patterns. J Neurosci 14, 1395-412.

Stoykova, A., Treichel, D., Hallonet, M. and Gruss, P. (2000). Pax6 modulates the dorsoventral patterning of the mammalian telencephalon. J Neurosci 20, 8042-50.

Strachan, T. and Read, A. P. (1994). PAX genes. Curr Opin Genet Dev 4, 427-38.

Strickler, A. G., Famuditimi, K. and Jeffery, W. R. (2002). Retinal homeobox genes and the role of cell proliferation in cavefish eye degeneration. Int J Dev Biol 46, 285-94.

Takechi, M. and Kawamura, S. (2005). Temporal and spatial changes in the expression pattern of multiple red and green subtype opsin genes during zebrafish development. J Exp Biol 208, 1337-45.

Tang, H. K., Singh, S. and Saunders, G. F. (1998). Dissection of the transactivation function of the transcription factor encoded by the eye developmental gene PAX6. J Biol Chem 273, 7210-21.

Thisse, B., Heyer, V., Lux, A., Alunni, V., Degrave, A., Seiliez, I., Kirchner, J., Parkhill, J. P. and Thisse, C. (2004). Spatial and temporal expression of the zebrafish genome by large-scale in situ hybridization screening. Methods Cell Biol 77, 505-19.

Tomarev, S. I. (1997). Pax-6, eyes absent, and Prox 1 in eye development. Int J Dev Biol 41, 835-42.

Tomarev, S. I., Callaerts, P., Kos, L., Zinovieva, R., Halder, G., Gehring, W. and Piatigorsky, J. (1997). Squid Pax-6 and eye development. Proc Natl Acad Sci U S A 94, 2421-6.

Ton, C. C., Hirvonen, H., Miwa, H., Weil, M. M., Monaghan, P., Jordan, T., van Heyningen, V., Hastie, N. D., Meijers-Heijboer, H., Drechsler, M. et al. (1991). Positional cloning and characterization of a paired box- and homeobox-containing gene from the aniridia region. Cell 67, 1059-74.

Tsujikawa, M. and Malicki, J. (2004). Genetics of photoreceptor development and function in zebrafish. Int J Dev Biol 48, 925-34.

Turque, N., Plaza, S., Radvanyi, F., Carriere, C. and Saule, S. (1994). Pax-QNR/Pax-6, a paired box- and homeobox-containing gene expressed in neurons, is also expressed in pancreatic endocrine cells. Mol Endocrinol 8, 929-38.

Umesono, K., Murakami, K. K., Thompson, C. C. and Evans, R. M. (1991). Direct repeats as selective response elements for the thyroid hormone, retinoic acid, and vitamin D3 receptors. Cell 65, 1255-66.

Underwood, H. and Siopes, T. (1984). Circadian organization in Japanese quail. J Exp Zool 232, 557-66.

Vallone, D., Gondi, S. B., Whitmore, D. and Foulkes, N. S. (2004). E-box function in a period gene repressed by light. Proc Natl Acad Sci U S A 101, 4106-11.

Vanecek, J. (1998). Melatonin inhibits release of luteinizing hormone (LH) via decrease of [Ca2+]i and cyclic AMP. Physiol Res 47, 329-35.

Varga, A. C. and Wrana, J. L. (2005). The disparate role of BMP in stem cell biology. Oncogene 24, 5713-21.

Vitalis, T., Cases, O., Engelkamp, D., Verney, C. and Price, D. J. (2000). Defect of tyrosine hydroxylase-immunoreactive neurons in the brains of mice lacking the transcription factor Pax6. J Neurosci 20, 6501-16.

Voisin, P., Guerlotte, J., Bernard, M., Collin, J. P. and Cogne, M. (1992). Molecular cloning and nucleotide sequence of a cDNA encoding hydroxyindole O-methyltransferase from chicken pineal gland. Biochem J 282 (Pt 2), 571-6.

Voisin, P., Guerlotte, J. and Collin, J. P. (1988). An antiserum against chicken hydroxyindole-O-methyltransferase reacts with the enzyme from pineal gland and retina and labels pineal modified photoreceptors. Brain Res 464, 53-61.

Vuilleumier, R., Besseau, L., Boeuf, G., Piparelli, A., Gothilf, Y., Gehring, W. G., Klein, D. C. and Falcon, J. (2006). Starting the zebrafish pineal circadian clock with a single photic transition. Endocrinology 147, 2273-9.

Walther, C. and Gruss, P. (1991). Pax-6, a murine paired box gene, is expressed in the developing CNS. Development 113, 1435-49.

Wawersik, S. and Maas, R. L. (2000). Vertebrate eye development as modeled in Drosophila. Hum Mol Genet 9, 917-25.

Wawersik, S., Purcell, P., Rauchman, M., Dudley, A. T., Robertson, E. J. and Maas, R. (1999). BMP7 acts in murine lens placode development. Dev Biol 207, 176-88.

Weaver, D. R., Stehle, J. H., Stopa, E. G. and Reppert, S. M. (1993). Melatonin receptors in human hypothalamus and pituitary: implications for circadian and reproductive responses to melatonin. J Clin Endocrinol Metab 76, 295-301.

Weissbach, H., Redfield, B. G. and Axelrod, J. (1960). Biosynthesis of melatonin: enzymic conversion of serotonin to N-acetylserotonin. Biochim Biophys Acta 43, 352-3.

Westerfield, M. (1993). The zebrafish book. University of Oregon Press. Available online (http://zfish.uoregon.edu/zf_info/zfbook.

Wiechmann, A. F. (1996). Hydroxyindole-O-methyltransferase mRNA expression in a subpopulation of photoreceptors in the chicken retina. J Pineal Res 20, 217-25.

Wiechmann, A. F., Bok, D. and Horwitz, J. (1985). Localization of hydroxyindole-O-methyltransferase in the mammalian pineal gland and retina. Invest Ophthalmol Vis Sci 26, 253-65.

Wiechmann, A. F. and Craft, C. M. (1993). Localization of mRNA encoding the indolamine synthesizing enzyme, hydroxyindole-O-methyltransferase, in chicken pineal gland and retina by in situ hybridization. Neurosci Lett 150, 207-11.

Wiechmann, A. F. and Wirsig-Wiechmann, C. R. (1993). Distribution of melatonin receptors in the brain of the frog Rana pipiens as revealed by in vitro autoradiography. Neuroscience 52, 469-80.

Wilson, D. S., Guenther, B., Desplan, C. and Kuriyan, J. (1995). High resolution crystal structure of a paired (Pax) class cooperative homeodomain dimer on DNA. Cell 82, 709-19.

Wilson, S. W. and Easter, S. S., Jr. (1991). Stereotyped pathway selection by growth cones of early epiphysial neurons in the embryonic zebrafish. Development 112, 723-46.

Wittbrodt, J., Shima, A. and Schartl, M. (2002). Medaka--a model organism from the far East. Nat Rev Genet 3, 53-64.

Wright, M. L. (2002). Melatonin, diel rhythms, and metamorphosis in anuran amphibians. Gen Comp Endocrinol 126, 251-4.

Wullimann, M. F. and Rink, E. (2001). Detailed immunohistology of Pax6 protein and tyrosine hydroxylase in the early zebrafish brain suggests role of Pax6 gene in

development of dopaminergic diencephalic neurons. Brain Res Dev Brain Res 131, 173-91.

Wullimann, M. F. and Rink, E. (2002). The teleostean forebrain: a comparative and developmental view based on early proliferation, Pax6 activity and catecholaminergic organization. Brain Res Bull 57, 363-70.

Xu, W., Rould, M. A., Jun, S., Desplan, C. and Pabo, C. O. (1995). Crystal structure of a paired domain-DNA complex at 2.5 A resolution reveals structural basis for Pax developmental mutations. Cell 80, 639-50.

Yamano, K., Araki, K., Sekikawa, K. and Inui, Y. (1994). Cloning of thyroid hormone receptor genes expressed in metamorphosing flounder. Dev Genet 15, 378-82.

Yamano, K. and Inui, Y. (1995). cDNA cloning of thyroid hormone receptor beta for the Japanese flounder. Gen Comp Endocrinol 99, 197-203.

Yamano, K. and Miwa, S. (1998). Differential gene expression of thyroid hormone receptor alpha and beta in fish development. Gen Comp Endocrinol 109, 75-85.

Yaoita, Y. and Brown, D. D. (1990). A correlation of thyroid hormone receptor gene expression with amphibian metamorphosis. Genes Dev 4, 1917-24.

Zachmann, A., Falcon, J., Knijff, S. C., Bolliet, V. and Ali, M. A. (1992). Effects of photoperiod and temperature on rhythmic melatonin secretion from the pineal organ of the white sucker (Catostomus commersoni) in vitro. Gen Comp Endocrinol 86, 26-33.

Zilberman-Peled, B., Ron, B., Gross, A., Finberg, J. P. and Gothilf, Y. (2006). A possible new role for fish retinal serotonin-N-acetyltransferase-1 (AANAT1): Dopamine metabolism. Brain Res 1073-1074, 220-8.

Ziv, L., Levkovitz, S., Toyama, R., Falcon, J. and Gothilf, Y. (2005). Functional development of the zebrafish pineal gland: light-induced expression of period2 is required for onset of the circadian clock. J Neuroendocrinol 17, 314-20.

Zuber, M. E., Gestri, G., Viczian, A. S., Barsacchi, G. and Harris, W. A. (2003). Specification of the vertebrate eye by a network of eye field transcription factors. Development 130, 5155-67.